Université de Toulouse

THÈSE

En vue de l'obtention du

DOCTORAT DE L'UNIVERSITÉ DE TOULOUSE

Délivré par :
Université Toulouse 3 Paul Sabatier (UT3 Paul Sabatier)

Cotutelle internationale avec :
Universidade Federal do Rio Grande do Sul, Instituto de Pesquisas Hidráulicas, Brasil

---

Présentée et soutenue par :
Rodrigo Cauduro Dias de PAIVA

Le

Titre :
Hydrologie du bassin Amazonien:
Compréhension et prévision fondées sur la modélisation hydrologique-hydrodynamique et la télédétection

---

École doctorale et discipline ou spécialité :
ED SDU2E : Hydrologie, Hydrochimie, Sol, Environnement

Unité de recherche :
Géosciences Environnement Toulouse (GET)

Directeur(s) de Thèse :

Walter Collischonn, Patrick Seyler et Marie-Paule Bonnet

Rapporteurs :

Otto Correa Rotunno Filho et Pierre Genthon

Autre(s) membre(s) du jury :

David Labat, Jean-Fraçois Crétaux, Carlos E. M. Tucci et Joel A. Goldenfum

Universidade Federal do Rio Grande do Sul
Instituto de Pesquisas Hidráulicas
Programa de Pós-Graduação em Recursos Hídricos e Saneamento Ambiental

Université de Toulouse 3 Paul Sabatier
Laboratoire Géosciences Environnement Toulouse
École Doctorale Sciences de l'Univers, de l'Environnement et de l'Espace

Tese de Doutorado

Hidrologia da bacia Amazônica:

Compreensão e previsão com base em modelagem hidrológica-hidrodinâmica e sensoriamento remoto

Rodrigo Cauduro Dias de Paiva

Orientadores:

Prof. Dr. Walter Collischonn (IPH/UFRGS), Dr. Patrick Seyler (GET/IRD) e Dra. Marie-Paule Bonnet (GET/IRD)

Relatores:

Prof. Dr. Otto Correa Rotunno Filho (COPPE/UFRJ) e Dr. Pierre Genthon (IRD/ Hydrosciences Montpellier)

Banca Examinadora:

Prof. Dr. David Labat (UPS), Dr. Jean-Fraçois Crétaux (CNES), Prof. Dr. Carlos Tucci (IPH/UFRGS) e Prof. Dr. Joel Goldenfum (IPH/UFRGS)

Porto Alegre, RS - Brasil
Fevereiro de 2012

Esta tese de doutorado foi desenvolvida em cotutela entre a *Universidade Federal do Rio Grande do Sul* (UFRGS) do *Brasil*, no *Instituto de Pesquisas Hidráulicas* (IPH), pelo *Programa de Pós-graduação em Recursos Hídricos e Saneamento Ambiental* (PPGRHSA), sob orientação do *Prof. Dr. Walter Collischonn*, e a *Université de Toulouse 3 Paul Sabatier* (UT3) da *França*, no laboratório *Géosciences Environnement Toulouse* (GET), pela escola doutoral *Sciences de l'Univers, de l'Environnement et de l'Espace* (SDU2E), na especialidade *Hydrologie, Hydrochimie, Sol, Environnement*, sob orientação do *Dr. Patrick Seyler* e *Dra. Marie-Paule Bonnet*, com financiamento do *Conselho Nacional de Desenvolvimento Científico e Tecnológico* (CNPq) do *Brasil*.

A minha avó Amabile (*in memoriam*)

Agradecimentos

A seguir, meus sinceros agradecimentos.

Começo agradecendo ao Prof. Walter Collischonn, pela amizade, pela orientação, por grandes ensinamentos passados durante a minha trajetória acadêmica e pelo exemplo de curiosidade e de entusiasmo por novos conhecimentos. À Dra. Marie-Paule Bonnet, pela orientação, pela amizade e por todos os ensinamentos, além da oportunidade de desenvolver este trabalho no GET em Toulouse, onde pude ter uma visão diferente das ciências hidrológicas no contexto das ciências da terra. E ao Dr. Patrick Seyler pelo apoio em Toulouse e pela direção da tese do lado da *Université de Toulouse 3 Paul Sabatier*.

Agradeço também aos Drs. Otto Rotunno e Pierre Genthon, que aceitaram serem relatores da minha tese, e a todos os outros membros da banca examinadora– os Drs. Joel Goldenfum, Carlos Tucci, David Labat e Jean-François Cretaux – por seus excelentes comentários e sugestões, de grande valor para este trabalho e com certeza para futuras pesquisas.

Sou grato às instituições onde este trabalho foi desenvolvido – a *Universidade Federal do Rio Grande do Sul* (UFRGS), o *Instituto de Pesquisas Hidráulicas* (IPH), o *Programa de Pós-graduação em Recursos Hídricos e Saneamento Ambiental* (PPGRHSA), a *Université de Toulouse 3 Paul Sabatier* (UT3), o laboratório *Géosciences Environnement Toulouse* (GET) e a escola doutoral *Sciences de l'Univers, de l'Environnement et de l'Espace* (SDU2E) - onde incluo todos os professores, pesquisadores, colegas e funcionários, por todo o apoio administrativo, técnico e científico e pelo ambiente propicio ao estudo e a novas ideias.

Devo também reconhecer o *Conselho Nacional de Desenvolvimento Científico e Tecnológico* (CNPq) pela bolsa de doutorado e também outras instituições como FINEP, IRD, CNRS e MHYZPA/INSU EC2CO pelo suporte financeiro. Além disto, organismos como a ANA, Hybam, SENHAMI, CPTEC/INPE, ESA e NASA pela cessão de dados hidrológicos e de sensoriamento remoto.

Agradeço ao colega e grande amigo Diogo Buarque, pela amizade e pelos mais diversos auxílios, com destaque para os relacionados à modelagem hidrológica da bacia Amazônica. Ao amigo e colega Adalberto Meller, com quem pude compartilhar as dificuldades inerentes da etapa de conclusão da tese, pelas discussões acerca dos resultados da tese. Ao prof. Clarke, que através do exemplo me ensinou sobre o pensamento claro e sobre pesquisa cientifica na área de hidrologia, também agradeço pela cooperação no estudo de dados de precipitação na Amazônia.

Minha gratidão se estende ao Dr. Luis Gustavo G. de Gonçalves pelos ensinamentos e apoio técnico-científico na área de assimilação de dados; ao Dr. Stephane Calmant pela ajuda em questões relacionadas à altimetria espacial; ao Dr. Frédéric Frappart pelo suporte em assuntos relacionados à gravimetria espacial e hidrologia da bacia Amazônica; ao prof. Carlos André pela colaboração no

projeto da Amazônia; a Dra. Joecila da Silva pela cessão de dados de altimetria espacial; ao Dr. F. Papa pelos dados de extensão de áreas alagadas estimada por satélite.

Sou também grato ao colega e amigo Augusto Getirana, pelas diversas ajudas/dicas durante a minha estadia em Toulouse e pela cooperação científica no tema de hidrologia de grandes bacias. Ao companheiro Jhan Carlo Espinoza, que entre divertidas conversas me deu importantes conselhos sobre a atividade de pesquisa. Ao prof. Tucci pelos ensinamentos e pelos auxílios acerca de hidrologia e modelagem hidrodinâmica. Também devo agradecer aos pesquisadores da Universidade de Bristol, na figura do prof. Paul Bates, Mark Trigg, Jeffrey Neal, Calum Baugh, entre outros, que me receberam em uma curta visita e proveram importantes comentários e sugestões acerca desta pesquisa.

Pelos comentários construtivos durante o processo de revisão dos artigos científicos relacionados a esta tese, agradeço aos Drs. P. Kumar, W. Buytaert, D. Fitzjarrald, M. Guimberteau, D. Yamazaki, D. Alsdorf, além de outros revisores anônimos e S. Mangiarotti e S. Shukla.

Também reconheço os importantes conhecimentos que tive a oportunidade de obter nos cursos de treinamento "*Earth Observation Understanding of the Water Cycle*" organizado pelo *Comittee on Space Research* na FUNCEME em Fortaleza, e "*Land Cover Change and Hydroclimate of La Plata bas.*", organizado pelo *Inter American Institute for Climate Change* na ITAIPU em Foz do Iguaçu.

Obrigado aos colegas do IPH e da sala de projetos, pela amizade, companheirismo, ajudas e discussões – Paulo, Fernando, Adrien (companheiro nas pesquisas amazônicas), Mino, Katiucia, Margarita, Karena, Rafael (todos eles), Carlos, Juan Martin, Márcio, Debora, Anderson, Rosane, Leandro, Davi, Saulo, Fernando Bike, Ruberto, Daniel e Ruti, Adriano, Vivi. Não posso me esquecer dos colegas e amigos de Toulouse, do GET e do observatoire Midi-Pyrénées, entre eles German, Joaquin, Eli, Elder, Charles, Fred, Tristan, Rodrigo, Florian, Stephanie, Jean Sebastien, Sakku, Romain, Aude, Stephane, Julia, Rebeca, Daniel, Cristina, Ana, Giana, Raul e Olivier. Também devo mencionar todos outros amigos que embora não sejam colegas de profissão foram sempre bons companheiros durante este período.

Sou muito grato a minha família – meus pais João Batista e Eloiza e meus irmãos Rafael e Carolina. Graças a eles, tive a oportunidade de viver com alegria em um ambiente de valorização e busca constante pelo conhecimento.

Mas acima de tudo, eu quero agradecer à minha amada Cláudia, que sempre esteve ao meu lado ao longo desta jornada de dificuldades inerentes, mas repleta de empolgantes descobertas.

Por fim, agradeço a todas outras pessoas não mencionadas aqui, mas que foram importantes na minha formação e no desenvolvimento deste trabalho.

Muito obrigado !

Resumo

Hidrologia da bacia Amazônica: Compreensão e previsão com base em modelagem hidrológica-hidrodinâmica e sensoriamento remoto

Autor: Rodrigo Cauduro Dias de Paiva

Orientadores: Walter Collischonn, Patrick Seyler e Marie-Paule Bonnet

A bacia Amazônica se destaca como o principal sistema hidrológico do mundo e pelo seu importante papel no sistema terrestre, influenciando o ciclo de carbono e o clima global. Recentes pressões antrópicas, como o desflorestamento, mudanças climáticas e a construção de barragens hidroelétricas, somados às crescentes cheias e secas extremas ocorridas nesta região, motivam o estudo da hidrologia da bacia Amazônica. Ao mesmo tempo, têm se desenvolvido métodos hidrológicos de modelagem e monitoramento via sensoriamento remoto que podem fornecer as bases técnicas para este fim. Este trabalho objetivou a compreensão e previsão da hidrologia da bacia Amazônica. Foram desenvolvidas e avaliadas diversas técnicas, incluindo de modelagem hidrológica-hidrodinâmica de larga escala, de assimilação de dados *in situ* e de sensoriamento remoto, e de previsão hidrológica. Este conjunto de técnicas foi utilizado para compreender o funcionamento da bacia Amazônica em termos de seus processos hidrológicos e sua previsibilidade hidrológica. O modelo hidrológico-hidrodinâmico de larga escala MGB-IPH foi utilizado para simular a bacia, sendo forçado com dados de chuva estimados por satélite. O modelo mostrou bom desempenho em uma validação detalhada contra observações de vazões e cotas *in situ* além de dados oriundos de sensoriamento remoto, incluindo níveis d'água de altimetria por radar, armazenamento d'água de gravimetria espacial e extensão de áreas alagadas. Mostrou-se a dominância das águas superficiais nas variações do armazenamento de água, a influência dos grandes corpos d'água sobre a variabilidade espacial da precipitação, além da importância das várzeas da inundação e efeitos de remanso sobre a propagação das ondas de cheia Amazônicas. As condições hidrológicas iniciais, com destaque para as águas superficiais, mostraram dominar a previsibilidade hidrológica nos grandes rios amazônicos, tendo assim a precipitação no futuro um papel secundário. Portanto, afim de melhor estimar os estados hidrológicos, de forma pioneira, foi desenvolvido um esquema de assimilação de dados para um modelo hidrológico-hidrodinâmico de larga escala para assimilar informações *in situ* e de altimetria por radar, cujo desempenho se mostrou satisfatório. Desenvolveu-se também um protótipo de sistema de previsão de vazões para a bacia Amazônica, baseado no modelo inicializado com condições iniciais ótimas do esquema de assimilação de dados e utilizando precipitação estimada por satélite disponível em tempo real. Os resultados foram promissores e o modelo foi capaz de prever vazões nos principais rios amazônicos com grande antecedência (~1 a 3 meses), antecipando, por exemplo, a grande seca de 2005. Estes resultados mostram o potencial da modelagem hidrológica de larga escala apoiada por informação de sensoriamento remoto na previsão de vazões com alta antecedência nas grandes bacias hidrográficas do mundo.

Palavras-chave: Amazônia, Processos Hidrológicos, Previsão Hidrológica, Modelagem Hidrológica-Hidrodinâmica, Sensoriamento Remoto, Assimilação de Dados, Altimetria por Radar

Résumé

Hydrologie du bassin Amazonien: Compréhension et prévision fondées sur la modélisation hydrologique-hydrodynamique et la télédétection

Autor: Rodrigo Cauduro Dias de Paiva

Directeurs: Walter Collischonn, Patrick Seyler et Marie-Paule Bonnet

Le bassin Amazonien est connu comme le plus grand système hydrologique du monde et pour son rôle important sur le système terre, influençant le cycle du carbone et le climat global. Les pressions anthropiques récentes, telles que la déforestation, les changements climatiques, la construction de barrage hydro-électriques, ainsi que l'augmentation des crues et sécheresse extrêmes qui se produisent dans cette région, motivent l'étude de l'hydrologie du bassin Amazonien. Dans le même temps, des méthodes hydrologiques de modélisation et de surveillance par observation satellitaire ont été développées qui peuvent fournir les bases techniques à cette fin. Ce travail a eu pour objectif la compréhension et la prévision du régime hydrologique du bassin Amazonien. Nous avons développé et évaluer des techniques de modélisation hydrologique-hydrodynamique de grande échelle, d'assimilation de données *in situ* et spatiales et de prévision hydrologique. L'ensemble de ces techniques nous a permis d'explorer le fonctionnement du bassin Amazonien en terme de processus physiques et de prévisibilité hydrologique. Nous avons utilisé le modèle hydrologique-hydrodynamique de grande échelle MGB-IPH pour simuler le bassin, le forçage précipitation étant fourni par l'observation spatiale. Les résultats de la modélisation sont satisfaisants lorsque validés à partir de données *in situ* de débit et de hauteurs d'eau mais également de données dérivées de l'observation spatiale incluant les niveaux d'eau déduits de l'altimétrie radar, le contenu en eau total issu de la gravimétrie satellitaire, l'extension des zones inondées. Nous avons montré que les eaux superficielles sont responsables en grande partie de la variation du stock total d'eau, l'influence des grands plans d'eau sur la variabilité spatiale des précipitations et l'influence des plaines d'inondation et des effets de remous sur la propagation des ondes de crues. Nos analyses ont montré le rôle prépondérant des conditions initiales, en particulier des eaux superficielles, pour la prévisibilité des grands fleuves Amazoniens, la connaissance des précipitations futures n'ayant qu'une influence secondaire. Ainsi, pour améliorer l'estimation des variables d'état hydrologiques, nous avons développé, pour la première fois, un schéma d'assimilation de données pour un modèle hydrologique-hydrodynamique de grande échelle, pour l'assimilation de données de jaugeages *in situ* et dérivées de l'altimétrie radar (débit et hauteur d'eau), dont les résultats se sont montrés satisfaisants. Nous avons également développé un prototype de système de prévision des débits pour le bassin Amazonien, basé sur le modèle initialisé avec les conditions initiales optimales fournies par le schéma d'assimilation de données, et en utilisant la pluie estimée par satellite disponible en temps réel. Les résultats ont été prometteurs, le modèle étant capable de prévoir les débits dans les principaux fleuves Amazoniens avec une antécédence importante (entre 1 et 3 mois), permettant d'anticiper, par exemple, la sècheresse extrême de 2005. Ces résultats démontrent le potentiel de la modélisation hydrologique appuyé par l'observation spatiale pour la prévision des débits avec une grande antécédence dans les grands bassins versant mondiaux.

Mots clés: Amazonie, Processus Hydrologiques, Prévision Hydrologique, Modélisation Hydrologique-Hydrodynamique, Télédétection, Assimilation de Données, Altimétrie par Radar

Abstract

Hydrology of the Amazon basin: Understanding and forecasting based on hydrologic-hydrodynamic modelling and remote sensing

Author: Rodrigo Cauduro Dias de Paiva

Advisors: Walter Collischonn, Patrick Seyler and Marie-Paule Bonnet

The Amazon basin is known as the world's main hydrological system and by its important role in the earth system, carbon cycle and global climate. Recent anthropogenic pressure, such as deforestation, climate change and the construction of hydropower dams, together with increasing extreme floods and droughts, encourage the research on the hydrology of the Amazon basin. On the other hand, hydrological methods for modeling and remotely sensed observation are being developed, and can be used for this goal. This work aimed at understanding and forecasting the hydrology of the Amazon River basin. We developed and evaluated techniques for large scale hydrologic-hydrodynamic modeling, data assimilation of both *in situ* and remote sensing data and hydrological forecasting. By means of these techniques, we explored the functioning of the Amazon River basin, in terms of its physical processes and its hydrological predictability. We used the MGB-IPH large scale hydrologic-hydrodynamic model forced by satellite-based precipitation. The model had a good performance when extensively validated against *in situ* discharge and stage measurements and also remotely sensed data, including radar altimetry-based water levels, gravimetric-based terrestrial water storage and flood inundation extent. We showed that surface waters governs most of the terrestrial water storage changes, the influence of large water bodies on precipitation spatial variability and the importance of the floodplains and backwater effects on the routing of the Amazon floodwaves. Analyses showed the dominant role of hydrological initial conditions, mainly surface waters, on hydrological predictability on the main Amazon Rivers, while the knowledge of future precipitation may be secondary. Aiming at the optimal estimation of these hydrological states, we developed, for the first time, a data assimilation scheme for both gauged and satellite altimetry-based discharge and water levels into a large scale hydrologic-hydrodynamic model, and it showed a good performance. We also developed a forecast system prototype, where the model is based on initial conditions gathered by the data assimilation scheme and forced by satellite-based precipitation. Results are promising and the model was able to provide accurate discharge forecasts in the main Amazon rivers even for very large lead times (~1 to 3 months), predicting, for example, the historical 2005 drought. These results point to the potential of large scale hydrological models supported with remote sensing information for providing hydrological forecasts well in advance at world's large rivers and poorly monitored regions.

Keywords: Amazon, Hydrological Processes, Hydrological Forecasts, Hydrologic-Hydrodynamic Modelling, Remote Sensing, Data Assimilation, Radar Altimetry

Sumário

Lista de abreviações

A-N - *Afternoon to Night period*

ANA - *Agência Nacional das Águas*

AS - *Altimetry Station*

CNPq - *Conselho Nacional de Desenvolvimento Científico e Tecnológico*

CPTEC - *Centro de Previsão do Tempo e Estudos Climáticos*

CRU CL 2.0 - *climatological dataset of the Climate and Research Unit*

DA - *Data Assimilation*

DEM - *Digital Elevation Model*

DJF - *December, January and February period*

EFAS - *European Flood Awareness System*

EKF - *Extended Kalman Filter*

EnKF - *Ensemble Kalman Filter*

ENSO - *El Niño - Southern Oscillation*

ENVISAT - *satéllite de observação terrestre da Agência Espacial Europeia*

ESA - *European Spatial Agency*

ESP - *Ensemble Streamflow Prediction*

FINEP - *Financiadora de Estudos e Projetos*

GET - *Laboratoire Géosciences Environnement Toulouse*

GIS - *Geographic Information System*

GLDAS - *Global Land Data Assimilation System*

GloFAS - *Global Flood Awareness System*

GRACE - *Gravity Recovery and Climate Experiment misson*

HD - *Hydrodynamic model*

HRU - *Hydrological Response Units*

HYBAM - *Hydrologie, Biogeochimie at Geodynamique du Bassin Amazonien*

ICEsat/GLAS - *Ice, Cloud, and Land Elevation Satellite/Geoscience Laser Altimeter System*

ICs - *Initial Conditions*

INPE - *Instituto de Pesquisas Espaciais*

IPH - *Instituto de Pesquisas Hidráulicas*

IRD - *Institut de Recherche pour le Développement*

ITCZ - *Intertropical Convergence Zone*

JJA - *June, July and August period*

MAM - *March, April and May period*

MC - *Muskingum Cunge model*

MFs -*Meteorological Forcings*

MGB-IPH - *Modelo de Grandes Bacias desenvolvido no Instituto de Pesquisas Hidráulicas*

NASA - *National Aeronautics and Space Administration*

N-M - *Night to Morning period*

reverse-ESP - *reverse Ensemble Streamflow Prediction*

SACZ - *South Atlantic Convergence Zone*

SDU2E - *École Doctorale Sciences de l'Univers, de l'Environnement et de l'Espace*

SENAMHI - *Servicio Nacional de Meteorologia e Hidrología*

SMOS - *Soil Moisture and Ocean Salinity mission*

SON - *September, October and November period*

SRTM - *Shuttle Radar Topography Mission*

SST - *Sea Surface Temperature*

SWOT - *Surface Waters and Ocean Topography mission*

TRMM - *Tropical Rainfall Measurement Mission*

TWS - *Terrestrial Water Storage*

UFRGS - *Universidade Federal do Rio Grande do Sul*

UT3 - *Université Toulouse 3 Paul Sabatier*

CAPÍTULO 1

Introdução

1.1. Introdução e contexto

1.1.1. Bacia Amazônica

A bacia Amazônica se destaca como um dos principais sistemas hidrológicos do mundo, drenando cerca de 6 milhões de km^2, e contribuindo com aproximadamente 15% do volume de água doce afluente aos oceanos [*Molinier et al.*, 1996]. Além de sua grande extensão, os seguintes fatores motivam o estudo da hidrologia da bacia Amazônica:

(i) Os seus processos hidrológicos podem exercer influência no clima tanto na escala local como global [*IPCC*, 2007], e no ciclo global de carbono e em particular nas emissões de metano e dióxido de carbono [*Richey et al.*, 2002; *Melack et al.*, 2004; *Aufdenkampe et al*., 2011], além de serem plano de fundo de outros importantes processos biogeoquímicos.

(ii) A Amazônia abriga uma das maiores florestas tropicais do mundo e um complexo ecossistema, que historicamente têm sido degradados por desmatamentos e introdução de pastagens e áreas agrícolas [*Leite et al*., 2012]. Tal desflorestamento tem importantes implicações devido às emissões do carbono estocado nas florestas para a atmosfera [*Leite et al*., 2012], além de potencialmente alterar o regime hidrológico [*Rodriguez et al.*, 2010], embora estes efeitos ainda não sejam completamente compreendidos.

(iii) Grande parte (~82%) da energia elétrica consumida no Brasil é de origem hidráulica [*EPE*, 2012], e a futura expansão do sistema hidrelétrico brasileiro passa pelo aproveitamento do potencial ainda pouco explorado dos rios Amazônicos [*BRASIL*, 2007a,b]. Diversas novas usinas hidroelétricas estão planejadas para os próximos anos e outras já estão em curso de construção como Belo Monte no rio Xingu e Jirau e Santo Antônio no rio Madeira. Entretanto, os possíveis impactos ambientais destes barramentos sobre o sistema Amazônico ainda não são inteiramente compreendidos.

(iv) Observa-se, recentemente, na bacia Amazônica um aumento na magnitude das cheias e secas em muitos dos seus principais tributários [e.g. *Espinoza et al.*, 2009b], com a ocorrência de importantes eventos hidrológicos extremos como as cheias de 2009 [*Chen et al*., 2010] e 2012, e as secas de 1996 [*Tomasella et al.*, 2010], 2005 [*Marengo et al*., 2008; *Zeng et al.*, 2008; *Chen et al.*, 2009] e 2010 [*Espinoza et al.*, 2011; *Marengo et al.*, 2011]. Estas cheias e secas causam importantes impactos sobre a população amazônica, que depende fortemente dos recursos hídricos para a produção de alimentos, transporte doméstico e comercial e produção de energia elétrica [*Marengo et al.*, 2008]. Além disto, a maior parte da

população está localizada ao longo dos grandes rios amazônicos onde a susceptibilidade às cheias é elevada. Neste sentido, o conhecimento quantitativo dos processos hidrológicos pode dar suporte à previsão e prevenção dos impactos de tais eventos extremos.

Somando-se a estes fatores, diversas características hidrológicas particulares encontradas na Amazônia motivam o estudo deste sistema. Esta região possui precipitações intensas e com alta variabilidade espacial, além de regime hidroclimático contrastante em diferentes regiões [*Espinoza et al.*, 2009a] e rios extremamente caudalosos. Grande parte dos rios Amazônicos encontra-se em áreas muito planas, onde efeitos de remanso e extensas áreas alagadas controlam os processos hidrológicos. Efeitos de remanso estão presentes tanto no período de cheias como de secas no curso principal do Amazonas [*Trigg et al.*, 2009], fazendo com que o efeito da maré seja identificado ao longo do próprio rio Amazonas até cerca de 1000 km a montante de sua foz [*Kosuth et al.*, 2009], e regulando o escoamento nos principais tributários amazônicos por efeito do próprio Amazonas sobre estes [*Meade et al.*, 1991]. Soma-se a isto as extensas áreas alagadas que são encontradas em grande parte da Amazônia [*Papa et al.*, 2010; *Hess et al.*, 2008; *Melack e Hess*, 2010], onde o escoamento d'água apresenta complexidades como grandes lagos interconectados [*Bonnet et al.*, 2008] e fluxo bidimensional [*Alsdorf et al.*, 2007a; *Alsdorf et al.*, 2010]. Além disto, estas várzeas possuem um importante papel no balanço de energia e interação entre a superfície e a atmosfera [*Mohamed et al.*, 2005; *Prigent et al.*, 2011], em ciclos globais de carbono [e.g. *Richey et al.*, 2002], na dinâmica do transporte de sedimentos [e.g. *Bourgoin et al.*, 2007; *Dunne et al.*, 1998] e nas condições químicas e ecológicas dos rios Amazônicos [*Junk*, 1997, *Richey et al.*, 2002, *Melack et al.*, 2004, *Moreira et al.*, 2004, *Seyler and Boaventura*, 2003].

1.1.2. Modelagem hidrológica na Amazônia

Neste sentido, modelos hidrológicos de base física são uma das principais ferramentas para (i) auxiliar na compreensão dos processos hidrológicos e sua relação com outros processos geofísicos, e para (ii) servir de base de Sistemas de Previsão Hidrológica visando à redução da vulnerabilidade da população local à eventos extremos.

A modelagem hidrológica na bacia amazônica é um tema de pesquisa em contínuo desenvolvimento. Os modelos de simulação hidrológica representam processos variáveis no tempo e espaço como infiltração e movimento de água no solo, balanço de energia e evapotranspiração e propagação de ondas de cheia em rios e planícies de inundação. Para

tanto, existe uma grande diversidade de modelos, alguns focados na simulação de processos de interface atmosfera-solo-planta [e.g. *Pitman*, 2003; *Wood et al.*, 1992], e outros mais focados na simulação de vazões em rios, propagação de ondas de cheia e estiagens [e.g. *Collischonn*, 2007; *Paiva*, 2011a].

Mais especificamente na bacia Amazônica e na simulação de águas superficiais, os modelos variam em função da complexidade, existindo modelos que (i) representam de forma simplificada o escoamento fluvial usando aproximações tipo reservatório linear ou onda cinemática e negligenciam as planícies de inundação [e.g. *Collischonn et al.*, 2008; *Getirana et al.*, 2010], (ii) modelos simplificados para o escoamento fluvial e com representação simplificada do escoamento nas várzeas de inundação [*Beighley et al.*, 2009; *Decharme et al.*, 2011; *Coe et al.*, 2008], (iii) modelos mais completos para o escoamento nos rios e com representação simplificada das várzeas [*Paiva et al., 2011*; *Paiva et al.*, 2012; *Yamazaki et al.*, 2011] e (iv) modelos detalhados da planície de inundação usando abordagem bidimensional [*Wilson et al.*, 2007] ou representando lagoas interconectadas [*Bonnet et al.*, 2008] mas para áreas restritas.

As limitações das diferentes abordagens de simulação se referem não somente a simplificações na representação de processos físicos, mas também em deficiências nos dados de entrada destes modelos. Sendo assim, o desenvolvimento de novas abordagens de simulação com a verificação do papel de diferentes processos hidrológicos além da verificação das principais fontes de erros ainda é um assunto em aberto na modelagem hidrológica de grandes bacias como a bacia Amazônica.

1.1.3. Sistemas de previsão hidrológica em grandes bacias

Apesar das limitações mencionadas acima, os modelos hidrológicos de base física recentemente passaram a ser utilizados em sistemas regionais e mesmo globais de monitoramento e previsão hidrológica em tempo real. Por exemplo, *Thielen et al.* [2009] apresentam a concepção do "*European Flood Awareness System - EFAS*", que se trata de um sistema alerta contra cheias para a Europa baseado em um modelo hidrológico distribuído forçado com previsões meteorológicas e utilizando a técnica de previsão probabilística. *Houborg et al.* [2012] apresentam as técnicas utilizadas no "*U.S. Drought Monitor*", que consiste em de um sistema de monitoramento em tempo real de secas nos Estados Unidos baseado em resultados de modelos hidrológicos de superfície. *Wood et al.* [2002] mostram um

sistema de previsão hidrológica sazonal para os Estados Unidos. Alguns estudos e protótipos de sistemas de previsão de vazões também foram desenvolvidos em algumas bacias brasileiras [*Tucci et al.*, 2003, *Collischonn et al.*, 2005; *Collischonn et al.*, 2007; *Meller*, 2012]. E por fim, *Alfieri et al.* [2012] apresentam a concepção e validações preliminares do "*Global Flood Awareness System - GloFAS*", que é uma extensão do sistema *EFAS* para a escala global.

Entretanto, sistemas de previsão hidrológica baseados em modelos físicos, com exceção do recente sistema global GloFAS, ainda não foram testados na região Amazônica e os estudos de previsão existentes na bacia são todos baseados em modelos estatísticos [e.g. *Uvo e Grahan*, 1998; *Uvo et al.*, 2000; *Schongart e Junk*, 2007; *Cappalaere et al.*, 1995].

1.1.4. Sensoriamento remoto de variáveis hidrológicas

Paralelamente às ferramentas de modelagem hidrológica, têm se desenvolvido nos últimos anos um grande número de técnicas de sensoriamento remoto para observação de variáveis hidrológicas, que permitem o monitoramento de grandes áreas remotas, como a Amazônia, com uma cobertura espaço-temporal muito superior a de observações *in situ*. Os produtos de sensoriamento remoto voltados para hidrologia desenvolvidos recentemente incluem:

- Métodos de estimativa dos níveis d'água através de altimetria espacial por radar [*Frappart et al.*, 2006; *Alsdorf et al.*, 2007; *Santos da Silva et al.*, 2010] com satélites como o TOPEX, Jason-2, ERS-2, ENVISAT, entre outros;
- Variação no armazenamento de água terrestre ("*Terrestrial Water Storage*") relativos a volumes estocados em águas subterrâneas, solo e planícies de inundação estimados pela missão de gravimetria GRACE "*Gravity Recovery and Climate Experiment*" [*Tapley et al.*, 2004];
- Umidade do solo com técnicas de micro-ondas da missão SMOS "*Soil Moisture and Ocean Salinity*" [*Kerr et al.*, 2001];
- Fluxos de energia e evapotranspiração [e.g. *Vinukollu et al.*, 2010];
- Extensão de áreas alagadas [e.g. *Hess et al.*, 2003; *Papa et al.*, 2010];
- Estimativas da precipitação com sensores de infravermelho e micro-ondas, como da missão TRMM "*Tropical Rainfall Measurement Mission*" [*Huffman et al.*, 2007];
- Dados topográficos de modelos digitais de elevação (DEMs) como da missão SRTM "*Shuttle Radar Topography Mission*" [*Farr et al.*, 2007], com cobertura quase global na escala de ~100 m e

- Áreas alagadas e níveis d'água da futura missão SWOT "*Surface Waters and Ocean Topography*" [*Durand et al.*, 2010].

Vários destes produtos de sensoriamento remoto vêm sendo utilizados para a compreensão dos processos hidrológicos na bacia Amazônica. Por exemplo, dados de variações no armazenamento de água terrestre da missão GRACE foram utilizados por *Chen et al.* [2010] e *Chen et al.* [2009] para estudar a cheia de 2009 e a seca de 2005, respectivamente. *Alsdorf et al.* [2007] utilizaram dados de radar para estimar variações nos níveis d'águas e avaliar a complexidade da dinâmica de inundação nas várzeas amazônicas. *Alsdorf et al.* [2010] utilizaram uma combinação de dados de sensoriamento remoto incluindo a missão GRACE para estimar os volumes d'água que são anualmente estocados e liberados nas várzeas de inundação na Amazônia. *Frappart et al.* [2011] estimaram os volumes d'água armazenados em estoques subterrâneos na bacia do rio Negro utilizando dados da missão GRACE, extensão de áreas alagadas de *Papa et al.* [2010] e altimetria espacial. Estas estimativas de sensoriamento remoto também poderiam ser utilizadas para a validação e investigação de erros de modelos hidrológicos ou ainda serem integrados com estes modelos.

1.1.5. Assimilação de dados

Neste sentido, as técnicas de assimilação de dados são uma alternativa para conciliar a recente grande quantidade de observações hidrológicas baseadas em sensoriamento remoto com modelos hidrológicos, com o objetivo de utilizar ambas as abordagens de forma ótima.

Assimilação de dados consiste basicamente em combinar dados de observações e informações de modelos de simulação para obter estimativa ótima do estado de um sistema [*Reichle*, 2008]. Utilizam-se normalmente métodos bayesianos [*Liu e Gupta*, 2007], em sua maioria baseados no filtro de Kalman [*Kalman*, 1960] como o "*Ensemble Kalman Filter"* [*Evensen*, 2003]. Este tipo de técnica pode ser utilizado em estudos retrospectivos onde se combinam dados históricos com resultados de modelos de simulação, a exemplo das reanálises de modelos meteorológicos [e.g. *Kalnay*, 1996]. Também pode ser utilizado para atualização de modelos hidrológicos de previsão em tempo real a fim de corrigir erros dos modelos no inicio da previsão e assim aumentar sua precisão [e.g. *Collischonn et al.*, 2005].

Diversas aplicações deste tipo de técnica em hidrologia já foram empregadas, incluindo a assimilação de diversos tipos de observações, tanto *in situ* como de sensoriamento

remoto, com diversos tipos de modelos e utilizando diferentes métodos, mas sendo a grande maioria utilizando a técnica "*Ensemble Kalman Filter*" [*Evensen*, 2003] ou suas variantes, conforme revisado em *Liu e Gupta* [2007], *Reichle* [2008] e *Liu et al.* [2012]. Algumas das aplicações abordam: a assimilação de informação de cobertura de neve ou umidade do solo por sensoriamento remoto em modelos de superfície [e.g. *Andreadis e Lettenmaier*, 2006; *Reichle et al.*, 2002]; a assimilação de níveis d'água *in situ* ou dados sintéticos da missão SWOT em modelos hidrodinâmicos em pequenos trechos de rios [*Neal et al.*, 2007; *Ricci et al.*, 2011; *Biancamaria et al.*, 2011; *Andreadis et al.*, 2007; *Durand et al.*, 2008]; a assimilação de dados de vazão em modelos hidrológicos distribuídos [*Clark et al.*, 2008; *McMillan et al.*, 2012; *Lee et al.*, 2012; *Thirel et al*., 2010]; entre outros. Existem inclusive sistemas de assimilação de dados terrestres que integram observações de sensoriamento remoto e modelos de simulação, como o LIS - "*Land Information System*" [*Kumar et al.*, 2008] e o GLDAS – "*Global Land Data Assimilation System*" [*Rodell et al.*, 2004] desenvolvidos pela Agência Espacial dos Estados Unidos, a NASA – "*National Aeronautics and Space Administration"*. Estes sistemas são focados em processos hidrológicos verticais (e.g. fluxos de energia, umidade do solo, cobertura de neve) visando prover informações para modelos de previsão meteorológica. Entretanto, apesar da existência de diversas aplicações de assimilação de dados em hidrologia, a utilização nos módulos de simulação de escoamento em rios e planícies de inundação em modelos hidrológicos de grande escala ainda é incomum.

1.2. Objetivos

Na breve introdução apresentada, argumentou-se sobre a importância da compreensão e previsão da hidrologia da bacia Amazônica ou outras grandes bacias hidrográficas, mas alertando para o atual desconhecimento sobre o funcionamento destes sistemas. Também foram apresentados os mais recentes tipos de técnicas que poderiam ser utilizadas para estes fins - incluindo modelagem hidrológica, sensoriamento remoto, assimilação de dados e previsão hidrológica - mas que também ainda são temas de pesquisa em aberto.

O objetivo desta tese é compreender e prever o funcionamento hidrológico de grandes bacias hidrográficas, mais especificamente a bacia Amazônica, com o suporte de modelos de simulação hidrológica-hidrodinâmica e monitoramento de variáveis hidrológicas por sensoriamento remoto. Mais especificamente, esta pesquisa visa:

- Desenvolver técnicas de modelagem hidrológica-hidrodinâmica de grande escala, de assimilação de dados *in situ* e de sensoriamento remoto e de previsão de vazões na bacia Amazônica.
- Avaliar o desempenho, os pontos fortes e as limitações de técnicas de modelagem hidrológica-hidrodinâmica de grande escala, de assimilação de dados *in situ* e de sensoriamento remoto e de previsão de vazões na bacia Amazônica.
- Compreender, com o suporte de modelagem hidrológica-hidrodinâmica e sensoriamento remoto, como funciona a bacia Amazônica em termos de seus processos hidrológicos dominantes e que fatores influenciam na sua previsibilidade hidrológica.

Neste sentido, são abordadas neste trabalho as seguintes questões científicas:

- Como é o desempenho de um modelo hidrológico-hidrodinâmico de grande escala na simulação de diferentes variáveis hidrológicas (vazões, níveis d'água, extensão de áreas alagadas, armazenamento d'água) na bacia Amazônica, se comparado com observações *in situ* e estimativas de sensoriamento remoto? Quais são as principais limitações e fontes de erros na modelagem hidrológica-hidrodinâmica em grandes bacias como a Amazônia? (Capítulo 2)
- Como se caracteriza o balanço hídrico da bacia Amazônica? Qual é o papel de diferentes compartimentos hidrológicos (águas superficiais, solo e águas subterrâneas) na variabilidade temporal do armazenamento total de água na Amazônia? Qual é o papel das várzeas de inundação e aspectos hidráulicos no escoamento fluvial para a propagação de ondas de cheias ao longo dos rios Amazônicos? (Capítulo 2)
- Como se caracteriza a variabilidade espacial da precipitação na Amazônia e qual é a influencia de grandes corpos d'água? Como isto se comporta em estimativas de precipitação por sensoriamento remoto? (Capítulo 3)

- Quais são as principais fontes de incerteza na previsão hidrológica na bacia Amazônica? O que é mais importante, o conhecimento preciso dos estados hidrológicos no inicio de uma previsão ou a precipitação no futuro? Quais são as variáveis hidrológicas mais importantes? Como este comportamento varia espacialmente e em função da antecedência da previsão e como este se relaciona com as características da bacia? (Capítulo 4)
- Como integrar observações de vazões e níveis d'água *in situ* e de sensoriamento remoto (altimetria espacial por radar) com modelos hidrológicos de grandes bacias através de técnicas de assimilação de dados? Como é o desempenho de um sistema de assimilação de dados baseado na técnica "*Ensemble Kalman Filter*"? É possível melhorar estimativas de vazões e níveis d'águas em rios não monitorados? Qual é a utilidade da assimilação de dados de altimetria espacial considerando sua relativa baixa resolução temporal e acurácia se comparados com dados *in situ*? (Capítulo 5)
- Seria possível desenvolver previsões de vazões em grandes bacias como a Amazônia com relativa precisão usando um modelo hidrológico-hidrodinâmico de grande escala baseado principalmente nas condições iniciais ótimas obtidas via assimilação de dados? Em que escalas espaciais e temporais? (Capítulo 5)

1.3. Organização do trabalho

A fim de responder aos objetivos da tese, foi desenvolvida uma série de estudos que são apresentados nos Capítulos 2 a 5 na forma de artigos, escritos baseados nas seguintes publicações:

Capítulo 2:

Paiva, R.C.D., Collischonn, W., Bonnet, M.-P., Buarque, D.C., Frappart, F., Calmant, S., Mendes, C.B. 2013. Large scale hydrologic and hydrodynamic modelling of the Amazon River basin. Water Resour. Res., 49, doi: 10.1002/wrcr.20067.

Capítulo 3:

Paiva, R.C.D., Buarque, D.C., Clarke, R.T., Collischonn, W., Allasia, D.G. 2011. Reduced precipitation over large water bodies in the Brazilian Amazon shown from TRMM data. Geophys. Res. Lett., 38, L04406, doi:10.1029/2010GL045277

Capítulo 4 :

Paiva, R.C.D., Collischonn, W., Bonnet, M.-P., de Gonçalves, L.G.G. 2012. On the sources of hydrological prediction uncertainty in the Amazon, Hydrol. Earth Syst. Sci., 16, 3127-3137, doi:10.5194/hess-16-3127-2012.

Capítulo 5:

Paiva, R.C.D., Collischonn, W., Bonnet, M.-P., de Gonçalves, L.G.G., Calmant, S., Getirana, A., Santos da Silva, J. Assimilating in situ and radar altimetry data into a large-scale hydrologic-hydrodynamic model for streamflow forecast in the Amazon River basin. To be submitted.

A Figura 1 apresenta uma visão geral dos temas abordados em cada capítulo e a relação entre eles. Apresenta-se a seguir e posteriormente no início de cada capítulo um resumo de suas respectivas contribuições e a relação com os demais capítulos.

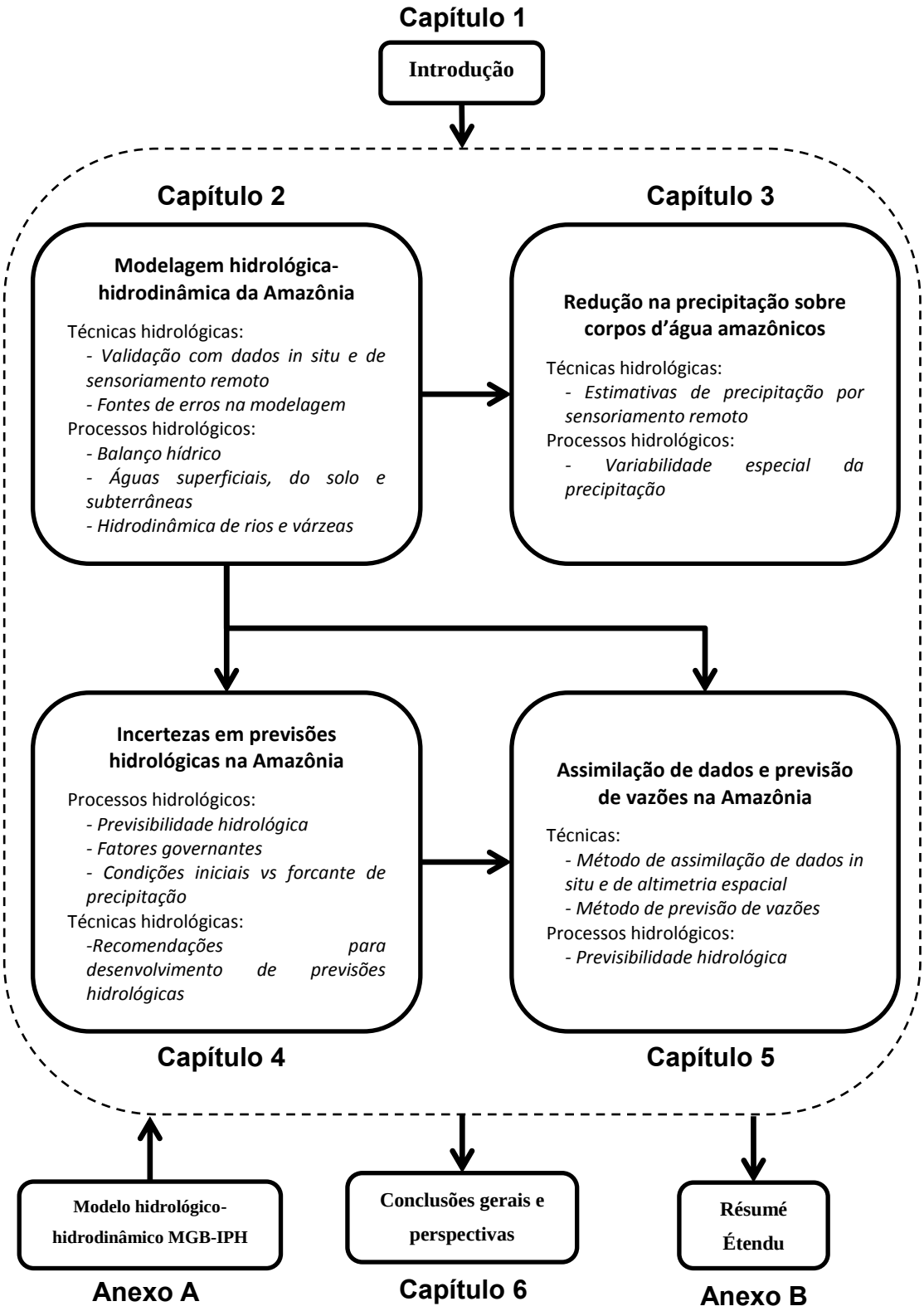

Figura 1. Visão geral e relação entre os principais temas abordados na tese.

A pesquisa desenvolvida nesta tese inicia-se no Capítulo 2 com um estudo de modelagem hidrológica-hidrodinâmica da bacia Amazônica, utilizado técnicas (modelo MGB-IPH) que se enquadram no estado da arte da modelagem física/conceitual de grandes bacias hidrográficas e sensoriamento remoto de variáveis hidrológicas. Em termos científicos, mas com um foco em técnicas hidrológicas, objetivo inicial deste capítulo é o de avaliar as limitações e as principais fontes de erros da modelagem hidrológica-hidrodinâmica na representação das principais variáveis hidrológicos na bacia Amazônica. Além disso, e com um olhar em processos hidrológicos, o funcionamento da bacia Amazônica é explorado através de resultados de simulação, incluindo aspectos como balanço hídrico, a contribuição das águas superficiais, no solo e subterrâneas na variabilidade do armazenamento d'água e o papel da hidráulica dos rios e várzeas de inundação na propagação de ondas de cheias ao longo dos rios Amazônicos. Paralelamente, a implementação de um modelo de simulação hidrológica da bacia Amazônica no Capítulo 2 tem uma finalidade operacional, considerando que fornece as bases técnicas para os estudos de previsão hidrológica e assimilação de dados que são apresentados nos capítulos seguintes (Capítulo 4 e 5).

Apresenta-se no Capítulo 3 um estudo acerca da variabilidade espacial da precipitação Amazônica estimada via sensoriamento remoto e a evidencia de uma redução na precipitação sobre grandes corpos d'água. A motivação para este estudo surgiu de uma análise preliminar de dados de precipitação nas etapas de preparação de informações para o estudo de modelagem do Capítulo 2. Neste momento, surpreendentemente verificou-se que a precipitação seria reduzida sobre os corpos d'água Amazônicos. As análises apresentadas neste capítulo se encontram de certa forma a parte do eixo principal da tese, visto que não são pré requisito para os estudos dos capítulos posteriores. Mas se enquadram dentro dos objetivos da tese de compreender o funcionamento da bacia Amazônica em termos de processos hidrológicos.

A parte inicial da tese (Capitulos 2 e 3), que é mais focada no funcionamento da bacia Amazônica em termos de processos hidrológicos, é seguida de estudos (Capítulo 4 e 5) que visam compreendê-la em termos de previsibilidade hidrológica e desenvolver técnicas voltadas a previsão de vazões.

No Capítulo 4 apresenta-se um estudo de previsibilidade na bacia Amazônica utilizando-se o modelo hidrológico-hidrodinâmico MGB-IPH baseado na implementação exposta no Capítulo 2. Mais especificamente, avalia-se a importância relativa das condições hidrológicas iniciais do modelo e dos forçantes meteorológicos como fontes de incerteza para a previsão de vazões na Amazônia. No contexto da pesquisa desenvolvida nesta tese, este

capítulo teve um papel fundamental – o de indicar a caminho a ser seguido para desenvolver previsões hidrológicas na bacia Amazônica usando em modelos de base física. Em resumo, os resultados mostram a importância do conhecimento das condições hidrológicas iniciais para a previsão de vazões nos principais rios Amazônicos mesmo para altos para horizontes de previsão, tendo a precipitação no futuro um papel secundário. Tais resultados sugerem a importância do desenvolvimento de técnicas de assimilação de dados para melhor estimar os estados hidrológicos no inicio das previsões, o que motivou o desenvolvimento do Capítulo 5.

Motivado por estes argumentos, neste Capítulo 5 apresenta-se o desenvolvimento e avaliação de um esquema de assimilação de dados no modelo hidrológico-hidrodinâmico MGB-IPH da bacia Amazônica, baseado em sua implementação do Capítulo 2. O esquema é baseado na técnica "*Ensemble Kalman Filter*", que se enquadra no estado da arte da integração de modelos com observações e tendo utilização crescente nos últimos anos em aplicações hidrológicas. Avaliou-se a assimilação de dados de vazões observadas *in situ* em estações fluviométricas, além de níveis d'água oriundos de altimetria espacial por radar, que complementam as observações hidrológicas convencionais permitindo o monitoramento mais detalhado com melhor cobertura espacial de grandes áreas remotas, como a Amazônia. Por fim, baseado nas conclusões do Capítulo 4 e no modelo desenvolvido no Capítulo 2, desenvolveu-se um protótipo de sistema de previsão de vazões para a bacia Amazônica, baseado no modelo inicializado com condições iniciais ótimas do esquema de assimilação de dados e utilizando precipitação estimada por satélite disponível em tempo real, que permitiu uma avaliação adicional acerca da previsibilidade do sistema Amazônico.

No Capítulo 6, apresenta-se um resumo das conclusões da tese assim como perspectivas para pesquisas futuras. O Capítulo Referencias Bibliográficas trás a lista de publicações citadas ao longo do manuscrito da tese, com exceção do corpo principal dos artigos apresentados nos Capítulos 2 a 5. O Anexo A exibe detalhes técnicos do modelo hidrológico-hidrodinâmico MGB-IPH utilizado nesta tese enquanto que o Anexo B apresenta um resumo expandido da tese em língua francesa.

CAPÍTULO 2

Large-scale hydrologic and hydrodynamic modelling of the Amazon River basin

Capítulo 2: Large-scale hydrologic and hydrodynamic modelling of the Amazon River basin

A pesquisa desenvolvida nesta tese inicia-se com um estudo de modelagem hidrológica-hidrodinâmica da bacia Amazônica utilizando técnicas que se enquadram no estado da arte da modelagem física/conceitual de grandes bacias hidrográficas e sensoriamento remoto de variáveis hidrológicas.

Avalia-se neste capítulo as limitações e as principais fontes de erros da modelagem hidrológica-hidrodinâmica na representação das principais variáveis hidrológicos na bacia Amazônica. O funcionamento da bacia Amazônica é explorado através de resultados de simulação, incluindo aspectos como balanço hídrico, a contribuição das águas superficiais, no solo e subterrâneas na variabilidade do armazenamento d'água e o papel da hidráulica dos rios e várzeas de inundação na propagação de ondas de cheias ao longo dos rios Amazônicos. Paralelamente, este capítulo tem uma finalidade operacional, visto que o objetivo também foi o de implementar um modelo de simulação na bacia Amazônica a fim de fornecer as bases técnicas para os estudos de previsão hidrológica que são apresentados nos Capítulos 4 e 5.

Utiliza-se o modelo hidrológico de base física MGB-IPH *"*Modelo de Grandes Bacias*"*, desenvolvido por *Collischonn et al.,* [2007] com um módulo de modelagem hidrodinâmica de grande escala desenvolvido recentemente por *Paiva et al.* [2011a], baseado nas equações de *Saint Venant* e em um modelo do tipo armazenamento para as várzeas de inundação. Algoritmos de geoprocessamento são utilizados para extrair informações do modelo digital de elevação (DEM) do SRTM [*Farr et al.*, 2007] para o modelo hidrodinâmico e o modelo foi forçado com estimativas de precipitação por satélite do TRMM 3B42 [*Huffman et al.,* 2007]. Maiores detalhes sobre o modelo hidrológico-hidrodinâmico são apresentados no Anexo A.

Apresenta-se uma validação detalhada do modelo utilizando-se observações hidrológicas convencionais (vazões e cotas de estações fluviométricas) e oriundas de recentes técnicas de sensoriamento remoto, incluindo níveis d'água estimados por altimetria espacial por radar do satélite ENVISAT [*Santos da Silva et al.,* 2010], extensão de áreas alagadas estimadas por dados de múltiplos satélites [*Papa et al.*, 2010] e variações no armazenamento de água terrestre oriundos da missão de gravimetria GRACE [*Frappart et al.,* 2010; 2011b].

Mostra-se que o modelo MGB-IPH com o módulo hidrodinâmico é capaz de representar os principais processos hidrológicos da bacia Amazônica, reproduzindo satisfatoriamente hidrogramas em diferentes escalas espaciais, mas principalmente nos grandes rios. Os resultados de simulação também concordam com observações de níveis d'água, extensão de áreas alagadas e variação no armazenamento d'água terrestre.

Entretanto, o modelo mostrou-se sensível principalmente aos dados de precipitação e a parâmetros relacionados à geometria de rios e várzeas de inundação. Grande parte dos erros ocorreu em áreas montanhosas e/ou pouco monitoradas, onde, possivelmente, existem erros importantes nos dados de precipitação utilizados (produto TRMM 3B42 estimado via sensoriamento remoto). A incerteza nos parâmetros relacionados aos rios e várzeas de inundação causou erros nos níveis água e extensão de áreas alagadas simulados, indicando a necessidade de desenvolvimento de melhores métodos para a estimativa destes parâmetros. São sugeridas algumas alternativas, como meios para correção do DEM SRTM para remover erros relacionados à vegetação, estimativa da largura dos rios por sensoriamento remoto ou o uso de dados da futura missão SWOT.

Os resultados do modelo em termos de balanço hídrico da bacia Amazônica são semelhantes a estudos anteriores e as taxas anuais médias de precipitação, evapotranspiração e vazão da bacia hidrográfica até Óbidos são P = 5.65 mm.dia^{-1}, ET = 2.72 mm.dia^{-1} e Q = 3.09 mm.dia^{-1}, respectivamente. O armazenamento d'água terrestre apresenta uma forte variação sazonal com amplitude média de 325 mm, e superando 750 mm na Amazônica central. As águas superficiais governam grande parte das variações do armazenamento d'água, sendo responsáveis por 56% da amplitude total de variação, seguidas pela água no solo (36%) e sendo as águas subterrâneas menos importantes (8%).

Os resultados mostram haver uma importante interação entre as vazões, níveis d'água e extensão de áreas alagadas, onde as várzeas de inundação atuam armazenando e liberando lentamente os volumes d'água dos rios durante a passagem das ondas de cheia, o que atenua e atrasa os hidrogramas em vários meses. Efeitos de remanso também se mostraram importantes na atenuação e atraso das ondas de cheia. Estes resultados mostram a importância de utilização de modelos hidrológicos complexos capazes de representar estes processos físicos.

Por fim, embora existam algumas limitações nos resultados de simulação apresentados, o modelo MGB-IPH mostra-se muito eficaz na representação de hidrogramas observados e consequentemente apropriado para servir de base para estudos de previsão de vazões na bacia Amazônica.

Capítulo 2: Large-scale hydrologic and hydrodynamic modelling of the Amazon River basin

This chapter is based on the following paper published at Water Resources Research:

Paiva, R.C.D., Collischonn, W., Bonnet, M.-P., Buarque, D.C., Frappart, F., Calmant, S., Mendes, C.B. 2013. Large scale hydrologic and hydrodynamic modelling of the Amazon River basin. Water Resour. Res., 49, doi: 10.1002/wrcr.20067

Abstract

In this paper, a hydrologic/hydrodynamic modelling of the Amazon River basin is presented using the MGB-IPH model with a validation using remotely-sensed observations. Moreover, the sources of model errors by means of the validation and sensitivity tests are investigated and the physical functioning of the Amazon basin is also explored. The MGB-IPH is a physically-based model resolving all land hydrological processes and here using a full 1D river hydrodynamic module with a simple floodplain storage model. River-floodplain geometry parameters were extracted from SRTM DEM and the model was forced using satellite-derived rainfall from TRMM3B42. Model results agree with observed *in situ* daily river discharges and water levels and with three complementary satellite-based products: (i) water levels derived from ENVISAT altimetry data; (ii) a global dataset of monthly inundation extent; and (iii) monthly terrestrial water storage (TWS) anomalies derived from GRACE. However, the model is sensitive to precipitation forcing and river–floodplain parameters. Most of the errors occur in westerly regions, possibly due to the poor quality of TRMM 3B42 rainfall dataset in these mountainous and/or poorly monitored areas. Also, uncertainty in river-floodplain geometry causes errors in simulated water levels and inundation extent, suggesting the need for improvement of parameter estimation methods. Finally, analyses of Amazon hydrological processes demonstrate that surface waters governs most of the Amazon TWS changes (56%), followed by soil water (36%) and ground water (8%). Moreover, floodplains play a major role in stream flow routing, although backwater effects are also important to delay and attenuate flood waves.

2.1. Introduction

The development of large-scale hydrological models has been a subject of important research topics in the past decades. These models, when used in forecast systems, may help reducing population vulnerability to natural hazards, particularly in the Amazon River basin, where extreme hydrological events have occurred in the past few years, such as the floods of 2009 and 2012 and the droughts in 1996, 2005 and 2010 [*Chen et al.*, 2010; *Tomasella et al.* 2010; *Marengo et al.*, 2008; *Espinoza et al.*, 2011, *Marengo et al.*, 2011]. Furthermore, complementary to observational studies [*e.g. Frappart et al.*, 2011a; *Azarderakhsh et al*., 2011; *Alsdorf et al.,* 2007a], simulation models can support the understanding and quantification of different Amazon hydrological processes such as evapotranspiration, soil and groundwater storages and river-floodplain hydrodynamics [e.g. *Costa and Foley,* 1997; *Trigg et al.* 2009].

Part of recent model developments concerns river and floodplain flow, which is an important factor in the Amazon hydrology. *Trigg et al.* [2009] showed that the Amazon flood wave is subcritical and diffusive. Consequently, backwater effects cause the influence of sea tides on the main river channel to be perceived more than ~1000 km upstream the river mouth [*Kosuth et al.*, 2009]. It also causes the influence of the main river over its tributaries [*Meade*, 1991] and controls droughts [*Tomasella et al.*, 2010]. Floodplain inundation is also an important issue [*Bonnet et al.*, 2008; *Alsdorf et al.*, 2007a; and *Alsdorf et al.*, 2010], playing a significant role in large-scale flood propagation [*Paiva et al.*, 2012; *Yamazaki et al.*, 2011], in sediment dynamics [*Bourgoin et al.*, 2007], in chemical and ecological conditions [*Junk*, 1997; *Richey et al*., 2002; *Melack et al.*, 2004; *Seyler and Boaventura*, 2003; among others] and in the climate system due to land surface and atmosphere interactions [*Mohamed et al.*, 2005; *Paiva et al*., 2011b; *Prigent et al.*, 2011].

Recent modelling developments used different kinds of approaches aiming at sufficiently representing physical processes, but considering computational and input data limitations. River hydrodynamics are generally represented by simplifications of *Saint Venant* equations, including a simplistic relation between water volume storage and discharge [e.g. *Coe et al*, 2008], kinematic wave models [*Decharme et al*. 2011; *Getirana et al.* 2012] or Muskingum Cunge type methods [*Collischonn et al., 2008*; *Beighley et al.*, 2009]; diffusive wave models [*Yamazaki et al.*, 2011] or a full hydrodynamic model [*Paiva et al.*, 2011a; *Paiva et al.*, 2012] where only the last two can represent the aforementioned backwater effects. Although the use of hydrodynamic models within large-scale distributed hydrological models is still uncommon, they also have been applied in other relatively large-scale problems [*Paz et al.*, 2010*; Biancamaria et al.*, 2009; *Lian et al.*, 2007]. When included, floodplain flows are modelled by different approaches: assuming storage areas having the same river water levels [e.g. *Paiva et al.*, 2011a; *Paiva et al.*, 2012; *Yamazaki et al.*, 2011] or considering water exchanges between river and floodplains as a function of river-floodplain water slope [e.g. *Decharme et al*. 2011]; adopting a composed river floodplain cross sections with 1D floodplain flow [e.g. *Beighley et al.*, 2009; *Getirana et al.*, 2012]; or considering 2 D floodplain flows [e.g. *Wilson et al.*, 2007; *Trigg et al.*, 2009]. In most of the cases, river bathymetry is approximated by a rectangular shape with parameters estimated as function of the upstream drainage area (or mean discharge) using empirical relations. Digital Elevation Models such as the SRTM DEM [*Farr et al.*, 2007] are used to estimate floodplain bathymetry and river bottom level or surface water slope. Model limitations can be due to the

simplifications on representing physical processes but also due to the deficiencies on the aforementioned input data. Consequently, model validations and investigations of the source of errors may guide the improvement of current models.

In this direction, additionally to *in situ* data commonly used for validation, remote sensing-derived hydrological datasets, such as river stages based on satellite altimetry measurements [*Alsdorf et al.*, 2007b; *Santos da Silva et al.*, 2010], inundation extent [*e.g. Hess et al.*, 2003; *Papa et al.*, 2010] or Terrestrial Water Storage (TWS) derived from the GRACE gravimetry from space mission [*Tapley et al.*, 2004], offer a new opportunity to compare and validate simulation outputs and improve these hydrological modelling approaches.

In this study, we present a hydrologic/hydrodynamic modelling of the Amazon River basin using the MGB-IPH hydrological model (*"Modelo de Grandes Bacias"*, *Collischonn et al.*, 2007) with a full river hydrodynamic module coupled with a simple floodplain storage model [*Paiva et al.*, 2011a] validated against remotely-sensed observations. We first present an extensive model validation based on comparisons between model outputs and i) *in situ* stream stages and discharges and also water levels derived from ENVISAT RA-2 satellite altimetry data from *Santos da Silva et al.* [2010]; ii) monthly inundation extent from a multisatellite product [*Papa et al.*, 2010]; and (iii) GRACE-based TWS from *Frappart et al.* [2010; 2011b]. Then, using the validation results and also sensitivity analyses, we determine the source of model errors in the Amazon, that may be extrapolated to other similar large-scale hydrological models Finally, the hydrological functioning of the Amazon River basin is explored using the model results, including aspects such as water balance, the surface, soil and ground water portioning and the role of river-floodplain hydraulics on stream flow routing.

2.2. Methods and datasets

2.2.1. The Hydrologic-Hydrodynamic Model

The MGB-IPH model is a large-scale distributed hydrological model that uses physical and conceptual equations to simulate land surface hydrological processes [*Collischonn et al.* 2007]. It uses a catchment-based discretization and the hydrological response units (HRUs) approach. The simulated vertical hydrological processes include soil

water budget using a bucket model, energy budget and evapotranspiration using Penman Monteith approach, interception and soil infiltration, surface runoff based on the variable contributing area concept and also subsurface and groundwater flow generation. The flow generated within the HRUs of each catchment is routed to the stream network using three linear reservoirs representing the groundwater, subsurface and surface flow. River flow routing is performed using a combination of either a Muskingum-Cunge (MC) method or a hydrodynamic model (HD).

The large-scale hydrodynamic model of MGB-IPH was developed by *Paiva et al.* [2011a] and applied to the Solimões River basin by *Paiva et al.* [2012]. This model differs from the MC model by its capacity to simulate flood inundation and backwater effects. The model solves the full 1-D *Saint-Venant* equations [*Cunge et al.*, 1980] for a river network using an implicit finite difference numeric scheme and a Gauss elimination procedure based on a modified skyline storage method. Flood inundation is simulated using a simple storage model [*Cunge et al.*, 1980], assuming that (i) the flow velocity parallel to the river direction is null on the floodplain, (ii) the floodplains act only as storage areas, (iii) the floodplain water level equals the water level at the main channel. Consequently, the river-floodplain lateral exchange equals $q_{fl} = (dz/dt)Afl(z)/dx$ where x and t are spatial and time dimensions and z is the river water level, and $Afl(z)$ is the flooded area inside a floodplain unit as described below. GIS-based algorithms are used to extract river and floodplain geometry parameters mainly from Digital Elevation Models (DEM) [*Paiva et al.*, 2011a]. Parameters from a rectangular-shaped river cross section are estimated using geomorphologic equations and the river bottom level is estimated from the DEM using corrections presented in *Paiva et al.* [2011a]. The algorithm delineates discrete "floodplain units" for each sub-reach and extracts a z vs Afl curve from the DEM for each of them. Corrections are applied on the DEM since SRTM signal does not penetrate vegetation or surface water and consequently does not provide ground elevation. Flood inundation results in terms of 2D water levels are computed based on 1D water level outputs and the DEM.

2.2.2. The Amazon River basin

The Amazon River basin (Fig. 1a) is known as the world's largest river basin. It has 6 million km^2 of surface area and drains ~15% of the total amount of fresh water dumped into oceans. This region exhibits high rainfall rates (average ~2200 mm.year^{-1}) with high spatial

variability [*Espinoza et al.*, 2009a]. Contrasting rainfall regimes are found in northern and southern parts of the basin, with the rainy season happening on June, July and August (on December, January and February) in the North (South) with more (less) defined wet and dry seasons occurring in the southern and eastern (northern and western) parts of the basin [*Espinoza et al.*, 2009a]. The Amazon basin is composed by three morphological units: the Andes with high altitudes and slopes, the Guyanese and Brazilian shields with moderate slopes and the Amazon plain with very low slopes. Extensive seasonally flooded areas are found at the Amazon plains [*Hess et al.*, 2003; *Papa et al.*, 2010]. Also, this region is characterized by complex river hydraulics, where the low river slopes cause backwater effects to control part of the river dynamics [*Meade*, 1991; *Paiva et al.*, 2012]. The abovementioned characteristics put together give rise to an interesting discharge regime. Rivers draining

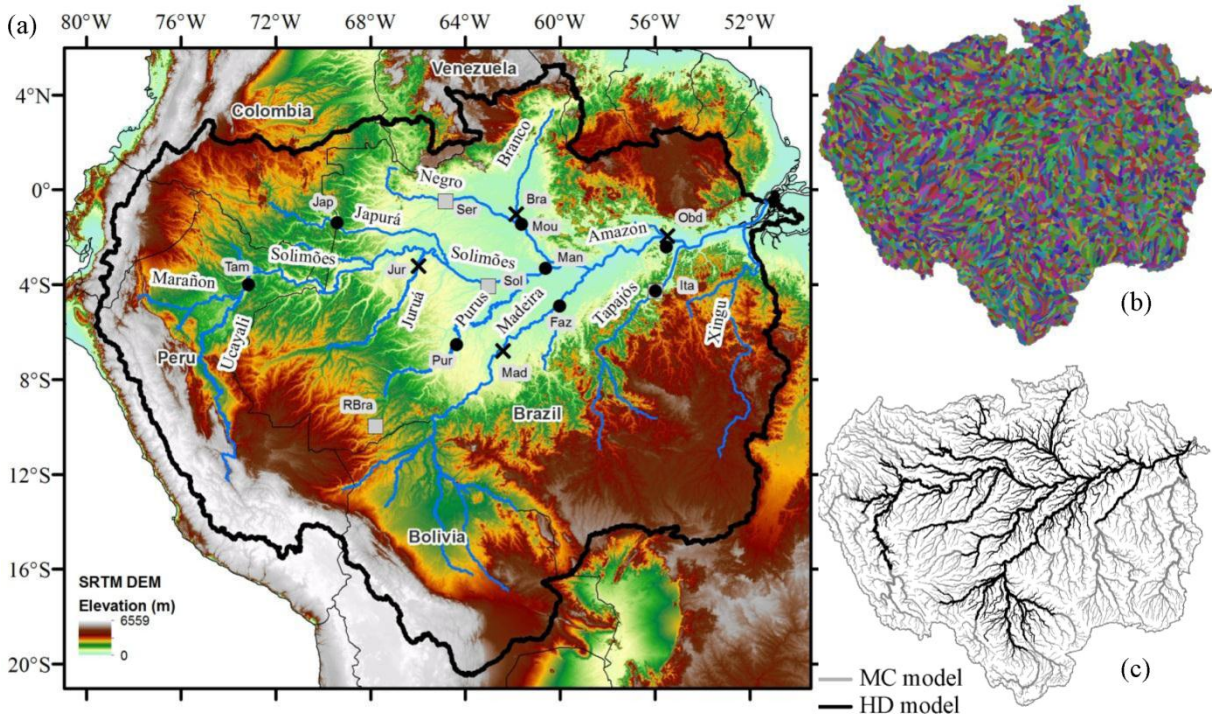

Figure 1. (a) Amazon River basin with its main tributaries, international limits, relief from SRTM DEM and some of the validation sites. Symbols for the location of the validation sites presented in Fig. 3 and 5 are as following: black circles for the gauge-based discharge series, grey rectangles for the gauge-based water level series, and black crosses for the altimetry-based water level series. Amazon River basin discretization into (b) catchments and (c) river reaches simulated using the Muskingum Cunge (MC) and hydrodynamic (HD) models.

southern areas have a maximum flow occurring from March to May and a minimum one from August to October [*Espinoza et al.*, 2009a]. In some other rivers a weaker seasonal regime can be found, in some cases due to rainfall characteristics and in others, such as the Solimões/Amazon main stem, due to the contribution of lagged hydrographs from northern

and southern areas. In the latter, high (low) water occurs generally from May to July (September to November).

2.2.3. Model discretization, parameter estimation and forcing data

The model discretization into river reaches, catchments, hydrodynamic computational cross sections and parameter estimation was carried out using the SRTM DEM [*Farr et al.*, 2007] with 15″ resolution (~ 500 m) (see Fig. 1a) and GIS based algorithms described in *Paiva et al.* [2011a]. The Amazon basin was discretized into 5763 catchments, ranging from 100 to 5000 km^2 (Fig. 1b).

An HRU map with 12 classes was developed using Brazilian and South American soil and vegetation maps [*RADAMBRASIL*, 1982; *Dijkshoorn et al.*, 2005; *Eva et al.*, 2002], and the Height Above the Nearest Drainage (HAND) terrain descriptor [*Rennó et al.*, 2008] to identify areas close to rivers where plant-groundwater interactions might take place.

To avoid excessive computing time, we used a combination of the Muskingum Cunge (MC) and hydrodynamic (HD) models (Fig. 1c). River reaches which were simulated with the HD model were selected using the following criteria: (i) river slope lower than 20cm.km^{-1}, based on *Ponce's* [1989] criteria for kinematic wave models and (ii) presence of large floodplains using DEM visual inspection. As a result, ~30% of the reaches were simulated using the HD model (Fig. 1c). River reaches were then discretized considering the distance between two computational cross sections $\Delta x = 10$ km, based on the criteria of the hydrodynamic model numerical scheme performance [*Castellarin et al.*, 2009; *Cunge et al.*, 1980; *Paiva et al.*, 2011a]. Temporal discretization for both HD and MC models were Δt = 3600 s, based on Courant criteria [*Cunge et al.*, 1980].

River geometry parameters, i.e. river width B [m] and maximum water depth H [m], were estimated as a function of the drainage area Ad [km^2], using geomorphologic equations developed from river cross sections surveys achieved at stream gauge locations provided by the Brazilian Water Resources Agency (ANA). We developed different sets of geomorphologic equations for six sub-basins within the Amazon defined by its major tributaries, as shown in Table 1 (also see Fig. 1a).

River bottom levels were estimated from the DEM using *Paiva et al.* [2011a] algorithms and $Hveg$ = 17 m (vegetation height) to eliminate DEM errors due to vegetation. Also, when using DEM to extract water level vs flooded area curves, all of its pixel values

(Z_{DEM}) were corrected using $Z^*_{DEM} = Z_{DEM} - Hveg$, except for areas with low vegetation, according to the HRU map.

Meteorological data were obtained from the CRU CL 2.0 dataset [*New et al.*, 2002], which provides monthly climatological values calculated using interpolated data from ground stations for the period between 1960 and 1990 at a spatial resolution of 10', which is in accordance with the low density of meteorological stations in the Amazon. We also used TRMM daily precipitation data provided by algorithm 3B42 [*Huffman et al.*, 2007], with a spatial resolution of $0.25^o \times 0.25^o$ for the 12-year period 1998–2009.

The MGB-IPH model parameters related to soil water budget were calibrated against discharge data from stream gauges using the MOCOM-UA optimization algorithm [*Yapo et al.*, 1998; *Collischonn et al.*, 2007] for the 1998-2005 time period, using the model performance statistics E_{NS}, E_{NSlog} and ΔV, described in the next section. For parameter calibration, model runs were used only within the MC model to avoid high computational costs and, therefore, we used only stream gauges located in river reaches simulated with the MC model (Fig. 1c). Gauges located in reaches simulated with the HD model were used only for validation. The calibration procedure optimized 6 parameters related to soil water budget for each HRU (the maximum water storage in the upper layer of soil *W*m; 3 equivalent hydraulic conductivities *K*bas, *K*int, *K*cap; the parameter from the variable contributing area model for runoff generation *b*), and 3 parameters related to surface, subsurface and base flow residence time (*C*s, *C*i and *TKB*), following *Collischonn et al.* [2007]. We optimized these parameters for each large river sub-basin, giving rise to tens of different parameter sets with the following median values and ranges (5% and 95% percentiles): *W*m = 282 (30-1800) mm, *b* = 0.48 (0.02-4.6), *K*bas = 1.2 (0.03-6.9) $mm.day^{-1}$, *K*int = 5.2 (0.2-200) $mm.day^{-1}$, *K*cap = 0.02 (0-0.26) $mm.day^{-1}$, *C*s = 12.4 (5.6-35.5), *C*i = 10.0 (3.9-1379), *TKB* = 99 (18-386) days. In some cases (~10%), calibrated parameters were out of these ranges, possibly due to input data errors (e.g. precipitation as discussed later) or even limitations in the model. Vegetation parameters used in energy balance and evapotranspiration computations (*e.g.* leaf area index, superficial resistance, albedo and vegetation height) were taken from *Shuttleworth* [1993]. The only parameter related to the hydrodynamic model is the Manning's coefficient and it was not calibrated using the MOCOM-UA algorithm. Instead, we used different values for different large river basins aiming at fitting hydrographs in the largest Amazonian rivers (0.035 in almost all the Amazon basin, 0.025 in the lower Madeira basin, 0.030 in the upper

Madeira, upper Solimões and upper Negro basins, 0.040 in upper part of Brazilian Solimões River).

Table 1. Geomorphologic equations developed to estimate river geometric parameters in computational cross sections: river width, *B* [m]; maximum water depth, *H* [m]; upstream drainage area *Ad* [km^2].

River Sub-Basin	River width [m]	Maximum water depth [m]	
Tapajós and Xingu	B=0.35.$Ad^{0.62}$	H=1.91.$Ad^{0.15}$	
Purus and Juruá	B=3.75.$Ad^{0.36}$	H=2.35.$Ad^{0.16}$	
Madeira	B=1.30.$Ad^{0.46}$	H=1.25.$Ad^{0.20}$	
Negro and Japurá	B=0.41.$Ad^{0.63}$	H=1.26.$Ad^{0.20}$	
Solimões	B=0.80.$Ad^{0.53}$	H=1.43.$Ad^{0.19}$	
Solimões/Amazon main stream	B=1.20.$Ad^{0.54}$	H=22	Ad < 400000 km^2
		H=20.86+2.86E-06.Ad	Ad < 2150000 km^2
		H=-1.04+1.30E-05.Ad	Ad > 2150000 km^2

2.2.4. Model validation approach

Discharge

Daily discharge results were compared with data from 111 stream gauges (Fig. 2) provided by the Brazilian Agency for Water Resources ANA ("*Agência Nacional das Águas*"), the Peruvian and Bolivian National Meteorology and Hydrology Services SENAMHI ("*Servicio Nacional de Meteorología e Hidrología*") and the Hydrology, Biogeochemistry and Geodynamic of the Amazon Basin (HYBAM) program (http://www.ore-hybam.org) for the 1999-2009 period. Values from the HYBAM database provided better discharge estimates in the central Amazon since it is based on both stages and water slope and, consequently, are able to represent looped rating curves.

Water level

Simulated daily water levels were validated against stream gauge records and radar altimetry data. We used 69 stream gauges for the 1998-2005 period, selected from ANA's database (see Fig. 5).

We also compared the computed water levels with ENVISAT satellite altimetry data. ENVISAT satellite has a 35-day repeat orbit and an 80 km inter-track distance. The database used is an extension of the one presented in *Santos da Silva et al.* [2010]. It consists of 212

altimetry stations (AS – deduced from the intersection of a satellite track with a water body) with water level time series reported to EGM08 geoid for the 2002-2009 period. Altimetry stations are located mainly along the Solimões, Amazon, Juruá, Japurá, Madeira, Negro and Branco Rivers (see Fig. 5). ENVISAT data selection techniques preconized by *Santos da Silva et al.* [2010] result in ~ 10 to 40 cm water level accuracy. Since water level model results are based on the SRTM DEM, it became necessary to convert ENVISAT water levels from their initial EGM08 geoidal reference to an EGM96 geoidal reference. We used the programs provided by the National Geospatial-Intelligence agency (http://earth-info.nga.mil/) to perform the conversion.

Flood Extent

Flood inundation results were compared to a multi-satellite monthly global inundation extent dataset at a ~25 x 25 km spatial resolution and available over the 1993 to 2004 period [*Papa et al.*, 2010]. This product was derived from multiple-satellite observations, including passive (Special Sensor Microwave Imager) and active (ERS scatterometer) microwaves along with visible and near-infrared imagery (advanced very high-resolution radiometer; AVHRR). This dataset was already used for validating other large-scale streamflow routing and flood models [e.g. *Decharme et al.*, 2011; *Yamazaki et al.*, 2011]. It is provided on an equal area grid of 0.25^{o}x0.25^{o} at the Equator where each pixel has 773km^2 of surface area. Considering this, for model validation, we computed daily water depth grids at a 15″ resolution (~500 m) based on simulated water levels and the DEM, as described in *Paiva et al.* [2011a], and then we resampled it into a ~25 x 25 km grid to compute monthly inundation extent only for the 1999-2004 time period.

Terrestrial water storage

The Gravity Recovery and Climate Experiment (GRACE) mission, launched in March 2002, provides measurements of the spatio-temporal changes in Earth's gravity field. Several recent studies have shown that GRACE data over the continents can be used to derive the monthly changes of the terrestrial water storage (TWS) [*Ramillien et al.*, 2005 and 2008; *Schmidt et al.*, 2008] with an accuracy of ~1.5 cm of equivalent water thickness when averaged over surfaces of thousands of square-kilometres. These TWS changes estimates over

land include all hydrological compartments, such as rivers, floodplains, lakes, soil and groundwater. We used the Level-2 land water solutions (RL04) produced by GFZ, JPL, and CSR with a spatial resolution of ~333 km, and an accuracy of 15-20 mm of water thickness. These are smoothed solutions using a 400 and 500 km halfwidth Gaussian filter and provided at $1x1^o$ and at a monthly time interval. They are also post-processed using an Independent Component Analysis (ICA) approach [*Frappart et al.*, 2010] which demonstrates a strong capacity for removing the north-south stripes polluting the GRACE solutions [*Frappart et al.*, 2011b].

To derive TWS estimates from the MGB-IPH model we used the following procedure. For each catchment, total water storage *S* (considering river, floodplain, surface, soil and ground waters) is related to precipitation (*P*), evapotranspiration (*ET*), river inflow (*I*) and outflow (*O*) by the continuity equation $dS/dt = (P - ET).A_d + I - O$, where A_d is the catchment drainage area and *t* is time. For each day, water storage was derived as $S_{t+1} = S_t + [(P_{t,t+1} - ET_{t,t+1}).A_d + I_{t,t+1} - O_{t,t+1}]\Delta t$ where Δt is the time interval, similarly as used by *Getirana et al.* [2011] at the basin scale for the Negro River basin.

Then, to derive model TWS estimates comparable with GRACE data, we smoothed MGB-IPH TWS values using a 450 km halfwidth Gaussian filter. Moreover, since the original GRACE spatial resolution is larger than 1^o x 1^o, we chose to resample both GRACE and MGB-IPH data to a 4^o x 4^o grid (Fig. 9). For each 4^o x 4^o pixel, TWS derived from GRACE was computed as a simple average of the 1^o x 1^o pixels and TWS from MGB-IPH model was estimated as the weighted mean of TWS of all catchments inside each 4^o x 4^o pixel, using catchment drainage area as weight. Finally, we computed TWS anomalies using the 2003-2009 long-term average.

Model performance statistics

MGB-IPH model results were compared to observations using some statistics commonly used in hydrological modelling studies: (i) Nash-Suttcliffe coefficient *ENS*; (ii) log-Nash-Suttcliffe coefficient *ENSlog* [*Collischonn et al.*, 2007], *i.e. ENS* computed using a logarithm transformation on discharge time series to focus on low flows; (iii) relative bias ΔV [%] or BIAS; and (iv) Pearson correlation coefficient *R.* A "delay index" *DI* [days] [*Paiva et al.*, 2012] was used to measure errors related to the time delay between simulated and observed hydrographs. It is computed using the cross correlation function $R_{xy}(m)$ from

simulated (x) and observed (y) time series, where DI equals the value of the time lag m where $R_{xy}(m)$ is at maximum. Positive (negative) DI values indicate delayed (advanced) simulated hydrographs. Furthermore, we measured the water level, the TWS and the flood extent amplitude error $A' = 100.(A_{calc}-A_{obs}) / A_{obs}$, where A_{calc} and A_{obs} are the simulated and observed amplitudes. The amplitude A of a given variable is defined here as the difference between its 95% and 5% percentiles. Due to differences in water levels datum reference and since GRACE actually measures TWS changes, for these variables all model performance statistics (except BIAS) were computed after removing the long-term average.

2.3 Model validation

2.3.1. Discharge

Validation against river discharges shows a good performance of the MGB-IPH model. According to Fig. 2, in 70% of the stream gauges the $ENS > 0.6$ and model represents mean discharge with accuracy, since volume errors $|\Delta V| < 15\%$ in 75% of the gauges. According to ENS and ΔV values (Fig. 2d), the model performs better in large rivers, although it is sufficiently good in the smaller ones ($ENS > \sim 0.5$ and $|\Delta V| < \sim 20\%$). The flood waves' timing is also well represented by the model and $DI < 5$ days in 70% of the stream gauges. DI values increase in large rivers and, for example, simulated flood wave is 5 to 15 days in advance in the Solimões/Amazon main stem. However, these values can be considered small if compared to the large flood traveling times of Amazon large rivers (a couple of months).

Most of the errors are concentrated in rivers draining westerly areas in Bolivia, Peru and Colombia, where the model underestimates discharges. However, these errors can compensate each other and provide feasible discharge results in downstream rivers. We speculate that such errors are a consequence of the poor quality of TRMM 3B42 rainfall datasets in these areas, which are poorly monitored and/or mountainous. This is supported by the sensitivity analysis of Section 2.4, which shows that errors in precipitation cause large changes in mean discharge and as well as in water depths and flood extent. Errors in satellite rainfall estimates over the Andean region of the Amazon were also shown by *Condom et al.* [2010] and by *Tian and Peters-Lidard* [2010] in a global map of uncertainties of satellite precipitation estimates.

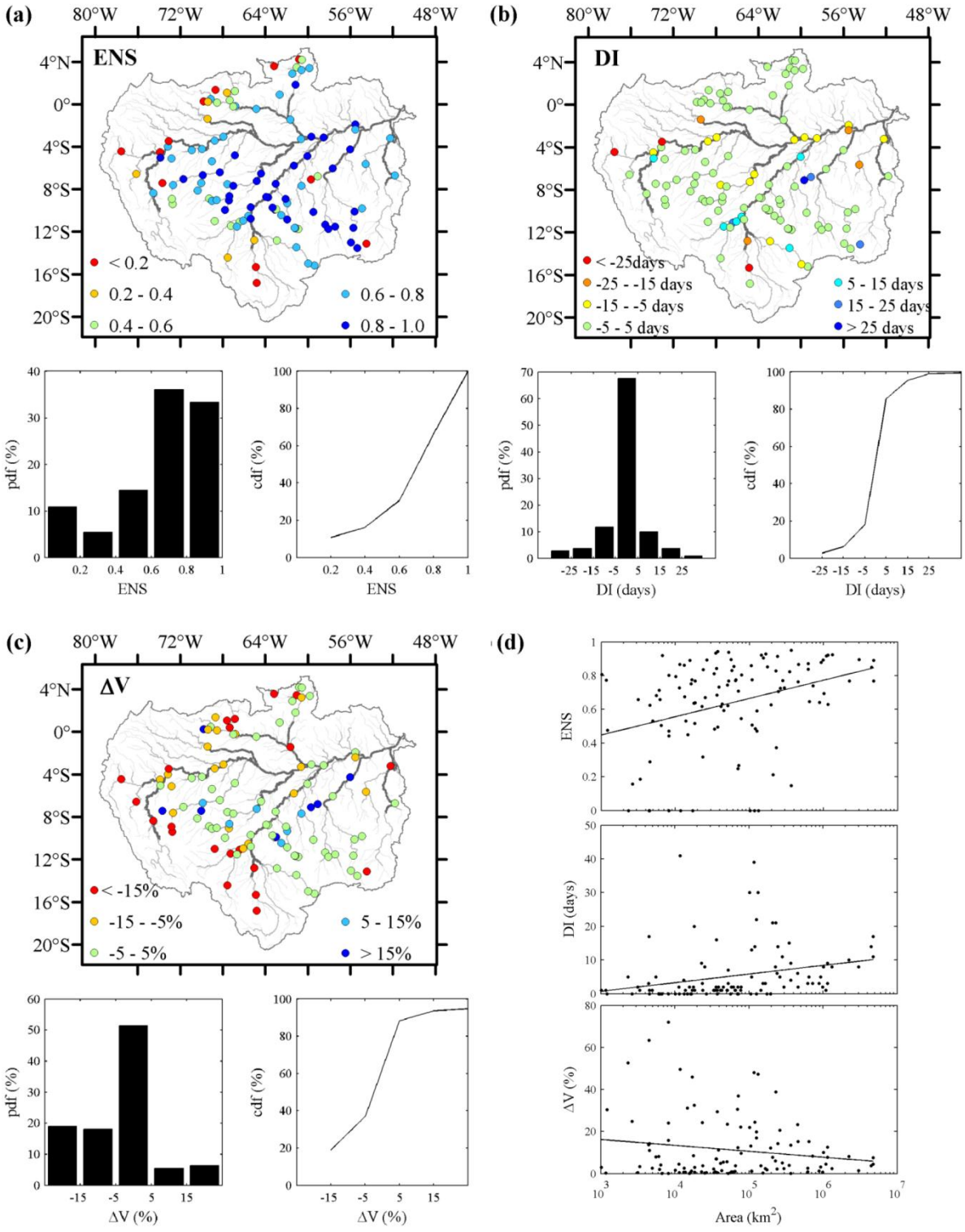

Figure 2. Validation of daily discharge derived from MGB-IPH model against stream gauge observations. Spatial distribution, probability (pdf) and cumulative (cdf) distribution functions of model performance statistics (a) Nash and Sutcliffe Index (*ENS*), (b) delay index (*DI*) and (c) volume error (ΔV) and (d) relation between upstream drainage area and model performance statistics.

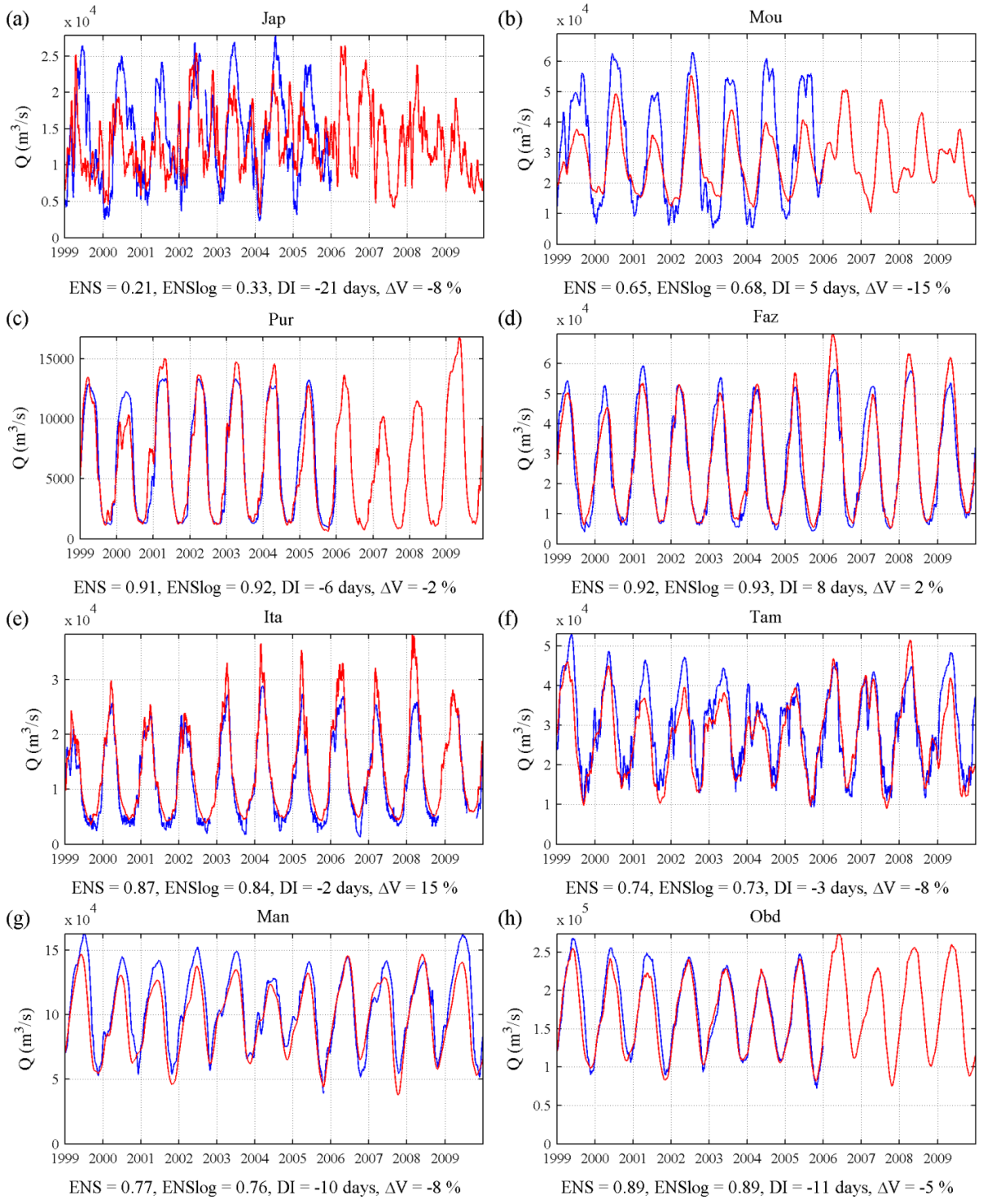

Figure 3. Observed (blue line) and simulated (red line) daily discharge in (a) Japurá River (Jap), (b) lower Negro River at Moura (Mou), (c) lower Purus River (Pur), (d) lower Madeira River at Fazenda Vista Alegre (Faz), (e) lower Tapajós River at Itaituba (Ita), (f) Solimões River at Tamshiyacu (Tam), (g) Solimões River close to confluence with Negro at Manacapuru (Man), and (h) Amazon River at Obidos (Obd). Sites are indicated in Fig. 1.

Results for the main Amazon tributaries are promising (Fig. 3). A very good model performance can be found in Juruá and Purus River basins, where the model is able to

represent complex (noisy) hydrographs in the upper part and flood waves attenuations as they travel downstream (see Fig. 3c for lower Purus). For the Madeira River basin, errors are found mostly in the Bolivian region (Fig. 2), but in most of Brazilian tributaries and in the Madeira main stem the discharge is well represented (Fig. 3d). Satisfactory model results are also found at Tapajós River basin (Fig. 3e), where hydrographs are mostly dominated by direct runoff and base flow, since large floodplains are not present (see Fig. 7). At Japurá River, which drains parts of the Andes of Colombia and Peru, the model results are poor, as shown in Fig. 3a. At Negro River basin, better results are found mostly in the Branco River basin (northeast) and worst results in the upper Negro River (northwest), but it shows improvement in lower Negro River.

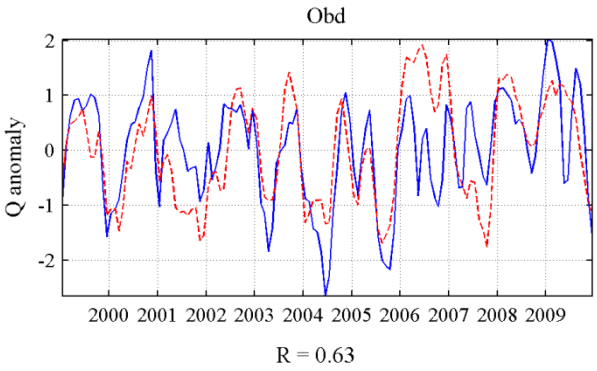

Figure 4. Observed (blue line) and simulated (red line) anomalies of monthly discharges in the Amazon River at Obidos (Obd).

Although there are large errors in the upper part of the Solimões river basin in Peru, flood waves are well represented in the Solimões/Amazon main stem, as shown in Fig. 3f and 3g at Tamshiyacu and Manacapuru, respectively. At Óbidos site, located close to the Amazon River outlet, results (Fig. 3h) show a good performance of the MGB-IPH model. *ENS* is high (0.89), the volume error is low (-4.6%) and flood wave is advanced in only -11 days. Hydrological extremes such as the 2005 drought and the 2009 flood are well represented (Fig. 3h) and the model captured inter-annual variability (Fig. 4).

2.3.2. Water levels

Validation against water levels from stream gauges shows that the model is performing well in the major tributaries of the Amazon (Fig. 5). $ENS > 0.60$ in 55% of the stream gauges and $R > 0.8$ in 80% of the cases. Water level results are similar to the

observations in large rivers, such as in the Solimões River (Fig. 6a) and also in smaller rivers where fast flood waves are present, such as in the Acre River in the upper Purus basin (Fig. 6b). Timing of flood waves are well represented in most gauges (*DI* < 5 days in 80% of the cases). Validation against ENVISAT satellite altimetry data also shows that the model performs well, mostly in central Amazon, Solimões, Juruá (Fig. 6d), Branco (Fig. 6e) and Madeira River and *ENS* > 0.6 in 60% of the virtual stations.

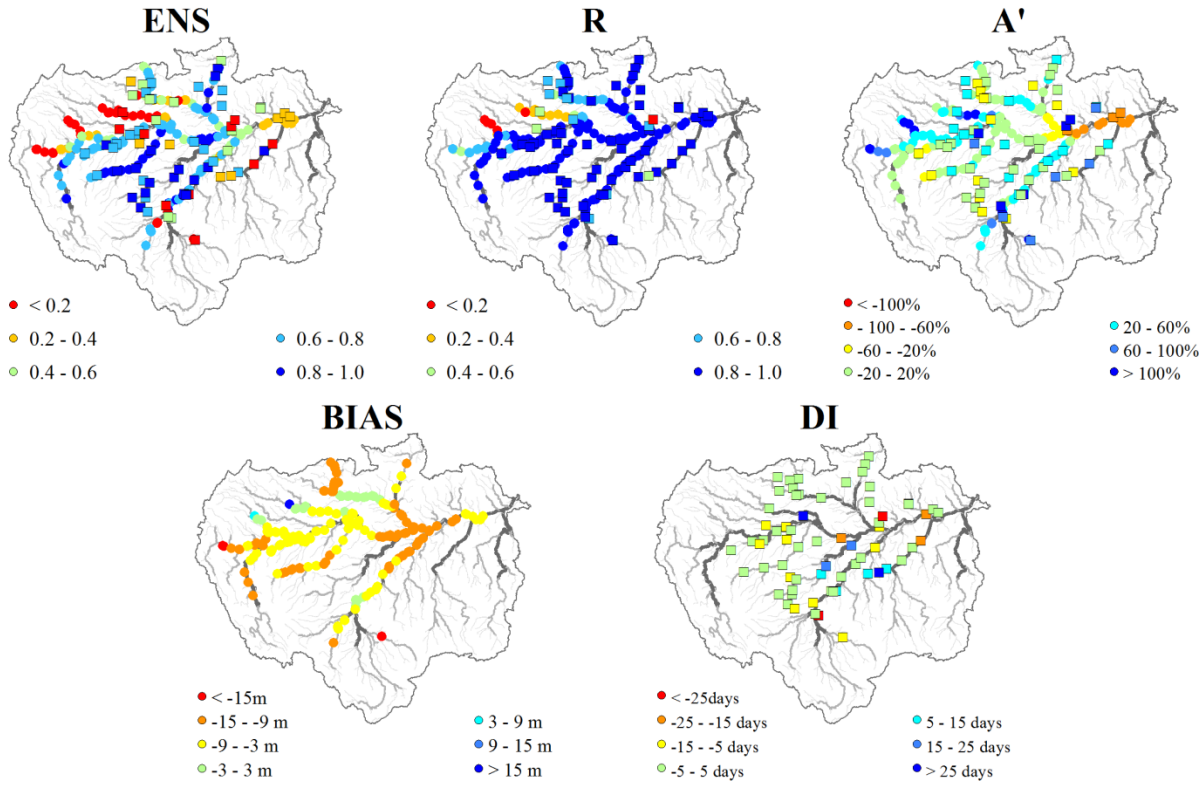

Figure 5. Validation of daily water levels derived from MGB-IPH model against stream gauge observations (squares) and ENVISAT satellite altimetry data (circles). Spatial distribution of model performance statistics Nash and Sutcliffe Index (*ENS*), Pearson correlation coefficient (*R*), amplitude error (*A'*), delay index (*DI*) and bias (*BIAS*).

However, large errors are found in some sites. A part of them is located in rivers draining poorly monitored and/or mountainous areas where discharges are also poorly simulated (see Section 2.3.1). In some of the stream gauges, despite the fact that the observed and simulated water levels are highly correlated and *DI* values are low, large amplitude errors are present, which indicates that model errors are due to the uncertainty of local cross section geometry, *e.g.* river width. In other sites located mainly close to a confluence with a large river (*e.g.* lower Tapajós River in Fig. 6c), there are large errors of timing and shape of flood waves, probably because either simulated or observed water levels are controlled by both

upstream flow and backwater effects. In this case, errors in river bottom level estimates could give rise to errors in the extension of backwater effects and in the timing of flood waves (similar to *Paiva et al.,* 2012). We also found a large bias between model and ENVISAT water levels, ranging from -3 to -15 m (Fig. 5). Smaller bias values were found by *Yamazaki et al*. [2012b] in the Amazon main stem, and differences may be associated to different methods for extracting errors from the DEM. In addition, important errors are found in lower Amazon River (Fig. 5 and 6f). The correlation with the observations is very high but the model strongly underestimates the amplitude of water levels. Such errors could be due to errors in river width estimates and also due to DEM, and therefore floodplain geometry errors, which cause errors in flood extent and consequently in river-floodplain volume exchanges, as supported by the sensitivity analysis presented in Section 2.4.

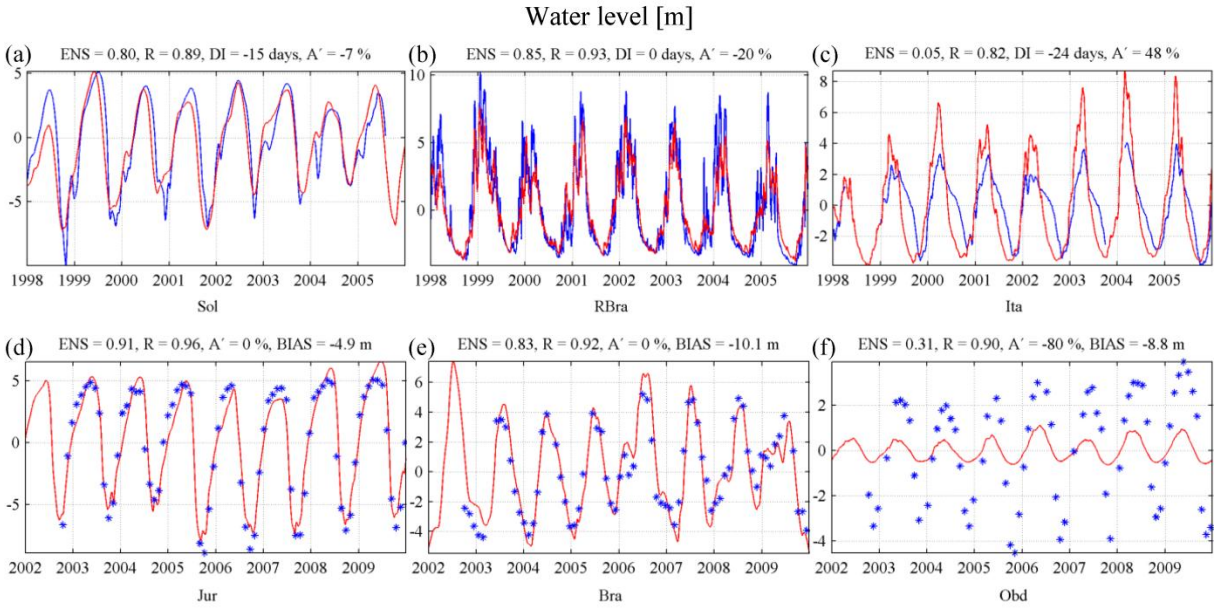

Figure 6. Simulated (red line) and observed daily water levels from stream gauges (blue line) and derived from ENVISAT satellite altimetry data (blue points) at (a) Solimões River (Sol), (b) upper Purus River basin at Acre River in Rio Branco (RBra), (c) lower Tapajós River at Itaituba (Ita), (d) lower Juruá River (Jur) (e) lower Branco River (Bra), (f) Amazon River at Óbidos (Obd). Sites are indicated in Fig. 1.

2.3.3. Flood extent

The overall inundation extent results from the MGB-IPH model are similar to remote sensing estimates from *Papa et al.* [2010] showing the seasonal variation of flood extent and the north-south contrast, with flood peaks occurring in DJF and MAM at the Bolivian Amazon, in MAM and JJA at central Amazon and JJA in the north (Fig. 7).

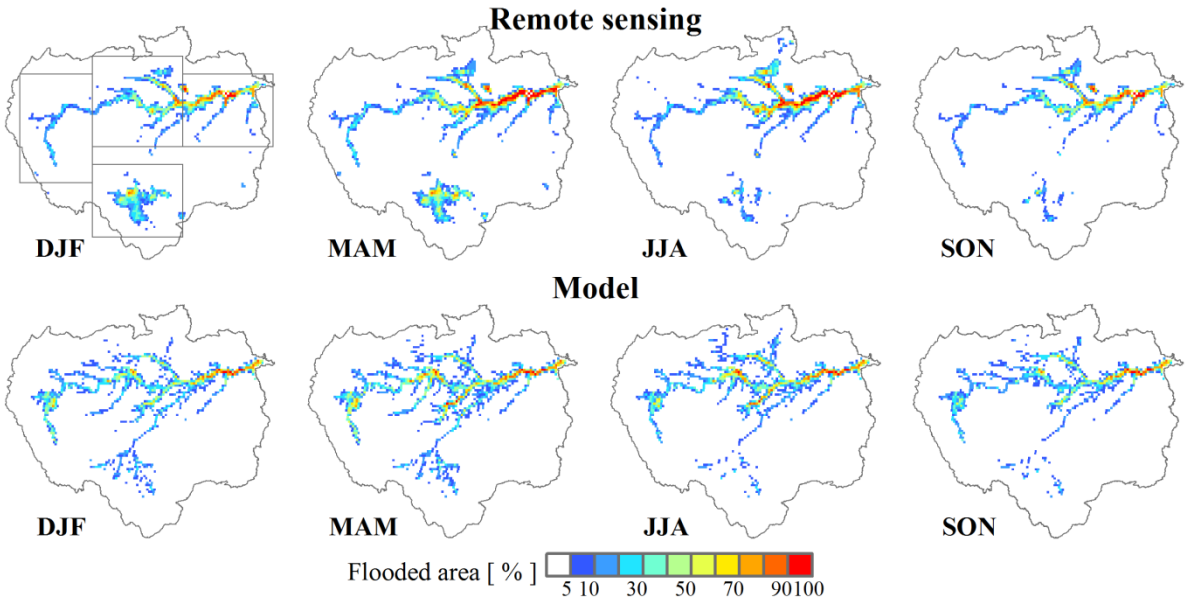

Figure 7. Seasonal variation of inundation extent derived from MGB-IPH model and remote sensing estimates from *Papa et al.* [2010]. Average values for DJF, MAM, JJA and SON seasons were computed for the 1999 to 2004 period.

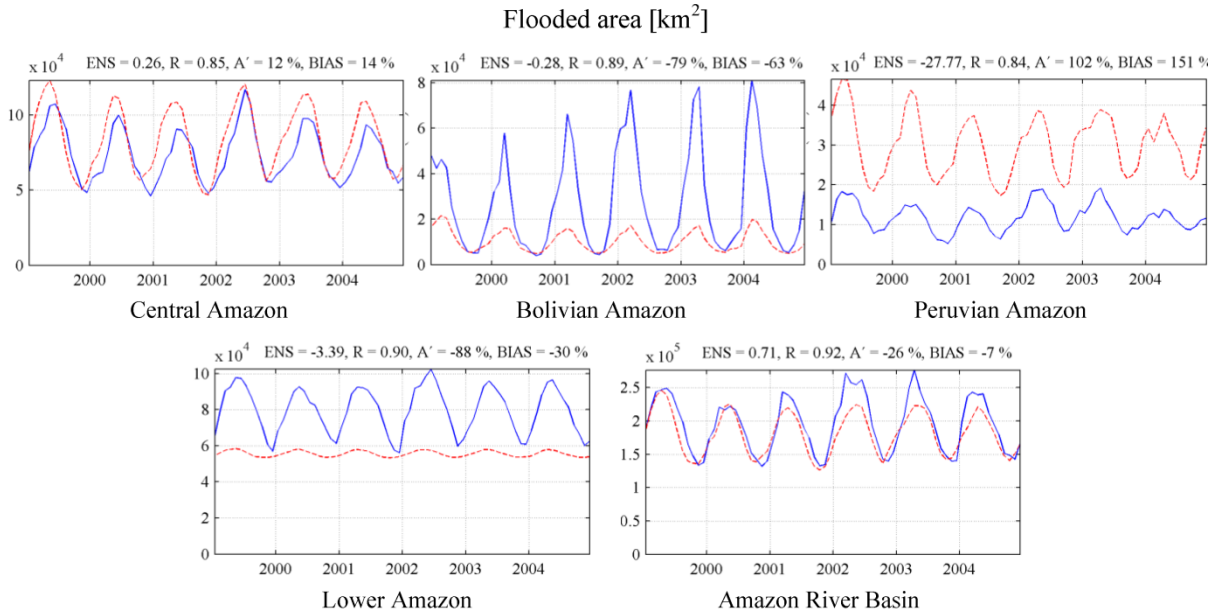

Figure 8. Monthly flooded area derived from MGB-IPH model (red dashed line) and remote sensing estimates from *Papa et al.* [2010] (blue line) at central Amazon (8°S 70°W to 2°N 60°W), Bolivian Amazon (18°S 70°W to 10°S 60°W), Peruvian Amazon (12°S 78°W to 0°S 70°W), lower Amazon (8°S 60°W to 0°S 50°W), and Amazon River basin. Regions are presented in Fig. 7.

The model provides total inundation extent similar to remote sensing estimates (Fig. 8) for the whole Amazon basin, with relatively good model performance statistics: *ENS* = 0.71, *R* = 0.92, *A'* = -26 % and *BIAS* = -7 %. However, analyses in different regions (rectangles in Fig. 7) show that errors are compensated when generating the overall estimate.

The best model results are found in central Amazon (Fig. 8), where a relatively low amplitude error (12%), bias (14%) and high correlation coefficient (0.85) are found. In the Peruvian Amazon (Fig. 8c) the model overestimates flood extent although the seasonal variation is well represented, while in the Bolivian Amazon (Fig. 8b), low water period and seasonal variation are well captured by the model, but flood at high water period is underestimated (DJF and MAM). In lower Amazon (Fig. 8d), bias is only -30 % and the seasonal variation is well represented (R = 0.90). However, the model underestimates the amplitude and flood at the high water period, leading to a low *ENS* value. This is in accordance with errors in water levels presented in Section 2.3.2.

It is noteworthy that a part of the errors could come from the remote sensing observations. A previous and similar dataset [*Prigent et al.*, 2007] seems to overestimate flood extent in the lower Amazon and underestimate it in the Solimões floodplain (central Amazon) if compared to *Hess et al.* [2003] dual season estimates for 1996 high water and 1995 low water periods.

Errors in flood extent may be due to uncertainty in river-floodplain geometry parameters, as presented in Section 2.4. For example, important errors are found in water levels and inundation extent in the lower Amazon River. In both cases, model results are highly correlated with observations, but the model underestimated the amplitude of water levels and flooded area. We speculate that the errors in lower Amazon River are due to river width errors and due to DEM errors. We used a coarser version of SRTM DEM with a ~500 m resolution instead of the ~90m, while floodplain flows can be partly controlled by smaller scale topography such as small channels [*Trigg et al*., 2012]. Besides, the SRTM DEM has systematic errors related to vegetation and surface water effects [*Sun et al.*, 2003]. We corrected these errors using methods presented in *Paiva et al.* [2011a] for river bottom level estimation and subtracting a constant value of *Hveg*=17 m in all DEM pixels, except where there is low vegetation. However, vegetation height may be variable even in forested areas. For example, in lower Amazon, large marginal lakes are present in floodplain [*e.g. Melack and Hess*, 2010; *Bonnet et al.*, 2008] and due to the correction applied in DEM, they are always flooded in the model simulation. Furthermore, a small water level variation leads to less river-floodplain volume exchanges.

2.3.4. Terrestrial water storage

Analyses show that the model provides TWS in good accordance with GRACE estimates. *ENS* values for TWS over the whole Amazon is 0.93, the correlation coefficient is high (0.97) and the amplitude error is low (12%). Fig. 9d shows that interannual variability is represented by the model, including the 2005 drought and the 2009 flood.

We also examined results in 21 square sub-regions with spatial resolution of 4° x 4°. *ENS* < 0.8 and *R* < 0.9 only in 5 areas, and these are found mostly in the northwest part of the Amazon and in upper Branco River basin, possibly due to the same errors reported in discharge results related to the precipitation forcing. Also, these areas are concentrated in the border of the river basin, where the Gaussian filter applied to the model results may have added errors. In other parts of the Amazon, results were provided in accordance with GRACE estimates (*e.g.* Fig. 9b and 9c). Amplitude errors are larger than 20% only in 5 sub-regions, located in west, but also in lower Amazon River. In the latter, errors are in accordance with the underestimation of water level and flood extent amplitude presented in Sections 2.3.2 and 2.3.3.

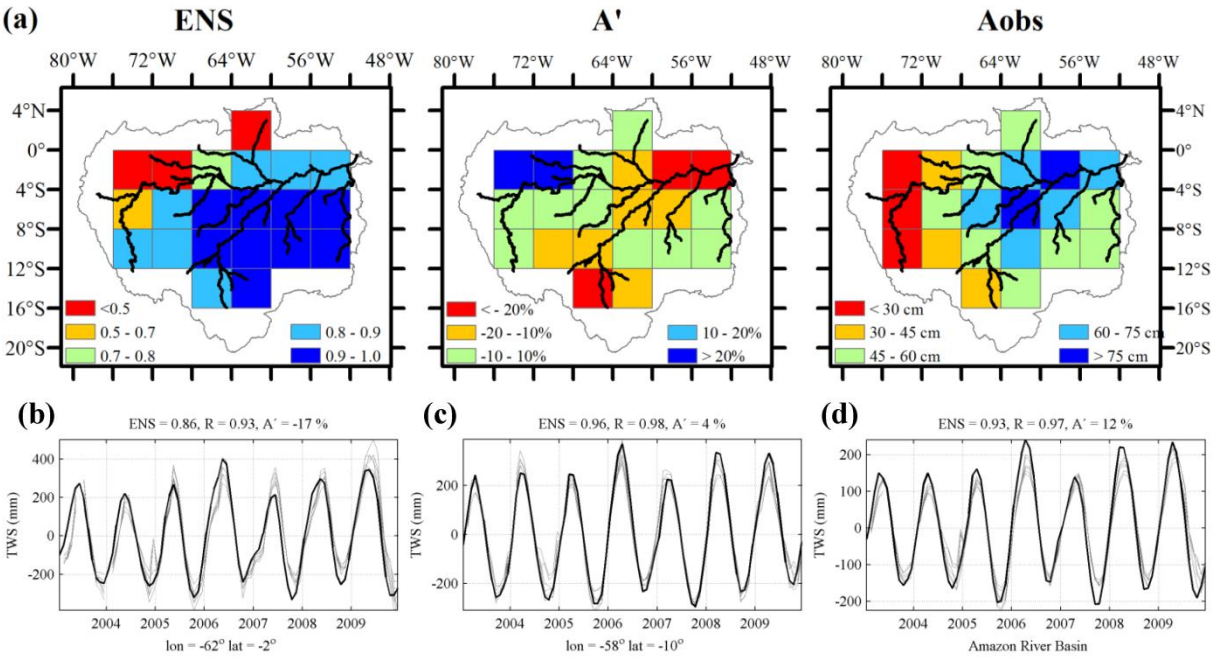

Figure 9. Validation of monthly Terrestrial Water Storage (TWS) derived from MGB-IPH model against GRACE estimates (2003-2009). (a) Spatial distribution of Nash and Sutcliffe Index (*ENS*), amplitude error (*A'*), observed amplitude (*Aobs*). Monthly time series of TWS derived from MGB-IPH model (black) and 6 GRACE solutions (grey) in (b) Lower Negro River Basin (4°x4° pixel centered in 62°W, 2°S),(c) Upper Tapajós River Basin (58°W, 10°S) and (d) Amazon River Basin. Statistics are presented for CSR solution with 400 km Gaussian filter.

2.4. Sensitivity analysis

We performed a sensitivity analysis to investigate the sources of model errors and also the physical functioning of the Amazon River basin. The model sensitivity to six model parameters/variables was evaluated: river width, manning's roughness coefficient, river bottom level, precipitation, flooded area and maximum soil storage. In all cases, each parameter/variable was equally perturbed in all Amazon river basin by the factors +50, +20, 0, -20 and -50%, except for river bottom level where we used +3,+1,0,-1,-3 m. Results were evaluated in terms of discharge close to the basin outlet at Óbidos station (Obd site at Fig. 1), water depth at central Amazon at Manacapuru station (Man site at Fig. 1) and total flooded area (Fig. 10 and 11) using climatological values computed from the 1999 to 2009 time period.

An important interaction between water levels, flooded areas and discharge occurs during flood waves traveling (Fig. 10). A decrease in river width causes a large increase in water depths and levels, consequently an increase of flooded areas occurs and flood waves are attenuated and delayed in a couple of months, causing minor flood flows and droughts, although the mean discharge does not change. Still, an increase in river width decreases water depth and flood inundation, resulting in advanced flood waves and major high water discharges. An explanation would be that larger amounts of water are stored and released across the floodplains, causing larger flow travel times. An inverse effect is observed perturbing manning's roughness coefficient. River width and manning coefficient results are similar to those discussed by *Yamazaki et al.* [2011] about river and floodplain interactions and flood wave travel times.

Increasing river bottom levels causes, at first, a smaller difference between river and floodplain bottom levels and as a result, flooding is easier to occur. Consequently, flood extension increases and the aforementioned effect takes place with a delayed flood wave. However, now water depth decreases possibly because larger amounts of water enter in floodplains.

Precipitation is the most sensitive variable (Fig. 10) and increasing it dramatically increases mean discharge, water depths and flood extent. Also, the same river-floodplain interaction takes place and flood waves are delayed and attenuated, although changes in mean values are much more pronounced.

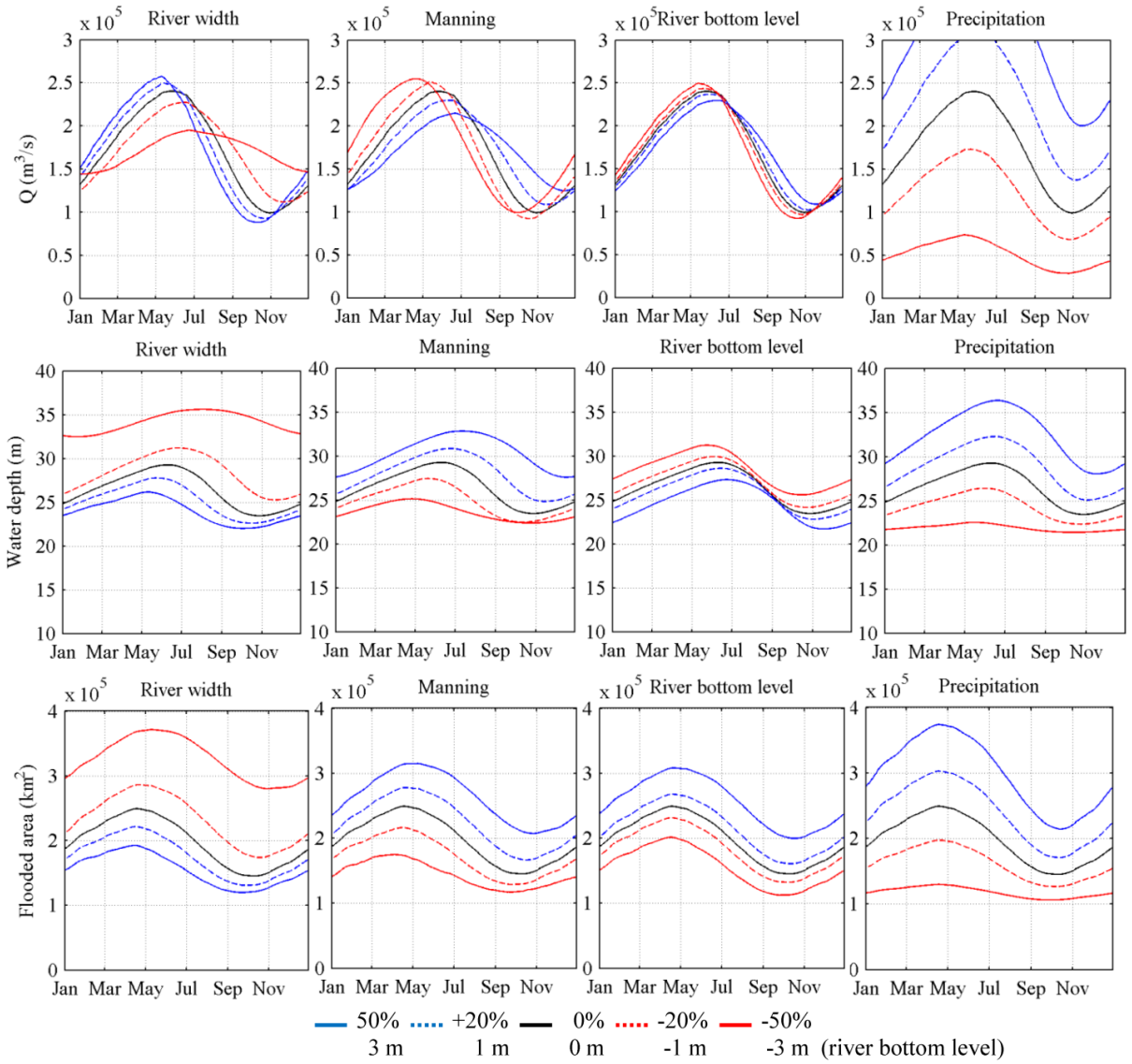

Figure 10. Sensitivity analysis: Climatology of discharge at Óbidos (Obd), water depth at Manacapuru (Man) and total flooded area derived from simulations using perturbed values of river width, manning coefficient, river bottom level and precipitation.

Positive changes in flooded areas (from the *z vs Afl* curve derived from the SRTM DEM) cause a similar effect than that observed in the river bottom level, with a decrease in water depths and delayed and attenuated flood waves (Fig. 11). Finally, we examined maximum soil water storage (Fig. 11), the most sensitive parameter of vertical water/energy balance of the MGB-IPH model [*Collischonn*, 2001]. Positive perturbations decrease all variables, probably because larger amounts of available water in the soil facilitate larger evapotranspiration rates. However, the sensibility of this parameter is not as pronounced as the others.

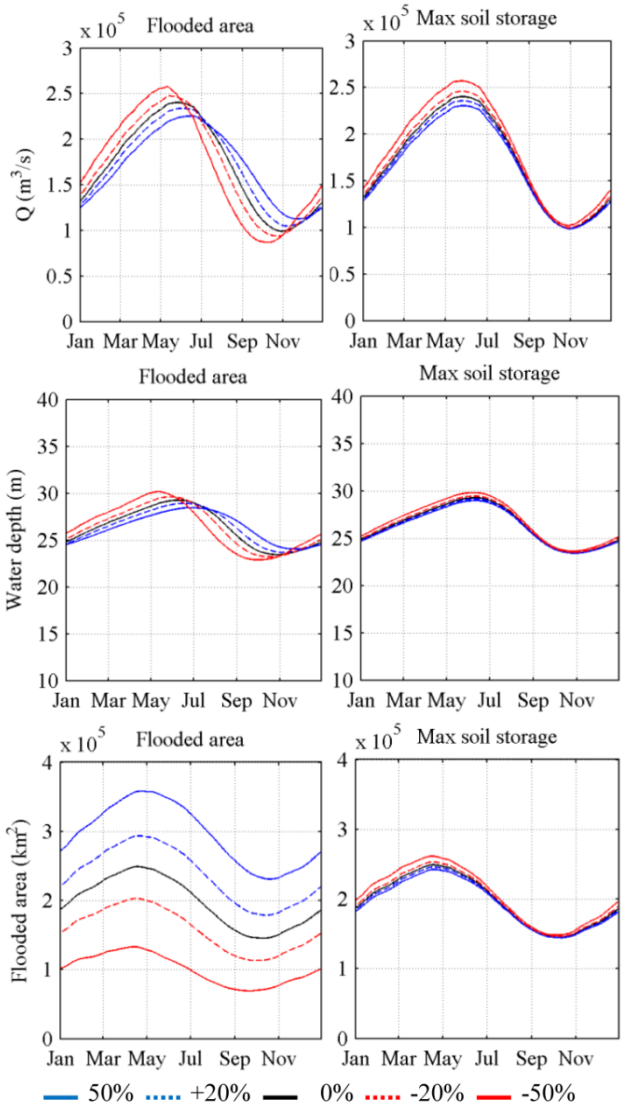

Figure 11. Sensitivity analysis: Climatology of discharge at Óbidos (Obd), water depth at Manacapuru (Man) and total flooded area derived from simulations using perturbed values of flooded area and maximum soil storage.

It is worth mentioning that we evaluated errors equally distributed over the entire basin, and that local uncertainties can cause different kinds of errors in discharges, water depths and flood extent. For example, errors in river width in a small reach may cause errors in both the mean and amplitude of water depths, and consequently in local flood extent, but may not have a major influence over other parts of the basin.

The analysis shows that input data uncertainty might play an important role in model errors. The model results are very sensitive to river – floodplain parameters, indicating the need to improve current estimation methods, which are based mostly in geomorphological relations and information from the SRTM DEM. These conclusions are consistent with

recommendations from other modelling studies using global river-flood models [*Decharme et al.*, 2011; *Yamazaki et al.*, 2011] and a flood inundation model [*Wilson et al.*, 2007]. Data from field campaigns could be used, but also methods using remote sensing to estimate river width and bottom level should be investigated, such as in *Durand et al.* [2010a]. Also, either a new DEM or a more sophisticated correction of the SRTM DEM is needed, removing vegetation height in forested areas and estimating bottom level of floodplain lakes. Vegetation effects could be removed, for example, using a global vegetation height map, such as in *Simard et al.* [2011]. Water level effects could be removed using a combination of satellite altimetry water levels and flood extent data, such as the techniques used by *Frappart et al.* [2008; 2011a] to estimate floodplain volumes variation. DEM corrections to allow better flow connectivity in small channels connecting floodplains such as presented by *Yamazaki et al.* [2012] could also be used. Additionally, data from the future Surface Water and Ocean Topography (SWOT) mission could also be employed [*Durand et al.*, 2010b].

2.5. Aspects of Amazon hydrological processes

2.5.1. Water balance

Fig. 12 presents the main components of water balance of the Amazon basin, comprising mean precipitation (*P*), evapotranspiration (*ET*) and discharge (*Q*) at Óbidos station rates derived from model results. Mean annual rates for the 1998-2009 period are $P = 5.65$ mm.day^{-1}, $ET = 2.72$ mm.day^{-1} and $Q = 3.09$ mm.day^{-1}. As discussed in Section 2.3.1., simulated discharge is similar to observations at Óbidos station, with a small bias equal to -4.6%. Mean precipitation, which is based on TRMM 3B42 v6 data, is slightly smaller (~6%) than values obtained in others: 6.0 mm.day^{-1} from *Espinoza et al.* [2009] based on 756 pluviometric stations; 6.3 mm.day^{-1} from *Azarderakhsh et al.* [2011] based on GPCP remote sensing data; 5.8 (5.2 – 8.6) mm.day^{-1} by *Marengo et al.* [2005] based on several rain gauges, remote sensing and reanalyses-based data. *ET* rates are also comparable with values obtained in other studies, although there are large differences between them: 2.27 mm.day^{-1} by *Azarderakhsh et al.* [2011] using global remote sensing-based products; 4.3 mm.day^{-1} by *Marengo et al.* [2005]; 3.23 mm.day^{-1} by *Ruhoff* [2011] using MOD16 remote sensing product but including the Tocantins basin; 3.2 mm.day^{-1} (at Negro basin), 2.9-3.8 mm.day^{-1}

and 2.6-3.0 mm.day^{-1} using modeling results by *Getirana et al.* [2010], *Costa and Foley* [1997] and *Beighley et al.*, [2009], respectively.

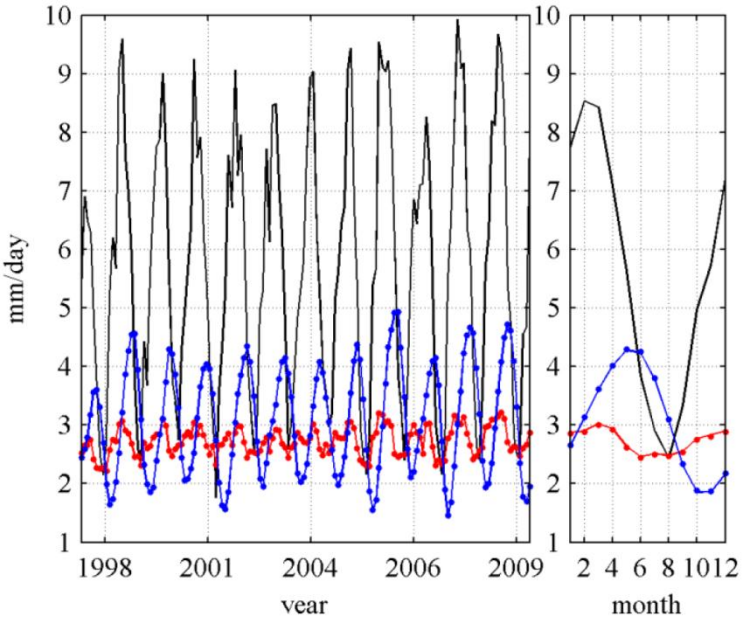

Figure 12. Water balance of the Amazon River basin. Monthly (left) and climatological (right) values of mean precipitation (black), evapotranspiration (red) and discharge close to the outlet at Óbidos (blue). Continuous lines (points) show simulation results (not) considering the influence of flood extent variability on evapotranspiration.

P exhibits a large seasonal variation, with larger rates (*P*>7mm.day^{-1}) between December and April with the maximum at February and March (P~8.5mm.day^{-1}) and minimum values at July and August (P~2.5mm.day^{-1}). The mean Amazon *ET* is almost constant along the year, without significant seasonal variations. The combination of *P* and *ET* rates causes a marked seasonal behaviour in discharge, with maximum (minimum) values of 4.3 (1.9) mm.day^{-1}, occurring in May-June (October-November). Discharge signal is delayed in 3 months if compared with *P*, showing the large water travel times along the Amazon rivers and floodplains.

Although the seasonally inundated floodplains play an important role in water transport throughout the Amazonian rivers, as demonstrated by the sensitivity analysis and by the results shown in next section, it seems not to have a major influence in water balance. Fig. 12 show a comparison of *Q* and *ET* results from two simulations, one considering the effect of seasonal flooded areas on *ET* (using methods described in *Paiva et al*., 2011a) and the other without such consideration, and the differences between them are insignificant. Although this is a preliminary analysis, and since *ET* from flooded forests is not completely represented

using the Penman Monteith approach, a possible explanation could be that (i) flooded areas represent a small part (less than 5%) of the total area of the Amazon and that (ii) *ET* in the Amazon is driven mostly by radiation [*Costa et al*., 2010] and not by water availability and consequently *ET* rates from flooded and nonflooded forests are similar.

2.5.2. Terrestrial water storage

In this section, the Amazon terrestrial water storage changes and the role of surface, soil and ground waters on TWS are explored. Analyses of Fig. 9 based on GRACE data show a marked seasonal variability of terrestrial water storage with large amplitude of variation (325 mm, mean of all GRACE solutions). Larger TWS variations are found mostly in central Amazon, with amplitudes of TWS larger than 750 mm, and smaller values are found in the Andean region (< 300 mm). To evaluate the main contributors of the TWS variations, we computed the water storage of three major hydrological compartments using model results, namely surface water (sum of river, floodplain and surface runoff storages), soil water and ground water and calculated the respective amplitude of variation as described in Section 2.2. The amplitude of variation of surface waters governs most of TWS changes in the Amazon basin (see Fig. 13), mostly in central Amazon and areas with large floodplains (see Fig. 7 and 13a). Soil water presents an important contribution on TWS changes in south-eastern areas; whilst ground water is the least important compartment in almost all regions. Surface waters dominate TWS variations for the whole Amazon area with a fraction of 56%, followed by soil (36%) and ground water storages (8%) (see Fig. 13b). Also, surface and soil water present similar seasonal variation, while groundwater storage presents a small delay. Results agree with *Han et al.* [2009] and *Frappart et al.* [2008], which indicated the dominant role of surface waters in TWS variations in the Amazon. The results also agree with *Frappart et al.* [2011a] that, using mostly remotely sensed datasets at the Negro river basin, showed that TWS changes are dominated by surface waters followed by soil and ground water with similar importance. Our results are also similar with *Kim et al.* [2009] estimates for the Amazon in a global study using modelling results, where river storage including shallow ground water (soil moisture) explained 73% (27%) of total TWS changes.

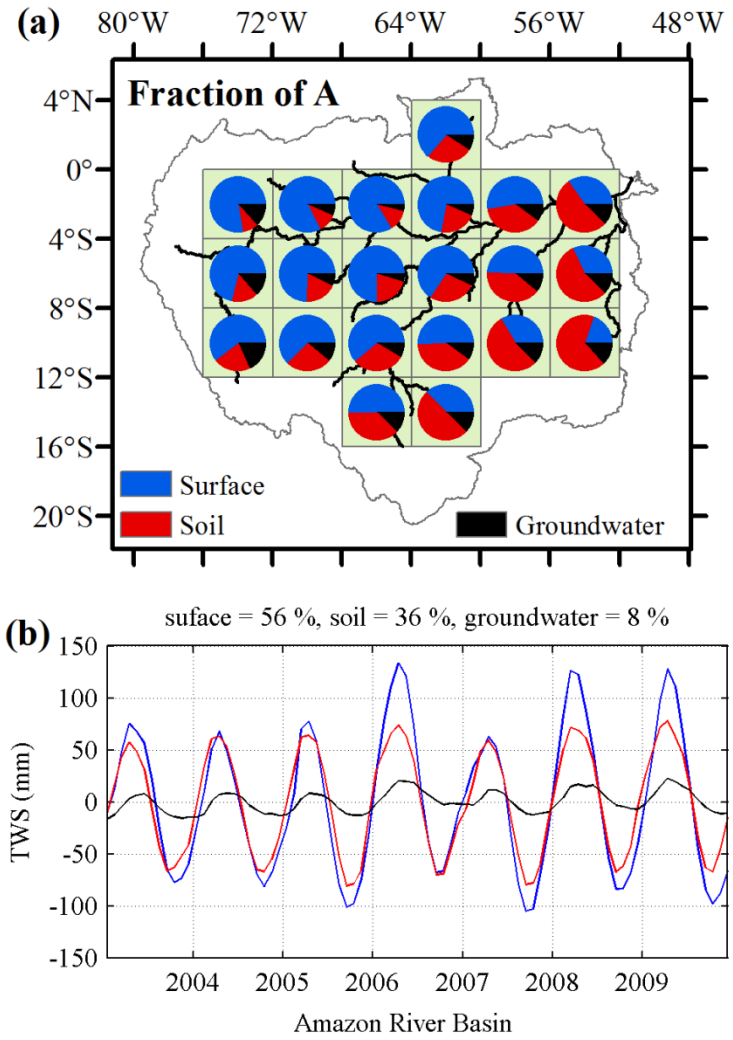

Figure 13. Fraction of terrestrial water storage divided into surface, soil and ground waters. (a) Spatial distribution of the fraction of TWS amplitude from each hydrological compartment. (b) Monthly time series of TWS from surface (blue), soil (red) and ground (black) waters.

2.5.3. River - floodplain hydraulics

To finish our analyses of the Amazon hydrological processes, river and floodplain processes are investigated and the importance of backwater effects and flood inundation in stream flow routing is evaluated. We compared discharge results from four model runs using the same parameters and model input forcings in all of them, but with different kinds of stream flow routing methods: (i) HDf - hydrodynamic model with floodplains, equal to model configuration used in the rest of the manuscript; (ii) MCf – Munskingum Cunge Todini with floodplains, using a nonlinear version of the Muskingum Cunge as presented by *Todini* [2007] and extended by *Pontes* [2011] to consider floodplains; (iii) HDn – hydrodynamic model without floodplains; (iv) MCn - Muskingum Cunge without floodplains. The Muskingum

Cunge based models, MCf and MCn, do not deal with backwater effects, since they are based on a kinematic wave approximation of the *Saint Venant* equations and do not consider neither the inertia nor the pressure forces, while HDn and MCn models do not represent flood inundation.

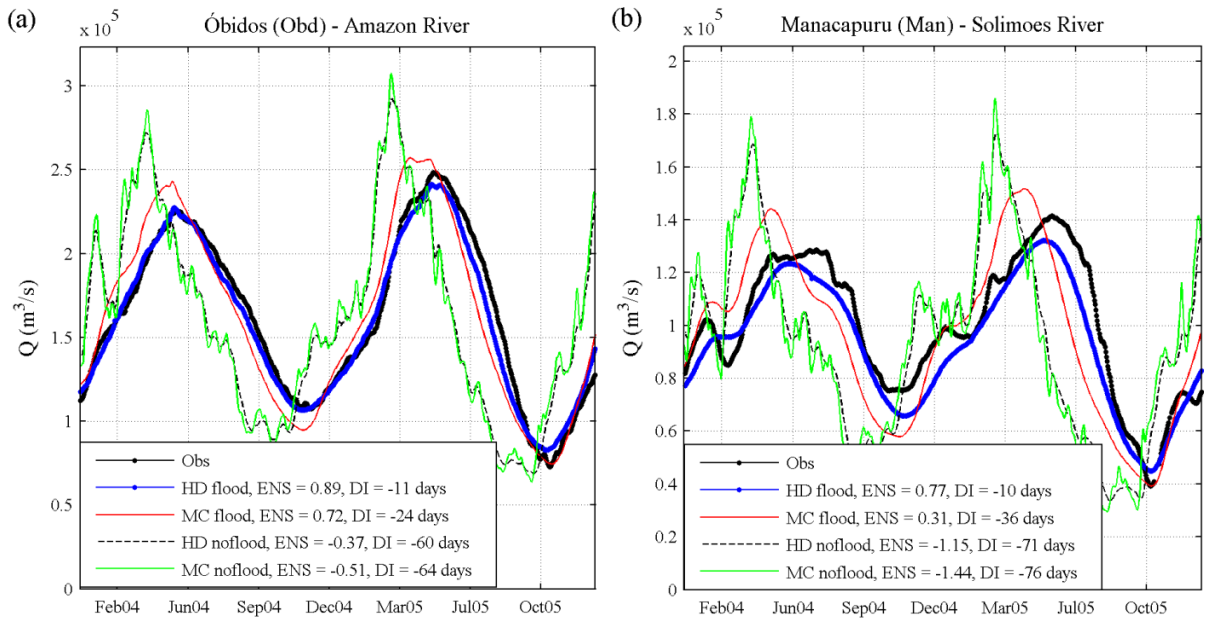

Figure 14. Observed (black line with dots) and simulated discharges at Óbidos (a) and Manacapuru (b) sites using hydrodynamic model with floodplains (blue line with dots), Muskingum Cunge with floodplains (red line), hydrodynamic model without floodplains (dashed black line) and Muskingum Cunge model without floodplains (grey line)

Results shown in Fig. 14 and in Table 2 indicate the better performance of the complete hydrodynamic model (HDf) in comparison with the other methods. Including backwater effects and floodplain storage generally delay and attenuates hydrographs, and simulations agree with observations (for example, *ENS* = 0.89 and 0.77 and *DI* = -11 and -10 days at Óbidos and Manacapuru stations respectively). Neither considering backwater effects nor floodplains (MC run) causes very advanced (*DI* = -64 and -76 days) and noisy hydrographs, with low *ENS* values (*ENS* = -0.51 and -1.44) and discarding only flood inundation (HDn run) causes a similar effect. However, to include floodplains only (MCf) is not sufficient to reproduce observed discharges (*ENS* = 0.72 and 0.31) and hydrographs still advanced about 15 and 25 days if compared to the most complete model (HDf). Possibly, the influence of floodplains is increased when the pressure term is present, as discussed in *Paiva et al.* [2012].

Table 2. Discharge model performance statistics Nash and Suttcliffe index (*ENS*) and delay index (*DI*) in days at gauging stations presented in Fig. 1 for simulations using hydrodynamic model with(out) floodplain – HDf (HDn) and Muskingum Cunge model with(out) floodplain – MCf (MCn).

		ENS				*DI* (days)			
Gauge	River	HDf	MCf	HDn	MCn	HDf	MCf	HDn	MCn
Jap	Japura	0.21	0.22	0.11	0.1	-21	-21	-27	-27
Mou	Negro	0.65	0.66	0.49	0.45	5	-6	-24	-26
Pur	Purus	0.91	0.74	0.66	0.61	-6	-18	-22	-24
Faz	Madeira	0.92	0.88	0.63	0.54	8	-4	-26	-29
Ita	Tapajós	0.87	0.84	0.85	0.85	-2	9	-5	-5
Tam	Solimões	0.74	0.67	0.21	0.04	-3	-11	-35	-39
Man	Solimões	0.77	0.31	-1.15	-1.44	-10	-36	-71	-76
Obd	Amazon	0.89	0.72	-0.37	-0.51	-11	-24	-60	-64

These results suggest that floodplains play a major role in flood wave attenuation and delay, but that backwater effects also cause important impacts. They are in accordance with preliminary analyses from *Paiva et al.* [2012], but they disagree with *Yamazaki et al.* [2011], who presented similar conclusions about floodplain storage but stated that backwater effects have a minor impact on hydrographs and are more important for representing water level profiles.

Although discussions from previous sections indicate that the model errors may arise from uncertainty in input data, results from this section show the importance of the model structure. Our approach is relatively complex in terms of river hydraulics since it uses full *Saint-Venant* equations, but is somehow simplified in terms of floodplain simulation. Consequently, it cannot fully represent all aspects of floodplain hydrodynamics such as bidirectional flows and river-floodplain water level dynamics [*Alsdorf et al.* 2007a; *Alsdorf et al.*, 2003; *Bonnet et al.*, 2008] and flow in small floodplain channels [*Trigg et al.*, 2012]. We believe that different flood inundation approaches [*e.g. Bonnet et al.*, 2008; *Paz et al.*, 2011; *Wilson et al.*, 2007; *Bates and De Roo*, 2000; *Neal et al*. 2012] coupled with full hydrodynamic models should still be tested to check its feasibility to represent all floodplain processes and the influence of these processes in large-scale stream flow routing and inundation dynamics.

2.6. Summary and conclusions

We present an extensive validation of the physically based large-scale hydrologic and hydrodynamic model MGB-IPH in the Amazon River basin using *in situ* and remote sensing

data sets. Sources of model errors, which can be extrapolated to other similar large scale models, were investigated by using model validation results and also supported by sensitivity tests. Finally, aspects of the physical functioning of the Amazon River basin are discussed taking advantage of the model results.

The model is able to reproduce observed hydrographs at different spatial scales, although performance is usually better in large rivers with large flood wave travel times. The model provides feasible water level results in most of the gauging stations and also at altimetry-based validation sites and overall inundation extent results similar to the remote sensing estimates. Discharge is well simulated even in regions where other hydrological variables are not well represented, as in the lower Amazon where some errors in water levels and flood extent can be found. Terrestrial water storage results also agree with GRACE-derived estimates.

Results from the sensitivity analysis indicate that model input data uncertainty may play an important role in model errors such as the ones presented in the model validation, although part of them can be due to the uncertainty in remote sensing data used here as observations. Precipitation forcing is the most sensitive variable, causing significant errors in mean discharge, water depth and flood extent. At the same time, important errors occur in westerly areas, which may be a consequence of the poor quality of TRMM 3B42 rainfall datasets in these areas, which are mountainous and/or poorly monitored.

The model results are also very sensitive to river-floodplain parameters, including river width and bottom level, Manning roughness coefficient and floodplain bathymetry. Important interactions between water levels, flooded areas and discharge errors are observed during the floodwaves traveling. Uncertainty in river and floodplain geometry, estimated through geomorphological relations and the SRTM DEM, causes errors in simulated water levels and inundation extent in some areas, indicating the need for improving current parameter estimation methods. These parameters are similar to the ones required in other large scale models and its uncertainty may cause errors in these models as well. Some alternatives to that could be the usage of newly remote sensing techniques for parameter estimation or corrections of the SRTM DEM to remove vegetation height in forested areas and to estimate bottom level of floodplains.

Overall water balance derived from model results is similar to estimates from previous studies. Mean annual rates of precipitation, evapotranspiration and discharge at Óbidos station are $P = 5.65$ mm.day^{-1}, $ET = 2.72$ mm.day^{-1} and $Q = 3.09$ mm.day^{-1}. TWS changes show

marked seasonal variability with a large amplitude of variation of 325 mm for all Amazon, and larger amplitude values (>750 mm) are found in central Amazon. Surface waters governs most of TWS changes in the Amazon basin (56%), mostly in central Amazon and in areas with large floodplains, while soil water presents an important contribution to TWS changes (36%), mainly in south-eastern areas and groundwater, it is the less important hydrological compartment (8%).

Finally, river and floodplain processes and the importance of backwater effects and flood inundation in stream flow routing were investigated. Results suggest that floodplains play a major role in flood wave attenuation and delay, but that backwater effects also cause important impacts, indicating the importance of including a flood inundation module and a complex *Saint Venant* equation approximation for river floodplain processes modelling in the Amazon. In contrast, although the seasonally inundated floodplains play an important role in water transport along Amazonian rivers, it seems not to have a major influence on evapotranspiration and water balance.

Acknowledgements

The authors are grateful for: the financial and operational support from the Brazilian agencies FINEP and ANA ("*Projeto de Integração e Cooperação Amazônica para a Modernização do Monitoramento Hidrológico*" ICA-MMH) and CNPq ("*Assimilação de Dados de monitoramento Espacial para a análise do regime hidrológico da Bacia Amazônica e a previsão de curto e médio prazos*") and the MHYZPA project funded by the French INSU EC2CO Cytrix program; the global inundation extent dataset provided by Fabrice Papa; the ENVISAT satellite altimetry data provided by Joecila Santos da Silva; the TRMM data supplied by NASA and associated agencies; the discharge data provided by ANA, Hybam, SENHAMI-Peru and SENHAMI-Bolivia; as well for the constructive comments from Dr. Praveen Kumar, editor of WRR, Dr. Augusto Getirana and other two anonymous Reviewers.

References

Alsdorf, D., Dunne, T., Melack, J., Smith, L., Hess, L. 2003. Diffusion modeling of recessional flow on central Amazonian floodplains. Geophysical Research Letters, 32, L21405.

Alsdorf, D., Bates, P., Melack, J., Wilson, M., Dunne, T. 2007a. The spatial and temporal complexity of the Amazon flood measured from space. Geophysical Research Ltrs, 34, L08402.

Alsdorf, D.E., Rodrıguez, E., Lettenmaier, D.P. 2007b. Measuring surface water from space. Reviews of Geophysics, 45, RG2002, doi:10Ð1029/2006RG000197.

Alsdorf, D., Han, S-C., Bates, P., Melack, J. 2010. Seasonal water storage on the Amazon floodplain measured from satellites. Remote Sensing of Environment, 114, 2448–2456.

Azarderakhsh, M., Rossow, W. B., Papa, F., Norouzi, H., Khanbilvardi, R. 2011. Diagnosing water variations within the Amazon basin using satellite data. J. Geophys. Res., 116, D24107, doi:10.1029/2011JD015997.

Bates, P.D., De Roo, A.P.J. 2000. A simple raster based model for flood inundation simulation. J. Hydrol., 236, 54–77.

Beighley, R.E., Eggert, K.G., Dunne, T., He, Y., Gummadi, V., Verdin, K.L. 2009. Simulating hydrologic and hydraulic processes throughout the Amazon River Basin. Hydrological Processes, 23, 8, 1221-1235.

Biancamaria, S., Bates, P.D., Boone, A., Mognard, N.M. 2009. Large-scale coupled hydrologic and hydraulic modelling of the Ob river in Siberia. Journal of Hydrology, 379, 136–150.

Bonnet, M.P., Barroux, G., Martinez, J.M., Seyler, F., Turcq, P.M., Cochonneau, G., Melack, J.M., Boaventura, G., Bourgoin, L.M., León, J.G., Roux, E., Calmant, S., Kosuth, P., Guyot, J.L., Seyler, F. 2008. Floodplain hydrology in an Amazon floodplain lake (Lago Grande de Curuaí). Journal of Hydrology, 349, 18 - 30.

Bourgoin, L.M., Bonnet, M.P., Martinez, J.M., Kosuth, P., Cochonneau, G., Turcq, P.M., Guyot, J.L., Vauchel, P., Filizola, N., Seyler, P. 2007. Temporal dynamics of water and sediment exchanges between the Curuaí floodplain and the Amazon River, Brazil. Journal of Hydrology, 335, 140-156.

Castellarin, A., Di Baldassarre, G., Bates, P. D., Brath, A. 2009. Optimal Cross-Sectional Spacing in Preissmann Scheme 1D Hydrodynamic Models. Journal of Hydraulic Engineering, 135, 2, 96-105.

Chen, J.L., Wilson, C.R., Tapley, B.D. 2010. The 2009 exceptional Amazon flood and interannual terrestrial water storage change observed by GRACE. Water Resour. Res., 46, W12526, doi:10.1029/2010WR009383.

Coe, M.T., Costa, M.H., Howard, E.A. 2008. Simulating the surface waters of the Amazon River basin: Impacts of new river geomorphic and flow parameterizations. Hydrological Processes 22, 14, 2542-2553.

Collischonn, W. 2001 Hydrologic simulation of large basins (in Portuguese). PhD Thesis, Inst. de Pesqui. Hidraul., Univ. Fed. do Rio Grande do Sul, Porto Alegre, Brazil.

Collischonn, W., Allasia, D.G., Silva, B.C., Tucci, C.E.M. 2007. The MGB-IPH model for large-scale rainfall-runoff modeling. Hydrological Sciences Journal, 52, 878-895.

Collischonn, B., Collischonn, W., Tucci, C. 2008 Daily hydrological modeling in the Amazon basin using TRMM rainfall estimates. Journal of Hydrology, 207.

Condom, T., Rau, P., Espinoza, JC. 2010 Correction of TRMM 3B43 monthly precipitation data over the mountainous areas of Peru during the period 1998–2007. Hydrol. Processes DOI: 10.1002/hyp.749.

Costa, M.H., Foley, J.A., 1997. Water balance of the Amazon Basin: dependence on vegetation cover and canopy conductance. Journal of Geophysical Research-Atmospheres 102(D20): 23973–23989.

Costa, M.H., Biajoli, M.C., Sanches, L., Malhado, A.C.M., Hutyra, L. R., da Rocha, H.R., Aguiar, R.G., de Araújo, A.C. 2010. Atmospheric versus vegetation controls of Amazonian tropical rain forest evapotranspiration: Are the wet and seasonally dry rain forests any different?, J. Geophys. Res., 115, G04021, doi:10.1029/2009JG001179.

Cunge, J.A., Holly, F.M., Verney, A. 1980. Practical Aspects of Computational River Hydraulics. Pitman Advanced Publishing Program.

Decharme, B., Alkama, R., Papa, F., Faroux, S., Douville, H., Prigent, C. 2011 Global off-line evaluation of the ISBA-TRIP flood model. Climate Dynamics.

Dijkshoorn, J.A., Huting, J.R.M., Tempel, P. 2005. Update of the 1:5 million Soil and Terrain Database for Latin America and the Caribbean (SOTERLAC; version 2.0). Report 2005/01, ISRIC – World Soil Information, Wageningen.

Durand, M., Rodríguez, E., Alsdorf, D., Trigg, M. 2010a. Estimating River Depth From Remote Sensing Swath Interferometry Measurements of River. IEEE journal of selected topics in applied earth observations and remote sensing, 3, 20-31.

Durand, M., Fu, L.L., Lettenmaier, D.P., Alsdorf, D.E., Rodríguez, E., Fernandez, D.E. 2010b. The surface water and ocean topography mission: Observing terrestrial surface water and oceanic submesoscale eddies. Proceedings Of the IEEE, 98, 5, 766−779.

Espinoza, J.C., Ronchail, J., Guyot, J.L., Cocheneau, G., Filizola, N., Lavado, W., de Oliveira, E., Pombosa, R., Vauchel, P. 2009. Spatio – Temporal rainfall variability in the Amazon Basin Countries (Brazil, Peru, Bolivia, Colombia and Ecuador). International Journal of Climatology, 29, 1574-1594.

Espinoza, J.C., Ronchail, J., Guyot, J. L., Junquas, C., Vauchel, P., Lavado, W., Drapeau, G., Pombosa, R. 2011. Climate variability and extreme drought in the upper Solimões River (western Amazon Basin): Understanding the exceptional 2010 drought. Geophys. Res. Lett., 38, L13406, doi:10.1029/2011GL047862.

Eva, H.D., De Miranda, E.E., Di Bella, C.M., Gond, V. 2002. A Vegetation map of South America. EUR 20159 EN. European Commission, Luxembourg.

Farr, T.G., Caro, E., Crippen, R., Duren, R., Hensley, S., Kobrick, M., Paller, M., Rodriguez, E., Rosen, P., Roth, L., Seal, D., Shaffer, S., Shimada, J., Umland, J.,Werner, M., Burbank, D., Oskin, M., Alsdorf, D. 2007. The shuttle radartopography mission. Reviews of Geophysics, 45, 2.

Frappart, F., Papa, F., Famiglietti, J.S., Prigent, C., Rossow, W.B., Seyler, F. 2008. Interannual variations of river water storage from a multiple satellite approach: a case study for the Rio Negro River basin. Journal of Geophysical Research, 113(D21), D21104, doi:10.1029/2007JD009438.

Frappart, F., Papa, F., Guntner, A., Werth, S., Santos da Silva, J., Tomasella, J., Seyler, F., Prigent, C., Rossow, W.B., Calmant, S., Bonnet, M.P. 2011a. Satellite-based estimates of groundwater storage variations in large drainage basins with extensive floodplains. Remote Sensing of Environment, 115, 6, 1588-1594.

Frappart, F., Ramillien, G., Maisongrande, P., Bonnet, M-P. 2010. Denoising satellite gravity signals by Independent Component Analysis. IEEE Geosciences and Remote Sensing Letters, 7, 3, 421-425, doi:10.1109/LGRS.2009.2037837.

Frappart, F., Ramillien, G., Leblanc, M., Tweed, S.O., Bonnet, M-P., Maisongrande, P. 2011b. An Independent Component Analysis approach for filtering continental hydrology in the GRACE gravity data. Remote Sensing of Environment, 115(1), 187-204, doi: 10.1016/j.rse.2010.08.017.

Getirana, A.C.V., Bonnet, M.-P., Rotunno Filho, O.C., Collischonn, W., Guyot, J.-L., Seyler, F., Mansur, W. J. 2010. Hydrological modelling and water balance of the Negro River basin: evaluation based on in situ and spatial altimetry data. Hydrological Processes, 24, 22, 3219-3236.

Getirana, et al. 2011. Calibração e Validação de Modelo Hidrológico com Observações In Situ, Altimetria e Gravimetria Espaciais. RBRH — Revista Brasileira de Recursos Hídricos, Volume 16 n.1 Jan/Mar 2011, 29-45.

Getirana, A.C.V., Boone, A., Yamazaki, D., Decharme, B., Papa, F., Mognard, N. 2012. The Hydrological Modeling and Analysis Platform (HyMAP): evaluation in the Amazon basin. J. Hydrometeorol., accepted for publication .

Han, S.-C., Kim, H., Yeo, I.-Y., Yeh, P., Oki, T., Seo, K.-W., Alsdorf, D., Luthcke, S.B. 2009. Dynamics of surface water storage in the Amazon inferred from measurements of inter-satellite distance change. Geophys. Res. Lett., 36, L09403, doi:10.1029/2009GL037910.

Hess, L.L., Melack, J.M., Novo, E.M.L.M., Barbosa, C.C.F., Gastil, M. 2003. Dual-season mapping of wetland inundation and vegetation for the central Amazon basin. Remote Sensing of Environment, 87, 404 – 428.

Huffman, G., Adler, R., Bolvin, D., Gu, G., Nelkin, E., Bowman, K., Hong, Y., Stocker, E., Wolff, D. 2007. The TRMM Multisatellite Precipitation Analysis (TCMA): quasi-global, multiyear, combined-sensor precipitation estimates at fine scales. J. Hydromet, 8, 38–55.

Junk, W.J. 1997. General aspects of floodplain ecology with special reference to Amazonian floodplains. In: Junk, W.J. (Ed.), The Central-Amazonian Floodplain: Ecology of a Pulsing System, Ecological Studies. Springer Verlag/Heidelberg, Berlin/New York, 3–22.

Kim, H., Yeh, P.J.-F., Oki, T., Kanae, S. 2009. Role of rivers in the seasonal variations of terrestrial water storage over global basins. Geophys. Res. Lett., 36, L17402, doi:10.1029/2009GL039006.

Kosuth, P., Callède, J., Laraque, A., Filizola, N., Guyot, J.L., Seyler, P., Fritsch, J.M., Guimarães, V. 2009. Sea-tide effects on flows in the lower reaches of the Amazon River. Hydrological Processes 23 (22), 3141-3150.

Lian, Y., Chan, I.-C., Singh, J., Demissie, M., Knapp, V., Xie, H. 2007. Coupling of hydrologic and hydraulic models for the Illinois River Basin. Journal of Hydrology, 344, 210–222.

Marengo, J.A. 2005. Characteristics and spatio-temporal variability of the Amazon River basin water budget. Climate Dynamics, 24: 11–22. DOI 10.1007/s00382-004-0461-6.

Marengo, J., Nobre, C., Tomasella, J., Oyama, M., de Oliveira, G., de Oliveira, R., Camargo, H., Alves, L. 2008. The drought in Amazonia in 2005. Journal of Climate, 21:495–516.

Marengo, J.A., Tomasella, J., Alves, L. M., Soares, W. R., Rodriguez, D.A. 2011. The drought of 2010 in the context of historical droughts in the Amazon region, Geophys. Res. Lett., 38, L12703, doi:10.1029/2011GL047436

Meade, R.H., Rayol, J.M., Da Conceição, S.C., Natividade, J.R.G. 1991. Backwater effects in the Amazon River basin of Brazil . Environmental Geology and Water Sciences, 18, 2, 105-114.

Melack, J.M., Hess, L.L., Gastil, M., Forsberg, B.R.., Hamilton, S.K., Lima, I.B.T., Novo, E.M.L.M. 2004. Regionalization of methane emissions in the Amazon basin with microwave remote sensing. Global Change Biol., 10, 530–544.

Melack, J.M., Hess, L.L. 2010. Remote sensing of the distribution and extent of wetlands in the Amazon basin. In Junk WJ, Piedade M (eds) Amazonian floodplain forests: ecophysiology, ecology, biodiversity and sustainable management. Ecological Studies, vol. 210, part 1. Springer, 43–59.

Mohamed, Y.A., van den Hurk, B.J.J.M., Savenije, H.H.G., Bastiaanssen, W.G.M. 2005. Impact of the Sudd wetland on the Nile hydroclimatology. Water Resour. Res., 41, W08420.

New, M., Lister, D., Hulme, M., Makin, I. 2002. A high-resolution data set of surface climate over global land areas. Climate Res., 21.

Neal, J.C., Schumann, G.J.-P., Bates, P D.D. 2012. A sub-grid channel model for simulating river hydraulics and floodplain inundation over large and data sparse areas. Water Resour. Res., doi:10.1029/2012WR012514, in press.

Paiva, R.C.D., Collischonn, W., Tucci, C.E.M. 2011a. Large scale hydrologic and hydrodynamic modeling using limited data and a GIS based approach. Journal of Hydrology, 406, 170–181

Paiva, R.C.D., Buarque, D.C., Clarke, R.T., Collischonn, W., Allasia, D.G. 2011b. Reduced precipitation over large water bodies in the Brazilian Amazon shown from TRMM data. Geophys. Res. Lett., 38, L04406, doi:10.1029/2010GL045277.

Paiva, R.C.D., Collischonn, W., Buarque, D.C. 2012. Validation of a full hydrodynamic model for large scale hydrologic modelling in the Amazon. Hydrol. Process. DOI: 10.1002/hyp.8425

Papa, F., Prigent, C., Aires, F., Jimenez, C., Rossow, W.B., Matthews, E. 2010. Interannual variability of surface water extent at the global scale, 1993–2004. J. Geophys. Res., 115, D12111, doi:10.1029/2009JD012674.

Paz, A.R., Bravo, J.M., Allasia, D., Collischonn, W., Tucci, C.E.M. 2010. Large-Scale Hydrodynamic Modeling of a Complex River Network and Floodplains. Journal of Hydrologic Engineering 15, 2, 152–165.

Paz, A.R.d., Collischonn, W., Tucci, C.E.M., Padovani, C.R. 2011. Large-scale modelling of channel flow and floodplain inundation dynamics and its application to the Pantanal (Brazil). Hydrological Processes, 25: 1498–1516, doi: 10.1002/hyp.7926.

Ponce, V.M. 1989. Engineering Hydrology. Prentice Hall.

Pontes, P.R.M. 2011. Comparing simplified hydrodynamic models for flow routing in rivers and channels (in Portuguese), PhD Thesis, Inst. de Pesqui. Hidraul., Univ. Fed. do Rio Grande do Sul, Porto Alegre, Brazil. http://hdl.handle.net/10183/35350

Prigent, C., Papa, F., Aires, F., Rossow, W. B., Matthews, E. 2007. Global inundation dynamics inferred from multiple satellite observations, 1993–2000. J. Geophys. Res., 112, D12107, doi:10.1029/2006JD007847.

Prigent, C., Rochetin, N., Aires, F., Defer, E., Grandpeix, J.-Y., Jimenez, C., Papa, F. 2011. Impact of the inundation occurrence on the deep convection at continental scale from satellite observations and modeling experiments. J. Geophys. Res., 116, D24118, doi:10.1029/2011JD016311.

RADAMBRASIL. 1982. Programa de Integração Nacional, Levantamento de Recursos Naturais. Ministério das Minas e Energia, Secretaria-Geral.

Ramillien, G., Famiglietti, J.S., Wahr, J. 2008. Detection of continental hydrology and glaciology signals from GRACE: A review. Surveys in Geophysics, 29, 4–5, 361−374, doi:10.1007/s10712-008-9048-9.

Ramillien, G., Frappart, F., Cazenave, A., Güntner, A. 2005. Time variations of the land water storage from an inversion of 2 years of GRACE geoids. Earth and Planetary Science Letters, 235, 283−301, doi:10.1016/j.epsl.2005.04.005

Renno, C.D., Nobre, A.D., Cuartas, L.A., Soares, J.V., Hodnett, M.G., Tomasella, J., Waterloo, M.J. 2009. HAND, a new terrain descriptor using SRTM-DEM: Mapping terra-firme rainforest environments in Amazonia. Remote Sensing of Environment, 12, 9, 3469-3481.

Richey, J.E., Melack, J.M., Aufdenkampe, A.K., Ballester, V.M., Hess, L.L. 2002. Outgassing from Amazonian rivers and wetlands as a large tropical source of atmospheric CO2. Nature 416, 617−620.

Ruhoff, A.L. 2011. Remote sensing applied to evapotranspiration estimation in tropical biomes (in Portuguese), PhD Thesis. Inst. de Pesqui. Hidraul., Univ. Fed. do Rio Grande do Sul, Porto Alegre, Brazil. http://hdl.handle.net/10183/32468

Santos da Silva, J.; Calmant, S.; Seyler, F.; Rotunno Filho, O.C.; Cochonneau, G.; Mansur, W.J. 2010. Water levels in the Amazon basin derived from the ERS 2 and ENVISAT radar altimetry missions. Remote Sensing of Environment, 114, 10, 2160-2181.

Schmidt, R., Flechtner, F., Meyer, U., Neumayer, K.-H., Dahle, Ch., Koenig, R., et al. 2008. Hydrological signals observed by the GRACE satellites. Surveys in Geophysics, 29, 319−334, doi:10.1007/s10712-008-9033-3.

Seyler, P., Boaventura, G.R. 2003. Distribution and partition of trace metals in the Amazon basin. Hydrol. Process., 17, 1345–1361.

Simard, M., Pinto, N., Fisher, J., Baccini, A. 2011. Mapping forest canopy height globally with spaceborne lidar. Journal of Geophysical Research, 116, G04021, 12, 2011, doi:10.1029/2011JG001708

Shuttleworth, W.J., 1993. Evaporation. In: Maidment, D.R. (Ed.), Handbook of Hydrology. McGraw-Hill, New York.

Sun, G., Ranson, K.J., Kharuk, V.I., Kovacs. K. 2003. Validation of surface height from shuttle radar topography mission using shuttle laser altimeter. Remote Sensing of Environment 88, 401–411.

Tapley, B.D., Bettadpur, S., Ries, J. C., Thompson, P.F., Watkins, M. 2004. GRACE measurements of mass variability in the Earth system. Science, 305, 503−505.

Tian, Y.; Peters-Lidard, C.D. 2010. A global map of uncertainties in satellite-based precipitation measurements. Geophys. Res. Letters 37, L24407, doi:10.1029/2010GL046008.

Todini, E. 2007. A mass conservative and water storage consistent variable parameter Muskingum-Cunge approach. Hydrol. Earth Syst. Sci., 11, 1645-1659, doi:10.5194/hess-11-1645-2007.

Tomasella, J., Borma, L.S., Marengo, J.A., Rodriguez, D.A., Cuartas, L.A., Nobre, C.A., Prado, M.C.R. 2010 The droughts of 1996–1997 and 2004–2005 in Amazonia: hydrological response in the river main-stem. Hydrol. Process.

Trigg, M.A., Wilson, M.D., Bates, P.D., Horritt, M.S., Alsdorf, D.E., Forsberg, B.R., Vega, M.C. 2009. Amazon flood wave hydraulics. Journal of Hydrology, 374, 92–105.

Trigg, M.A., Bates, P.D.D., Wilson, M.D., Schumann, G.J.-P., Baugh, C.A. 2012, Floodplain channel morphology and networks of the middle Amazon River. Water Resour. Res., doi:10.1029/2012WR011888, in press.

Wilson, W., Bates, P., Alsdorf, D., Forsberg, B., Horritt, M., Melack, J., Frappart, F., Famiglietti, J. 2007, Modeling large-scale inundation of Amazonian seasonally flooded wetlands. Geophys. Res. Lett., 34, L15404, doi:10.1029/2007GL030156.

Yapo, P.O., Gupta, H.V., Sorooshian, S. 1998. Multi-objective global optimization for hydrologic models. Journal of Hydrology, 204, 83-97.

Yamazaki, D., Kanae, S., Kim, H., Oki, T. 2011. A physically based description of floodplain inundation dynamics in a global river routing model. Water Resour. Res., 47, W04501, doi:10.1029/2010WR009726.

Yamazaki, D., Lee, H., Alsdorf, D.E., Dutra, E., Kim, H., Kanae, S., Oki, T. 2012. Analysis of the water level dynamics simulated by a global river model: a case study in the Amazon River. Water Resources Research, doi:10.1029/2012WR011869http://www.agu.org/pubs/crossref/pip/2012WR011869.shtml

Yamazaki, D., Baugh, C., Bates, P.D., Kanae, S., Alsdorf, D.E., Oki, T. 2012. Adjustment of a spaceborne DEM for use in floodplain hydrodynamic modelling. J. Hydrol., 436-437, 81-91, doi:10.1016/j.jhydrol.2012.02.045

CAPÍTULO 3

Reduced precipitation over large water bodies in the Brazilian Amazon shown from TRMM data

Capítulo 3: Reduced precipitation over large water bodies in the Brazilian Amazon shown from TRMM data

Neste capítulo, apresenta-se um estudo da variabilidade especial da precipitação na Amazônia brasileira utilizando dados de sensoriamento remoto da missão TRMM ("*Tropital Rainfall Measurement Mission*") [*Huffman et al.*, 2007]. A motivação para este estudo surgiu de uma análise preliminar dos dados de precipitação do produto TRMM 3B42 na etapa de preparação de dados para a modelagem hidrológica e hidrodinâmica da bacia Amazônica (Capítulo 2), quando se verificou que, surpreendentemente, a precipitação era reduzida sobre os grandes corpos d'água amazônicos. A partir disto, surgiram as seguintes questões: A redução na precipitação estimada pelo TRMM 3B42 sobre os grandes corpos d'água amazônicos seria significativa? Esta redução seria artificial, causada por questões técnicas das estimativas de sensoriamento remoto do TRMM 3B42? Ou seria real e uma característica das precipitações na Amazônia explicada por algum fenômeno físico?

Em resumo, os resultados mostram uma clara redução na precipitação média anual e número de dias chuvosos do TRMM 3B42 sobre os grandes corpos d'água amazônicos, como os rios Solimões, Amazonas, Tapajós e Negro e o reservatório de Balbina, confirmados por testes estatísticos. Este comportamento é variável ao longo do dia, sendo mais marcado durante a tarde quando grande parte da precipitação é de origem convectiva e se invertendo à noite e pela manhã. Estas características não estão de acordo com problemas técnicos das estimativas de precipitação por sensoriamento remoto relatados em estudos anteriores. Por outro lado, os padrões aqui identificados estão de acordo com o fenômeno chamado de brisa fluvial, causado por diferenças no balanço de energia na água e na floresta, que poderia causar uma maior formação de nuvens e precipitação sobre a floresta durante o dia e o contrário à noite, descrido em outros trabalhos na região.

Os resultados sugerem que a precipitação média da bacia Amazônica pode estar sendo sistematicamente subestimada, já que grande parte dos postos pluviométricos da região localiza-se em cidades situadas junto aos maiores rios. Tal resultado tem importantes implicações em estudos hidrológicos, nas validações das estimativas de precipitação de sensoriamento remoto, e em aplicações de modelagem hidrológica, como ilustrado no Capítulo 2, onde os resultados de simulação são fortemente sensíveis a erros na precipitação.

Capítulo 3: Reduced precipitation over large water bodies in the Brazilian Amazon shown from TRMM data

This chapter is based on the following paper published at Geophysical Research Letters:

Paiva, R. C. D., D. C. Buarque, R. T. Clarke, W. Collischonn, Allasia, D. G. 2011. Reduced precipitation over large water bodies in the Brazilian Amazon shown from TRMM data. Geophys. Res. Lett., 38, L04406, doi:10.1029/2010GL045277.

Abstract

Tropical Rainfall Measurement Mission (TRMM) data show lower rainfall over large water bodies in the Brazilian Amazon. Mean annual rainfall (*P*), number of wet days (rainfall > 2mm) (*W*) and annual rainfall accumulated over 3-hour time intervals (P_{3hr}) were computed from TRMM 3B42 data for 1998-2009. Reduced rainfall was marked over the Rio Solimões/Amazon, along most Amazon tributaries and over the Balbina reservoir. In a smaller test area, a heuristic argument showed that *P* and *W* were reduced by 5% and 6.5% respectively. Allowing for TRMM 3B42 spatial resolution, the reduction may be locally greater. Analyses of diurnal rainfall patterns showed that rainfall is lowest over large rivers during the afternoon, when most rainfall is convective, but at night and early morning the opposite occurs, with increased rainfall over rivers, although this pattern is less marked. Rainfall patterns reported from studies of smaller Amazonian regions therefore exist more widely.

3.1. Introduction

In the Amazon basin, uncertainty in rainfall causes difficulties in the study of hydrological processes, hydroclimatic variability [e.g. *Espinoza et al.,* 2009], biogeochemical analysis and hydrological modeling [e.g., *Coe et al.*, 2008*; Collischonn et al.,* 2008], whilst the value of ground-level estimates of rainfall is limited by low raingauge density in a region where convective rainfall is spatially highly variable. Estimation of rainfall characteristics by remote sensing, using satellite-derived data from TRMM [*Huffman et al.,* 2007] and CMORPH [*Joyce et al.,* 2004] is an attractive alternative, giving better spatial cover of rainfall fields. *Pereira Filho et al* [2010] analyzed hourly rainfall for a four-year record from CMORPH and concluded that convection over the Amazon region is often more organized than had previously been thought, and that satellite-derived rainfall estimates can be an important source of rainfall information where *in situ* observations are lacking. However, the use of remote-sensed rainfall estimates is not without problems: *Tian and Peters-Lidard* [2007], for example, reported systematic positive errors in TRMM 3B42 rainfall estimates for

pixels associated withinland water-bodies, and speculate that this inconsistency results from deficiencies in the TRMM assumptions about water-surface emissivity.

In the Amazon, raingauges are preferentially sited along rivers where most settlements lie [*Oliveira and Fitzjarrald,* 1993*; de Gonçalves et al.,* 2006*; Fitzjarrald et al.,* 2008]. However, meso-scale circulations close to large rivers such as river breezes may also affect rainfall distribution locally [*Silva Dias et al* 2004*; Fitzjarrald et al.* 2008] and lead to reduced rainfall [*Garstang and Fitzjarrald* 1999].

River breezes result from differences in sensible and latent heat fluxes over land and water, enhancing cloudiness over land during daytime, whilst skies over water remain clear; at nighttime, the opposite occurs. *Garstang and Fitzjarrald* [1999] stated that away from large Amazonian rivers, convergence zones lead to enhanced rainfall over forest and diminished rainfall near rivers, and that daytime enhancement/diminution has a greater net effect on rainfall near rivers than the reverse night-time situations.

River breezes has been observed and modeled over limited areas by several authors [*Ribeiro and Adis,* 1984*; Oliveira and Fitzjarrald,* 1993*,* 1994*; Silva Dias et al.,* 2004*; Fitzjarrald et al.,* 2008]. Reduced annual rainfall in riverine areas near Manaus in central Amazonia has also been reported [*Ribeiro and Adis,* 1984*; Garstang and Fitzjarrald,* 1999*; Cutrim et al., 2000*]. *Fitzjarrald et al.* [2008], analyzing data from raingauges near the Amazon-Tapajos confluence, found that stations near large rivers missed the afternoon convective rain, but that this deficit was more than compensated by additional nocturnal rainfall. *Silva Dias et al.* [2004] used high-resolution numerical simulation to explore the atmospheric circulation near the Amazon-Tapajos confluence, concluding that, since most long-term climate stations lie near to Amazonian rivers, measurements taken very close to them must be interpreted with care.

Since raingauges are often sited near large rivers, it is possible that raingauge-derived estimates of Amazon rainfall may be biased. Such a bias would have important implications for hydrological modeling, water resource management, and the calibration and validation of remote-sensed rainfall estimates using raingauge data [*Oliveira and Fitzjarrald,* 1993*,* e.g. *de Gonçalves et al.* 2006*; Hughes,* 2006]. Using TRMM 3B42 records, this paper therefore explores rainfall spatial variability in the Brazilian Amazon and the evidence for lower rainfall near its large rivers. The paper presents results from TRMM 3B42 data analyses, and does not seek to elucidate physical mechanisms.

3.2. Data and Methods

The area studied is that part of the Amazon River basin lying within Brazilian territory, shown in Fig. 1. TRMM rainfall were provided by algorithm 3B42 [*Huffman et al.*, 2007], with spatial resolution of $0.25^o \times 0.25^o$ and temporal resolution of three hours, for the 12-year period 1998-2009. Data were selected within a grid defined by latitudes $+6^o$ to -17^o and longitudes -74^o to -47^o. This paper reports results of analyses of three variables. These are: 1) mean annual rainfall, P; 2) mean annual number of wet days, W, defined here as days with rainfall greater than a threshold of 2 mm (as in *Buarque et al*, 2010); and 3) mean annual rainfall accumulated in each 3-hour time interval of the TRMM 3B42 temporal resolution, P_{3hr}. Analysis consisted of two steps. In the first, annual means of P and W were calculated for 1998-2009. In the second, the diurnal variation of rainfall was evaluated using P_{3hr}. For

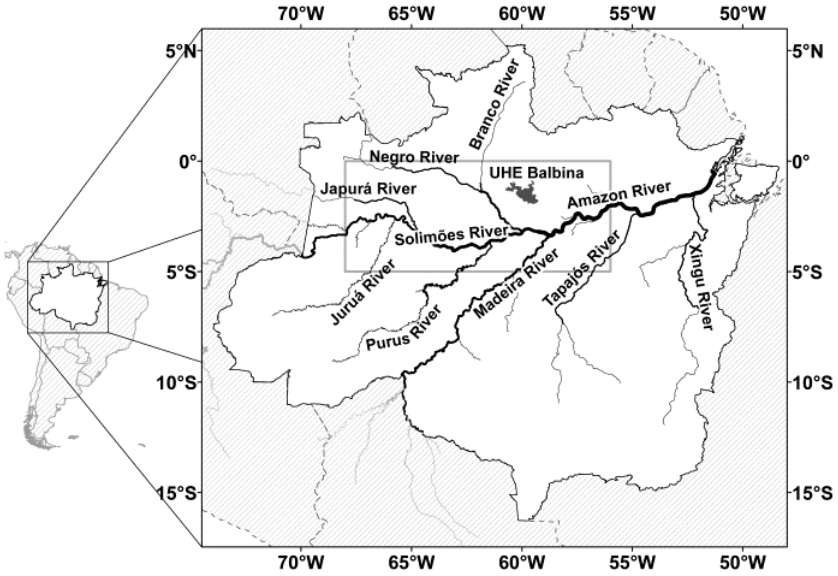

Figure 1. Brazilian Amazon river basin (white), river network and test area (rectangle in central Amazon).

both steps, rainfall reductions near large water bodies were tested for statistical significance. A proper significance test (in which a hypothesis is proposed, and additional data are collected to test it) was not possible given the context, but the following argument gives a reasonable substitute, despite being partly subjective and not fully rigorous. A test area in the central Amazon was selected which extended from longitude 68^o W to 56^o W and from the equator to 5^o S (see Fig. 1). Away from its river system, spatial distribution of rainfall within this area is relatively homogeneous and free from the large regional differences seen in Fig. 2; any remaining spatial trend in P, W and P_{3hr} was removed by linear regression

$X^* = a_1\lambda + a_2\varphi + a_3$, where λ and φ are the latitude and longitude of points within the test area. The variable used in the test procedure was the regression residual $X' = X - X^*$, where X is P, W or P_{3hr} at a TRMM 3B42 grid-point. In what follows, all primed variables denote residuals derived from such regressions. The TRMM 3B42 grid-points were divided into two groups ("Water" and "No Water") according to whether they were near to major rivers or other water bodies, using a 100 m resolution map of central Amazon wetlands [*Hess et al.*, 2003]. The fraction of wetland within each TRMM 3B42 grid-square was computed: grid-squares with more than 20% wetland were classified as "Water", the remainder as "No Water". Grid-squares were identified where P, W or P_{3hr} was significantly smaller than the "No Water" grid points, by means of a *t*-test [e.g., *Wilks,* 2006], where one mean was the grid-square value, and the other the mean of the "No Water" grid-squares. A second *t*-test for difference between the "Water" and "No Water" sample means was also performed [*Wilks,* 2006]. All tests used a 5% significance level. Finally, since the values obtained from neighboring TRMM 3B42 grid-points will be spatially correlated, an effective sample size was therefore computed for the means entering each *t*-test, by adapting, to a space of two dimensions, an expression for the equivalent number of independent observations in a serially-correlated time series [e.g., *Cressie,* 1993]. This expression is $N' = N(1-\rho) / (1+\rho)$ where N is the original sample size and ρ is the lag-one serial correlation; in the present context, ρ was averaged over the two grid directions.

3.3. Results

Fig. 2a, showing P for 1998-2009, gives a general picture of rainfall spatial variability shown by the TRMM 3B42 data-set. Some well-known regional characteristics are apparent, such as the higher rainfall in the Rio Negro headwaters and near the Amazon's mouth; and the E-W and N-S gradients in P. The figure shows an apparent reduction near large rivers, an effect which stands out clearly along the Rios Solimões/Amazon, especially near the confluences with the Negro and Tapajós, and along most Amazon tributaries: Madeira, Purus, Juruá and Japurá, but particularly along the Tapajós and Negro. This reduction is consistent with the conclusions of other studies over more limited regions [e.g. *Ribeiro and Adis,* 1984*; Garstang and Fitzjarrald* 1999*; Cutrim et al.* 2000], although it does not agree with the findings of *Fitzjarrald et al.* [2008], perhaps due to the scale of TRMM 3B42 data. The site of the Balbina reservoir (2,400 km^2) stands out in the figure, with rainfall lower than in

surrounding areas. A reduction in *W* along larger rivers is also evident (Fig. 2b) and more marked than in Fig. 2a, especially downstream of the confluence of the Rios Negro and Solimões, over the Balbina reservoir, and near the Amazon- Tapajós confluence.

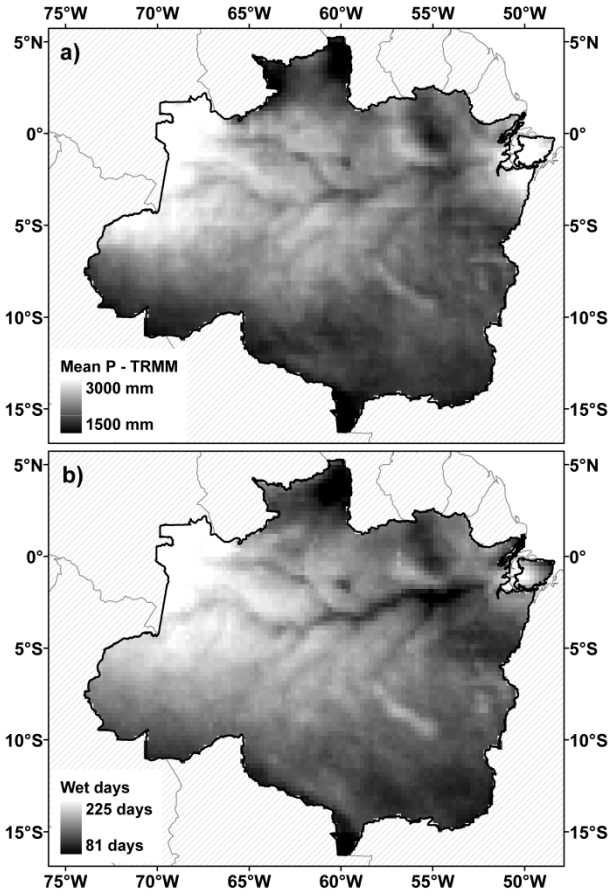

Figure 2. (a) Mean annual rainfall and (b) mean number of wet days from TRMM 3B42 data (1998-2009).

Fig. 3a shows the test area with the largest rivers and the Balbina reservoir, together with the TRMM 3B42 grid points classified as "Water" in black. Based on the values in Table 1, the relative difference between *P* and *W* from areas within the influence of large water bodies ("Water"), and from areas without ("No Water"), are -5% ((-82.5 – 41.2)/2486) and -6.5% ((-7.3 – 3.7)/169.8), respectively. Trend removal was necessary for computing these differences because "Water" pixels are not uniformly distributed (see Fig. 3a), being more concentrated to the west of the test area, and because there is also a strong E-W gradient in *P* (Fig. 2). The pooled lag-one spatial correlation for both variables was ρ=0.84. In a first statistical test, it was found that *P* and *W* were significantly smaller at "Water" than at "No Water" grid-points ($p<0.05$), confirming the lower rainfall near large water bodies. In the second test, Fig. 3b shows TRMM 3B42 grid-points in the test area where *P* is lower than the

mean for "No Water" grid-points. These are concentrated along the Solimões/Amazon and Negro rivers, but reductions also appear near the Balbina reservoir and at a grid-point on the Tapajós. Similar results were also found for *W*, given in Fig. 3c, but with more grid-points with smaller values concentrated along Rio Solimões/Amazon. A sensitivity analysis of the threshold value for grid-squares to be classified as "Water" confirmed that results from the statistical tests and the consequent conclusions were unchanged when the threshold ranged from 5% to 50%.

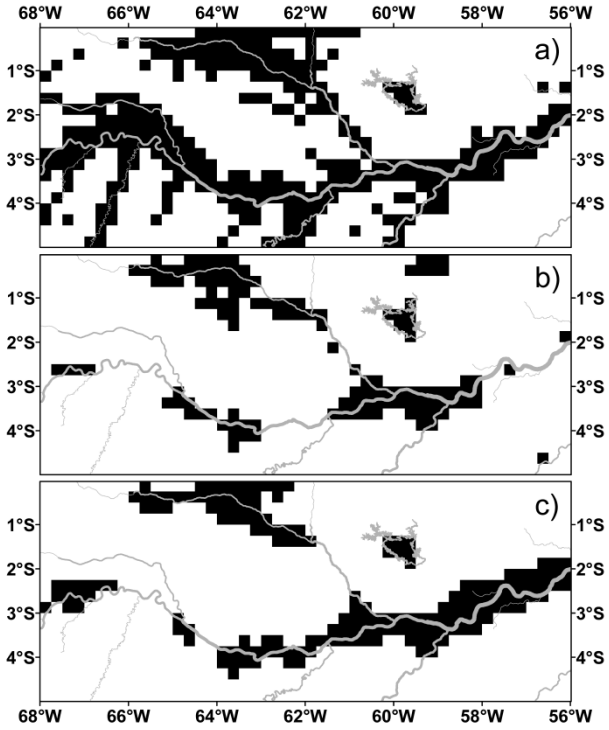

Figure 3. (a) TRMM 3B42 grid-squares constituting the "Water" group; (b) grid-squares with lower *P* than grid-squares in the "No Water" group, ($p<0.05$); and (c) grid-squares with smaller *W* then for the "No Water" group ($p<0.05$).

Table 1. Sample Size, Effective Sample Size, and Mean and Standard Deviation of Residuals After Trend Removal in *P* and *W* [(a)].

Region	*N*	*N*'	*P* [mm]		*W* [days]	
			Mean	SD	Mean	SD
Water	320	28	-82.5	147.2	-7.3	10.9
No Water	640	57	41.2	129.1	3.7	7.7
All grid points [(b)]	960	84	2486	211.7	169.8	18.4

[(a)] *N*, number of TRMM 3B42 grid-points; *N*′, effective sample size; SD, standard deviation. Values from grid-squares denoted by "Water", "No Water".

[(b)] Statistics computed using original *P* and *W* values.

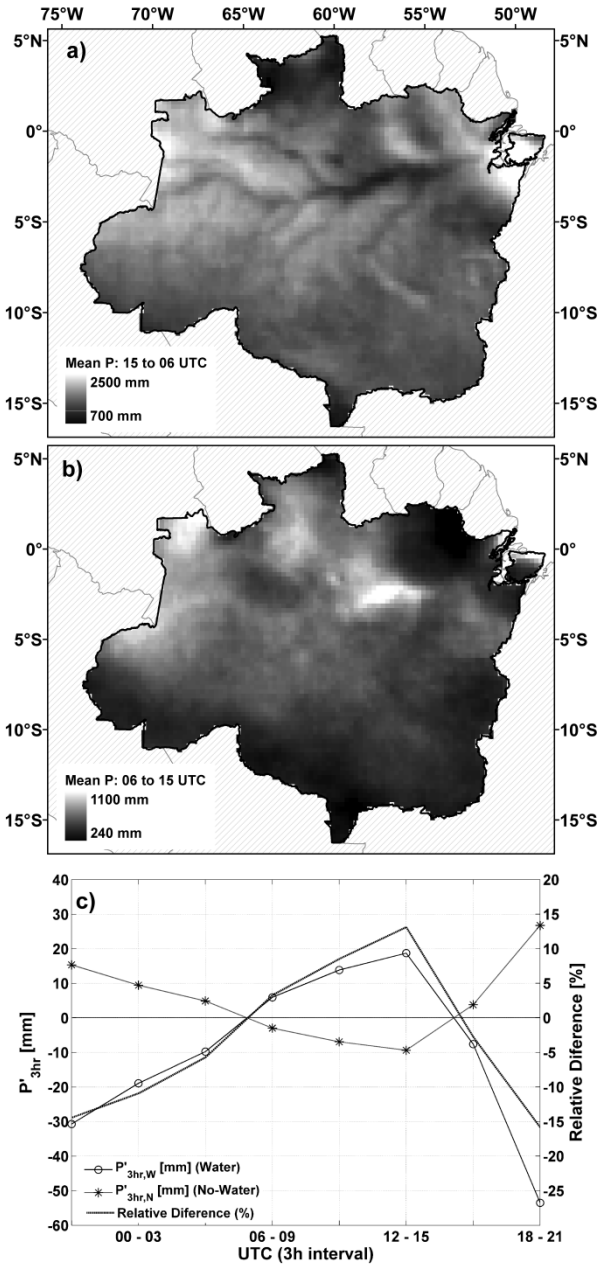

Figure 4. *P* occurring between (a) 06 and 15 UTC; and (b) between 15 and 06 UTC. In (c), diurnal variation of P'_{3hr} averaged over grid-points denoted by "Water" (line with stars) and by "No Water" (line with circles) and its relative difference (bold line).

Fig. 4a and 4b show mean annual rainfall occurring during afternoon-night (A-N) period (15 to 06 UTC, or approximately 11 to 02 h in local time) and during night-morning (N-M) period (06 to 15 UTC or approximately 02 to 11 h in local time). The lower rainfall near large rivers is very marked in the A-N period and is even more pronounced than in Fig. 2a, mainly over the Rio Amazon. During the N-M period the opposite is found. A large increase in *P* is observed along the Rio Amazon between its confluences with Rios Madeira and Tapajós, with a less pronounced increase in *P* along the Rios Negro and Solimões and

Balbina reservoir. Fig. 4c shows the diurnal variation of averaged P'_{3hr} in the "Water" ($P'_{3hr,W}$) and "No Water" ($P'_{3hr,N}$) grid-points of the test area. Detailed information concerning diurnal variation of precipitation is presented in Table 2.

Table 2. Summary of diurnal variation in rainfall [(a)]

Time Interval	Total P_{3hr}	P'_{3hr} Mean		P'_{3hr} S.D.		p [(b)]	Rel.Dif.
UTC	(%)	Water	No Water	Water	No Water		
00-03	10	-18.9	9.5	50.1	71.1	0.15	-11%
03-06	10	-9.8	4.9	64.1	84.4	0.35	-6%
06-09	11	6.0	-3.0	57.1	64.3	0.64	3%
09-12	10	13.9	-6.9	44.6	49.4	0.89	9%
12-15	9	18.7	-9.4	44.2	45.2	0.94	13%
15-18	17	-7.6	3.8	83.3	94.2	0.32	-3%
18-21	20	-53.5	26.8	99.2	103.5	**0.01**	-16%
21-00	13	-30.7	15.4	54.1	63.1	**0.01**	-14%

[(a)] fraction of P (1998-2009); mean and standard deviation (S.D.) of P'_{3hr} from grid-points denoted by "Water" and "No Water"; probability (p) of observed difference between $P'_{3hr,N}$ and $P'_{3hr,W}$, on the null hypothesis of no difference in rainfall between "Water" and "No Water"; and relative difference between $P'_{3hr,W}$ and $P'_{3hr,N}$.

[(b)] Significant values are marked in bold.

The reduction of $P'_{3hr,W}$ and the increase of $P'_{3hr,N}$ occurs during afternoon and early evening, with a relative peak difference of -16 % between 18 and 21 UTC. In fact, this effect occurs in all 3-hour intervals between 15-06 UTC, which are the wettest, accounting for 70% of total annual rainfall. The increase of $P'_{3hr,W}$, and the decrease of $P'_{3hr,N}$, are observed during the night and morning.

The relative differences between $P'_{3hr,W}$ and $P'_{3hr,N}$ are larger for rainfall occurring in most 3-hour intervals than those found for P'. However, these differences are only statistically significant for the 18-21 UTC and the 21-00 UTC time intervals, where the lower rainfall near rivers is observed. The increased P near large rivers during the N-M period was not statistically significant although evident in Fig. 4b.

The overall reduction of rainfall over water bodies reported here runs counter to the TRMM 3B42 systematically-positive errors over inland water bodies reported by *Tian and Peters-Lidard* [2007] in southeastern USA. However, the lower rainfall over large rivers is significant during afternoon, when most rainfall is convective, in agreement with *Yang and Smith* [2008]. The observed inversion and timing of the rainfall pattern over large rivers is

supported by other observations [*Cutrim et al.,* 2000*; Fitzjarrald et al.,* 2008*; Negri et al.,* 2000] and by the descriptions of river breeze effects on precipitation [*Garstang and Fitzjarrald,* 1999].

Although quantitative estimates of reduction in rainfall over large Amazonian water bodies have been given here, they cannot be regarded as fully definitive measures, since (among other limitations) the test area was selected subjectively. Furthermore, the spatial resolution of TRMM 3B42 (~ 25 km) may be larger than the width of most Amazon rivers: when TRMM 3B42 mean annual rainfall is computed at a grid-point, the corresponding grid-square may include areas remote from the water body itself, so that the reduction in rainfall close to large water bodies may well be locally higher than reported in this study.

3.4. Conclusion

The reportedly-lower rainfall over large water bodies in the Brazilian Amazon was explored using TRMM 3B42 rainfall data. Three descriptors of rainfall (mean annual total, *P*; mean number of days with more than 2 mm of rain, *W*; and mean annual rainfall accumulated in 3-hour intervals, P_{3hr}) were analyzed. It is concluded that:

(i) Visually, the TRMM 3B42 data show a very clear reduction in *P* and *W* near large water bodies. This effect is particularly marked along the course of the Solimões/Amazon rivers, along the major tributaries (particularly along the Rios Tapajós and Negro), and near the extensive Balbina reservoir;

(ii) This visual evidence was complemented by a quantitative analysis within a selected test area, using an analytical procedure similar to a statistical significance test. This showed that both *P* and *W* were lower near large water bodies, by 5% and 6.5% respectively;

(iii) The reduction in rainfall near large rivers is greatest during the afternoon (15 to 06 UTC), when most rainfall is convective. An opposite pattern occurring during night-morning (06- 15 UTC) is clearly discernible, although not statistically significant using the approximate test-procedure used.

(iv) The observed reduction of precipitation over large water bodies and its diurnal variation is not consistent with errors over inland water bodies in TRMM 3B42 data reported by *Tian and Peters-Lidard* [2007] but is in accordance with other observational studies and description of river breeze effects on precipitation.

Factors that include the uncertainty in TRMM 3B42 rainfall estimates and the scale of the TRMM 3B42 grid suggest that the quantitative estimates of rainfall reduction close to large rivers reported here should not be regarded as definitive; and reductions in P, W and P_{3hr} may well be locally greater than those given.

Acknowledgments

The authors are grateful for support from the Brazilian agencies FINEP and ANA; the TRMM data supplied by NASA and associated agencies; and for constructive comments of Professor David Fitzjarrald, Jhan Carlo Espinoza Villar, and anonymous reviewers.

References

Buarque, D.C., Clarke, R.T., Mendes, C.A.B. 2010. Spatial correlation in precipitation trends in the Brazilian Amazon. J. Geophys. Res., 115, D12108, doi:10.1029/2009JD013329.

Coe, M.T., Costa, M.H., Howard, E.A. 2008. Simulating the surface waters of the Amazon River basin: Impacts of new river geomorphic and flow parameterizations. Hydrol. Processes, 22, 14, 2542–2553, doi:10.1002/hyp.6850.

Collischonn, B., Collischonn, W., Tucci, C.E.M. 2008. Daily hydrological modeling in the Amazon basin using TRMM rainfall estimates. J. Hydrol., 360, 1–4, 207–216, doi:10.1016/j.jhydrol.2008.07.032.

Cressie, N.A.C. 1993. Statistics for Spatial Data. Rev. ed., Wiley, New York.

Cutrim, E.M., Martin, D.W., Butzow, D.G., Silva, I.M., Yulaeva, E. 2000. Pilot analysis of hourly rainfall in central and eastern Amazonia. J. Clim., 13, 1326–1334, doi:10.1175/1520-0442(2000)013<1326:PAOHRI>2.0.CO;2.

de Gonçalves, L.G.G., Shuttleworth, W.J., Nijssen, B., Burke, E.J., Marengo, J.A., Chou, S.C., Houser, P., Toll, D.L. 2006. Evaluation of model-derived and remotely sensed precipitation products for continental South America. J. Geophys. Res., 111, D16113, doi:10.1029/2005JD006276.

Espinoza, J.C., Ronchail, J., Guyot, J.L., Cochonneau, G., Naziano, F., Lavado, W., de Oliveira, E., Pombosa, R., Vauchel, P. 2009. Spatiotemporal rainfall variability in the Amazon basin countries (Brazil, Peru, Bolivia, Colombia, and Ecuador). Int. J. Climatol., 29,11, 1574–1594, doi:10.1002/joc.1791.

Fitzjarrald, D.R., Sakai, R.K., Moraes, O.L.L., Cosme de Oliveira, R., Acevedo, O.C., Czikowsky, M.J., Beldini, T. 2008. Spatial and temporal rainfall variability near the Amazon-Tapajós confluence. J. Geophys. Res., 113, G00B11, doi:10.1029/2007JG000596.

Garstang, M., Fitzjarrald, D.R. 1999. Observations of Surface to Atmosphere Interactions in the Tropics. Oxford Univ. Press, Oxford, U. K.

Hess, L.L., Melack, J.M., Novo, E.M.L.M., Barbosa, C.C.F., Gastil, M. 2003. Dual-season mapping of wetland inundation and vegetation for the central Amazon basin. Remote Sens. Environ., 87, 404–428, doi:10.1016/j.rse.2003.04.001.

Huffman, G., Adler, R., Bolvin, D., Gu, G., Nelkin, E., Bowman, K., Hong, Y., Stocker, E., Wolff, D. 2007. The TRMM Multisatellite Precipitation Analysis (TCMA): Quasi-global, multiyear, combined-sensor precipitation estimates at fine scales. J. Hydrometeorol., 8, 38–55, doi:10.1175/JHM560.1.

Hughes, D.A. 2006. Comparison of satellite rainfall data with observations from gauging station networks. J. Hydrol., 327, 3–4, 399–410, doi:10.1016/j.jhydrol.2005.11.041.

Joyce, R.J., Janowiak, J.E., Arkin, P.A., Xie, P. 2004. CMORPH: A method that produces global precipitation estimates from passive microwave and infrared data at high spatial and temporal resolution. J. Hydrometeorol., 5, 487–503, doi:10.1175/1525-7541(2004)005<0487:CAMTPG>2.0.CO;2.

Negri, A.J., Anagnostou, E.N., Adler, R.F. 2000. A 10-yr climatology of Amazonian rainfall derived from passive microwave satellite observations. J. Appl. Meteorol., 39, 1, 42–56, doi:10.1175/1520-0450(2000)039<0042:AYCOAR>2.0.CO;2.

Oliveira, A.P., Fitzjarrald, D.R. 1993. The Amazon river breeze and the local boundary layer: I. Observations. Boundary Layer Meteorol., 63, 141–162, doi:10.1007/BF00705380.

Oliveira, A.P., Fitzjarrald, D.R. 1994. The Amazon river breeze and the local boundary layer: II. Linear analysis and modeling. Boundary Layer Meteorol., 67, 75–96, doi:10.1007/BF00705508.

Pereira Filho, A.J., Carbone, R.E., Janowiak, J.E., Arkin, P., Joyce, R., Hallak, R., Ramos, C.G.M. 2010. Satellite rainfall estimates over South America—Possible applicability to the water management of large watersheds. J. Am. Water Resour. Assoc., 46, 2, 344–360, doi:10.1111/j.1752-1688.2009.00406.x.

Ribeiro, M.N.G., Adis, J. 1984. Local rainfall variability—A potential bias for bioecological studies in the central Amazon. Acta Amazon., 14, 159–174.

Silva Dias, M.A.F., Silva Dias, P.L., Longo, M., Fitzjarrald, D.R., Denning, A.S. 2004. River breeze circulation in eastern Amazonia: Observations and modeling results. Theor. Appl. Climatol., 78, 111–122, doi:10.1007/s00704-004-0047-6.

Tian, Y., Peters-Lidard, C.D. 2007. Systematic anomalies over inland water bodies in satellite-based precipitation estimates. Geophys. Res. Lett., 34, L14403, doi:10.1029/2007GL030787.

Wilks, D.S. 2006. Statistical Methods in the Atmospheric Sciences. 2nd ed., 467, Academic, San Diego, Calif.

Yang, S., Smith, E.A. 2008. Convective–stratiform precipitation variability at seasonal scale from 8 yr of TRMM observations: Implications for multiple modes of diurnal variability. J. Clim., 21, 4087–4114, doi:10.1175/2008JCLI2096.1.

CAPÍTULO 4

On the sources of hydrological prediction uncertainty in the Amazon

Capítulo 4: On the sources of hydrological prediction uncertainty in the Amazon

Os erros nos resultados de sistemas de previsão hidrológica baseados em modelos hidrológicos de base física são oriundos de: (i) incertezas na estrutura e parâmetros do modelo hidrológico, (ii) incertezas nos forçantes meteorológicos futuros e (iii) incertezas das condições hidrológicas iniciais no momento da previsão [*Liu e Gupta*, 2007]. Sendo assim, o conhecimento da importância relativa de cada um destes termos pode indicar as ações prioritárias no desenvolvimento de sistemas de previsão hidrológica, podendo ser a melhora da estrutura do modelo, dos forçantes meteorológicas ou das estimativas das condições iniciais através de sistemas de assimilação de dados.

Neste capítulo, apresenta-se um estudo de previsibilidade na bacia Amazônica utilizando-se o modelo MGB-IPH baseado na implementação exposta no Capítulo 2. Avalia-se a importância relativa das condições hidrológicas iniciais do modelo e dos forçantes meteorológicos, mais especificamente precipitação, como fontes de incerteza para a previsão de vazões na Amazônia. No contexto da pesquisa desenvolvida nesta tese, este capítulo teve um papel fundamental – o de indicar a caminho a ser seguido para desenvolver previsões hidrológicas na bacia Amazônica usando em modelos de base física.

Para este estudo utiliza-se uma abordagem desenvolvida por *Wood and Lettenmaier* [2008], que compara a incerteza de previsões de vazão geradas a partir de um modelo forçado a partir de conjunto de condições hidrológicas iniciais e com a de previsões geradas com a mesma condição inicial, porém com diferentes forçantes meteorológicas. De posse dos dois conjuntos de previsões, avaliou-se a partir de qual antecedência a incerteza na previsão devido a erros na precipitação começam a ser mais importantes que a incertezas nas condições iniciais do modelo hidrológico. Pesquisou-se também como estes resultados variam espacialmente e em função da estação do ano, que variáveis de estado são as mais importantes e como os resultados se relacionam com as características da bacia Amazônica.

Em resumo, os resultados mostram que, para horizontes de previsão até cerca de 1 a 3 meses, as condições hidrológicas inicias do modelo são mais importantes que as forcantes meteorológicas na previsão de vazões nos principais rios Amazônicos. Destaca-se a importância de variáveis de estado relacionadas a águas superficiais como vazões e níveis d'água nos rios e volumes nas várzeas de inundação.

Os resultados sugerem a potencialidade de um sistema baseado em um modelo hidrológico forçado com dados meteorológicos históricos e usando condições iniciais ótimas para previsão de vazões em tempo real na bacia Amazônica. Além disso, mostra-se a importância do desenvolvimento de técnicas de assimilação de dados em modelos

hidrológicos para estimar os estados hidrológicos a serem utilizados no inicio de cada previsão. Tais conclusões motivaram o desenvolvimento do Capítulo 5, onde são desenvolvidas e avaliadas técnicas de assimilação de dados e vazões e níveis d'água e previsões hidrológicas na bacia Amazônica.

Capítulo 4: On the sources of hydrological prediction uncertainty in the Amazon

This chapter is based on the following paper published at Hydrology and Earth System Sciences:

Paiva, R.C.D., Collischonn, W., Bonnet, M.P., and de Gonçalves, L.G.G. 2012. On the sources of hydrological prediction uncertainty in the Amazon. Hydrol. Earth Syst. Sci., 16, 3127-3137, doi:10.5194/hess-16-3127-2012.

Abstract

Recent extreme events in the Amazon River basin and the vulnerability of local population motivate the development of hydrological forecast systems using process based models for this region. In this direction, the knowledge of the source of errors in hydrological forecast systems may guide the choice on improving model structure, model forcings or developing data assimilation systems for estimation of initial model states. We evaluate the relative importance of hydrologic initial conditions and model meteorological forcings errors (precipitation) as sources of stream flow forecast uncertainty in the Amazon River basin. We used a hindcast approach that compares Ensemble Streamflow Prediction (ESP) and a reverse Ensemble Streamflow Prediction (reverse-ESP). Simulations were performed using the physically-based and distributed hydrological model MGB-IPH, comprising surface energy and water balance, soil water, river and floodplain hydrodynamics processes. Model was forced using TRMM 3B42 precipitation estimates. Results show that uncertainty on initial conditions play an important role for discharge predictability even for large lead times (~ 1 to 3 months) on main Amazonian Rivers. Initial conditions of surface waters state variables are the major source of hydrological forecast uncertainty, mainly in rivers with low slope and large floodplains. Initial conditions of groundwater state variables are important mostly during low flow period and in the southeast part of the Amazon, where lithology and the strong rainfall seasonality with a marked dry season may be the explaining factors. Analyses indicate that hydrological forecasts based on a hydrological model forced with historical meteorological data and optimal initial conditions, may be feasible. Also, development of data assimilation methods is encouraged for this region.

4.1. Introduction

Recent extreme hydrological events have occurred in the past years in the Amazon River basin, such as the 2009 flood [*Chen et al.,* 2010] and the 1996 [*Tomasella et al.,* 2010], 2005 [*Marengo et al.,* 2008; *Zeng et al.,* 2008; *Chen et al.,* 2009] and 2010 [*Espinoza et al.,* 2011, *Marengo et al.,* 2011] droughts. These extreme events caused several impacts on local population, since most settlements lie along the Amazon and its main tributaries where susceptibility to floods is large. Also, local population strongly depends on these rivers for transportation of people and goods, agriculture, generation of hydroelectricity, among others. The vulnerability to hydrological extremes could be reduced with information provided by Hydrological Forecast Systems.

Currently, the attempts for developing hydrological forecasts in the Amazon are all based in statistical methods. *Uvo and Grahan* [1998] and *Uvo et al.* [2000] developed seasonal water level and discharge forecasts (March-May period) for 6 river stream gauges in the Brazilian Amazon, including Belo Monte, Samuel and Balbina reservoirs sites and also Negro River at Manaus, based on rain gauge data, streamflow data and Pacific and Atlantic Ocean sea surface temperatures (SSTs) using a canonical correlation analysis in the first and an artificial neural network approach in the latter. The authors conclude that, in the Amazon, it is possible to forecast seasonal runoff one season in advance with a certain degree of accuracy using empirical models, SST and/or precipitation data, with correlation coefficient between observed and estimated discharges ranging from -0.38 to 0.74 in *Uvo and Grahan* [1998] and from 0.53 to 0.86 in *Uvo et al.* [2000]. *Schongart and Junk* [2007] presented retrospective forecasts of the maximum water level in Central Amazonia (Manaus) using El Niño - Southern Oscillation (ENSO) indices. *Cappalaere et al.* [1996] developed flood forecasts methods for Central Amazonia (Manaus) for lead times ranging from 10 to 60 days, using statistical-type modelling of the stage time series recorded at the main river gauges in the Brazilian Amazon basin.

However, hydrological forecast systems based on physically based hydrological models such as *Wood et al.* [2002], *Collischonn et al.* [2005] or *Thielen et al.* [2009] were not evaluated in the region, although hydrological modelling of the Amazon is being continually developed [e.g. *Beighley et al.*, 2009; *Decharme et al.*, 2008; *Coe et al.*, 2007; *Getirana et al.*, 2010; *Paiva et al.*, 2011; *Paiva et al.*, 2012a,b ; *Trigg et al.*, 2009; *Yamazaki et al.*, 2011, *Guimberteau et al.*, 2012].

Prediction errors of the hydrological forecast systems arise from uncertainty on: (i) model structure and parameters, (ii) atmospheric forcing such as precipitation and (iii) initial states (e.g. preceding soil moisture or volume of water stored in rivers and floodplains). The type of model forcings can range from simple climatology to an ensemble of historical meteorology [*Day*, 1985] or to more complex weather forecasts obtained from General or Regional Circulation Models [e.g. *Collischonn et al.*, 2005; *Wood et al.*, 2002]. In contrast, several data assimilation methods [*Reichle*, 2008; *Liu and Gupta*, 2007] can be employed to improve initial states estimates. Numerous hydrologic remote sensing products that can be assimilated are been developed in current years, such as: river water levels from nadir altimeters [*Alsdorf et al.*, 2007; *Santos da Silva et al.*, 2010], Terrestrial Water Storage from GRACE mission [*Tapley et al.*, 2004a,b; *Chen et al.*, 2009], soil moisture estimates from

SMOS mission [*Kerr et al.*, 2001], flooded inundation extent [*Hess et al.*, 2003; *Papa et al.*, 2010; *Prigent et al.*, 2007], energy fluxes and evapotranspiration [e.g. *Vinukollu et al.*, 2011] and in future flooded extent with water level from the SWOT mission [*Durand et al.*, 2010]. Therefore, the knowledge of the relative importance of each source of errors plays an important role on the hydrological predictability and also supports the choice of technique to be first developed: improving model structure, improving or looking for better model forcings or developing data assimilation systems for better initial conditions estimates. In the later case, it is also important to evaluate what are the key state variables and what data to assimilate.

In this direction, *Wood and Lettenmaier* [2008] developed an approach to evaluate the relative importance of errors in hydrologic initial conditions and model meteorological forcings as sources of hydrologic uncertainty. Latter, *Shukla and Lettenmaier* [2011] and *Shukla et al.* [2011a] applied this approach to evaluate seasonal forecasts of cumulative runoff and soil moisture in the United States and globally, respectively. We use a similar approach to evaluate the relative importance of hydrologic initial conditions and model meteorological forcings errors (precipitation) as sources of stream flow forecast uncertainty in the Amazon River basin. We assess (i) when each of these features are more important, i.e. at which lead time uncertainty arising from meteorological forcings errors becomes larger than from initial conditions errors and in which season (ii) where, i.e. in which rivers; (iii) what are the key state variables contributing for uncertainty; and (iv) how it relates to Amazon River basin characteristics.

4.2. Methods

4.2.1. Amazon River basin

The Amazon River basin is the largest hydrological system of the world. It has an area of approximately 6 million km^2, is responsible for ~15% of fresh water released into the oceans and covers several South American countries, including Brazil, Bolivia, Peru, Colombia, Ecuador, Venezuela and Guiana (Fig. 1a). The Amazon consists of three main morphological units, namely the Andes, Amazon plain and the Guyanese and Brazilian shields (Fig. 1). Extensive seasonally flooded areas are found at the Amazon plains [*Hess et al.*, 2003; *Papa et al.*, 2010; *Prigent et al.*, 2007] (see Fig. 1b), which store and release large

amounts of water from the rivers and consequently attenuate and delay flood waves into several days or months [*Paiva et al.*, 2012a,b].

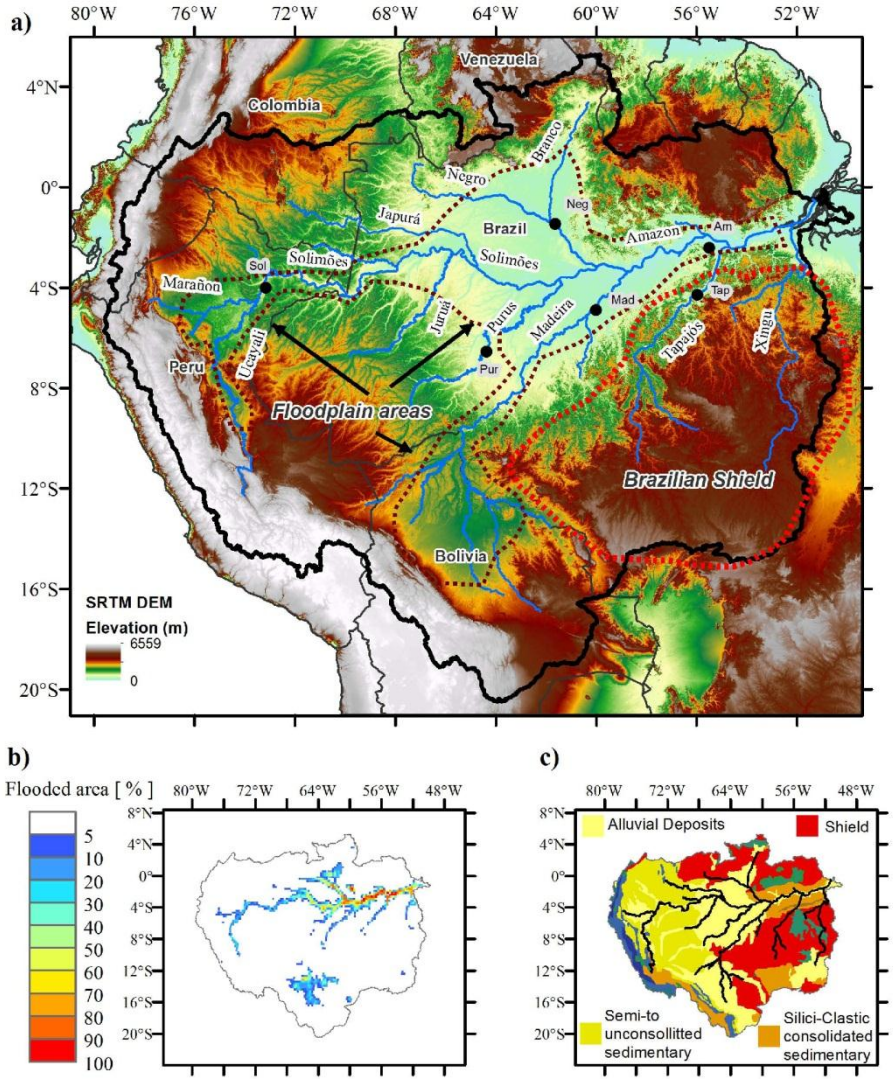

Figure 1. (a) Amazon River basin with main tributaries, international limits, relief from SRTM DEM [*Farr et al.*, 2007] and sites used in analyses (black circles), (b) Mean flooded area (%) derived from *Papa et al.* [2010] and (c) Lithological map derived from *Durr et al.* [2005].

Due to its size, the Amazon basin presents important spatial rainfall variability, as briefly described below following *Espinoza et al.* [2009a]. Extremely rainy regions (more than 3000 mm.year^{-1}) are found in the northeast, in the Amazon delta exposed by the intertropical convergence zone (ITCZ) and at southeast close to the South Atlantic Convergence Zone (SACZ). Rainfall decreases towards southeast (~1500 – 2000 mm.year^{-1}) and also in the Andes as function of altitude (rainfall is generally less than 1000 mm.year^{-1} in areas over 3000 m). Concerning the seasonal cycle, contrasting rainfall regimes are found in northern and southern parts of the basin, with rainy season in June, July and August – JJA (in

December, January and February - DJF) in the North (South). Seasonal variability, with defined wet and dry seasons, is present at southern and eastern parts of the basin, including Xingu, Tapajós, Madeira, Purus and Juruá river basins, but also at northern areas from Branco river basins (see Fig. 1a). Areas located at Northwest (Maranon, Japurá and Negro river basins) exhibit weaker seasonal regime with large amounts of rainfall rates during the role year (see Fig. 1a).

Table 1. Gauging stations from Fig. 1a with summary of discharge regime, MGB-IPH model skill and results.

ID	Station	River	Area (10^3km^2)	Q_{mean} (10^3m^{3}s^{-1})	Q_{min} (10^3 m^{3}s^{-1})	Q_{max} (10^3 m^{3}s^{-1})	s_{VC} (10^3 m^{3}s^{-1})	E_{NS}	T (days)
Sol 10075000	Tamshiyacu	Upper Solimões	724	29.5	14.5 (Sep)	43.0 (May)	0.35	0.74	37
Neg 14840000	Moura	Negro	648	31.4	10.7 (Jan)	55.6 (Aug)	0.59	0.65	56
Mad 15860000	Faz. Vista Alegre	Madeira	1320	26.9	6.5 (Sep)	53.0 (Apr)	0.65	0.92	53
Tap 17730000	Itaituba	Tapajós	461	11.2	3.5 (Sep)	22.8 (Mar)	0.64	0.87	41
Pur 13880000	Canutama	Purus	238	6.4	1.3 (Oct)	12.8 (Apr)	0.71	0.91	34
Am 17050001	Obidos	Amazon	4714	182.8	98.6 (Nov)	250.1 (Jun)	0.31	0.77	72

Q_{mean} – mean discharge, Q_{min} and Q_{max} – minimum and maximum monthly discharge derived from climatology with respective time of occurrence, s_{VC} – seasonal coefficient of variability computed as the ratio between the standard deviation of monthly discharges and Q_{mean}, E_{NS} – Nash and Suttcliffe index from simulated and observed discharges, T values as described in 4.2.2 and 4.3.1.

Spatial variability in the discharge regime is also observed in the Amazon, as described by *Espinoza et al.* [2009b] and as can be seen in Table 1. Rivers draining southern areas such as the Xingu, Tapajós, Madeira, Purus and Juruá (Fig. 1a) exhibit a southern tropical regime, with a maximum from March to May (MAM) and a minimum from August to October (Table 1). A northern tropical regime is found at Branco River, where maximum flow occurs during June to August and minimum during December to March. Other rivers have weaker seasonal regimes (see s_{VC} values from Table 1), in some cases due to rainfall characteristics (e.g. Negro and Japura Rivers) and in the Solimões/Amazon main stem, due to the contribution of lagged hydrographs from northern and southern areas. In the latter, high water occurs generally from May to July and low water from September to November and 1-3 months earlier in upper Solimões due to the flood wave travel time.

4.2.2. ESP versus rev-ESP approach

We used a hindcast approach developed by *Wood and Lettenmaier* [2008] that contrasts Ensemble Streamflow Prediction (ESP) and a reverse Ensemble Streamflow Prediction (reverse-ESP) (see Fig. 2). This approach uses ensemble model runs from a large scale distributed and process based hydrological model to evaluate the relative importance of errors in hydrologic initial conditions - ICs (e.g. soil moisture, groundwater storage, river discharge, floodplain storage, etc.) and model meteorological forcings – MFs (e.g. precipitation, surface air temperature, incoming solar radiation, etc.) as sources of stream flow forecast uncertainty.

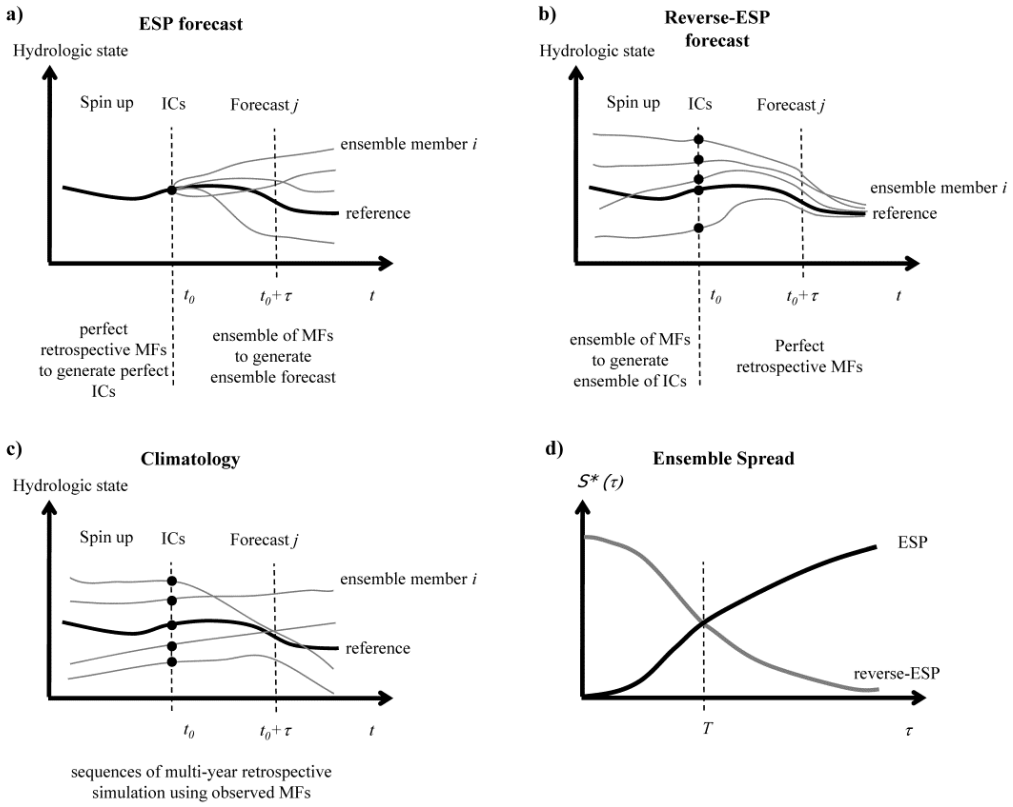

Figure 2. Schematic representation of evolution of hydrologic states in spinup and forecast for (a) ESP approach, (b) reverse-ESP approach, (c) climatology and (d) relative ensemble spread *S** as function of lead time τ. Modified from *Wood and Lettenmaier* [2008].

In the ESP [*Day*, 1985], the model uses "perfect" initial conditions and runs forced by an ensemble of observed meteorological data from past years (see Fig. 2a). An estimate of "perfect" initial conditions is computed using a hydrological model driven by observed meteorological forcings up to the time of forecast (e.g. forecast starts with model states from

15 June 2000). Then, an ensemble forecast is obtained using observed meteorological data resampled from past years (e.g. meteorological data from 15 June to 25 September of years 1998, 1999, …, 2009). As a result, ESP shows a proxy of stream flow forecast uncertainty due to meteorological forcing errors [*Wood and Schaake*, 2008]. In contrast, in reverse-ESP the model runs from an ensemble of simulated initial conditions from past years forced by a perfect forecast (see Fig. 2b). The initial conditions ensemble is obtained using the hydrological model forced by observed meteorological data resampled from past years during the spinup period (up to the date of forecast) (e.g. model initial states from 15 June of years 1998, 1999, …, 2009). Observed meteorological data from current year is used as perfect meteorological forecast (e.g. meteorological data form 15 June to 25 September 2000). Consequently, the reverse-ESP produces a proxy of stream flow forecast uncertainty due to model initial conditions errors. Model climatology (Fig. 2c), where either initial conditions and meteorological forcings are unknown, is used as a reference for comparing ESP and reverse-ESP model runs.

We use the ensemble spread (either for ESP, reverse-ESP and model climatology) as a measure of uncertainty in stream flow forecasts. For a given forecast j starting at the time interval t_0 and at τ lead time, the ensemble spread S is computed as the mean square deviation using simulated discharge Q_{sim} as a reference:

$$S(\tau, j) = \frac{1}{N}\sum_{i=1}^{N}\left(Q_{\text{ens}i} - Q_{\text{sim}}\right)^2 \quad (1)$$

where N is the ensemble size, $Q_{\text{ens}i}$ is stream flow from ensemble member i . The indexes t and τ were omitted for simplicity. S is computed for the ESP (S_{ESP}), reverse-ESP ($S_{\text{rev-ESP}}$) and model climatology (S_{CLIM}) ensembles. For a proper evaluation of stream flow uncertainty in different time periods, the model climatology is used as a reference and relative spreads are computed as $S^*_{\text{ESP}} = S_{\text{ESP}} / S_{\text{CLIM}}$ and $S^*_{\text{rev-ESP}} = S_{\text{rev-ESP}} / S_{\text{CLIM}}$. Finally, results are averaged from all forecasts:

$$S^*(\tau) = \frac{1}{M}\sum_{j=1}^{M} S^*(\tau, j) \quad (2)$$

where M is the total number of forecasts performed in the test period and $S^*(\tau)$ is the relative ensemble spread as function of the lead time τ.

The comparison of the spread of both sets of ensembles allows the evaluation of the relative importance of the initial conditions and meteorological forcings on model predictability as functions of lead time (see Fig. 2d). Moreover, a proxy of the river "memory" T can be obtained by verifying in which lead time τ the spread of ESP ensemble becomes larger than the reverse-ESP:

$$T = min(\tau) \mid S^*_{\text{rev-ESP}}(\tau) < S^*_{\text{ESP}}(\tau) \quad (3)$$

4.2.3. Hydrological model

We used the MGB-IPH model [*Collischonn et al.*, 2007; *Paiva et al.*, 2011a], which is a large scale, distributed and process based hydrological model with a hydrodynamic module described in *Paiva et al.* [2011]. It simulates surface energy and water balance and also discharge, water level and flood inundation on a complex river network. We used results from a model application in the Amazon River basin (Fig. 1a) presented in *Paiva et al.* [2012b], as briefly described below. The model was forced using TRMM 3B42 precipitation estimates [*Huffman et al.*, 2007], with spatial resolution of 0.25^o x 0.25^o and daily time step for a period spanning 12 years (1998 - 2009) and meteorological data obtained from the CRU CL 2.0 dataset [*New et al.*, 2002]. Stream gauge data were provided by the Brazilian Agency for Water Resources (ANA), the Peruvian and Bolivian National Meteorology and Hydrology Services (both SENAMHI) and the HYBAM program (Hydrology, Biogeochemistry and Geodynamic of the Amazon Basin, http://www.ore-hybam.org/). The model parameters related to soil water budget were calibrated using discharge data from part of the stream gauges (47 stations). Then, the model was validated against discharge and water level data from stream gauge stations (111 and 69 sites, respectively), water levels derived from ENVISAT satellite altimetry data [*Santos da Silva et al.*, 2010] (212 sites), Terrestrial Water Storage from GRACE mission [*Tapley et al.*, 2004a,b] and flood inundations extent from *Papa et al.* [2010]. Comparisons between simulations and observations showed relatively high Nash and Suttcliffe index (E_{NS}) values and a good model performance. E_{NS} values were larger than 0.6 in ~70% of discharge gauges and Table 1 shows E_{NS} ranging from 0.65 to 0.91 at the 6 discharge gauging stations analyzed in Section 4.3.1. (Fig. 1a). Also, E_{NS} values where larger than 0.6 in ~60% of the water level stations derived from satellite altimetry.

Similarly, total Amazon flood extent and terrestrial water storage agreed with observations with E_{NS} values of 0.71 and 0.93, respectively.

4.2.4. Model runs

We performed 6 different model runs: (i) a retrospective simulation from which the ensemble of model climatology is derived and used as initial conditions for rev-ESP runs; (ii) a ESP run; (iii) a reverse-ESP run; and three restricted reverse-ESP runs, where in the first only (iv) surface waters state variables (river discharge and water level, floodplain storage and surface runoff) are considered, in the second only (v) soil moisture state variable is considered and in the latter only (vi) groundwater state variables are considered. In all model runs, simulations used the 1998 to 2009 time period and ensembles have 12 members. ESP and reverse-ESP model runs generated 4 forecasts per year with up to 100 days lead time starting at 15 March, 15 June, 15 September and 15 December. Note that since we are using meteorological data obtained from the CRU CL 2.0 dataset [*New et al.*, 2002], which provides only climatological values, uncertainty of meteorological variables different from precipitation is not accounted. We choose this simplification because MGB-IPH model using CRU CL 2.0 showed a reasonable performance when results were compared with observations [*Paiva et al.*, 2012b] and most of Amazon discharge variability is due to precipitation variability.

4.3. Results

4.3.1. Forecast uncertainty in main rivers

We first explore forecast uncertainty results in 6 sites located in the main tributaries of Amazon River basin (see Fig.2a and Table 1) using the 2003/2004 hydrological year as an example (Fig. 3). Results show to be different for each site, although some characteristics are found in all of them.

In upper Solimões River, discharge starts to rise in September, and the spread of the ESP run rapidly surpasses the spread of the reverse-ESP run, showing that the importance of uncertainties in meteorological forcings is larger than from initial conditions (Fig. 3a). This situation changes in the other forecasts (at high water period in forecasts starting in 15

December and 15 March and in flow recession starting in 15 June) when the uncertainty in initial conditions appears to be more important than meteorological forcings. On average, the spread of the ESP ensemble S^*_{ESP} takes 37 days to surpass the spread of the reverse-ESP ensemble (T =37 days in Fig. 3b).

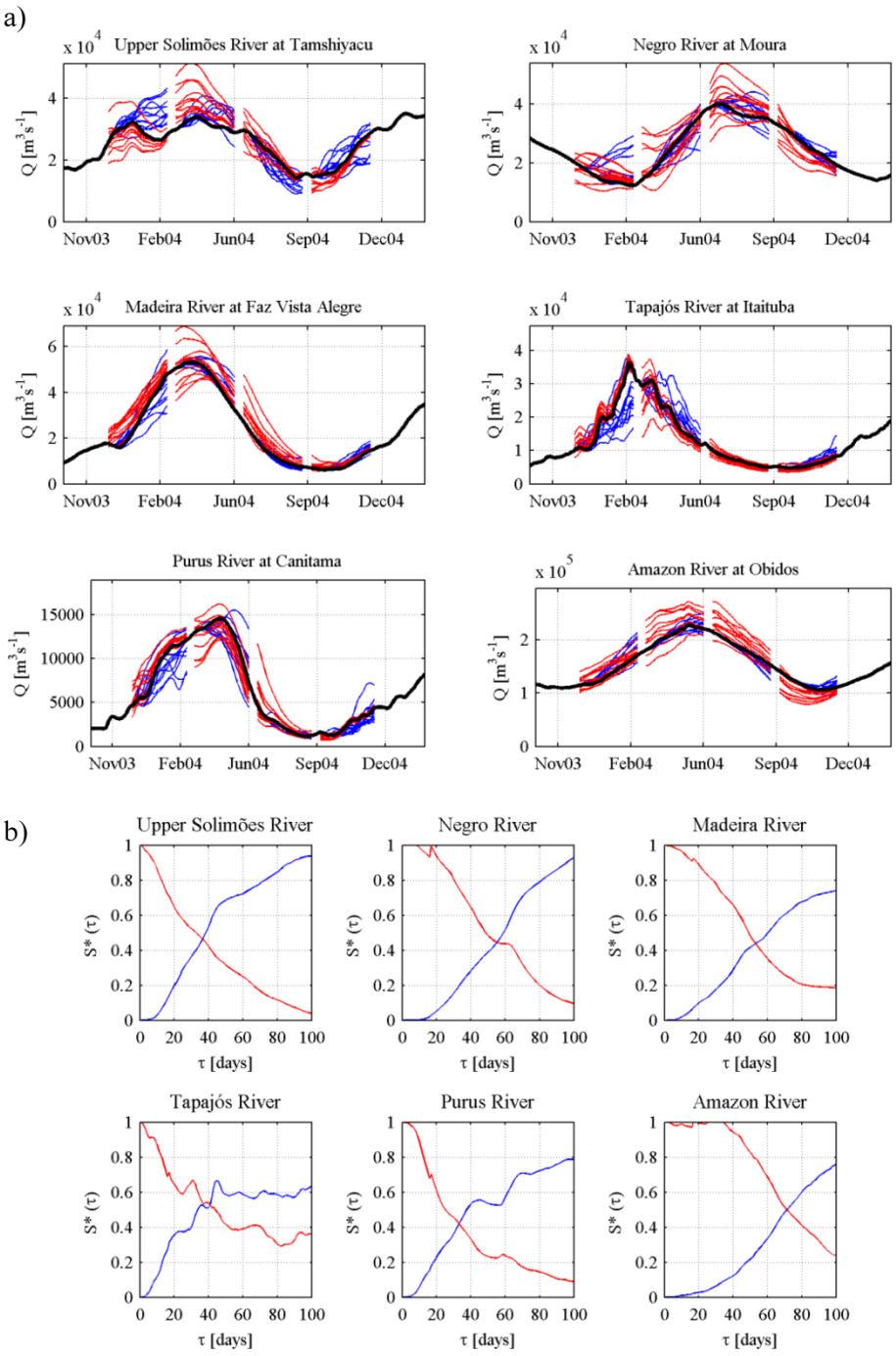

Figure 3. Retrospective simulation (black), ESP (blue) and reverse-ESP (red) (a) discharge results and (b) relative ensemble spread $S^*(\tau)$ as function of the lead time τ. Results are presented at upper Solimões (Sol), Negro (Neg), Madeira (Mad), Tapajós (Tap), Purus (Pur) and Amazon (Am) Rivers at sites shown in Fig. 1a.

At the Negro River site, discharges rise during the MAM period, and differently from upper Solimões River, the forecast uncertainty due to initial conditions shows to be comparable with uncertainty due to meteorological forcings even for large lead times (Fig. 3a). This characteristic is also present at high water (JJA) and flow recession periods (SON and DJF), and as a consequence only after 56 days uncertainty in meteorological forcings becomes more important than in initial conditions (Fig. 3b).

At the rivers draining the southeast part of the Amazon with a southern tropical regime, namely Madeira, Purus and Tapajós Rivers, some common features are found. In DJF period, when discharge slowly starts to rise, and in MAM period, when it increases rapidly almost to flood peak, initial conditions uncertainties are important at the beginning of forecasts but the weight of meteorological forcings uncertainty becomes larger for smaller lead times. In contrast, at high water periods (JJA), flow recession and low water period (SON), the spread of reverse-ESP ensemble greatly surpasses the spread of the ESP ensemble, showing that initial conditions errors may have a large influence in flow forecasts uncertainty (Fig. 3a). *T* values of Purus, Tapajós and Madeira Rivers showed to be different and approximately 34, 41 and 53 days, respectively (Fig. 3b).

In the Amazon main stem, analysis show that the spread of reverse-ESP ensemble greatly surpass the spread of ESP ensemble in all periods of the year, including high water (MAM), low water (SON), rising (DJF) and falling (JJA) periods (Fig. 3a). Uncertainty in meteorological forcings becomes more important than in initial conditions only after 72 days (Fig. 3b).

Meteorological forcings seem to play an important role in forecast uncertainty at the rising water period, but this is not valid or not so strong in some of the largest rivers, such as Solimões, Negro and Amazon. Perhaps this is due to the flood travel times in these rivers and the contribution of lagged hydrographs from areas with different hydrological regimes (Section 4.2.1.). In all rivers, the influence of initial conditions greatly surpasses MF's in high water period and mostly in flow recession and low water period. This characteristic in flow recession and low water period is very strong in rivers with southern tropical regime, where rainfall seasonality is stronger and there is a very marked dry season [*Espinoza et al.*, 2009a; *Espinoza et al.*, 2009b], as described in Section 4.2.1. In all Amazon large rivers, *T* values can be considered very large, ranging from ~30 days at Purus Rivers to ~70 days in the Amazon River, showing that uncertainty on initial conditions may play an important role for hydrological predictability even for large lead times (~ 2 or 3 months).

4.3.2. Spatial analysis

We investigate the spatial distribution of *T* values, indicating at which lead time uncertainty in meteorological forcings becomes more important that initial conditions for hydrological predictability and serving as a proxy of river "memory". According to Fig. 4a, large *T* values are found at almost all Amazonian Rivers. *T* values smaller than 10 days are found mostly in headwater and in the Andean region at west part of the Amazon, where high river slopes are present (see also Fig. 1a). In most of Amazon main tributaries, including Solimões, Juruá, Purus, Madeira, Tapajós, Xingu and Negro River, it is larger than 30 days and in Amazon main stem it is between 2 and 3 months. Results show that initial conditions may be the main source of discharge forecast uncertainty even for large lead times (~ 1 to 3 months) in most Amazonian Rivers.

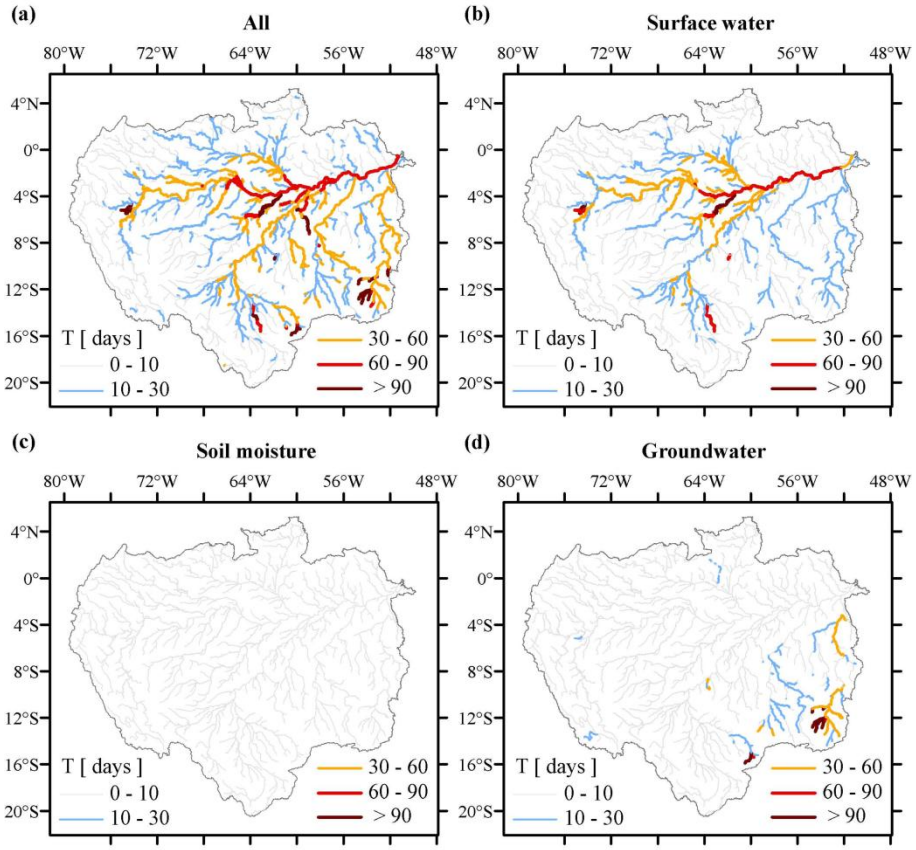

Figure 4. Spatial distribution of *T* values considering (a) all, (b) surface water, (c) soil moisture and (d) groundwater model states variables. Results are shown only in rivers reaches with upstream drainage area larger than 3000 km^2.

Results from restricted reverse-ESP runs (Fig. 4b, 4c and 4d) show larger *T* values in analyzes considering only surface waters state variables (Fig. 4b). This suggests that initial conditions of surface waters state variables, which include river discharge and water levels, surface runoff and floodplain storage, are the major source of hydrological forecast uncertainty. This characteristic is present mostly in Solimões, Negro, Purus, Japurá, Madeira and Amazon Rivers that are located in low slope regions (Fig. 1a) with large seasonally inundated floodplains (see Fig. 1b), as described in Section 4.2.1. *T* values in analyses using soil moisture restricted reverse-ESP run (Fig. 4c) are always less than 10 days, showing that initial conditions of soil moisture are not as important as initial conditions of other state variables. Finally, groundwater state variables showed to be important mostly in Tapajós and Xingu River basins located at southeast part of the Amazon.

The relatively importance of meteorological forcings and initial conditions as sources of hydrological prediction uncertainty is variable according to the period of the year, as shown by seasonal analyses of *T* values (Fig. 5). At rivers draining extensive floodplains, such as Solimões, Negro, Juruá, Madeira and Purus, *T* values are always large, especially in high water and falling period (MAM and JJA, see also Fig. 3). In these time periods, *T* values larger than 90 days are found in the Amazon main stem.

The southeast part of the basin, including Xingu, Tapajos and Brazilian Madeira River basins, presents the most pronounced seasonal variation of *T* values. At high water periods (DJF and MAM, see also Fig. 3), *T* values range from 10 to 30 days. But it increases a lot in low water period (JJA, SON) reaching values larger than 90 days. It shows that in this region, initial conditions are more important for hydrological prediction during low flows.

Results show that in rivers with extensive floodplains, initial conditions of surface waters state variables are the major source of prediction uncertainty and its importance increases during high water and falling period. This behavior may be related to the large flood wave travel times of these rivers, where these flood waves are delayed because floodplains store large volumes of water and release it slowly [*Paiva et al.,* 2012a,b].

On the other hand, at southeast part of the basin, mainly at Tapajós and Xingu Rivers, initial conditions play an important role for prediction of low flows and groundwater state variables showed to be important. This region is the one that presents the strongest rainfall seasonality with a marked dry season as discussed in Section 4.2.1. and by *Espinoza et al.* [2009a,b]. It is also located mostly in the Brazilian Shield, where lithological characteristics differ from the rest of the basin (Fig. 1a and 2c). So, a possible explanation for this behavior is

that during low flows period, river discharge may be dominated by base flow, which is directly related to groundwater storage.

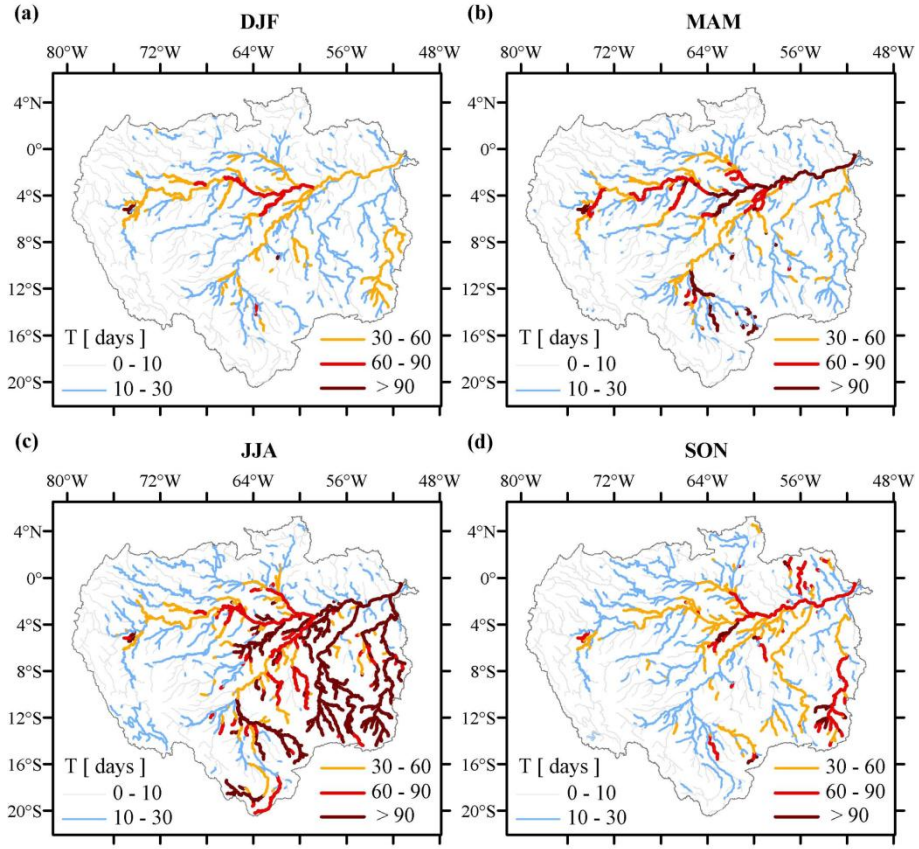

Figure 5. Spatial distribution of *T* values considering (a) DJF, (b) MAM, (c) JJA and (d) SON time periods. Results are shown only in rivers reaches with upstream drainage area larger than 3000 km^2.

Finally, in a first comparison, our results disagree with *Shukla et al.* [2011b], who applied the same methodology in a global analysis, founding results that show that meteorological forcings uncertainty dominate the hydrological prediction uncertainty in the Amazon, even for shorter lead times. However, the results are not fully comparable since we evaluated river discharge while the authors studied cumulative runoff, which do not take into account flow routing throughout river, floodplain and groundwater reservoirs. Consequently, the water time traveling throughout these hydrological compartments and the associated memory to initial water storage in these reservoirs are not considered, and that is probably the reason for the disagreement between results.

4.4. Conclusion

We investigate the importance of model initial conditions and meteorological forcings as sources of hydrological predictions uncertainty in the Amazon River basin. Our investigations show that in the Amazon River basin:

(i) Uncertainty on initial conditions may play an important role for discharge forecasts even for large lead times (~ 1 to 3 months) on main Amazonian Rivers. This suggests that an Ensemble Streamflow Prediction approach (ESP), based on a hydrological model forced with historical meteorological data and using optimal initial conditions, may be feasible for hydrological forecasting even for large lead times (~ 1 to 3 months). Also, development of data assimilation methods is encouraged for reducing model initial conditions uncertainty.

(ii) Initial conditions of surface waters state variables are the major source of hydrological forecast uncertainty, mainly in rivers with low slope and large floodplains, such as Solimões, Juruá, Japurá, Madeira, Negro and Amazon Rivers. Initial conditions of groundwater state variables are important mostly in southeast part of the Amazon, in Tapajós as Xingu Rivers. Soil moisture is not as important as other state variables as a source of hydrological prediction uncertainty.

(iii) The relatively importance of meteorological forcings and initial conditions as sources of hydrological prediction uncertainty is variable according to the period of the year.

(iv) At rivers draining extensive floodplains, initial conditions are more important in all time periods but especially in high water and falling period (MAM and JJA). This can be related to the large flood wave travel times of these rivers, where these flood waves are delayed because floodplains store large volumes of water and release it slowly.

(v) Meteorological forcings are more important in the beginning of rainy season when hydrographs are rising, especially at the rivers draining southeast.

(vi) At southeast part of the basin, mainly at Tapajós and Xingu Rivers, initial conditions play an important role for prediction of low flows (JJA, SON) and groundwater state variables showed to be important. A possible reason is that this region is the one that presents the strongest rainfall seasonality with a marked dry season. Lithology may be an explaining factor, since this region is located mostly over the Brazilian Shield.

Other kind of errors, such as in model structure and parameter, may also play an important role in hydrological predictability. However, we choose not to focus on it supposing

that the hydrological model is already calibrated with sufficient skill and that the main source of errors in a forecast situation would be in initial conditions and meteorological forcings.

Results indicate that hydrological forecasts based on physically based and distributed hydrological models forced with past climate and optimal initial conditions may be feasible in the Amazon River basin and possibly in other world large rivers. It should also be mentioned the potentiality of recent remote sensing developments for providing past meteorological forcings (e.g. Tropical Rainfall Measurement Mission, Huffman et al., 2007, and others) and information to update model states, such as radar altimetry based water levels or discharge derived from previous [*Alsdorf et al.*, 2007, *Santos da Silva et al.*, 2010] or the future SWOT mission [*Durand et al.*, 2010].

Acknowledgments

The authors are grateful for: the financial support from the Brazilian agencies FINEP and ANA ("*Projeto de Integração e Cooperação Amazônica para a Modernização do Monitoramento Hidrológico*" ICA-MMH) and CNPq ("*Assimilação de Dados de monitoramento Espacial para a análise do regime hidrológico da Bacia Amazônica e a previsão de curto e médio prazos*"); the TRMM data supplied by NASA and associated agencies; the global inundation extent dataset provided by Dr. Fabrice Papa; as well for the constructive comments from Dr. Sylvain Mangiarotti and Dr. Shraddhanand Shukla, and also from Dr. Wouter Buytaert, editor from HESS, Dr. Matthieu Guimberteau and the other anonymous reviewer.

References

Alsdorf, D.E., Rodrıguez, E., Lettenmaier, D.P. 2007b. Measuring surface water from space. Reviews of Geophysics, 45: RG2002, DOI:10Ð1029/2006RG000197.

Beighley, R.E., Eggert, K.G., Dunne, T., He, Y., Gummadi, V., Verdin, K.L. 2009. Simulating hydrologic and hydraulic processes throughout the Amazon River Basin. Hydrological Processes, 23, 8, 1221-1235.

Cappelaere, B., Lubès-Niel, H., Berkhoff, C., Thépaut, H., Guyot, J.L., de Oliveira, E. Rodrigues, M. 1996. Prévisions des crues de l'Amazone. In: /. 'hydrologie tropicale: géoscience et outil pour le développement (Actes de la conférence de Paris, mai 1995), 355-366, IAHS Publ, 238.

Chen, J.L.,Wilson, C.R., Tapley, B.D., Zang, Z.L., Niu, G.Y. 2009. The 2005 drought event in the Amazon River basin as measured by GRACE and estimated by climate models. J. Geophys. Res., 114, B05404, doi:10.1029/2008JB006056.

Chen, J.L., Wilson, C.R., Tapley, B.D. 2010. The 2009 exceptional Amazon flood and interannual terrestrial water storage change observed by GRACE. Water Resour. Res., 46, W12526, doi:10.1029/2010WR009383.

Coe, M.T., Costa, M.H., Howard, E.A. 2008. Simulating the surface waters of the Amazon River basin: Impacts of new river geomorphic and flow parameterizations. Hydrological Processes, 22, 14, 2542-2553.

Collischonn, W., Haas, R., Andreolli, I., Tucci, C.E.M. 2005. Forecasting river Uruguay flow using rainfall forecasts from a regional weather-prediction model. J. Hydrol., 305, 87-98.

Collischonn, W., Allasia, D.G., Silva, B.C., Tucci, C.E.M. 2007. The MGB-IPH model for large-scale rainfall-runoff modeling. Hydrological Sciences Journal, 52, 878-895.

Day, G.N. 1985. Extended streamflow forecasting using NWSRFS. J. Water Resour. Plann. Manage., 111, 157–170.

Decharme, B., Douville, H., Prigent, C., Papa, F., Aires F. 2008. A new river flooding scheme for global climate applications: Off-line evaluation over South America. J. Geophys. Res., 113, D11110, doi:10.1029/2007JD009376.

Durand, M., Fu, L.L., Lettenmaier, D.P., Alsdorf, D.E., Rodríguez, E., Fernandez, D.E. 2010a. The surface water and ocean topography mission: Observing terrestrial surface water and oceanic submesoscale eddies. Proceedings Of the IEEE, 98, 5, 766−779.

Durr, H.H., Meybeck, M., Durr, S.H. 2005. Lithologic composition of the Earth's continental surfaces derived from a new digital map emphasizing riverine material transfer. Global Biogeochem. Cy., 19, GB4S10, doi:10.1029/2005GB002515.

Espinoza, J.C., Ronchail, J., Guyot, J.L., Cocheneau, G., Filizola, N., Lavado, W., de Oliveira, E., Pombosa, R., Vauchel, P. 2009a. Spatio-Temporal rainfall variability in the Amazon Basin Countries (Brazil, Peru, Bolivia, Colombia and Ecuador). International Journal of Climatology, 29, 1574-1594.

Espinoza, J.C., Guyot, J.L, Ronchail, J., Cocheneau, G., Filizola, N., Fraizy, P., Labat, D., de Oliveira, E., Ordonez, J.J., and Vauchel, P. 2009b. Contrasting regional discharge evolutions in the Amazon Basin, J. Hydrol., 375, 297–311.

Espinoza, J.C., Ronchail, J., Guyot, J.L., Junquas, C., Vauchel, P., Lavado, W., Drapeau, G., Pombosa, R. 2011. Climate variability and extreme drought in the upper Solimões River (western Amazon Basin): Understanding the exceptional 2010 drought. Geophys. Res. Lett., 38, L13406, doi:10.1029/2011GL047862.

Farr, T.G., Caro, E., Crippen, R., Duren, R., Hensley, S., Kobrick, M., Paller, M., Rodriguez, E., Rosen, P., Roth, L., Seal, D., Shaffer, S., Shimada, J., Umland, J.,Werner, M., Burbank, D., Oskin, M., Alsdorf, D. 2007. The shuttle radartopography mission. Reviews of Geophysics, 45, 2, RG2004, doi:10.1029/2005RG000183.

Getirana, A.C.V., Bonnet, M.-P., Rotunno Filho, O.C., Collischonn, W., Guyot, J.-L., Seyler, F., Mansur, W.J. 2010. Hydrological modelling and water balance of the Negro River basin: evaluation based on in situ and spatial altimetry data. Hydrological Processes, 24, 22, 3219-3236.

Guimberteau, M., Drapeau, G., Ronchail, J., Sultan, B., Polcher, J., Martinez, J.-M., Prigent, C., Guyot, J.-L., Cochonneau, G., Espinoza, J. C., Filizola, N., Fraizy, P., Lavado, W., De Oliveira, E., Pombosa, R., Noriega, L., and Vauchel, P. 2012. Discharge simulation in the sub-basins of the Amazon using ORCHIDEE forced by new datasets. Hydrol. Earth Syst. Sci., 16, 911-935, doi:10.5194/hess-16-911-2012.

Hess, L.L., Melack, J.M., Novo, E.M.L.M., Barbosa, C.C.F., Gastil, M. 2003. Dual-season mapping of wetland inundation and vegetation for the central Amazon basin. Remote Sensing of Environment, 87, 404-428.

Huffman, G., Adler, R., Bolvin, D., Gu, G., Nelkin, E., Bowman, K., Hong, Y., Stocker, E., Wolff, D. 2007. The TRMM Multisatellite Precipitation Analysis (TCMA): quasi-global, multiyear, combined-sensor precipitation estimates at fine scales. J. Hydromet, 8, 38–55.

Liu, Y., Gupta, H.V. 2007. Uncertainty in hydrologic modeling: Toward an integrated data assimilation framework. Water Resour. Res., 43, W07401, doi:10.1029/2006WR005756.

Kerr, Y., Waldteufel, P., Wigneron, J.-P., Martinuzzi, J.-M., Font, J., and Berger, M. 2001. Soil moisture retrieval from space: The soil moisture and ocean salinity (SMOS) mission. IEEE T. Geosci. Remote Sens., 39, 1729-1736.

Marengo, J., Nobre, C., Tomasella, J., Oyama, M., de Oliveira, G., de Oliveira, R., Camargo, H., Alves, L. 2008. The drought in Amazonia in 2005. Journal of Climate, 21, 495–516.

Marengo, J.A., Tomasella, J., Alves, L.M., Soares, W.R., Rodriguez, D.A. 2011. The drought of 2010 in the context of historical droughts in the Amazon region. Geophys. Res. Lett., 38, L12703, doi:10.1029/2011GL047436.

New, M., Lister, D., Hulme, M., Makin, I. 2002. A high-resolution data set of surface climate over global land areas. Climate Res., 21, 1-25.

Paiva, R.C.D., Collischonn, W., Tucci, C.E.M. 2011. Large scale hydrologic and hydrodynamic modeling using limited data and a GIS based approach. Journal of Hydrology, 406, 170–181.

Paiva, R.C.D., Collischonn, W., Buarque, D.C. 2012a. Validation of a full hydrodynamic model for large scale hydrologic modelling in the Amazon. Hydrol. Process., in press, DOI: 10.1002/hyp.8425.

Paiva, R.C.D., Collischonn, W., Bonnet, M.P., Buarque, D.C., Frappart, F., Calmant, S., Mendes, C.B. 2012b. Large scale hydrologic and hydrodynamic modelling of the Amazon River basin. Water Resour. Res. (in review)

Papa, F., Prigent, C., Aires, F., Jimenez, C., Rossow, W.B., Matthews, E. 2010. Interannual variability of surface water extent at the global scale, 1993–2004. J. Geophys. Res., 115, D12111, doi:10.1029/2009JD012674.

Prigent, C., Papa, F., Aires, F., Rossow, W., Matthews, E.: Global inundation dynamics inferred from multiple satellite observations, 1993–2000. J. Geophys. Res., 112, 1993-2000.

Reichle, R.H. 2008. Data assimilation methods in the Earth sciences. Adv. Water Resour., 31, 1411–1418.

Santos da Silva, J., Calmant, S., Seyler, F., Rotunno Filho, O.C., Cochonneau, G., Mansur, W.J. 2010. Water levels in the Amazon basin derived from the ERS 2 and ENVISAT radar altimetry missions. Remote Sensing of Environment, 114, 10, 2160-2181.

Schongart, J., Junk,W.J. 2007. Forecasting the flood-pulse in Central Amazonia by ENSO-indices. J. Hydrol., 335, 124-132.

Shukla, S., Lettenmaier, D. P. 2011. Seasonal hydrologic prediction in the United States: understanding the role of initial hydrologic conditions and seasonal climate forecast skill. Hydrol. Earth Syst. Sci., 15, 3529-3538, doi:10.5194/hess-15-3529-2011.

Shukla, S., Sheffield, J., Wood, E. F., Lettenmaier, D. P. 2011. Relative contributions of initial hydrologic conditions and seasonal climate forecast skill to seasonal hydrologic prediction globally. Abstract H51N-05 presented at 2011 Fall Meeting, AGU, San Francisco, Calif., 5–9 December, 2011.

Tapley, B. D., Bettadpur, S., Watkins, M., and Reigber, C. 2004a. The gravity recovery and climate experiment: mission overview and early results. Geophys. Res. Lett., 31, L09607, doi:10.1029/2004GL019920.

Tapley, B.D., Bettadpur, S., Ries, J.C., Thompson, P.F., Watkins, M. 2004b. GRACE measurements of mass variability in the Earth system. Science, 305, 503-505.

Thielen, J., Bartholmes, J., Ramos, M.-H., de Roo, A. 2009. The European Flood Alert System – Part 1: Concept and development, Hydrol. Earth Syst. Sci., 13, 125-140, doi:10.5194/hess-13-125- 2009.

Tomasella, J., Borma, L.S., Marengo, J.A., Rodriguez, D.A., Cuartas, L.A. Nobre, C.A., Prado, M.C.R. 2010. The droughts of 1996–1997 and 2004–2005 in Amazonia: hydrological response in the river main-stem. Hydrol. Process., 25, 8, 1228-1242, DOI: 10.1002/hyp.7889.

Trigg, M.A., Wilson, M.D., Bates, P.D., Horritt, M.S., Alsdorf, D.E., Forsberg B.R., Vega, M.C. 2009. Amazon flood wave hydraulics. Journal of Hydrology, 374, 92–105.

Uvo, C.B., Graham, N. E. 1998. Seasonal runoff forecast for northern South America: A statistical model. Water Resour. Res., 34, 12, 3515-3524, doi:10.1029/98WR02854, 1998.

Uvo, C.B., Tölle, U., Berndtsson, R. 2000. Forecasting discharge in Amazonia using artificial neural networks. International Journal of Climatology, 20, 1495-1507, doi: 10.1002/1097-0088(200010)20:12<1495::AID-JOC549>3.0.CO;2-F.

Vinukollu, R.K., Wood, E.F., Ferguson, C.R., and Fisher, J.B. 2011. Global Estimates of Evapotranspiration for Climate Studies using Multi-Sensor Remote Sensing Data: Evaluation of Three Process-Based Approaches. Remote Sens. Environ., 115, 801-823, doi:10.1016/j.rse.2010.11.006.

Wood, A.W., Lettenmaier, D. P. 2008. An ensemble approach for attribution of hydrologic prediction uncertainty. Geophys. Res. Lett., 35, L14401, doi:10.1029/2008GL034648.

Wood, A.W., Schaake J.C. 2008. Correcting errors in streamflow forecast ensemble mean and spread. J. Hydrometeorol., 9, 132-148.

Wood, A.W., Maurer, E., Kumar, A., Lettenmaier, D.P. 2002. Long-range experimental hydrologic forecasting for the eastern United States. Journal of Geophysical Research, 107, D20, 4429, doi:10.1029/2001JD000659.

Yamazaki, D., Kanae, S., Kim, H., Oki, T. 2011. A physically n dynamics in a global river routing model. Water Resour. Res., 47, W04501, doi:10.1029/2010WR009726.

Zeng, N., Yoon, J.H., Marengo, J.A., Subuamaniam, A., Nobre, C.A., Mariotti, A., and Neelin, J.D. 2008. Causes and impact of the 2005 Amazon drought. Environ. Res. Lett., 3, 014002, doi:10.1088/1748-9326/3/1/014002.

CAPÍTULO 5

Assimilating *in situ* and radar altimetry data into a large-scale hydrologic-hydrodynamic model for streamflow forecast in the Amazon River basin

Capítulo 5: Assimilating *in situ* and radar altimetry data into a large-scale hydrologic-hydrodynamic model for streamflow forecast in the Amazon River basin

O Capítulo 2 apresenta modelagem hidrológica e hidrodinâmica da bacia Amazônica onde se pode observar como os modelos não são capazes de reproduzir com perfeição dados observados. Por outro lado, recentes técnicas de sensoriamento remoto vêm complementando observações hidrológicas convencionais *in situ*, permitindo o monitoramento mais detalhado de grandes áreas remotas, como a Amazônia. No Capítulo 4, apresenta-se um estudo de previsibilidade na bacia Amazônica e os resultados sugerem que seria possível gerar previsões baseadas principalmente nas condições hidrológicas no instante da previsão, que poderiam ser estimadas com maior precisão a partir da assimilação de dados observados.

Motivado por estes argumentos, neste capítulo apresenta-se o desenvolvimento e avaliação de um esquema de assimilação de dados no modelo hidrológico-hidrodinâmico MGB-IPH da bacia Amazônica, baseado em sua implementação do Capítulo 2. Utiliza-se a técnica "*Ensemble Kalman Filter*" para assimilar dados de vazões e níveis d'água oriundos de observações *in situ* e de altimetria por radar. Explora-se também a utilidade deste sistema para gerar previsões de vazões na bacia Amazônica.

Em resumo, os resultados mostram o bom desempenho do esquema de assimilação de dados, melhorando as estimativas do modelo nos postos fluviométricos utilizados na assimilação e também transferindo informações para trechos de rio não monitorados. A assimilação de dados de altimetria por radar também melhora os resultados do modelo nos grandes rios e a nível diário, mesmo considerando que este tipo de dado possui uma baixa resolução temporal (~35 dias). Os testes de previsões de vazões são promissores, mostrando ser possível gerar previsões nos grandes rios Amazônicos com relativa precisão e para altas antecedências, e.g. >90 dias ao longo do rio Solimões/Amazonas. Estes resultados indicam existir um grande potencial no desenvolvimento de sistemas de previsões hidrológicas para grandes bacias incluindo áreas pouco monitoradas, utilizando modelagem baseada em processos e sensoriamento remoto.

Capítulo 5: Assimilating *in situ* and radar altimetry data into a large-scale hydrologic-hydrodynamic model for streamflow forecast in the Amazon River basin

This chapter is based on the following paper to be submitted:

Paiva, R. C. D., Collischonn, W., Bonnet, M. P., de Gonçalves, L. G. G., Calmant, S., Getirana, A., Santos da Silva, J. Assimilating in situ and radar altimetry data into a large-scale hydrologic-hydrodynamic model for streamflow forecast in the Amazon River basin, (To be submitted).

Abstract

We present the development and evaluation of a data assimilation framework for gauged and radar altimetry-based discharge and water levels into a large scale hydrologic-hydrodynamic model, aiming at providing stream flow forecasts at the Amazon River basin. We used the process-based hydrological model MGB-IPH coupled with a river hydrodynamic module using a storage model for floodplains. The Ensemble Kalman Filter was implemented to assimilate information from hundreds of gauging stations and altimetry stations developed from ENVISAT satellite data. Model state variables errors were generated by corrupting precipitation forcing, considering log-normally distributed, time and spatially correlated errors. The EnKF performed well assimilating *in situ* discharge, by improving model estimates at assimilations sites and also transferring information to ungauged rivers reaches. The assimilation of altimetry data improves results at a daily basis in terms of water levels and discharges with minor degree, even though radar altimetry data has a low temporal resolution. Sensitivity tests highlighted the importance of the magnitude of precipitation errors and that of their spatial correlation, while temporal correlation showed to be dispensable. The deterioration of model performance at some unmonitored reaches indicates the need for proper characterization of model errors and spatial localization techniques for hydrological applications. Finally, we evaluated stream flow forecasts for the Amazon basin based on initial conditions gathered by the data assimilation scheme and using the ensemble stream flow prediction approach where the model is forced by past meteorological forcings. Forecasts agreed with observations and remain meaningful at large rivers even for very large lead times, e.g. >90 days at the Solimões/Amazon main stem. Results point to the potential of hydrological forecasts at world's large rivers and poorly monitored regions by using remote sensing information.

5.1. Introduction

Surface waters play an important role in terrestrial water cycle and global earth system, regulating freshwater discharge from land into oceans [*Oki and Kanae*, 2006] and also land-atmosphere exchanges of water, energy [*Krinner*, 2003; *Decharme et al.*, 2011] and gases such as methane [*Gedney et al.*, 2004]. Moreover, it affects directly society that uses it for drinking water and also transportation of people and goods, agriculture and production of hydroelectricity. More specific to the Amazon basin, important extreme hydrological events have occurred recently, namely the 2009 and 2012 floods and the 1996, 2005 and 2010 droughts [*Chen et al.*, 2010; *Tomasella et al.* 2010; *Marengo et al.*, 2008; *Espinoza et al.*,

2011, *Marengo et al.*, 2011]. These events caused several impacts on local population that strongly depends on the rivers and is very vulnerable to floods since most settlements lie along the rivers.

In situ measurements of river stage and discharge at stream gauges are the most conventional alternative for monitoring surface waters, although observation networks are rather sparse at several regions such as the Amazon basin. Alternatively, radar altimetry techniques are being developed in past years to monitor water levels [e.g. *Santos da Silva et al.*, 2010; *Alsdorf et al.*, 2007] or discharges using rating curves [e.g. *Leon et al.*, 2006; *Papa et al.*, 2010a; *Getirana and Peters-Lidard*, 2012]. If compared to *in situ* gauges in remote regions, these satellite instruments can provide observations with much better spatial resolution, but with worse temporal sampling. Moreover, the forthcoming Surface Water and Ocean Topography (SWOT) mission [*Durand et al.*, 2010a] is designed to provide high resolution images of inland water surface elevation for rivers, lakes, wetlands and reservoirs using a swath mapping radar altimeter with high frequency repeat orbit. Additionally, it may also be possible to derive discharge estimates from SWOT data by using specially developed algorithms [e.g. *Durand et al.*, 2010b].

In contrast, there are several efforts on hydrological modeling to simulate processes as river and floodplain dynamics in large river basins such as the Amazon [*Paiva et al.*, 2012; *Paiva et al.*, 2013 *Yamazaki et al.*, 2011; *Getirana et al.*, 2012; *Decharme et al.*, 2011; *Coe et al.*, 2008; *Wilson et al.*, 2007; *Trigg et al.*, 2009]. These models can potentially provide detailed information on surface waters, both spatially and temporally, but such estimates are somehow imperfect due to uncertainty in model structure, parameters and forcing data [*Liu and Gupta*, 2007].

Data assimilation (DA) methods are an alternative to optimally merge uncertain model predictions with both *in situ* and the newly remote sensing observations of surface waters. The aim of DA techniques is to "produce physically consistent representations or estimates of the dynamical behaviour of a system by merging the information present in imperfect models and uncertain data in an optimal way to achieve uncertainty quantification and reduction" [*Liu and Gupta*, 2007]. Such methods can also be used to estimate initial states of hydrological models for forecasting the aforementioned extreme events. Although there are some hydrological regional/global forecast systems founded on physically-based hydrological models [e.g. *Wood et al.*, 2002; *Thielen et al.*, 2009; *Alfieri et al.*, 2012], and also several physical modeling

experiments in the Amazon basin, as previously mentioned, current attempts for developing hydrological forecasts in this basin are mostly based on statistical methods [e.g. *Uvo and Grahan*, 1998; *Uvo et al.*, 2000]. Furthermore, *Paiva et al*. [2012b] showed that, for lead times up to 3 months, uncertainty of initial conditions plays a major role for discharge predictability on main Amazonian Rivers, if compared to the importance of precipitation forcing, suggesting the importance of DA techniques for streamflow forecasts in this region.

Research on data assimilation in the scope of hydrology has increased in past years with various applications using Kalman filters (e.g. the Ensemble Kalman Filter – EnKF, developed by *Evensen*, 2003), particle filters or variational methods, as extensively reviewed in *Liu and Gupta* [2007], *Reichle* [2008] and *Liu et al.* [2012]. These applications include a wide range of observations, both *in situ* and remotely sensed, data assimilation methods and models representing different hydrological processes, at different spatial scales and with several objectives, such as: the assimilation of snow [*Andreadis and Lettenmaier*, 2006] and soil moisture [*Reichle et al.*, 2002] data into land surface models using the EnKF; assimilation of *in situ* water level measurements into a small scale 1 D hydrodynamic model for flood forecast using Kalman filtering methods [*Neal et al.*, 2007; *Ricci et al.*, 2011]; assimilation of synthetic SWOT data into hydrodynamic models at restricted areas using the EnKF and some variations [*Biancamaria et al.*, 2011; *Andreadis et al.*, 2007; *Durand et al.*, 2008]; assimilation of discharge data into distributed hydrological models [*Clark et al.*, 2008; *McMillan et al.*, 2012; *Lee et al.*, 2012; *Thirel et al*., 2010; *Rakovec et al.*, 2012] using the EnKF or variational methods; simultaneous assimilation of soil moisture and discharge data into a distributed hydrological model using variational DA [*Lee et al.*, 2011]; assimilation of radar altimetry data of reservoir water levels using the EnKF [*Pereira-Cardenal et al.*, 2011]; development of a modelling platform (Land Information System - LIS) to merge multiple *in situ* and remotely sensed observations with land surface models [*Kumar et al*., 2008]; merging water levels information derived from a satellite Synthetic Aperture Radar (SAR) image and digital terrain model (DTM) with a 1 D hydrodynamic model for estimating river discharge [*Neal et al.*, 2009]; among others. Although there is an extensive bibliography on hydrological data assimilation, the current state of the art regional/global hydrological prediction systems [e.g. *Thielen et al.*, 2009; *Alfieri et al.*, 2012] still do not incorporate advanced data assimilation systems for updating model initial states. Also, the assimilation of

discharge and water levels from *in situ* and remotely sensed observations into regional/global hydrologic-hydrodynamic models is still uncommon.

In this paper, we present the development and evaluation of a data assimilation framework for both gauged and radar altimetry-based discharge and water levels into a large scale hydrologic-hydrodynamic model of the Amazon River basin using the EnKF. We also explore the usefulness of such system to provide streamflow forecasts when forced by past remotely sensed precipitation data and based mostly on model initial conditions. This paper is in the context of recent developments of techniques for integrating information from hydrological models with newly remotely sensed data such as the forthcoming SWOT mission and also in the context of regional/global hydrological forecast systems including large, poorly gauged river basins. Through our experimental results, we explore questions such as: is an EnKF-based DA scheme feasible for assimilating discharge and water level data into large scale hydrologic-hydrodynamic models? Is it able to improve discharge and water level estimates at sites where data were assimilated and also at ungauged rivers? Does the assimilation of radar altimetry data also improve model estimates at large river basins, considering that it has lower temporal resolution and accuracy if compared to gauged *in situ* data? Would it be possible to provide accurate streamflow forecasts at large basins such as the Amazon using a large scale hydrologic-hydrodynamic model based mostly on the initial hydrological states gathered by the DA scheme? At which spatial and temporal scales?

5.2. Methods

5.2.1. The hydrologic-hydrodynamic model

We used the MGB-IPH model [*Collischonn et al.*, 2007], which is a large scale, distributed and process-based hydrological model with a hydrodynamic module described in *Paiva et al.* [2011]. It simulates surface energy and water balance and also discharge, water level and flood inundation on a complex river network. Vertical hydrological processes include soil water budget using a bucket model, energy budget and evapotranspiration using the Penman Monteith approach, and also surface, subsurface and groundwater flow generation, among others. The flow generated within each catchment is routed to the stream

network using a linear reservoir type model. River flow routing is performed using a combination of either a Muskingum-Cunge (MC) method or a hydrodynamic model (HD).

The hydrodynamic model of MGB-IPH [*Paiva et al.*, 2011] solves the full 1 D *Saint-Venant* equations for the river network and flood inundation is simulated using a simple model assuming that the floodplains act only as storage areas. River-floodplain parameters (river width, bottom levels, roughness coefficient, floodplain bathymetry) are estimated using GIS-based algorithms from the Shuttle Radar Topography Mission (SRTM) Digital Elevation Model (DEM) [*Farr et al.*, 2007] and using geomorphological relations.

5.2.2. The Ensemble Kalman Filter

The goal of data assimilation is to combine the uncertain and complementary information from measurements and simulation models into an optimal estimate of the hydrological fields of interest, providing a general framework for dealing with uncertainty from measurements and also input, output and model structure [*Reichle*, 2008; *Liu and Gupta*, 2007; *Liu et al.* 2012; *Vrugt et al.*, 2005].

A great part of the hydrological applications of data assimilation methods uses schemes based on the Kalman filter [*Kalman*, 1960], specially the Ensemble Kalman Filter [*Evensen*, 2003; Evensen, 2009], which is also used in this study and is briefly described below. The model representing the dynamics of the simulated system can be described in a discrete form by the process equation:

$$\mathbf{x}_{k+1} = M(\mathbf{x}_k, \mathbf{u}_k, \boldsymbol{\theta}) + \mathbf{q}_k \quad (1)$$

where $\mathbf{x}$ is a vector of state variables, $\mathbf{u}$ and $\boldsymbol{\theta}$ represent model forcings and parameters, M is the nonlinear model operator that relates model states from time interval t_k to $t_{k+1} = t_k + \Delta t$, and $\boldsymbol{q}_k$ represents errors due to uncertainty in model structure, parameter, forcings and antecedent states. In this study, $\mathbf{x}$ is composed by all MGB-IPH model state variables, including soil moisture, storage and discharge from surface, subsurface and groundwater reservoirs, soil temperature, canopy storage and river discharge and water level. The measurement equation is defined by:

$$\mathbf{y}_k = H(\mathbf{x}_k) + \boldsymbol{\varepsilon}_k \quad (2)$$

where **y** is the vector of observations, **ε** is the vector of observation errors and *H* is the observation operator which relates model state variables **x** to the observations **y**. In our case, observations include river discharges or water levels at selected sites.

In the context of forecast systems and sequential data assimilation methods, at each time interval, the model is integrated in time using eq. 1 to provide a forecast (or background) $\mathbf{x}^f_{k+1}$ and whenever an observation is available the forecast errors are computed as [$\mathbf{y}_{k+1}$ - $H(\mathbf{x}^f_{k+1})$]. Therefore, the goal of data assimilation is to obtain an optimal estimate of model state variables $\mathbf{x}^a$ (called analysis) given model and observation errors. In the case of the original Kalman Filter [*Kalman*, 1960], the DA problem is solved using a linear estimator assuming that (i) model and observation operators (*M* and *H*) are linear; (ii) observation errors are unbiased and both temporally and spatially uncorrelated; (iii) model errors are unbiased and temporally uncorrelated; and (iv) there is no correlation between model and observation errors. Consequently, an unbiased and minimum variance estimate of model states is obtained by:

$$\mathbf{x}^a = \mathbf{x}^f + \mathbf{K}\left(\mathbf{y} - \mathbf{H}\mathbf{x}^f\right) \tag{3}$$

$$\mathbf{K} = \mathbf{P}^f\mathbf{H}^T\left[\mathbf{H}\mathbf{P}^f\mathbf{H}^T + \mathbf{R}\right]^{-1} \tag{4}$$

where **K** is the Kalman gain, **P** is the covariance of model errors **q**, and **R** is the covariance of measurement errors **ε**. The Kalman filter also provides the maximum likelihood solution of the DA problem when model and measurement errors are assumed to be also Gaussian. However, the applicability of the KF is limited since most hydrological systems exhibit nonlinear dynamics [*Liu and Gupta*, 2007] and the assumptions about model errors (e.g. Gaussian, unbiased, among others) are not always valid. Moreover, both the original KF and also its non-linear version, the Extended KF (EKF), have additional drawbacks when applied in large and complex systems with lots of state variables (e.g. distributed hydrological models) due to extra programming and heavy computational requirements associated with the storage and forward integration of the error covariance matrix **P** [*Vrugt et al.*, 2005].

Otherwise, *Evensen* [2003] presented the Ensemble Kalman Filter (EnKF), which is a stochastic or Monte Carlo alternative for the deterministic EKF [*Evensen*, 2009]. In this method, the observations and model states are perturbed using *a priori*-known errors and by

means of the model operator *M*, the algorithm generates an ensemble of model trajectories from which the time evolution of model errors and error covariance matrix can be sampled:

$$\mathbf{P}^f \cong \mathbf{P}_e^f = \overline{\left(\mathbf{x}^f - \overline{\mathbf{x}^f}\right)\left(\mathbf{x}^f - \overline{\mathbf{x}^f}\right)^T}\ ,\ \mathbf{P}^a \cong \mathbf{P}_e^a = \overline{\left(\mathbf{x}^a - \overline{\mathbf{x}^a}\right)\left(\mathbf{x}^a - \overline{\mathbf{x}^a}\right)^T} \quad (5)$$

Each ensemble member is then updated using the same analysis equation from the original KF (eq. 3 and 4). Alternatively, efficient computational implementations of the EnKF are presented in *Evensen* [2003, 2004 and 2009] (see http://enkf.nersc.no/ for Fortran codes) where the explicit computation and storage of **P** are not required. We used the square root scheme presented in *Evensen* [2004, 2009] where the perturbation of measurements is not performed, in order to reduce sampling errors.

For linear systems and with large ensemble sizes, the EnKF provides the same solution as the KF method. However, it is noteworthy that it does not fully take into account non-Gaussian errors nor solve the Bayesian update equation for non-Gaussian probability distribution functions. Still, it is a computational efficient analysis scheme for nonlinear models that provides a satisfactory solution, although it is suboptimal, that somehow lies between a linear Gaussian update and a full Bayesian computation [*Evensen*, 2009].

5.2.3. Uncertainty in precipitation forcing

We perturbed model states variables by adding a noise in precipitation forcing, considering (i) that this is the most uncertain model input [*Liu et al.*, 2012] and possibly the most important source of model uncertainty and (ii) that this is a proper method to generate physically coherent model errors. A similar approach performed satisfactorily in other hydrological applications of DA methods such as *Andreadis and Lettenmaier* [2006] and *Biancamaria et al.* [2011]. Precipitation values were corrupted using a log-normally distribution as presented by *Nijjsen and Lettenmaier* [2004] and also applied by *Andreadis and Lettenmaier* [2006]:

$$P_c = \frac{1+\beta}{\sqrt{E^2+1}} \exp\left(\sqrt{\ln\left[E^2+1\right]}\ s\right) P \quad (6)$$

where P_c [mm.Δt^{-1}] is the perturbed daily precipitation, P [mm.Δt^{-1}] is the unperturbed daily precipitation, E is the relative error [%], β is the relative bias and $s \sim N(0,1)$ is a normally

distributed and spatially correlated random variable with zero mean and unit variance. Spatially correlated pseudo random fields ***w*** were generated by means of the algorithm based on the two dimensional Fourier transform presented in *Evensen* [2003] (see http://enkf.nersc.no/ for Fortran codes), having zero mean, unit variance and isotropic covariance function decreasing to the e^{-1} value at the distance τ_x called spatial decorrelation length. At each spatial location, temporal correlation was also considered using the following equation for simulating the time evolution of errors [*Evensen*, 2003]:

$$s_k = \alpha s_{k-1} + \sqrt{1-\alpha^2}\, w_{k-1} \tag{7}$$

where k is the time interval, s_k is a sequence of time correlated errors with zero mean and unit variance (input for eq. 6) and α determines the time decorrelation of the stochastic forcing, e.g., α = 0 generates a sequence of white noise while α = 1 removes the stochastic forcing. The parameter α is determined by:

$$\alpha = 1 - \frac{\Delta t}{\tau_t} \tag{8}$$

where τ_t is the temporal decorrelation length, that determines that s decreases by the ratio e^{-1} after a time period $t = \tau_t$ if the stochastic term w is excluded.

5.2.4. Measurement errors

Water level (z) and discharge (Q) observations errors were modeled using the following relations:

$$z_c = z + \varepsilon_z \;,\; \varepsilon_z \sim N\left(0\,,\, \sigma_z{}^2\right) \tag{9}$$

$$Q_c = Q + \varepsilon_Q \;,\; \varepsilon_Q \sim N\left(0\,,\, \left(\sigma_Q Q\right)^2\right) \tag{10}$$

where z_c [m] and Q_c [$m^3.s^{-1}$] are the corrupted values of z [m] and Q [$m^3.s^{-1}$], ε_z [m] and ε_Q [$m^3.s^{-1}$] are the normally distributed errors with parameters σ_z [m] and σ_Q [%] of z and Q, respectively. The formulation of discharge errors allows representing larger uncertainties for high stage levels than for low flows due to uncertainties in discharge rating curves, as pointed out by *Clark et al.* [2008]. Alternatively, simulated and observed discharges were also

transformed into the log space before the assimilation, following *Clark et al.* [2008]. In this case, observation errors were modeled by:

$$Q_c = \varepsilon'_Q Q \ , \ \varepsilon'_Q \sim \log N\left(1, \sigma'^{\,2}_Q\right) \tag{11}$$

where now ε'_Q is a log-normally distributed error with unit mean and standard deviation σ'_Q [%], similar to eq. 10. At log space, standard deviation is given by $\sigma'_{\log Q} = \sqrt{\log\left(\sigma'^{\,2}_Q + 1\right)}$.

5.3. Experimental design

5.3.1. Amazon basin

The study area is the Amazon River basin, known as the largest hydrological system of the world (~6 million km^2 of surface area) and contributing with ~15% to the total fresh water released into the oceans. The Amazon basin is characterized by extensive seasonally flooded areas [*Hess et al.*, 2003; *Papa et al.*, 2010b; *Melack and Hess*, 2010], which store and release large amounts of water from the rivers and consequently attenuate and delay flood waves in several days or months [*Paiva et al.*, 2012a; *Paiva et al.*, 2013; *Yamazaki et al.*, 2011]. Also, complex river hydraulics are present, where the low river slopes cause backwater effects that control part of river dynamics [*Meade*, 1991; *Trigg et al.*, 2009; *Tomasella et al.*, 2010; *Paiva et al.*, 2012a; *Paiva et al.*, 2013]. Additionally, this region presents high precipitation rates (average ~2200 mm.year^{-1}) with high spatial variability and contrasting rainfall regimes in the northern (rainfall peak at JJA) and southern (rainfall peak at DJF) parts of the basin, with more defined wet and dry seasons occurring in southern and eastern regions [*Espinoza et al.*, 2009].

5.3.2. Model implementation

We used a MGB-IPH implementation on the Amazon basin developed by *Paiva et al.* [2013], as briefly described below. The model was forced using meteorological data obtained from the CRU CL 2.0 dataset [*New et al.*, 2002] and remotely sensed precipitation estimates from the TRMM 3B42 v6 product [*Huffman et al.*, 2007], with spatial resolution of 0.25^o x 0.25^o and daily time step for a period spanning 12 years (1998 - 2009). The model parameters

related to soil water budget were calibrated using daily discharge data from stream gauges (see next section for description of gauged data). Then, the model was validated against daily discharge and water level data from stream gauge stations, water levels derived from ENVISAT satellite altimetry data [*Santos da Silva et al.*, 2010] (212 sites with 35-day repeat orbit), monthly Terrestrial Water Storage from GRACE mission [*Frappart et al.* 2010; 2011b] and monthly flood inundation extent from *Papa et al.* [2010b]. Simulations agreed with observations, with relatively high Nash and Suttcliffe index (E_{NS}) values: $E_{NS} > 0.6$ in ~70% of discharge gauges, $E_{NS} > 0.6$ in ~60% of the water level stations derived from satellite altimetry, $E_{NS} = 0.71$ for total flood extent and $E_{NS} = 0.93$ for terrestrial water storage.

Since this study aimed at applications of data assimilation to hydrological forecasting, we also used a real time precipitation product to force the MGB-IPH model. We choose to use the TRMM Merge product [*Rozante et al.*, 2010], which is a near to real time precipitation estimate based on TRMM 3B42RT [*Huffman et al.*, 2007] merged with data from *in situ* gauges and provided by the Brazilian center for weather forecasts and climate studies CPTEC (*Centro de Previsão do Tempo e Estudos Climáticos*), a division of the Brazilian National Institute for Space Research INPE (*Instituto Nacional de Pesquisas Espaciais*).

5.3.3. Discharge and water level observations

We evaluated the assimilation of three types of data: (1) *in situ* discharge observations; (2) remotely sensed water levels derived from the ENVISAT radar altimeter; and (3) remotely sensed discharge estimates derived from radar altimetry water levels and rating curves.

In situ daily discharge from 109 stream gauges were provided by the Brazilian agency for water resources ANA (*Agência Nacional das Águas*), the Peruvian and Bolivian national meteorology and hydrology services SENAMHI (*Servicio Nacional de Meteorología e Hidrología*) and the French ORE-HYBAM program (*Hydrologie, Biogeochimie and Geodynamique du Bassin Amazonien*, http://www.ore-hybam.org). We also used stage data from 66 ANA gauge stations, but only for validation purposes.

Remotely sensed water levels were obtained from the ENVISAT satellite altimeter. The ENVISAT satellite has a 35-day repeat orbit and an 80 km inter-track distance at the Equator. The database used is an extension of the one presented in *Santos da Silva et al.* [2010], consisting in 212 altimetry stations (AS – deduced from the intersection of a satellite

track with a water body) with water level time series for the 2002-2009 period. ENVISAT data selection techniques preconized by *Santos da Silva et al.* [2010] result in ~ 10 to 40 cm water level accuracy. Due to differences in water levels datum reference, the comparisons between simulated and observed water levels were performed in terms of anomalies, i.e. after removing the long-term average.

Altimetry-based discharge data was developed by *Getirana and Peters-Lidard* [2012] for the Amazon basin, following the methodology first presented by *Leon et al.* [2006] in the Negro River sub-basin. This dataset was constructed using a rating-curve-based methodology deriving water discharge from ENVISAT altimetry data at 475 altimetric stations (AS). The stage-discharge relations at each AS were built based on satellite altimetry and outputs from a global flow routing (GFR) scheme [*Getirana et al.*, 2012]. A second experiment was performed in this study using observed discharges at gauge stations to force the GFR scheme at downstream reaches. Validation of the methodology against observed discharges at 90 sites showed a mean relative error of 27% for the experiment using *in situ* discharge within the GFR scheme. We assimilated data only from the 287 ASs located downstream of a gauging station where results were improved in the second experiment.

5.3.4. DA scheme parameters

The first sensitivity experiments used the following standard parameters of the DA scheme. Ensemble size of the EnKF was set as $N = 200$. Precipitation fields were corrupted considering the following error parameters: precipitation relative error $E = 25\%$, and precipitation relative bias $\beta = 1.0$ following *Andreadis and Lettenmaier* [2006]; temporal decorrelation length of precipitation errors $\tau_t = 10$ days; and spatial decorrelation length of precipitation errors $\tau_x = 1.0^o$, similarly to *Andreadis and Lettenmaier* [2006] and *Clark et al.* [2008]. The parameter of water level measurements error was set as $\sigma_z = 0.20$ m, based on the accuracy of ENVISAT estimates provided by *Santos da Silva et al.* [2010]. We computed the mean relative error between *in situ* discharge measurements and values provided by rating curves at 87 gauging stations from the ANA database as a surrogate of the discharge error parameter σ_Q. The median value of all stations was 13 %, while *Clark et al.* [2008] used 10% in its DA experiments. Therefore, we choose to also use $\sigma_Q = 10\%$ for simplicity. We used σ_Q

= 27% for assimilation of satellite based discharge data, based on the error value found in *Getirana and Peters-Lidard* [2012].

5.3.5. Data assimilation experiments

We performed three data assimilation experiments, namely: (i) *In situ* discharge assimilation (Exp 1) (ii) Radar altimetry assimilation (Exp 2) and (iii) Assimilation of discharge series based on satellite altimetry (Exp 3).

In the first experiment, we tested: (Exp. 1a) the assimilation of discharge from almost all gauge stations (80%) using a few of them for validation (20%); (Exp. 1b) the assimilation of only 12 stations (~10%) located at some of the major tributaries to emulate the situation of using only telemetric stream gauges for real time applications; (Exp. 1c) the assimilation of discharge from almost all gauge stations, similar to (Exp. 1a), but without transforming discharge into the log space (Section 5.2.4.). Moreover, we explored the sensibility of the DA scheme to some of its parameters, namely the ensemble size N, precipitation relative error E and temporal and spatial decorrelation lengths of precipitation errors τ_t, and τ_x.

The second experiment (Exp. 2) evaluated the assimilation of ENVISAT radar altimetry water level anomalies. Stage data from *in situ* gauges were used for model verification. Simulations were also compared in terms of discharge using *in situ* data to evaluate the impact of water level assimilation in discharge estimates.

In the third experiment (Exp. 3), we assessed the assimilation of discharge derived from radar altimetry water level. Discharge data from stream gauges were used for verification.

In all cases, simulations started in 1998 and ran to 2002 for model spin-up. The year of 2003 was used for the spin-up of the DA scheme, where no update was performed in the first months allowing the system to develop a coherent correlation structure, following *Andreadis and Lettenmaier* [2006]. To access the DA scheme performance, model simulations using (EnKF simulation) or not (Open-loop simulation) data assimilation were compared. Results were evaluated for the two year period 2004-2005 by means of the following model performance statistics that compares simulation results with observations: (i) the Nash-Suttcliffe coefficient E_{NS} ranging from -∞ to 1 (optimum) and (ii) changes in root mean square error $\Delta rms = 100.(rms_2 - rms_1) / rms_1$, ranging from -100% (optimum) to ∞, where

rms_1 and rms_2 are root mean squared errors from Open-loop and EnKF simulations, respectively.

5.3.6. Prospects of streamflow forecasting

Hindcast streamflow forecasts were generated using an ensemble streamflow prediction (ESP) approach [*Day*, 1985], as described below. The model uses an estimate of initial conditions derived from the DA scheme and runs forced by an ensemble of observed meteorological data from past years. An estimate of initial conditions is computed during the spin-up period using a hydrological model driven by observed meteorological forcings, updated using data assimilation of observations up to the time of forecast (e.g. forecast starts with model states from June 1st of 2010). Then, an ensemble forecast is obtained using observed meteorological data resampled from past years (e.g. meteorological data from June 1st to September 1st of years 1998, 1999, …, 2009).

Precipitation from TRMM Merge was used during spin-up period, while during forecast the model was forced with TRMM 3B42 data for the period spanning 12 years (1998 - 2009) and, consequently, the forecast ensemble had 12 members. The DA scheme used the configuration from Exp. 1b where *in situ* discharge data were assimilated to update model states before starting a forecast. ESP runs generated decadal forecasts up to 90 days lead time and starting at every 1st, 10th and 20th day of the month for the two year period of 2004-2005.

For simplicity reasons, forecasts were evaluated only by deterministic means by averaging ensemble values into a single forecast. We used the skill score SS_{cli} which compares the performance of the model forecasts with a control forecast based on climatology [*Wilks*, 2006]:

$$SS_{cli} = 1 - \frac{\sum_t (Q_{obs}^t - Q_{for}^t)^2}{\sum_t (Q_{obs}^t - Q_{cli}^t)^2} \tag{12}$$

where t is the time interval, Q_{obs} is daily discharge observed at stream gauge stations, Q_{for} is forecasted discharge, Q_{cli} is the climatological value of discharge on day t computed from observations. SS_{cli} ranges from $-\infty$ to 1 (optimum) and positive values show an improvement over a forecast based on climatology.

5.4. Results and discussion

5.4.1. In situ discharge assimilation

We start our analysis evaluating the sensibility of the DA scheme performance to some of its parameters, as presented in Fig. 1. The objective of such examination is to verify which parameters are the most important ones and if the DA performance is improved by using values of these parameters that are different from the first guess ones based on previous studies (see Section 5.3.4.). The configuration of Exp. 1a was used, where *in situ* discharge data were assimilated. Results were evaluated in terms of mean changes in root mean squared error (Δ*rms*) between observed and simulated discharges, computed for two samples, the first including stream gauges used for data assimilation and the latter only the validation ones. Larger decreases in the *rms* error indicate better performance of the DA scheme.

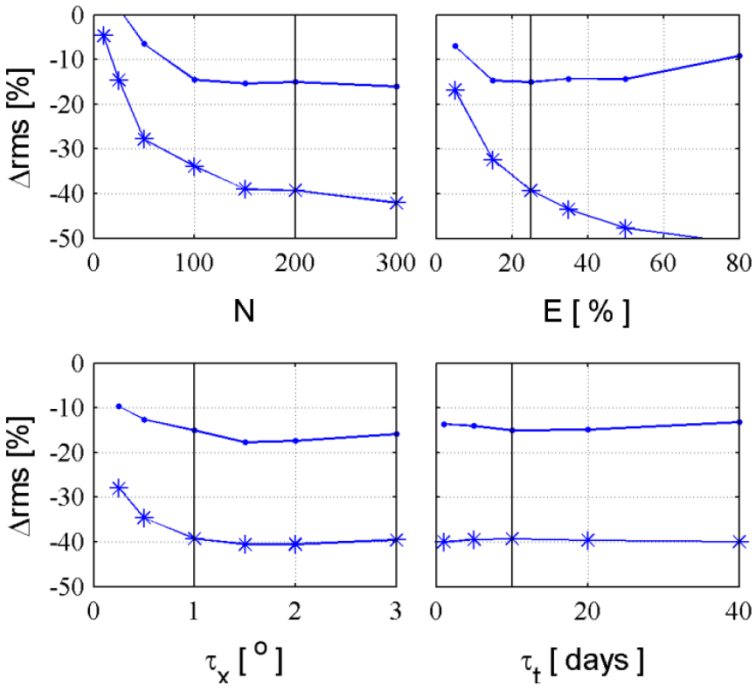

Figure 1. Sensitivity tests of DA scheme parameters. Mean change in root mean square error (Δ*rms*) for the assimilation (line with stars) and validation (line with dots) stream gauges as function of ensemble size (*N*), precipitation relative error (*E*) and spatial (τ_x) and temporal (τ_t) decorrelation lengths of precipitation errors. First guess values are represented by the black line.

According to the analysis, the DA scheme strongly depends on the ensemble size *N*. Small *N* values produce small improvements in discharge results and larger values enhance the DA performance (smaller Δ*rms* values), although the improvement rate is small for *N* values larger than 150 members. Such behaviour is possibly due to numerical reasons, since a larger *N* enable a better sampling of model covariance errors from the ensemble, as discussed by *Evensen* [2009]. The DA scheme is also very sensitive to precipitation relative error *E* and increasing *E* values improves DA performance. However, if *E* is larger than 50%, Δ*rms* increases in validation sites causing worse results (see Fig. 1). Possibly, larger precipitation errors cause larger model uncertainty and consequently the DA scheme gives more weight to observations, but it starts to degrade model results at different locations after some point. A moderate dependence to the τ_x parameter was found and spatial correlation of precipitation errors showed to be of importance, since the performance degrades for smaller decorrelation lengths. The best results were obtained for 1.5^o for both the assimilation and validation samples. Finally, a weak sensibility to the τ_t parameter was found, which indicates that considering temporal correlation in precipitation errors is not as important as spatial correlation.

Based on the sensitivity tests, we used the following new parameter values for the further experiments: $N = 200$ (unchanged), $E = 50\%$, $\tau_x = 1.5^o$ and $\tau_t = 10$ days (unchanged). However, it is noteworthy that these parameter values related to precipitation errors, although providing better results for data assimilation, may not realistically represent errors in the TRMM Merge dataset or the spatially variable satellite precipitation errors presented in *Tian and Peters-Lidard* [2010]. That is possibly because we considered that model uncertainty comes from precipitation errors and neglected other sources such as parameter and model structural errors [*Liu and Gupta*, 2007]. Therefore, and since the first guess values were not fully justified in the previous studies [*Andreadis and Lettenmaier*, 2006; *Clark et al.*, 2008], we preferred to use the parameter values where the DA scheme performs better.

We first evaluate results from the Exp. 1a. The DA scheme improves results by decreasing model errors in almost all stream gauges (blue sites in Fig. 2a), including both assimilation and validation sites. On average, E_{NS} values increase from 0.71 to 0.94 and the *rms* error decreases by 49% (Table 1). For example, at an assimilation site located on the Negro River (Fig. 3a), when the EnKF is used, the discharge estimates are much closer to observations if compared with the open-loop simulation. The E_{NS} index increases from 0.62 to

0.91 and the *rms* error decreases by 51%. Similarly, results also improve at validation sites, although with a smaller degree, and the E_{NS} index increases from 0.60 to 0.73, with a reduction in *rms* error of -16% (Table 1), as illustrated at a validation site located at upper Juruá River basin (Fig. 3b). Such results demonstrate that the DA scheme improves model discharge estimates, not only at sites where data were assimilated but possibly at ungauged rivers reaches as well.

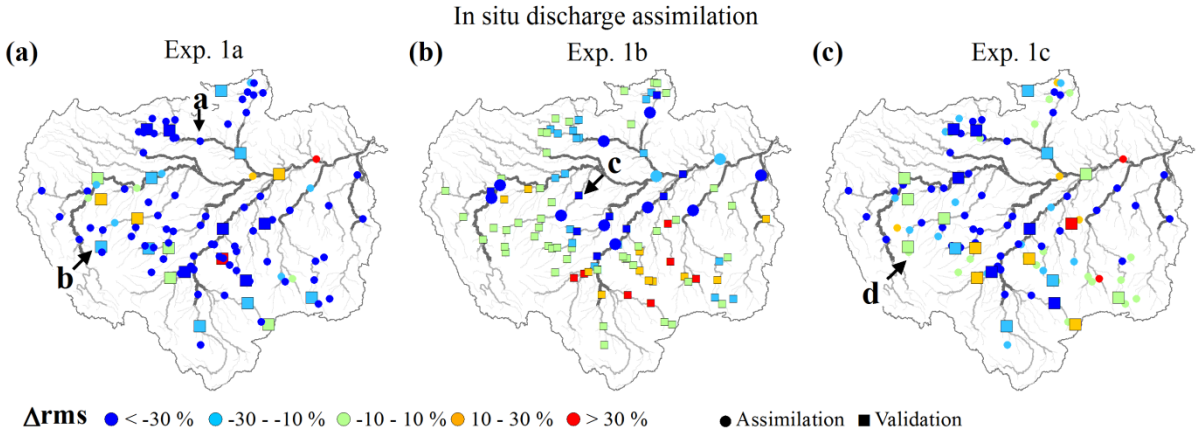

Figure 2. Evaluation of *in situ* discharge assimilation. Spatial distribution of change in root mean square error (Δ*rms*) in stream gauges used for data assimilation (circles) and validation (squares) considering the assimilation of (a) almost all gauges (Exp. 1a), (b) only 12 gauges (Exp. 1b) and (c) almost all gauges but without log transformation (Exp. 1c).

Table 1. Summary of the performance of *in situ* discharge data assimilation (Exp 1): median Nash and Suttcliffe index (E_{NS}) in simulation (Open-loop) and assimilation (EnKF) modes and mean change in root mean square error (Δ*rms*).

Sites		Exp. 1a[2]		Exp. 1b[3]		Exp. 1c[4]	
		E_{NS}	Δ*rms* (%)	E_{NS}	Δ*rms* (%)	E_{NS}	Δ*rms* (%)
All	Open-loop	0.68	-	0.68	-	0.68	-
	EnKF	0.93	-42	0.72	-8	0.85	-25
Assimilation	Open-loop	0.71	-	0.89	-	0.71	-
	EnKF	0.94	-49	0.98	-51	0.88	-29
Validation	Open-loop	0.60	-	0.65	-	0.60	-
	EnKF	0.73	-16	0.67	-3	0.67	-10
Large rivers[1]	Open-loop	0.79	-	0.79	-	0.79	-
	EnKF	0.94	-34	0.87	-23	0.95	-40

[1] Stream gauges located at rivers reaches with upstream drainage area larger than 10^5 km^2.

[2] Exp. 1a – data assimilation using discharge from 80% of the stream gauges.

[3] Exp. 1b – data assimilation using discharge from 10% of the stream gauges.

[4] Exp. 1c – equal Exp. 1a but without transforming discharge into the log space.

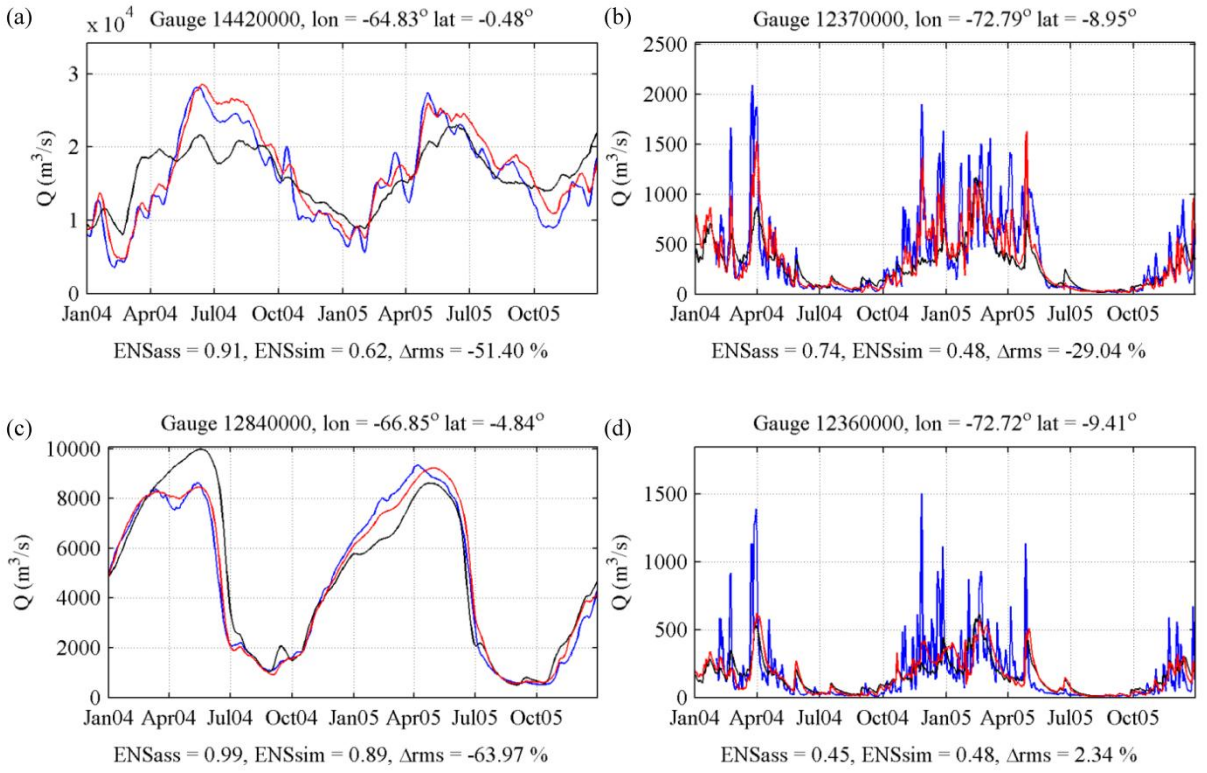

Figure 3. Discharge derived from *in situ* observation (blue line), open-loop simulation (black line) and EnKF simulation (red line) at (a) Negro River (assimilation site, Exp. 1a), (b) upper Juruá River (validation site, Exp. 1a), (c) lower Juruá River (validation site Exp. 1b) and upper Juruá River (assimilation site, Exp. 1c). Site are indicated Fig. 2.

In Exp. 1b, results improve at assimilation sites - E_{NS} increases from 0.89 to 0.98 and the *rms* error decreases by 50% (Table 1). However, since data from only a few gauges were assimilated, there is no important improvement (Δrms = -3%) if all validation sites are examined together. As expected, according to Fig. 2b the DA scheme improves discharge estimates mostly at large rivers (e.g. Fig. 3c), where E_{NS} increases from 0.79 to 0.87 while Δrms equals -23%. But at smaller rivers, in most cases the DA scheme has minor effect on simulated discharges (green squares at Fig. 2b) or in some cases it degrades results.

In previous studies conducted over smaller basins [e.g. in *Clark et al.*, 2008; and in others summarised by *Lee et al.*, 2012], the attempt to transfer information to neighbour or upstream ungauged river reaches was unsuccessful and corrupted model results, while in our case (Exp. 1b) the DA scheme degraded model outputs mostly at smaller basins and improved results at larger rivers. Such behaviour possibly happens because the state estimation in distributed hydrological models is subject to overfitting due to the large dimensionality of the model state space, and consequently, when limited data is available, the data assimilation may

update state variables at some lumped fashion such as the sub-basin scale, as explained by *Lee et al*. [2012].

Finally, we compare the use (Exp. 1a) or not (Exp. 1c) of the transformation of discharge values into the log space before data assimilation. The performance of the DA scheme degrades if the log transformation is not used, and in this case Δ*rms* increases to -29% and -10% for the assimilation and validation samples respectively, instead of the -49% and -16% values obtained in the Exp. 1a. *Clark et al.* [2008] argue that the EnKF with log transformation performs better because relationships between streamflow and model states are non-linear and state updates are exceptionally large when differences between model and observed values are high. However, the worst performance was observed mostly at smaller river reaches (see Fig. 2c) as illustrated in Fig. 3c. Also, DA performs better at gauging stations in large rivers and Δ*rms* increases from -34% (Exp. 1a) to -40% (Exp. 1c). Apparently, when the log transformation is not used, the DA scheme gives more weight to large discharge values (~10^3 to ~10^5 $m^3.s^{-1}$) at large rivers while observations at the smaller ones (< ~10^3 $m^3.s^{-1}$) are not fully taken into account. These results indicate the importance of using the log space transformation also to deal with very different discharge magnitudes, including the ones arising from different spatial scales but also concerning to flood and drought flows.

5.4.2. Radar altimetry data assimilation

In this section, the assimilation of water levels derived from ENVISAT altimetry is evaluated (Exp. 2). Stage and discharge data observed at *in situ* gauging stations were used for validation purposes.

The DA scheme improves water level simulations at altimetry stations used for assimilation (Fig. 4a), as illustrated in Fig. 5a. On average, *rms* decreases by 56% and E_{NS} values increase from 0.66 to 0.96 (Table 2). Simulated water level accuracy also increases when compared to *in situ* stage data (Δ*rms* = -13%). However, the improvement is more evident if only gauging stations located at rivers where altimetry data were assimilated (Fig. 4b and 5b). In this case, mean Δ*rms* equals -43% and E_{NS} changes from 0.75 to 0.94 (Table 2), similar to what was obtained at altimetry stations. At other sites, the DA scheme has a minor effect on simulated water levels or even degrades results in some cases. Similar results

were found for the *in situ* discharge validation sample (Fig. 4c). Assimilating water level data improves discharge estimates (Δ*rms* = -15 %) mostly at the same rivers in which altimetry data is available (e.g. Fig. 5c). But it also degrades results at some of the other river reaches.

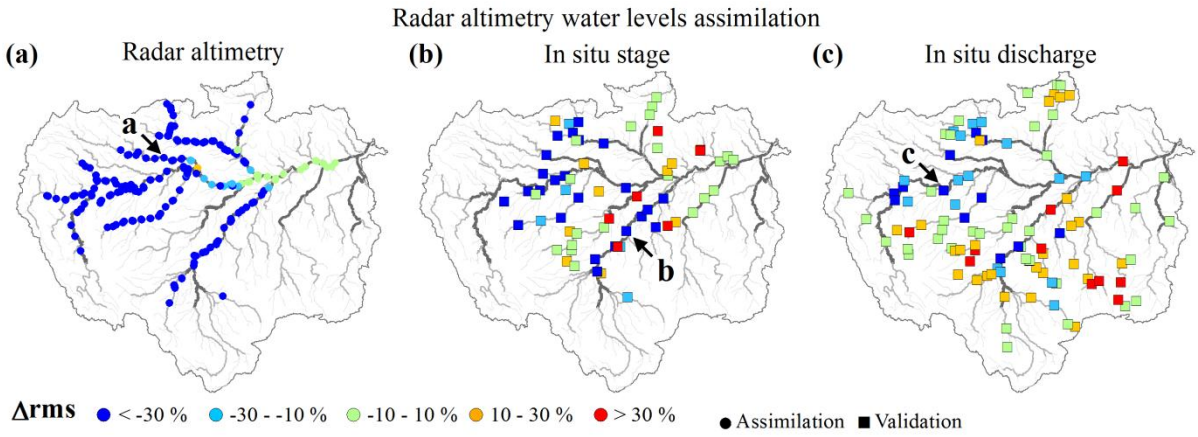

Figure 4. Evaluation of ENVISAT radar altimetry data assimilation. Spatial distribution of change in root mean square error (Δ*rms*) at (a) altimetry stations used for data assimilation and stream gauges with (b) stage and (c) discharge data used for verification.

Table 2. As Table 1 but for Exp. 2.

Sites			E_{NS}	Δ*rms* (%)
All	Radar altimetry Assimilation	Open-loop	0.66	-
		EnKF	0.96	-56.0
	In situ stage Validation	Open-loop	0.64	-
		EnKF	0.74	-13
	In situ discharge Validation	Open-loop	0.68	-
		EnKF	0.68	1
Inside ENVISAT domain[(1)]	*In situ* stage Validation	Open-loop	0.75	-
		EnKF	0.94	-44
	In situ discharge Validation	Open-loop	0.79	-
		EnKF	0.86	-15

[(1)] Upstream and downstream at least one altimetry station.

Furthermore, the DA scheme can degrade results in some reaches where no data were assimilated. Such a problem is possibly caused by spurious correlations in the model covariance matrix from the EnKF due to a poor sampling from the ensemble. Aiming to avoid spurious correlations, methods such as covariance localization or local analysis [*Sakov and Bertino*, 2010] could be used to constrain the influence of observations based on distance

criteria as already used in atmospheric or ocean applications. However, in our view, a particular localization criteria should be developed for hydrological applications, since the correlation between the model states can be a function of an Euclidean distance in some cases (e.g. soil moisture) or in others, of a distance measured following the rivers' path (e.g. river discharge and water levels).

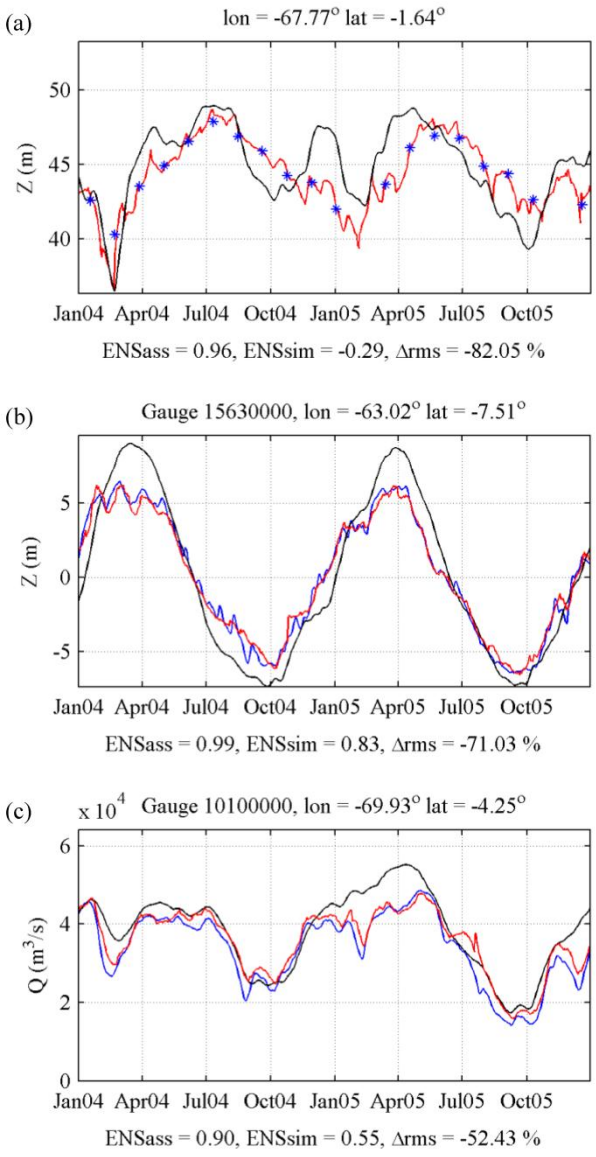

Figure 5. Observation (blue line), open-loop simulation (black line) and EnKF simulation (red line) at (a) Japurá River altimetry site, (b) Madeira River *in situ* stage site (c) Solimões River *in situ* discharge site. Sites are indicated in Fig. 4.

Results from this experiment demonstrate that the assimilation of radar altimetry data into large scale hydrologic models can improve simulations, mainly in terms of water levels

but also in discharge. Even though ENVISAT data is provided at a 35-day temporal resolution, its assimilation can improve model results at a daily basis as illustrated in Fig. 5b and 5c possibly due to the low temporal variability of Amazonian hydrographs and the fact that ENVISAT measurements are non-simultaneous.

5.4.3. Assimilation of discharge series based on satellite altimetry

In the last DA experiment (Exp. 3), we evaluate the assimilation of discharge data derived from ENVISAT water level. Therefore, the data assimilated into the model has the same high spatial coverage and low temporal sampling as altimetry water levels have, but it also contains discharge information which is the most important hydrological variable of the model. *In situ* discharge data were also used for validation.

The DA scheme was able to assimilate altimetry-based discharges increasing the agreement between these observations and model results in most of the altimetry stations (Fig. 6a), as exemplified in Fig. 7a. In average, the *rms* error between altimetry-based discharges and model results decreased 23% (Table 3), which represents a smaller improvement if compared to the assimilation of *in situ* discharge (Δrms = -49% in Exp. 1a). Since observation errors are larger in the altimetry-based discharges, the DA scheme gives more weight to background model results and updated discharge values are not so close to measurements. The comparison of model results with *in situ* discharge data (Fig. 6b) shows that errors decrease mostly at gauging stations located at rivers where altimetry data were assimilated (e.g. Fig. 7b). At these sites, E_{NS} changes from 0.76 to 0.80 and the mean Δrms is -14% (Table 3), which is comparable to the improvement obtained in the altimetry data assimilation (Exp. 2, Table 2) over discharge results (Δrms = -15%), but smaller than the enhancement of water level results (Δrms = -43%). Moreover, similarly to Exp. 2, at gauging stations located outside the assimilation domain, the DA scheme has a minor effect on simulated discharge or degrades results in some cases.

Results from this section show the potential of assimilating discharge data derived from satellite altimetry into large scale hydrological models instead of *in situ* discharge or satellite water levels, even though such data has lower temporal resolution and accuracy if compared to data gathered at *in situ* gauging stations.

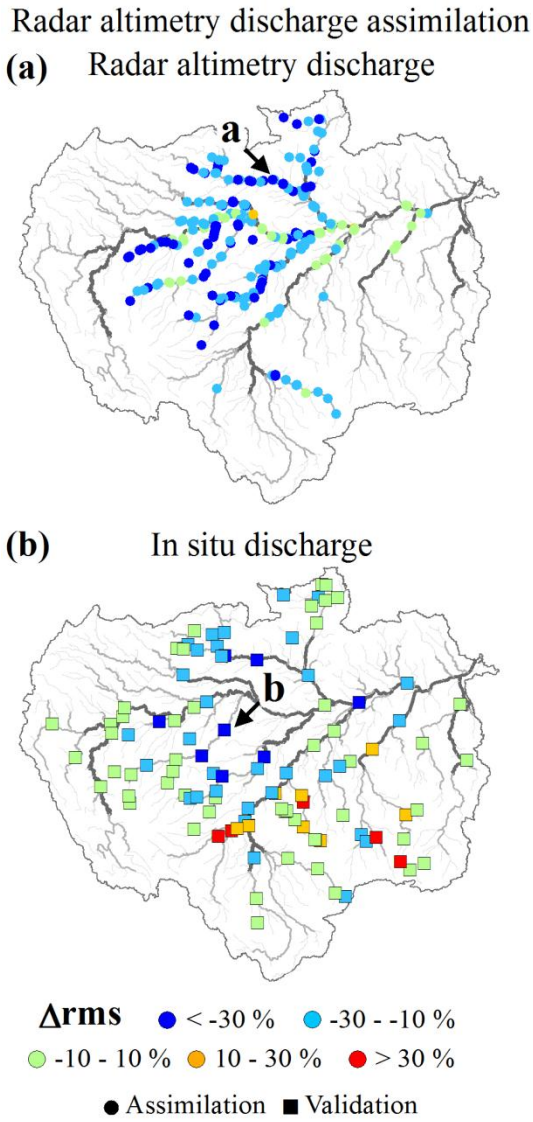

Figure 6. Evaluation of ENVISAT radar altimetry discharge assimilation. Spatial distribution of change in root mean square error (Δ*rms*) at (a) altimetry stations used for data assimilation and (b) stream gauges with discharge data used for validation.

Table 3. As Table 1 but for Exp. 3.

Sites			E_{NS}	Δ*rms* (%)
All	Altimetry discharge Assimilation	Open-loop	0.62	-
		EnKF	0.79	-23
	In situ discharge Validation	Open-loop	0.68	-
		EnKF	0.72	-5
Inside ENVISAT Domain (1)	*In situ* discharge Validation	Open-loop	0.76	-
		EnKF	0.80	-15

(1) Upstream and downstream at least one altimetry station.

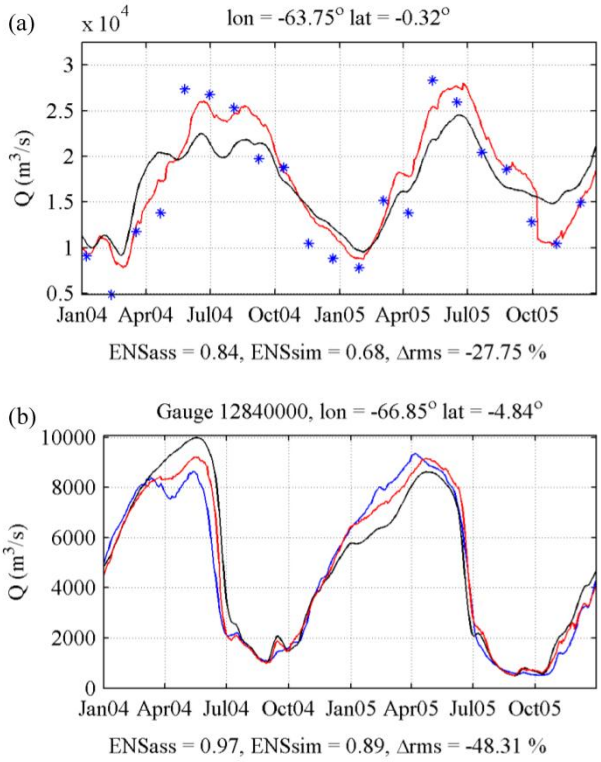

Figure 7. Observation (blue line), open-loop simulation (black line) and EnKF simulation (red line) of discharge at (a) Negro River altimetry site and (b) Juruá River *in situ* site. Sites are indicated in Fig. 6.

5.4.4. Prospects of streamflow forecasting

We now assess the potential of a large scale hydrologic-hydrodynamic model coupled with a DA scheme to provide streamflow forecasts in the Amazon basin. Since hydrological initial states governs discharge predictability at the large Amazonian rivers (discussed by *Paiva et al.*, 2012b), we have chosen to generate forecasts starting with initial states gathered by the DA scheme and then using the ensemble streamflow prediction approach – ESP [*Day*, 1985], where the model is run forced by an ensemble of observed meteorological data from past years. Since this is a first attempt, we have chosen to evaluate forecasts using only the DA scheme configuration from Exp. 1b, where the model is updated using discharge data from 12 gauging stations located on the Amazon and its main tributaries.

We first evaluate hindcast forecasts at the Solimões/Amazon mainstem, including upper Solimões River at Tamishiyacu, Solimões River at Manacapuru and Amazon River at Óbidos (Fig. 8). The model was able to forecast discharges with relatively high accuracy even for very large lead times (90 days). In all cases, forecasts are markedly better than simply

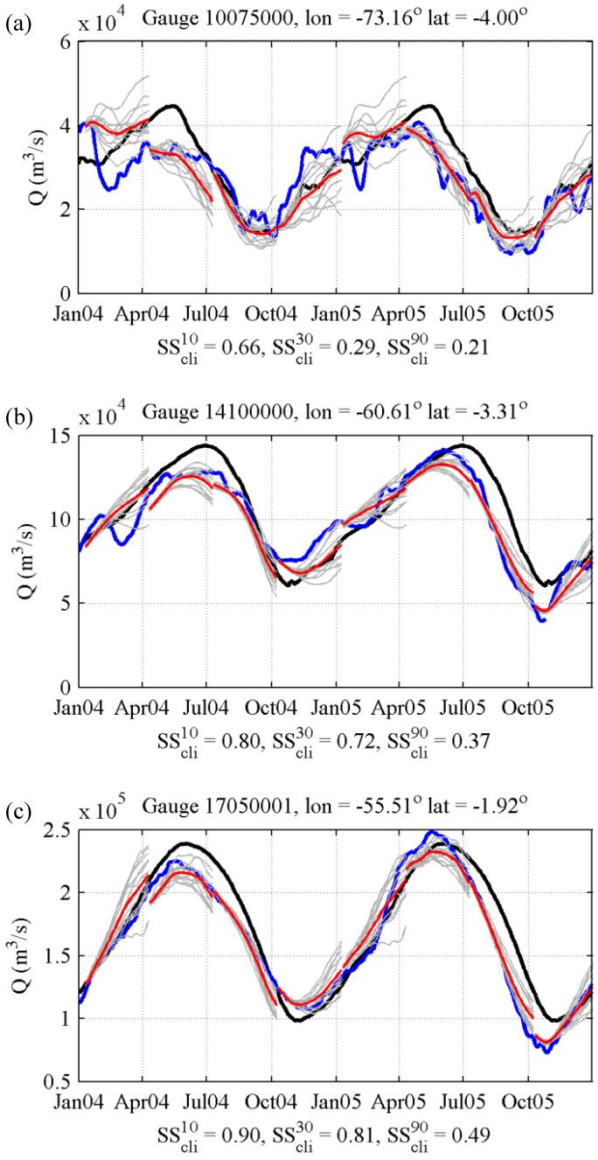

Figure 8. Evaluation of streamflow forecasts. Observed (blue), climatological (black) discharges, ensemble forecasts (grey) together with ensemble mean (red) at (a) Upper Solimões River at Tamishiyacu, (b) Solimões River at Manacapuru and (c) Amazon river at Óbidos. Presented forecasts started each 10th Jan, Apr, Jul and Oct. Sites are indicated in Fig. 9.

using discharge climatology, as shown by positive values of SS_{cli} skill score (Fig. 8). As expected, the agreement between model values and observations decreases as function of lead time, and, for example, SS_{cli} decreases from 0.90 to 0.49 for forecasts 10 and 90 days ahead at Óbidos station. But it remains very high, showing that it would be possible to produce accurate forecasts at the Amazon main river for even larger lead times. Model performance also increases from the upper to the lower part of the Solimões/Amazon River, and at the same time, the spread of the ESP ensemble at large lead times increases upstream and

decreases downstream. Such behaviour is explained by the fact that in larger rivers, the hydrological predictability is much more influenced by the current volumes of water stored upstream than by future precipitation forcing, as discussed by *Paiva et al.* [2012b].

Analysis from Fig. 8 also demonstrates that the model successfully predicted the severe 2005 drought at the Solimões/Amazon main stem. At this year, discharges dropped ~1 month earlier than normal (Fig. 8) and river levels fell to historically low levels causing navigation to be suspended [*Marengo et al.*, 2008]. Even so, the model was able to predict this low flows ~90 days ahead.

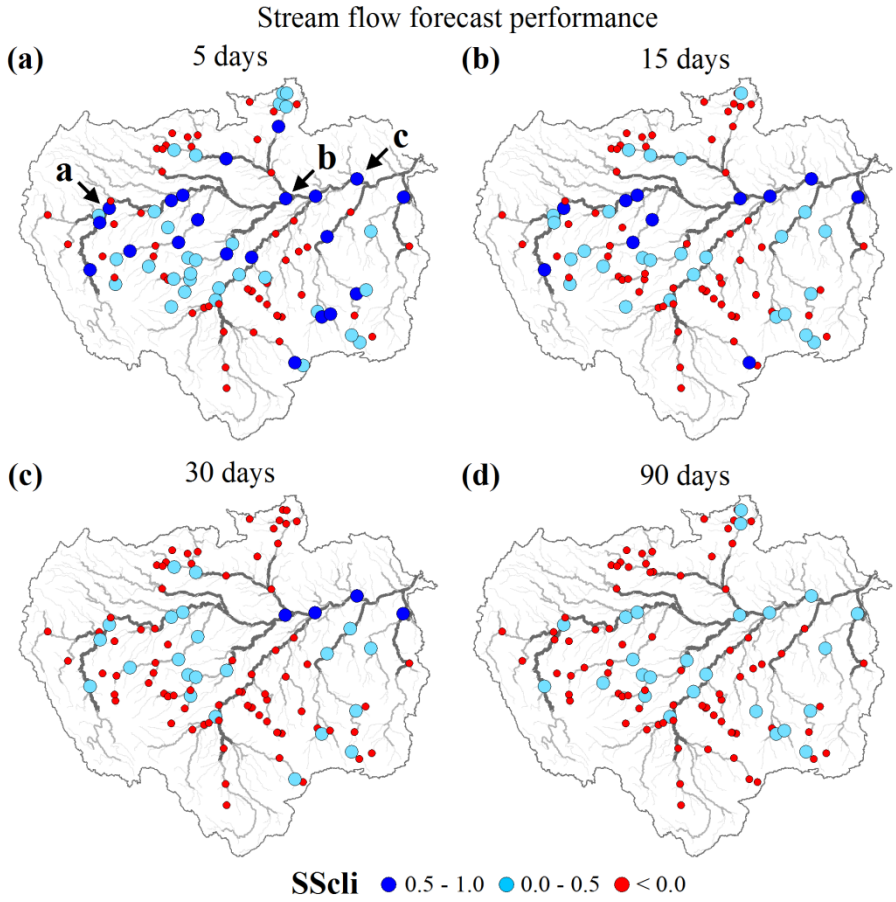

Figure 9. Evaluation of streamflow forecasts. Spatial distribution of the skill score SS_{cli} for (a) 5, (b) 15, (c) 30 and (d) 90 days lead time.

We now evaluate forecasts at gauging stations located all over the Amazon basin. Forecasts for a smaller lead time of 5 days or even 15 days (Fig. 9a and 9b) were relatively accurate with positive SS_{cli} values at several gauging stations located at both upstream and downstream rivers. However, the quality of the forecasts decreased as a function of lead time (30 and 90 days, Fig. 9c and 9d). It becomes very poor at smaller rivers and remains

meaningful with positive SS_{cli} values mainly at gauging stations with large draining areas. For 90 days lead time, SS_{cli} index remains positive at almost all stations along the Solimões/Amazon main stem and in some of the main tributaries. This behavior is also illustrated at Fig. 10. SS_{cli} values are usually higher at gauging stations located in rivers draining large areas and decrease with lead time. For instance, if only stations gauging rivers with drainage area larger than 10^5 km^2 or $4x10^5$ km^2 are considered, on average, forecasts remain better than climatology (SS_{cli} >0) up to ~15 and ~25 days lead time, respectively. On the other hand, if only the largest rivers are taken into account (>10^6 km^2), SS_{cli} values are high and always positive, which demonstrates the good performance of the model forecasts. SS_{cli} is also high at stream gauges used for data assimilation where forecasts are usually better, SS_{cli} is close to one for small lead times, as expected, and becomes negative after ~55 days.

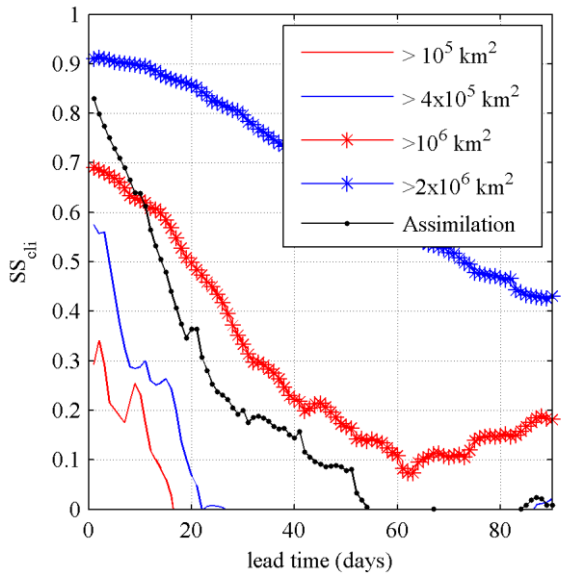

Figure 10. Median skill score SS_{cli} of stream flow forecasts at gauging stations as function of lead time. Different curves show results considering gauges with different drainage areas (red and blue lines) and only gauges used for data assimilation (black line with dots).

5.5. Summary and conclusions

We presented the development and evaluation of a data assimilation scheme for both gauged and satellite altimetry-based discharge and water levels into a large scale hydrologic-hydrodynamic model of the Amazon River basin using the Ensemble Kalman Filter - EnKF. We also evaluated hindcast forecasts based on this system using the ensemble streamflow

prediction approach, where the model was forced by an ensemble of past precipitation forcing from TRMM mission.

According to our results, the data assimilation scheme performed well in assimilating *in situ* and remotely sensed discharge and water levels into the large scale hydrologic-hydrodynamic model. The assimilation of *in situ* discharge showed that EnKF can improve discharge estimates at assimilation gauges but, differently from previous studies at smaller basins [e.g. *Clark et al.*, 2008; and others summarised by *Lee et al.*, 2012], also transfer information to ungauged rivers by improving results at validation sites, although with a smaller degree. The assimilation of discharge data at a reduced number of gauging stations located at larger rivers improves results mostly at the large reaches but it degrades results at some smaller basins. Also, the transformation of discharge measurements into the log space proved to be important to deal with very different discharge magnitudes arising from different spatial scales or from contrasting flood and recession flows.

The assimilation of satellite altimetry data improved model water levels, and also discharges with minor extent, mostly at the same river reaches where altimetry stations are located. Assimilating altimetry-based discharge also improved model estimates, although with minor degree if compared to the *in situ* discharge assimilation, probably due to the larger errors in remotely sensed observations. However, in both cases, even though radar altimetry data has low temporal resolution (35 days), its assimilation can improve model results at a daily basis, possibly due to its higher spatial resolution and the low temporal variability of Amazonian hydrographs.

The sensitivity analysis of the parameter from the DA scheme highlighted the importance of the magnitude of precipitation errors and that of their spatial correlation, while temporal correlation showed to be dispensable.

The deterioration of model performance at some unmonitored reaches may be due to the large dimensionality of state space in distributed hydrological models compared to the available information. Consequently, data assimilation may update state variables at some lumped fashion such as the sub-basin scale, as explained by *Lee et al*. [2012]. This problem can be also due to spurious correlations that can arise by numerical reasons and could be avoided by using proper spatial localization methods [e.g. *Sakov and Bertino*, 2010] developed for hydrological applications to constrain the influence of measurements. Additionally, the DA scheme could benefit from a better characterization of model errors,

where not only precipitation but other sources of uncertainty, such as in model parameters and structure could be included, as suggested by *Liu et al.* [2012].

Although limitations still exist, results are encouraging. This kind of DA scheme could also be easily employed to other similar regional/global scale hydrological models [e.g. *Yamazaki et al.*, 2011; *Decharme et al.*, 2011; *Alfieri et al.*, 2012]. It has also the potential to improve by assimilating remotely sensed water levels gathered by other satellite missions as the existing ones, or the altimetry missions to be launched in the coming years by European Spatial Agency ESA, namely the SENTINEl-3 constellation and the forthcoming SWOT mission [*Durand et al.*, 2010a]. Moreover, the altimetry-based discharge assimilation can improve when better discharge estimates become available, such as the ones under development for the future SWOT mission [*Durand et al.*, 2010b].

Finally, the model was able to provide relatively accurate streamflow forecasts in the Amazon basin. For smaller lead times (~ 5 to 15 days), forecasts agreed with observations in lots of gauging stations and for larger lead times (>30 days) they remained meaningful mostly at larger rivers. Forecasts were usually better at stream gauges used for data assimilation, especially for smaller lead times. Along the Solimões/Amazon main stem, forecast were highly accurate even for very large lead times (90 days) and the model was capable to successfully predict the record 2005 drought at the Solimões/Amazon River well in advance. These results demonstrate the potential for developing stream flow forecasts with large lead times at the world's large river basins, such as the Amazon, founded on large scale hydrological models based mostly on initial states gathered with proper DA schemes, and using past climate with the ESP approach. Also, results point to the potentiality of providing hydrological forecasts at poorly monitored regions by using mostly remotely sensed information.

Acknowledgements

The authors are grateful for: the financial and operational support from the Brazilian agencies FINEP and ANA ("*Projeto de Integração e Cooperação Amazônica para a Modernização do Monitoramento Hidrológico*" ICA-MMH) and CNPq-IRD ("*Assimilação de Dados de monitoramento Espacial para a análise do regime hidrológico da Bacia Amazônica e a previsão de curto e médio prazos*"); the ENVISAT satellite altimetry data supplied by

ESA; the TRMM data supplied by NASA and associated agencies; the TRMM Merge data provided by CPTEC/INPE; the discharge and stage data provided by ANA, Hybam, SENHAMI-Peru and SENHAMI-Bolivia; the EnKF Fortran codes provided by Geir Evensen; the support from Fernando Fan in processing precipitation data; as well as for the constructive comments from Adalberto Meller and Jeffrey Neal.

References

Alfieri, L., Burek, P., Dutra, E., Krzeminski, B., Muraro, D., Thielen, J., and Pappenberger, F. 2012. GloFAS – global ensemble streamflow forecasting and flood early warning. Hydrol. Earth Syst. Sci. Discuss., 9, 12293-12332, doi:10.5194/hessd-9-12293-2012.

Alsdorf, D.E., Rodrıguez, E., Lettenmaier, D.P. 2007. Measuring surface water from space. Reviews of Geophysics, 45: RG2002, DOI:10Ð1029/2006RG000197.

Andreadis, K.M., Lettenmaier, D.P. 2006. Assimilating remotely sensed snow observations into a macroscale hydrology model. Advances in Water Resources, 29, 6, 872-886.

Andreadis, K.M., Clark, E.A., Lettenmaier, D.P., Alsdorf, D.E. 2007. Prospects for river discharge and depth estimation through assimilation of swath-altimetry into a raster-based hydrodynamics model. Geophys. Res. Lett., 34, L10403, doi:10.1029/2007GL029721.

Biancamaria, S., Durand, M., Andreadis, K.M., Bates, P.D., Boone, A., Mognard, N.M., Rodriguez, E., Alsdorf, D.E., Lettenmaier, D.P., Clark, E.A. 2011. Assimilation of virtual wide swath altimetry to improve Arctic river modeling. Remote Sensing of Environment, 115, 2, 373-381.

Chen, J.L., Wilson, C.R., Tapley, B.D. 2010. The 2009 exceptional Amazon flood and interannual terrestrial water storage change observed by GRACE. Water Resour. Res., 46, W12526, doi:10.1029/2010WR009383.

Clark, M.P., Rupp, D.E., Woods, R.A., Zheng, X., Ibbitt, R.P., Slater, A.G., Schmidt, J., Uddstrom, M.J. 2008. Hydrological data assimilation with the ensemble Kalman filter: Use of streamflow observations to update states in a distributed hydrological model. Adv. Water Res., 31, 1309-1324, doi:10.1016/j.advwatres.2008.06.005.

Coe, M.T., Costa, M.H., Howard, E.A. 2008. Simulating the surface waters of the Amazon River basin: Impacts of new river geomorphic and flow parameterizations. Hydrological Processes, 22, 14, 2542-2553.

Collischonn, W., Allasia, D.G., Silva, B.C., Tucci, C.E.M. 2007. The MGB-IPH model for large-scale rainfall-runoff modeling. Hydrological Sciences Journal, 52, 878-895.

Day, G.N. 1985. Extended streamflow forecasting using NWSRFS. J. Water Resour. Plann. Manage., 111, 157–170.

Decharme, B., Alkama, R., Papa, F., Faroux, S., Douville, H., Prigent, C., 2011. Global off-line evaluation of the ISBA-TRIP flood model. DOI 10.1007/s00382-011-1054-9.

Durand, M., Fu, L.L., Lettenmaier, D.P., Alsdorf, D.E., Rodríguez, E., Fernandez, D.E. 2010a. The surface water and ocean topography mission: Observing terrestrial surface water and oceanic submesoscale eddies. Proceedings Of the IEEE, 98, 5, 766−779.

Durand, M., Rodríguez, E., Alsdorf, D., Trigg, M. 2010b. Estimating River Depth From Remote Sensing Swath Interferometry Measurements of River. IEEE journal of selected topics in applied earth observations and remote sensing, 3, 20-31.

Durand, M., Andreadis, K.M., Alsdorf, D.E., Lettenmaier, D.P., Moller, D., Wilson, M. 2008. Estimation of bathymetric depth and slope from data assimilation of swath altimetry into a hydrodynamic model. Geophys. Res. Lett., 35, L20401, doi:10.1029/2008GL034150.

Espinoza, J.C., Ronchail, J., Guyot, J.L., Cocheneau, G., Filizola, N., Lavado, W., de Oliveira, E., Pombosa, R., Vauchel, P. 2009. Spatio-Temporal rainfall variability in the Amazon Basin Countries (Brazil, Peru, Bolivia, Colombia and Ecuador). International Journal of Climatology, 29, 1574-1594.

Espinoza, J.C., Ronchail, J., Guyot, J.L., Junquas, C., Vauchel, P., Lavado, W., Drapeau, G., Pombosa, R. 2011. Climate variability and extreme drought in the upper Solimões River (western Amazon Basin): Understanding the exceptional 2010 drought. Geophys. Res. Lett., 38, L13406, doi:10.1029/2011GL047862.

Evensen, G. 2003. The ensemble Kalman filter: theoretical formulation and practical implementation. Ocean Dynamics, 53, 343 – 367.

Evensen, G. 2004. Sampling strategies and square root analysis schemes for the EnKF. Ocean Dyn., 54, 539–560.

Evensen, G. 2009. Data assimilation, The Ensemble Kalman Filter. 2nd ed., Springer.

Farr, T.G., Caro, E., Crippen, R., Duren, R., Hensley, S., Kobrick, M., Paller, M., Rodriguez, E., Rosen, P., Roth, L., Seal, D., Shaffer, S., Shimada, J., Umland, J.,Werner, M., Burbank, D., Oskin, M., Alsdorf, D. 2007. The shuttle radartopography mission. Reviews of Geophysics, 45, 2.

Frappart, F., Ramillien, G., Maisongrande, P., Bonnet, M-P. 2010. Denoising satellite gravity signals by Independent Component Analysis. IEEE Geosciences and Remote Sensing Letters, 7, 3, 421-425, doi:10.1109/LGRS.2009.2037837.

Frappart, F., Ramillien, G., Leblanc, M., Tweed, S.O., Bonnet, M-P., Maisongrande, P. 2011b. An Independent Component Analysis approach for filtering continental hydrology in the GRACE gravity data. Remote Sensing of Environment, 115, 1, 187-204, doi: 10.1016/j.rse.2010.08.017.

Gedney, N., Cox, P.M., Huntingford, C. 2004. Climate feedback from wetland methane emission. Geophys Res Lett, 31, L20503, doi:10.1029/2004GL020919.

Getirana, A.C.V., Boone, A., Yamazaki, D., Decharme, B., Papa, F., and Mognard, N. 2012. The Hydrological Modeling and Analysis Platform (HyMAP): evaluation in the Amazon basin. J. Hydrometeorol., accepted for publication, 2012.

Getirana, A.C.V., Peters-Lidard, C. 2012. Water discharge estimates from large radar altimetry datasets in the Amazon basin. Hydrol. Earth Syst. Sci. Discuss., 9, 7591-7611, doi:10.5194/hessd-9-7591-2012.

Hess, L.L., Melack, J.M., Novo, E.M.L.M., Barbosa, C.C.F., Gastil, M. 2003. Dual-season mapping of wetland inundation and vegetation for the central Amazon basin. Remote Sensing of Environment, 87, 404-428.

Huffman, G., Adler, R., Bolvin, D., Gu, G., Nelkin, E., Bowman, K., Hong, Y., Stocker, E., Wolff, D. 2007. The TRMM Multisatellite Precipitation Analysis (TCMA): quasi-global, multiyear, combined-sensor precipitation estimates at fine scales. J. Hydromet, 8, 38–55.

Kalman, R.E. 1960. A new approach to linear filtering and prediction problems. Transactions of the AMSE – Journal of Basic Engineering, 82 D, 35-45.

Krinner, G., 2003. Impact of lakes and wetlands on boreal climate, J. Geophys. Res., 108(D16), 4520, doi:10.1029/2002JD002597.

Kumar, S.V., Reichle, R.H., Peters-Lidard, C.D., Koster, R.D., Zhan, X., Crow, W.T., Eylander, J.B., Houser, P.R. 2008. A Land Surface Data Assimilation Framework using the Land Information System: Description and Applications. Advances in Water Resources, 31, 1419-1432, DOI:10.1016/j.advwatres.2008.01.013

Lee, H., Seo, D.-J., Koren, V. 2011. Assimilation of streamflow and in situ soil moisture data into operational distributed hydrologic models: Effects of uncertainties in the data and initial model soil moisture states. Advances in Water Resources, 34, 1597–1615, /10.1016/j.advwatres.2011.08.012.

Lee, H., Seo, D.-J., Liu, Y., Koren, V., McKee, P., and Corby, R. 2012. Variational assimilation of streamflow into operational distributed hydrologic models: effect of spatiotemporal scale of adjustment. Hydrol. Earth Syst. Sci., 16, 2233-2251, doi:10.5194/hess-16-2233-2012.

Leon, J.G., Calmant, S., Seyler, F., Bonnet, M-P., Cauhopé, M., Frappart, F. 2006. Rating curves and average water depth at the Upper Negro river from satellite altimetry and modeled discharges. Journal of Hydrology, 328, 3-4, 481-496.

Liu, Y., Gupta, H.V. 2007. Uncertainty in hydrologic modeling: Toward an integrated data assimilation framework. Water Resour. Res., 43, W07401, doi:10.1029/2006WR005756.

Liu, Y., Weerts, A.H., Clark, M., Hendricks Franssen, H.-J., Kumar, S., Moradkhani, H., Seo, D.-J., Schwanenberg, D., Smith, P., van Dijk, A.I.J.M., van Velzen, N., He, M., Lee, H., Noh, S. J., Rakovec, O., Restrepo, P. 2012. Advancing data assimilation in operational hydrologic forecasting: progresses, challenges, and emerging opportunities. Hydrol. Earth Syst. Sci., 16, 3863-3887, doi:10.5194/hess-16-3863-2012.

Marengo, J., Nobre, C., Tomasella, J., Oyama, M., de Oliveira, G., de Oliveira, R., Camargo, H., Alves, L. 2008. The drought in Amazonia in 2005. Journal of Climate, 21, 495–516.

Marengo, J.A., Tomasella, J., Alves, L.M., Soares, W.R., Rodriguez, D.A. 2011. The drought of 2010 in the context of historical droughts in the Amazon region. Geophys. Res. Lett., 38, L12703, doi:10.1029/2011GL047436.

McMillan, H.K., Hreinsson, E.Ö., Clark, M.P., Singh, S.K., Zammit, C., Uddstrom, M.J. 2012. Operational hydrological data assimilation with the Retrospective Ensemble Kalman Filter: use of observed discharge to update past and present model states for flow forecasts. Hydrol. Earth Syst. Sci. Discuss., 9, 9533-9575, doi:10.5194/hessd-9-9533-2012.

Meade, R.H., Rayol, J.M., Da Conceição, S.C., Natividade, J.R.G. 1991. Backwater effects in the Amazon River basin of Brazil. Environmental Geology and Water Sciences, 18, 2, 105-114.

Melack, J.M., Hess, L.L. 2010. Remote sensing of the distribution and extent of wetlands in the Amazon basin. In: Junk, W.J., Piedade, M. (eds) Amazonian floodplain forests: ecophysiology, ecology, biodiversity and sustainable management. Ecological Studies, vol. 210, part 1. Springer, 43–59.

Neal, J.C., Schumann, G.J.-P., Bates, P.D., Buytaert, W., Matgen, P., Pappenberger, F. 2009. A data assimilation approach to discharge estimation from space. Hydrological Processes, 23, 25, 3641-3649, ISSN: 1099-1085 10.1002/hyp.7518.

Neal, J.C., Atkinson, P.M. Hutton, C.W. 2007. Flood inundation model updating using ensemble Kalman filter and spatially distributed measurements. Journal of Hydrology, 336, 401-415.

New, M., Lister, D., Hulme, M., Makin, I. 2002. A high-resolution data set of surface climate over global land areas. Climate Res., 21.

Nijssen, B., Lettenmaier, D. 2004. Effect of precipitation sampling error on simulated hydrological fluxes and states: Anticipating the Global Precipitation Measurement satellites. J. Geophys. Res., 109, D02103, doi:10.1029/2003JD003497.

Oki, T., Kanae, S. 2006. Global hydrological cycles and world water resources. Science, 313, 1068–1072, doi:10.1126/science.1128845.

Paiva, R.C.D., Collischonn, W., Tucci, C.E.M. 2011. Large scale hydrologic and hydrodynamic modeling using limited data and a GIS based approach. Journal of Hydrology, 406, 170–181.

Paiva, R.C.D., Collischonn, W., Buarque, D.C. 2012a. Validation of a full hydrodynamic model for large scale hydrologic modelling in the Amazon. Hydrol. Process., DOI: 10.1002/hyp.8425.

Paiva, R.C.D., Collischonn, W., Bonnet, M.P., de Gonçalves, L.G.G. 2012b. On the sources of hydrological prediction uncertainty in the Amazon, Hydrol. Earth Syst. Sci., 16, 3127-3137, doi:10.5194/hess-16-3127-2012.

Paiva, R.C.D., Collischonn, W., Bonnet, M.-P., Buarque, D.C., Frappart, F., Calmant, S., Mendes, C.B. 2013. Large scale hydrologic and hydrodynamic modelling of the Amazon River basin. Water Resour. Res., doi: 10.1002/wrcr.20067, (Accepted for publication).

Papa, F., Durand, F., Rossow, W.B., Rahman, A., Bala, S.K. 2010a. Satellite altimeter-derived monthly discharge of the Ganga-Brahmapoutra River and its seasonal to interannual variations from 1993 to 2008. J. Geophys. Res., 115, C12013, doi:10.1029/2009JC006075.

Papa, F., Prigent, C., Aires, F., Jimenez, C., Rossow, W.B., Matthews, E. 2010b. Interannual variability of surface water extent at the global scale, 1993–2004. J. Geophys. Res., 115, D12111, doi:10.1029/2009JD012674.

Pereira-Cardenal, S.J., Riegels, N.D., Berry, P.A.M., Smith, R.G., Yakovlev, A., Siegfried, T.U., Bauer-Gottwein, P. 2011. Real-time remote sensing driven river basin modeling using radar altimetry. Hydrol. Earth Syst. Sci., 15, 241-254, doi:10.5194/hess-15-241-2011, 2011.

Rakovec, O., Weerts, A.H., Hazenberg, P., Torfs, P.J.J.F., and Uijlenhoet, R. 2012. State updating of a distributed hydrological model with Ensemble Kalman Filtering: effects of updating frequency and observation network density on forecast accuracy. Hydrol. Earth Syst. Sci., 16, 3435-3449, doi:10.5194/hess-16-3435-2012.

Reichle, R.H., Mclaughlin, D.B., Entekhabi, D. 2002. Hydrologic Data Assimilation with Ensemble Kalman Filter. Monthly Weather Review, 130, 103-114.

Reichle, R.H. 2008. Data assimilation methods in the Earth sciences. Adv. Water Resour., doi:10.1016/j.advwatres.2008.01.001.

Ricci, S., Piacentini, A., Thual, O., Le Pape, E., Jonville, G. 2011. Correction of upstream flow and hydraulic state with data assimilation in the context of flood forecasting. Hydrol. Earth Syst. Sci., 15, 3555-3575, doi:10.5194/hess-15-3555-2011.

Rozante, J.R., Moreira, D.S., de Goncalves, L.G.G., Vila, D.A. 2010. Combining TRMM and Surface Observations of Precipitation: Technique and Validation over South America. Wea. Forecasting, 25, 885–894, doi: http://dx.doi.org/10.1175/2010WAF2222325.1

Santos da Silva, J., Calmant, S., Seyler, F., Rotunno Filho, O.C., Cochonneau, G., Mansur, W.J. 2010. Water levels in the Amazon basin derived from the ERS 2 and ENVISAT radar altimetry missions. Remote Sensing of Environment, 114, 10, 2160-2181.

Thielen, J., Bartholmes, J., Ramos, M.-H., de Roo, A. 2009. The European Flood Alert System – Part 1: Concept and development, Hydrol. Earth Syst. Sci., 13, 125-140, doi:10.5194/hess-13-125- 2009.

Thirel, G., Martin, E., Mahfouf, J.-F., Massart, S., Ricci, S., and Habets, F. 2010. A past discharges assimilation system for ensemble streamflow forecasts over France – Part 1: Description and validation of the assimilation system. Hydrol. Earth Syst. Sci., 14, 1623-1637, doi:10.5194/hess-14-1623-2010.

Tian, Y., Peters-Lidard, C.D. 2010. A global map of uncertainties in satellite-based precipitation measurements. Geophys. Res. Letters, 37, L24407, doi:10.1029/2010GL046008.

Tomasella, J., Borma, L.S., Marengo, J.A., Rodriguez, D.A., Cuartas, L.A. Nobre, C.A., Prado, M.C.R. 2010. The droughts of 1996–1997 and 2004–2005 in Amazonia: hydrological response in the river main-stem. Hydrol. Process., 25, 8, 1228-1242, DOI: 10.1002/hyp.7889.

Trigg, M.A., Wilson, M.D., Bates, P.D., Horritt, M.S., Alsdorf, D.E., Forsberg B.R., Vega, M.C. 2009. Amazon flood wave hydraulics. Journal of Hydrology, 374, 92–105.

Uvo, C.B., Graham, N. E. 1998. Seasonal runoff forecast for northern South America: A statistical model. Water Resour. Res., 34, 12, 3515-3524, doi:10.1029/98WR02854, 1998.

Uvo, C.B., Tölle, U., Berndtsson, R. 2000. Forecasting discharge in Amazonia using artificial neural networks. International Journal of Climatology, 20, 1495-1507, doi: 10.1002/1097-0088(200010)20:12<1495::AID-JOC549>3.0.CO;2-F.

Vrugt, J.A., Diks, C.G.H., Gupta, H.V., Bouten, W., Verstraten, J.M. 2005. Improved treatment of uncertainty in hydrologic modeling: Combining the strengths of global optimization and data assimilation. Water Resour. Res., 41, W01017, doi:10.1029/2004WR003059.

Wilks, D.S. 2006. Statistical Methods in the Atmospheric Sciences. 2st ed. Academic Press, 467.

Wilson, W., Bates, P., Alsdorf, D., Forsberg, B., Horritt, M., Melack, J., Frappart, F., Famiglietti, J. 2007. Modeling large-scale inundation of Amazonian seasonally flooded wetlands. Geophys. Res. Lett., 34, L15404, doi:10.1029/2007GL030156.

Wood, A.W., Maurer, E., Kumar, A., Lettenmaier, D.P. 2002. Long-range experimental hydrologic forecasting for the eastern United States. Journal of Geophysical Research, 107, D20, 4429, doi:10.1029/2001JD000659.

Yamazaki, D., Kanae, S., Kim, H., Oki, T. 2011. A physically n dynamics in a global river routing model. Water Resour. Res., 47, W04501, doi:10.1029/2010WR009726.

CAPÍTULO 6

Conclusões gerais e perspectivas

6.1. Conclusões

Como funciona a hidrologia de grandes bacias hidrográficas, mais especificamente da bacia Amazônica?

É possível prever o seu funcionamento, antecipando cheias e secas, e fornecendo informações quantitativas para o gerenciamento dos recursos hídricos?

Que fatores dominam a previsibilidade hidrológica na bacia Amazônica?

Como as mais recentes técnicas de modelagem hidrológica-hidrodinâmica de grande escala e observação via sensoriamento remoto podem auxiliar para estes fins?

Estas são as questões que motivaram o desenvolvimento desta tese. Para tanto, foram desenvolvidas e avaliadas técnicas de modelagem hidrológica-hidrodinâmica de grande escala, de assimilação de dados *in situ* e de sensoriamento remoto nestes modelos e de previsão de vazões. Este conjunto de técnicas foi utilizado para o estudo da bacia Amazônica em termos de seus processos hidrológicos e de sua previsibilidade hidrológica.

Estes temas e diversas questões científicas específicas foram abordados em uma série de estudos, apresentados nos Capítulos 2 a 5, cujas conclusões são apresentadas a seguir.

6.1.1. Modelagem hidrológica e hidrodinâmica

A bacia Amazônica foi simulada utilizando-se um modelo hidrológico e hidrodinâmico que se enquadra no estado da arte da modelagem física/conceitual de grandes bacias hidrográficas. Utiliza-se o modelo hidrológico MGB-IPH *"*Modelo de Grandes Bacias*"*, desenvolvido por *Collischonn et al.* [2007] com um módulo de modelagem hidrodinâmica de grande escala desenvolvido recentemente por *Paiva et al.* [2011a], que utiliza as equações de *Saint Venant* para simular o escoamento nos rios e em um modelo do tipo armazenamento nas várzeas de inundação.

O modelo foi amplamente validado utilizando-se observações hidrológicas convencionais (vazões e cotas de estações fluviométricas) e oriundas de recentes técnicas de sensoriamento remoto, incluindo níveis d'água estimados por altimetria espacial por radar do satélite ENVISAT [*Santos da Silva et al.,* 2010], extensão de áreas alagadas estimadas por dados de múltiplos satélites [*Papa et al.,* 2010] e variações no armazenamento de água terrestre oriundos da missão de gravimetria GRACE [*Frappart et al.,* 2010; 2011b]. Em

resumo, os resultados mostram um bom desempenho deste modelo, cujos resultados concordam com as observações mencionadas acima.

Entretanto, algumas limitações foram observadas, como erros de vazões, níveis d'água e áreas inundadas simulados em algumas regiões específicas, podendo ser explicadas por incertezas em alguns dados e parâmetros de entrada. A precipitação é a variável mais sensível de todas, e os erros na estimativa desta variável de entrada podem causar erros importantes em todas as variáveis de saída, como vazões, níveis d'água e extensão de áreas alagadas médias. Paralelamente, foram encontrados erros em áreas no oeste Amazônico, possivelmente em consequência da baixa qualidade das estimativas de precipitação por satélite nesta região, que é ao mesmo tempo montanhosa e pouco monitorada. O modelo também se mostrou sensível a parâmetros relacionados a características dos rios e várzeas de inundação, como largura e nível de fundo dos rios, coeficiente de rugosidade de Manning e batimetria das várzeas. A incerteza nestes parâmetros, que foram estimados baseados no modelo digital de elevação do SRTM [*Farr et al.*, 2007] e relações geomorfológicas, causou erros em níveis d'água e áreas alagadas em algumas regiões, indicando a necessidade de melhores métodos para suas estimativas. Estas conclusões concordam e complementam estudos anteriores, como os de *Yamazaki et al.* [2011] e *Decharme et al.* [2011].

6.1.2. Hidrologia da bacia Amazônica

O funcionamento hidrológico da bacia Amazônica foi estudado utilizando-se resultados de modelagem e observações de sensoriamento remoto.

O balanço hídrico geral da bacia Amazônica obtido via resultados de simulação concorda com estimativas de estudos anteriores. Conforme os resultados, as taxas médias de precipitação, evapotranspiração e vazão próxima foz em Óbidos são: $P = 5.65$ mm.dia^{-1}, $ET = 2.72$ mm.dia^{-1} e $Q = 3.09$ mm.dia^{-1}. A Amazônia apresenta uma marcada variabilidade sazonal no armazenamento de água terrestre, com altas amplitudes de variação de 325 mm, chegando a valores maiores que 750 mm na Amazônica central. Tal variabilidade é dominada pela dinâmica das águas superficiais (56%), principalmente na Amazônia central, que possui grandes várzeas de inundação. A água no solo também é responsável por parte (36%) da variabilidade no armazenamento d'água na bacia, e as águas subterrâneas não apresentam uma grande contribuição (8%) para este processo.

Investigou-se também o papel das várzeas de inundação e efeitos de remanso na propagação das grandes cheias Amazônicas. Uma importante interação entre os níveis d'água,

áreas alagadas e vazões ocorre durante a passagem das ondas de cheia. As várzeas de inundação atuam armazenando volumes d'água extravasados pelo rio, atenuando e atrasando as ondas de cheia, atraso este de vários meses nos grandes rios amazônicos. Os efeitos de remanso também possuem um papel importante, embora menor, e se não representados também causam hidrogramas adiantados em relação aos observados. Estes resultados indicam a importância da utilização de aproximações quase completas das equações de *Saint Venant* e da representação das várzeas de inundação na modelagem da bacia Amazônica ou outras bacias semelhantes. Embora as várzeas tenham um papel importante no movimento das águas Amazônicas, a sua variação sazonal aparentemente não influencia as taxas de evapotranspiração e o balanço hídrico desta bacia.

Através de estimativas de precipitação de sensoriamento remoto da missão TRMM, estudou-se a variabilidade espacial da precipitação na Amazônia brasileira. Em resumo, os resultados mostram uma clara redução na precipitação média anual e número de dias chuvosos sobre os grandes corpos d'água amazônicos. Este comportamento é mais marcado durante a tarde, quando grande parte da precipitação é de origem convectiva, e se invertendo a noite e pela manhã. Tal fenômeno não está de acordo com problemas técnicos das estimativas de precipitação por sensoriamento remoto relatados de estudos anteriores. Por outro lado, os resultados apresentados concordam com outros estudos observacionais em pequena escala na região amazônica, que mencionam um fenômeno chamado de brisa fluvial, causado por diferenças no balanço de energia na água e na floresta, que poderia causar uma maior formação de nuvens e precipitação sobre a floresta durante o dia e o contrário à noite. Como grande parte dos postos pluviométricos da bacia Amazônica localiza-se ao longo dos rios, as estimativas de precipitação baseadas em pluviômetros podem estar sendo sistematicamente subestimadas, tendo importantes implicações sobre estudos nesta região. Entretanto, o estudo aqui apresentado não é totalmente conclusivo, e este fenômeno poderia ser confirmado através da análise de dados radares meteorológicos instalados *in situ*.

6.1.3. Assimilação de dados in situ e de altimetria por radar

Investigou-se também acerca da integração de modelos de simulação com observações, tanto de estações fluviométricas como de sensoriamento remoto, com o objetivo de melhorar as estimativas destes modelos. De forma pioneira, foi desenvolvido um esquema de assimilação de dados para um modelo hidrológico-hidrodinâmico de grande escala para assimilar informações *in situ* e de altimetria por radar. O esquema é baseado na técnica

"*Ensemble Kalman Filter*" para atualizar todas as variáveis de estado do modelo e foi avaliado na bacia Amazônica.

O desempenho deste sistema provou-se satisfatório na assimilação de dados de vazão de níveis d'água *in situ* e de altimetria por radar no modelo hidrológico-hidrodinâmico de grande escala. A assimilação de vazões *in situ* demonstrou que este esquema melhora as estimativas do modelo nos postos fluviométricos utilizados para assimilação, mas diferentemente de tentativas de estudos anteriores, também transfere informações para locais não monitorados melhorando os resultados, embora que em um menor grau.

A assimilação de dados de altimetria por radar do satélite ENVISAT melhora estimativas de níveis d'água e vazões, principalmente nos rios onde observações foram assimiladas. Um aspecto interessante é que, embora os dados dos radares altimétricos tenham uma baixa resolução temporal (35 dias), a sua assimilação melhora os resultados do modelo em nível diário, possivelmente pela alta resolução espacial deste dado e a baixa variabilidade temporal da inundação amazônica.

Em alguns casos o esquema degrada os resultados em locais não monitorados, podendo ser devido à (i) grande dimensionalidade do espaço de variáveis de estado de modelos hidrológicos distribuídos, se comparado com a informação contida nos dados assimilados; (ii) imperfeita caracterização dos erros do modelo hidrológico; (iii) correlações espúrias que surgem devido a questões numéricas do método. Assim, ainda existe o potencial de aperfeiçoar este tipo de esquema de assimilação de dados, através do uso de mais dados observados, um melhor conhecimento acerca dos erros do modelo hidrológico e o desenvolvimento de métodos de localização para restringir espacialmente a influencia das observações.

6.1.4. Previsão hidrológica

As características de previsibilidade hidrológica na bacia Amazônica foram inicialmente estudadas a fim de guiar o desenvolvimento de um protótipo de sistema de previsão hidrológica. Os resultados deste estudo inicial mostram que a incerteza nas condições hidrológicas iniciais domina a previsibilidade hidrológica nos grandes rios amazônicos, mesmo para altos horizontes de previsão (1 a 3 meses), sendo mais importante que a incerteza da precipitação no futuro. Destaca-se a importância de variáveis de estado relacionadas a águas superficiais como vazões, níveis d'água e volumes nas várzeas de inundação, principalmente em rios com baixa declividade e grandes várzeas de inundação,

possivelmente devido ao alto tempo de viagem das ondas de cheia neste tipo de ambiente. O estado das águas subterrâneas mostrou-se importante principalmente nas estiagens no sudoeste da bacia, caracterizado por uma maior sazonalidade e por encontrar-se sobre a formação geológica do Escudo Brasileiro. Incertezas no forçante de precipitação mostraram-se importantes nos rios menores e no inicio da estação chuvosa durante a subida dos hidrogramas em algumas regiões especificas. Os resultados indicaram a possibilidade de desenvolver previsões hidrológicas para a bacia Amazônica baseadas principalmente nas condições hidrológicas iniciais, além de motivar o desenvolvimento de técnicas de assimilação de dados para estimar estes estados hidrológicos no inicio das previsões.

Com base nestes argumentos, desenvolveu-se pela primeira vez um protótipo de sistema de previsão de vazões para a bacia Amazônica, baseado no modelo hidrológico-hidrodinâmico da Amazônia, inicializado com condições iniciais ótimas estimadas pelo esquema de assimilação de dados utilizando precipitação estimada por sensoriamento remoto disponível em tempo real. Empregou-se a técnica "*Ensemble Streamflow Prediction*", onde considerando desconhecer-se a precipitação no futuro, utiliza-se um conjunto dados de precipitação dos anos passados para forcar o modelo.

Os resultados deste sistema mostraram-se promissores e o modelo foi capaz de prover previsões satisfatórias na bacia Amazônica. No caso de baixos horizontes de previsão (5 a 15 dias), as previsões concordam os dados observados em muitas as estações fluviométricas enquanto que para maiores horizontes (> 30 dias) as previsões continuam informativas principalmente nos grandes rios. Os resultados normalmente são melhores nos postos fluviométricos utilizados para assimilação de dados, como esperado. As previsões tem grande acurácia ao longo do rio principal Solimões/Amazonas, mesmo para horizontes de previsão muito elevados (90 dias), sendo capaz de prever, por exemplo, a grande seca de 2005 com grande antecedência. Estes resultados mostram o potencial da modelagem hidrológica de grande escala apoiada por informação de sensoriamento remoto na previsão de vazões com alta antecedência nas grandes bacias do mundo, como a bacia Amazônica.

6.2. Perspectivas

Os resultados desta tese, em conjunto com outras pesquisas recentes, apontam para diversas perspectivas de pesquisa envolvendo a compreensão e previsão da hidrologia de grandes bacias hidrográficas.

6.2.1. Modelagem física de grande escala

As análises do presente estudo demonstram que uma das limitações da modelagem de grande escala baseada em processos é relacionada aos parâmetros de entrada, destacando-se o conhecimento limitado acerca de parâmetros relacionados a rios e planícies de inundação. Isto poderia ser contornado com as novas técnicas de sensoriamento remoto que vem sendo desenvolvidas. A batimetria das várzeas de inundação é normalmente estimada com dados de elevação do SRTM, que possui erros sistemáticos devido ao sinal do SRTM não penetrar a vegetação. Este erro poderia ser tratado com o auxilio de um recente mapa global de altura de vegetação de *Simard et al.* [2011] desenvolvido com dados do satellite ICEsat/GLAS ("*Ice, Cloud, and Land Elevation Satellite/Geoscience Laser Altimeter System*"). Por outro lado, a largura dos rios atualmente é estimada por meio de relações geomorfológicas empíricas através da vazão média ou área de drenagem. Inclusive, *Andreadis et al.* [em revisão] desenvolveram recentemente uma base de dados global de largura e profundidade d'água em rios baseado neste conceito. Mas a largura dos rios poderia ser estimada com imagens de sensoriamento remoto, utilizando, por exemplo, as técnicas de extração automática desenvolvidos por *Pavelsky e Smith* [2007]. Adicionalmente, dados da futura missão SWOT ("*Surface Waters and Ocean Topography*") [*Durand et al.*, 2010], que fornecerá informação de níveis d`água e áreas inundadas em alta resolução espacial, poderão ser utilizados para estimar a batimetria de rios e várzeas de inundação.

Por outro lado, existe ainda a necessidade de aperfeiçoar os modelos no que tange a representação física de diferentes processos hidrológicos. Os resultados desta tese demonstraram a importância da representação detalhada da hidráulica fluvial com equações de *Saint Venant* quase completas e o papel das várzeas de inundação. Entretanto, outros processos ainda deveriam ser incorporados nos modelos de simulação de grande escala. Por exemplo, diversos trabalhos apontam para a complexidade presente nas várzeas de inundação Amazônicas, com escoamento bidirecional e complexidade nas trocas d'água entre rios e planícies [*Alsdorf et al.* 2007a; *Alsdorf et al.*, 2003; *Bonnet et al.*, 2008] além de escoamento em pequenos canais [*Trigg et al*., 2012]. Estes aspectos poderiam ser representados com diferentes tipos de abordagens de simulação detalhada das várzeas de inundação [*e.g. Bonnet et al.*, 2008; *Paz et al.*, 2011; *Wilson et al.*, 2007; *Bates and De Roo*, 2000; *Neal et al*. 2012]. Outros aspectos também merecem atenção, como a interação entre águas superficiais e subterrâneas recentemente abordado por *Vergnes e Decharme* [2012] e *Miguez-Machu e Fan* [2012a,b]. A representação da hidrologia de grandes bacias hidrográficas também poderia

melhorar com a maior resolução espacial dos modelos. Para tanto, *Wood et al.* [2011] alertam para a necessidade do desenvolvimento de modelos hidrológicos de alta resolução para o domínio global, indicando diversos temas de pesquisa e obstáculos científicos a serem vencidos.

6.2.2. Compreensão de processos hidrológicos via estudos de simulação

As análises desta tese, em conjunto com outras pesquisas recentes, mostram como é possível usar modelos hidrológicos baseados em processos para a compreensão do funcionamento hidrológico de grandes bacias, respondendo a questões cientificas sobre estes sistemas e não servindo somente como ferramenta de suporte para projetos de engenharia como historicamente empregados no passado. Especificamente nesta tese, estudou-se o papel de aspectos hidráulicos e das várzeas de inundação sobre a propagação das ondas de cheia Amazônicas, além do papel de diferentes compartimentos hidrológicos na variação do armazenamento d'água na bacia. Mas diversas outras questões podem ser investigadas e respondidas com o aperfeiçoamento destes modelos. Além disto, a incorporação de um grande volume de informações através de assimilação de dados nestes modelos também pode permitir o estudo e caracterização dos diversos fluxos hidrológicos em diferentes regiões/biomas do globo, como normalmente se utiliza em reanálises meteorológicas para estudos climáticos. Além disso, a avaliação de modelos concorrentes baseados em diferentes hipóteses sobre o funcionamento hidrológico de um sistema também pode auxiliar para estes fins. Por exemplo, este tipo de abordagem foi utilizada no Capitulo 2 para verificação da importância das várzeas e efeitos de remanso, e também em outros estudos recentes, como em *Neal et al.* [2012] na investigação do funcionamento do delta interior do rio Niger, e em *Miguez-Machu e Fan* [2012a,b] que estudaram a importância das águas subterrâneas no ciclo hidrológico amazônico.

6.2.3. Prevendo impactos antrópicos sobre a hidrologia Amazônica

O desflorestamento [*Leite et al*., 2012] na bacia Amazônica pode gerar importantes impactos sobre a sua hidrologia, que apesar de já estudados recentemente [*Rodriguez et al.*, 2010] não são completamente compreendidos. Além disto, supostas mudanças climáticas são esperadas [*IPCC*, 2007] havendo a necessidade de sua avaliação sobre a hidrologia amazônica. Soma-se a isto a construção de novas grandes barragens hidroelétricas nos rios

Amazônicos, cujos impactos sobre o sistema Amazônico ainda não são inteiramente compreendidos. Os impactos destes diferentes tipos de pressão antrópica sobre a hidrologia amazônica poderiam ser avaliados com o auxilio de modelos hidrológicos de grande escala como o desenvolvido nesta tese.

6.2.4. Assimilação de dados de sensoriamento remoto

Desenvolveu-se nesta tese técnicas de assimilação de dados de vazões e altimetria por radar em modelos hidrológicos de grande escala, e os resultados foram encorajadores. Estas técnicas podem ser utilizadas para o desenvolvimento de reanálises hidrológicas que seriam utilizadas em estudos retrospectivos, a exemplo dos eventos hidrológicos extremos ocorridos recentemente na Amazônia. O mesmo esquema de assimilação de dados também poderia facilmente ser aplicado em outros modelos regionais ou globais similares [e.g. *Yamazaki et al.*, 2011; *Decharme et al.*, 2011; *Alfieri et al.*, 2012; *Getirana et al.*, 2012]. Existe também o potencial de melhorar os resultados apresentados nesta tese através da assimilação de dados de novas missões a serem lançadas no futuro, como a constelação SENTINEL-3 da ESA ("*European Spatial Agency*") ou a futura missão SWOT [*Durand et al.*, 2010].

6.2.5. Previsão hidrológica

Os resultados apresentados mostram o potencial do uso de modelos hidrológicos baseados em processos para a previsão de vazões em grandes bacias. Mais ainda, modelos hidrológicos apoiados principalmente em informação de sensoriamento remoto, como estimativas de precipitação e níveis d'água de altimetria por radar. Por outro lado, alguns sistemas continentais/globais operacionais de previsão hidrológica já estão sendo desenvolvidos [*Thielen et al.*, 2009; *Wood et al.*, 2002; *Alfieri et al.*, 2012]. Neste sentido, as técnicas de assimilação de dados e previsão hidrológica baseada principalmente nas condições iniciais e informação de sensoriamento remoto poderiam ser implementadas em sistemas operacionais deste tipo.

Referencias bibliográficas

Alfieri, L., Burek, P., Dutra, E., Krzeminski, B., Muraro, D., Thielen, J., and Pappenberger, F. 2012. GloFAS – global ensemble streamflow forecasting and flood early warning. Hydrol. Earth Syst. Sci. Discuss., 9, 12293-12332, doi:10.5194/hessd-9-12293-2012.

Alsdorf, D., Bates, P., Melack, J., Wilson, M., Dunne, T. 2007a. The spatial and temporal complexity of the Amazon flood measured from space. Geophysical Research Ltrs, 34, L08402.

Alsdorf, D.E., Rodrıguez, E., Lettenmaier, D.P. 2007b. Measuring surface water from space. Reviews of Geophysics, 45: RG2002, DOI:10Ð1029/2006RG000197.

Alsdorf, D., Han, S-C., Bates, P., Melack, J. 2010. Seasonal water storage on the Amazon floodplain measured from satellites. Remote Sensing of Environment, 114, 2448–2456.

Andreadis, K.M., Lettenmaier, D.P. 2006. Assimilating remotely sensed snow observations into a macroscale hydrology model. Advances in Water Resources, 29, 6, 872-886.

Andreadis, K.M., Clark, E.A., Lettenmaier, D.P., Alsdorf, D.E. 2007. Prospects for river discharge and depth estimation through assimilation of swath-altimetry into a raster-based hydrodynamics model. Geophys. Res. Lett., 34, L10403, doi:10.1029/2007GL029721.

Aufdenkampe, A.K., Mayorga, E., Raymond, P.A., Melack, J.M., Doney, S.C., Alin, S.R., Aalto, R.E., Yoo, K. 2011. Riverine coupling of biogeochemical cycles between land, oceans, and atmosphere. Frontiers in Ecology and the Environment, 9, 53-60, DOI: 10.1890/100014.

Beighley, R.E., Eggert, K.G., Dunne, T., He, Y., Gummadi, V., Verdin, K.L. 2009. Simulating hydrologic and hydraulic processes throughout the Amazon River Basin. Hydrological Processes, 23, 8, 1221-1235.

Biancamaria, S., Durand, M., Andreadis, K.M., Bates, P.D., Boone, A., Mognard, N.M., Rodriguez, E., Alsdorf, D.E., Lettenmaier, D.P., Clark, E.A. 2011. Assimilation of virtual wide swath altimetry to improve Arctic river modeling. Remote Sensing of Environment, 115, 2, 373-381.

Bonnet, M.P, Barroux, G., Martinez, J.M., Seyler, F., Turcq, P.M., Cochonneau, G., Melack, J.M., Boaventura, G., Bourgoin, L.M., León, J.G., Roux, E., Calmant, S., Kosuth, P., Guyot, J.L., Seyler, F. 2008. Floodplain hydrology in an Amazon floodplain lake (Lago Grande de Curuaí). Journal of Hydrology, 349, 18-30.

Bourgoin, L.M., Bonnet, M.P., Martinez, J.M., Kosuth, P., Cochonneau, G., Turcq, P.M., Guyot, J.L., Vauchel, P., Filizola, N., Seyler, P. 2007. Temporal dynamics of water and sediment exchanges between the Curuaí floodplain and the Amazon River, Brazil. Journal of Hydrology, 335, 140-156.

Brasil. 2007a. Plano Nacional de Energia 2030. Empresa de Pesquisa Energética, Rio de Janeiro: EPE, 408.

Brasil. 2007b. Plano Nacional de Energia 2030 v.3. Geração hidrelétrica. Ministério de Minas e Energia, Empresa de Pesquisa Energética.

Cappelaere, B., Lubès-Niel, H., Berkhoff, C., Thépaut, H., Guyot, J.L., de Oliveira, E. Rodrigues, M. 1996. Prévisions des crues de l'Amazone. In: /. 'hydrologie tropicale: géoscience et outil pour le développement (Actes de la conférence de Paris, mai 1995), 355-366, IAHS Publ, 238.

Chen, J.L.,Wilson, C.R., Tapley, B.D., Zang, Z.L., Niu, G.Y. 2009. The 2005 drought event in the Amazon River basin as measured by GRACE and estimated by climate models. J. Geophys. Res., 114, B05404, doi:10.1029/2008JB006056.

Chen, J.L., Wilson, C.R., Tapley, B.D. 2010. The 2009 exceptional Amazon flood and interannual terrestrial water storage change observed by GRACE. Water Resour. Res., 46, W12526, doi:10.1029/2010WR009383.

Clark, M.P., Rupp, D.E., Woods, R.A., Zheng, X., Ibbitt, R.P., Slater, A.G., Schmidt, J., Uddstrom, M.J. 2008. Hydrological data assimilation with the ensemble Kalman filter: Use of streamflow observations to update states in a distributed hydrological model. Adv. Water Res., 31, 1309-1324, doi:10.1016/j.advwatres.2008.06.005.

Coe, M.T., Costa, M.H., Howard, E.A. 2008. Simulating the surface waters of the Amazon River basin: Impacts of new river geomorphic and flow parameterizations. Hydrological Processes, 22, 14, 2542-2553.

Collischonn, W., Allasia, D.G., Silva, B.C., Tucci, C.E.M. 2007. The MGB-IPH model for large-scale rainfall-runoff modeling. Hydrological Sciences Journal, 52, 878-895.

Collischonn, B., Collischonn, W., Tucci, C. 2008. Daily hydrological modeling in the Amazon basin using TRMM rainfall estimates. Journal of Hydrology, 207.

Collischonn, W., Tucci, C.E.M., Clarke, R.T., Chou, S.C., Ghuilhon, L.G., Cataldi, M., Allasia, D.G. 2007. Medium-range reservoir inflow predictions based on quantitative precipitation forecasts. Journal of Hydrology (Amsterdam), 344, 112-122.

Decharme, B., Alkama, R., Papa, F., Faroux, S., Douville, H., Prigent, C., 2011. Global off-line evaluation of the ISBA-TRIP flood model. DOI 10.1007/s00382-011-1054-9.

Dunne, T., Mertes, L.A.K., Meade, R.H., Richey, J.E., Forsberg, B.R. 1998. Exchanges of sediment between the flood plain and channel of the amazon river in brazil. Geological Society of America Bulletin, 110, 450-467.

Durand, M., Andreadis, K.M., Alsdorf, D.E., Lettenmaier, D.P., Moller, D., Wilson, M. 2008. Estimation of bathymetric depth and slope from data assimilation of swath altimetry into a hydrodynamic model. Geophys. Res. Lett., 35, L20401, doi:10.1029/2008GL034150.

Durand, M., Fu, L.L., Lettenmaier, D.P., Alsdorf, D.E., Rodríguez, E., Fernandez, D.E. 2010a. The surface water and ocean topography mission: Observing terrestrial surface water and oceanic submesoscale eddies. Proceedings Of the IEEE, 98, 5, 766−779.

EPE. 2012. Balanço Energético Nacional 2012: Ano base 2011. Empresa de Pesquisa Energética (Brasil), Rio de Janeiro, 282.

Espinoza, J.C., Ronchail, J., Guyot, J.L., Cocheneau, G., Filizola, N., Lavado, W., de Oliveira, E., Pombosa, R., Vauchel, P. 2009a. Spatio-Temporal rainfall variability in the Amazon Basin Countries (Brazil, Peru, Bolivia, Colombia and Ecuador). International Journal of Climatology, 29, 1574-1594.

Espinoza, J.C., Guyot, J.L, Ronchail, J., Cocheneau, G., Filizola, N., Fraizy, P., Labat, D., de Oliveira, E., Ordonez, J.J., and Vauchel, P. 2009b. Contrasting regional discharge evolutions in the Amazon Basin, J. Hydrol., 375, 297–311.

Espinoza, J.C., Ronchail, J., Guyot, J.L., Junquas, C., Vauchel, P., Lavado, W., Drapeau, G., Pombosa, R. 2011. Climate variability and extreme drought in the upper Solimões River (western Amazon Basin): Understanding the exceptional 2010 drought. Geophys. Res. Lett., 38, L13406, doi:10.1029/2011GL047862.

Evensen, G. 2003. The ensemble Kalman filter: theoretical formulation and practical implementation. Ocean Dynamics, 53, 343 – 367.

Farr, T.G., Caro, E., Crippen, R., Duren, R., Hensley, S., Kobrick, M., Paller, M., Rodriguez, E., Rosen, P., Roth, L., Seal, D., Shaffer, S., Shimada, J., Umland, J.,Werner, M., Burbank, D., Oskin, M., Alsdorf, D. 2007. The shuttle radartopography mission. Reviews of Geophysics, 45, 2.

Frappart,F., Papa, F., Guntner, A., Werth, S., Santos da Silva, J., Tomasella, J., Seyler, F., Prigent, C., Rossow, W.B., Calmant, S., Bonnet, M.P. 2011a. Satellite-based estimates of groundwater storage variations in large drainage basins with extensive floodplains. Remote Sensing of Environment, 115, 6, 1588-1594.

Frappart, F., Calmant, S., Cauhopé, M., Seyler, F., Cazenave, A. 2006. Preliminary results of ENVISAT RA-2-derived water levels validation over the Amazon basin. Remote Sensing of Environment, 100, 252-264.

Getirana, A.C.V., Bonnet, M.-P., Rotunno Filho, O.C., Collischonn, W., Guyot, J.-L., Seyler, F., Mansur, W.J. 2010. Hydrological modelling and water balance of the Negro River basin: evaluation based on in situ and spatial altimetry data. Hydrological Processes, 24, 22, 3219-3236.

Hess, L.L., Melack, J.M., Novo, E.M.L.M., Barbosa, C.C.F., Gastil, M. 2003. Dual-season mapping of wetland inundation and vegetation for the central Amazon basin. Remote Sensing of Environment, 87, 404-428.

Houborg, R., Rodell, M., Li, B., Reichle, R., Zaitchik, B. 2012. Drought indicators based on model assimilated GRACE terrestrial water storage observations. Wat. Resour. Res., 48, W07525, doi:10.1029/2011WR011291.

Huffman, G., Adler, R., Bolvin, D., Gu, G., Nelkin, E., Bowman, K., Hong, Y., Stocker, E., Wolff, D. 2007. The TRMM Multisatellite Precipitation Analysis (TCMA): quasi-global, multiyear, combined-sensor precipitation estimates at fine scales. J. Hydromet, 8, 38–55.

IPCC. 2007. Climate Change 2007: The Physical Science Basis. Contribution of Working Group I to the Fourth Assessment Report of the Intergovernmental Panel on Climate Change. [Solomon, S., Qin, D., Manning, M., Chen, Z., Marquis, M., Averyt, K.B., Tignor, M., Miller, H.L. (eds.)], Cambridge University Press, Cambridge, United Kingdom and New York, NY, USA, 996.

Junk, W.J. 1997. General aspects of floodplain ecology with special reference to Amazonian floodplains. In: Junk, W.J. (Ed.), The Central-Amazonian Floodplain: Ecology of a Pulsing System, Ecological Studies. Springer Verlag/Heidelberg, Berlin/New York, 3–22.

Kalman, R.E. 1960. A new approach to linear filtering and prediction problems. Transactions of the AMSE – Journal of Basic Engineering, 82 D, 35-45.

Kalnay, E. et al. 1996. The NCEP/NCAR 40-years reanalysis project. Bull. Am. Meteorol. Soc., 77, 437-471.

Kerr, Y., Waldteufel, P., Wigneron, J.-P., Martinuzzi, J.-M., Font, J., and Berger, M. 2001. Soil moisture retrieval from space: The soil moisture and ocean salinity (SMOS) mission. IEEE T. Geosci. Remote Sens., 39, 1729-1736.

Kosuth, P., Callède, J., Laraque, A., Filizola, N., Guyot, J.L., Seyler, P., Fritsch, J.M., Guimarães, V. 2009. Sea-tide effects on flows in the lower reaches of the Amazon River. Hydrological Processes, 23, 22, 3141-3150.

Kumar, S.V., Reichle, R.H., Peters-Lidard, C.D., Koster, R.D., Zhan, X., Crow, W.T., Eylander, J.B., Houser, P.R. 2008. A Land Surface Data Assimilation Framework using the Land Information System: Description and Applications. Advances in Water Resources, 31, 1419-1432, DOI:10.1016/j.advwatres.2008.01.013

Lee, H., Seo, D.-J., Liu, Y., Koren, V., McKee, P., and Corby, R. 2012. Variational assimilation of streamflow into operational distributed hydrologic models: effect of spatiotemporal scale of adjustment. Hydrol. Earth Syst. Sci., 16, 2233-2251, doi:10.5194/hess-16-2233-2012.

Leite, C. C., Costa, M.H., Soares-Filho, B.S., de Barros Viana Hissa, L. 2012. Historical land use change and associated carbon emissions in Brazil from 1940 to 1995. Global Biogeochem. Cycles, 26, GB2011, doi:10.1029/2011GB004133.

Liu, Y., Gupta, H.V. 2007. Uncertainty in hydrologic modeling: Toward an integrated data assimilation framework. Water Resour. Res., 43, W07401, doi:10.1029/2006WR005756.

Liu, Y., Weerts, A.H., Clark, M., Hendricks Franssen, H.-J., Kumar, S., Moradkhani, H., Seo, D.-J., Schwanenberg, D., Smith, P., van Dijk, A.I.J.M., van Velzen, N., He, M., Lee, H., Noh, S. J., Rakovec, O., Restrepo, P. 2012. Advancing data assimilation in operational hydrologic forecasting: progresses, challenges, and emerging opportunities. Hydrol. Earth Syst. Sci., 16, 3863-3887, doi:10.5194/hess-16-3863-2012.

Marengo, J., Nobre, C., Tomasella, J., Oyama, M., de Oliveira, G., de Oliveira, R., Camargo, H., Alves, L. 2008. The drought in Amazonia in 2005. Journal of Climate, 21, 495–516.

Marengo, J.A., Tomasella, J., Alves, L.M., Soares, W.R., Rodriguez, D.A. 2011. The drought of 2010 in the context of historical droughts in the Amazon region. Geophys. Res. Lett., 38, L12703, doi:10.1029/2011GL047436.

McMillan, H.K., Hreinsson, E.Ö., Clark, M.P., Singh, S.K., Zammit, C., Uddstrom, M.J. 2012. Operational hydrological data assimilation with the Retrospective Ensemble Kalman Filter: use of observed discharge to update past and present model states for flow forecasts. Hydrol. Earth Syst. Sci. Discuss., 9, 9533-9575, doi:10.5194/hessd-9-9533-2012.

Meade, R.H., Rayol, J.M., Da Conceição, S.C., Natividade, J.R.G. 1991. Backwater effects in the Amazon River basin of Brazil. Environmental Geology and Water Sciences, 18, 2, 105-114.

Melack, J.M., Hess, L.L., Gastil, M., Forsberg, B.R., Hamilton, S.K., Lima, I.B.T., Novo, E.M.L.M. 2004. Regionalization of methane emissions in the Amazon basin with microwave remote sensing. Global Change Biol., 10, 530–544.

Melack, J.M., Hess, L.L. 2010. Remote sensing of the distribution and extent of wetlands in the Amazon basin. In: Junk, W.J., Piedade, M. (eds) Amazonian floodplain forests: ecophysiology, ecology, biodiversity and sustainable management. Ecological Studies, vol. 210, part 1. Springer, 43–59.

Meller, A. 2012. Previsão de cheias por conjunto em curto prazo. Tese de Doutorado, Inst. de Pesqui. Hidraul., Univ. Fed. do Rio Grande do Sul, Porto Alegre, Brasil.

Miguez-Macho, G., Fan Y. 2012a. The role of groundwater in the Amazon water cycle: 1. Influence on seasonal streamflow, flooding and wetlands. J. Geophys. Res., 117, D15113, doi:10.1029/2012JD017539.

Miguez-Macho, G., Fan Y. 2012b. The role of groundwater in the Amazon water cycle: 2. Influence on seasonal soil moisture and evapotranspiration. J. Geophys. Res., 117, D15114, doi:10.1029/2012JD017540.

Mohamed, Y.A., van den Hurk , B.J.J.M., Savenije, H.H.G., Bastiaanssen, W.G.M. 2005. Impact of the Sudd wetland on the Nile hydroclimatology. Water Resour. Res., 41, W08420.

Molinier M., Guyot J.L., Oliveira E., Guimarães V. 1996. Les régimes hydrologiques de l'Amazone et de ses affluents. In L'hydrologie tropicale. IAHS Publ., 238, 209-222.

Moreira-Turcq, P., Jouanneau, J.M., Turcq, B., Seyler, P., Weber, O., Guyot, J.L. 2004. Carbon sedimentation at lago grande de Curuai, a floodplain lake in the low Amazon region; insights into sedimentation rates. Palaeogeogr. Palaeoclimatol. Palaeoecol., 214, 27–40.

Neal, J.C., Atkinson, P.M. Hutton, C.W. 2007. Flood inundation model updating using ensemble Kalman filter and spatially distributed measurements. Journal of Hydrology, 336, 401-415.

Paiva, R.C.D., Collischonn, W., Tucci, C.E.M. 2011. Large scale hydrologic and hydrodynamic modeling using limited data and a GIS based approach. Journal of Hydrology, 406, 170–181.

Paiva, R.C.D., Collischonn, W., Buarque, D.C. 2012a. Validation of a full hydrodynamic model for large scale hydrologic modelling in the Amazon. Hydrol. Process., DOI: 10.1002/hyp.8425.

Papa, F., Prigent, C., Aires, F., Jimenez, C., Rossow, W.B., Matthews, E. 2010. Interannual variability of surface water extent at the global scale, 1993–2004. J. Geophys. Res., 115, D12111, doi:10.1029/2009JD012674.

Pitman, A.J., 2003. The evolution of, and revolution in, land surface schemes designed for climate models. Int. J. Climatol., 23, 479–510.

Prigent, C., Rochetin, N., Aires, F., Defer, E., Grandpeix, J.-Y., Jimenez, C., Papa, F. 2011. Impact of the inundation occurrence on the deep convection at continental scale from satellite observations and modeling experiments. J. Geophys. Res., 116, D24118, doi:10.1029/2011JD016311.

Reichle, R.H., Mclaughlin, D.B., Entekhabi, D. 2002. Hydrologic Data Assimilation with Ensemble Kalman Filter. Monthly Weather Review, 130, 103-114.

Reichle, R.H. 2008. Data assimilation methods in the Earth sciences. Adv. Water Resour., doi:10.1016/j.advwatres.2008.01.001.

Ricci, S., Piacentini, A., Thual, O., Le Pape, E., Jonville, G. 2011. Correction of upstream flow and hydraulic state with data assimilation in the context of flood forecasting. Hydrol. Earth Syst. Sci., 15, 3555-3575, doi:10.5194/hess-15-3555-2011.

Richey, J.E., Melack, J.M., Aufdenkampe, A.K., Ballester, V.M., Hess, L.L. 2002. Outgassing from Amazonian rivers and wetlands as a large tropical source of atmospheric CO2. Nature, 416, 617-620.

Rodell, M., Houser, P.R., Jambor, U., Gottschalck, J., Mitchell, K., Meng, C.-J., Arsenault, K., Cosgrove, B., Radakovich, J., Bosilovich, M., Entin, J.K., Walker, J.P., Lohmann, D., Toll, D. 2004. The Global Land Data Assimilation System. BAMS, 381-394.

Rodriguez, D.A., Tomasella, J., Linhares, C. 2010. Is the forest conversion to pasture affecting the hydrological response of Amazonian catchments? Signals in the Ji-Paraná Basin. Hydrol. Process., 24, 1254-1269, doi: 10.1002/hyp.7586.

Santos da Silva, J., Calmant, S., Seyler, F., Rotunno Filho, O.C., Cochonneau, G., Mansur, W.J. 2010. Water levels in the Amazon basin derived from the ERS 2 and ENVISAT radar altimetry missions. Remote Sensing of Environment, 114, 10, 2160-2181.

Schongart, J., Junk,W.J. 2007. Forecasting the flood-pulse in Central Amazonia by ENSO-indices. J. Hydrol., 335, 124-132.

Seyler, P., Boaventura, G.R. 2003. Distribution and partition of trace metals in the Amazon basin. Hydrol. Process., 17, 1345-1361.

Tapley, B.D., Bettadpur, S., Ries, J.C., Thompson, P.F., Watkins, M. 2004. GRACE measurements of mass variability in the Earth system. Science, 305, 503-505.

Thielen, J., Bartholmes, J., Ramos, M.-H., de Roo, A. 2009. The European Flood Alert System – Part 1: Concept and development, Hydrol. Earth Syst. Sci., 13, 125-140, doi:10.5194/hess-13-125- 2009.

Thirel, G., Martin, E., Mahfouf, J.-F., Massart, S., Ricci, S., and Habets, F. 2010. A past discharges assimilation system for ensemble streamflow forecasts over France – Part 1: Description and validation of the assimilation system. Hydrol. Earth Syst. Sci., 14, 1623-1637, doi:10.5194/hess-14-1623-2010.

Tomasella, J., Borma, L.S., Marengo, J.A., Rodriguez, D.A., Cuartas, L.A. Nobre, C.A., Prado, M.C.R. 2010. The droughts of 1996–1997 and 2004–2005 in Amazonia: hydrological response in the river main-stem. Hydrol. Process., 25, 8, 1228-1242, DOI: 10.1002/hyp.7889.

Trigg, M.A., Wilson, M.D., Bates, P.D., Horritt, M.S., Alsdorf, D.E., Forsberg B.R., Vega, M.C. 2009. Amazon flood wave hydraulics. Journal of Hydrology, 374, 92–105.

Trigg, M.A., Bates, P.D.D., Wilson, M.D., Schumann, G.J.-P., Baugh, C.A. 2012. Floodplain channel morphology and networks of the middle Amazon River. Water Resour. Res., doi:10.1029/2012WR011888, in press.

Tucci, C.E.M., DIAS, P.L.S., CLARKE, R.T., SAMPAIO, G.O., COLLISCHONN, W. 2003. Long-term flow forecasts based on climate and hydrologic modeling: Uruguay river basin. Water Resources Research, 39, 7, 1-2.

Uvo, C.B., Graham, N. E. 1998. Seasonal runoff forecast for northern South America: A statistical model. Water Resour. Res., 34, 12, 3515-3524, doi:10.1029/98WR02854, 1998.

Uvo, C.B., Tölle, U., Berndtsson, R. 2000. Forecasting discharge in Amazonia using artificial neural networks. International Journal of Climatology, 20, 1495-1507, doi: 10.1002/1097-0088(200010)20:12<1495::AID-JOC549>3.0.CO;2-F.

Vergnes, J.-P., Decharme, B. 2012. A simple groundwater scheme in the TRIP river routing model: global off-line evaluation against GRACE terrestrial water storage estimates and observed river discharges. Hydrol. Earth Syst. Sci., 16, 3889-3908, doi:10.5194/hess-16-3889-2012.

Vinukollu, R.K., Wood, E.F., Ferguson, C.R., and Fisher, J.B. 2011. Global Estimates of Evapotranspiration for Climate Studies using Multi-Sensor Remote Sensing Data: Evaluation of Three Process-Based Approaches. Remote Sens. Environ., 115, 801-823, doi:10.1016/j.rse.2010.11.006.

Wilson, W., Bates, P., Alsdorf, D., Forsberg, B., Horritt, M., Melack, J., Frappart, F., Famiglietti, J. 2007. Modeling large-scale inundation of Amazonian seasonally flooded wetlands. Geophys. Res. Lett., 34, L15404, doi:10.1029/2007GL030156.

Wood, A.W., Lettenmaier, D. P. 2008. An ensemble approach for attribution of hydrologic prediction uncertainty. Geophys. Res. Lett., 35, L14401, doi:10.1029/2008GL034648.

Wood, A.W., Maurer, E., Kumar, A., Lettenmaier, D.P. 2002. Long-range experimental hydrologic forecasting for the eastern United States. Journal of Geophysical Research, 107, D20, 4429, doi:10.1029/2001JD000659.

Wood, E.F., Lettenmaier, D.P., Zartarian, V.G. 1992. A land-surface hydrology parameterization with subgrid variability for general circulation models. J. Geophys. Res., 97, 2717-2728.

Wood, E.F., et al. 2011 Hyperresolution global land surface modeling: Meeting a grand challenge for monitoring Earth's terrestrial water. Water Resour. Res., 47, W05301, doi:10.1029/2010WR010090.

Yamazaki, D., Kanae, S., Kim, H., Oki, T. 2011. A physically n dynamics in a global river routing model. Water Resour. Res., 47, W04501, doi:10.1029/2010WR009726.

Zeng, N., Yoon, J.H., Marengo, J.A., Subuamaniam, A., Nobre, C.A., Mariotti, A., and Neelin, J.D. 2008. Causes and impact of the 2005 Amazon drought. Environ. Res. Lett., 3, 014002, doi:10.1088/1748-9326/3/1/014002.

ANEXO A

The MGB-IPH large-scale hydrologic-hydrodynamic model: A brief description

A.1. General overview

The MGB-IPH model ("*Modelo Hidrológico de Grandes Bacias*") is a large scale distributed hydrological model developed by *Collischonn et al.* [2007]. It is similar to other large scale hydrological models such as LARSIM [*Ludwig and Bremicker*, 2006] and VIC [*Liang et al.*, 1994; *Nijssem et al.*, 1997]. It is a process-based model that uses physical and conceptual equations to simulate the terrestrial hydrological cycle: soil water budget, energy budget and evapotranspiration, interception, superficial, sub-superficial and groundwater flow generation and river flow routing (see Fig. 1). The MGB-IPH model was applied in several South American basins for different purposes [e.g. *Collischonn et al.*, 2005; *Collischonn et al.*, 2008; *Getirana et al.*, 2010; *Paiva et al. 2011*; *Paiva et al.*, 2012]. For the modeling of the Amazon basin, *Paiva et al.* [2011] improved MGB-IPH flow routing scheme by adding a full hydrodynamic module which includes a simplified representation of the floodplain inundation [*Paiva et al.*, 2011]. Some of the model concepts are presented below.

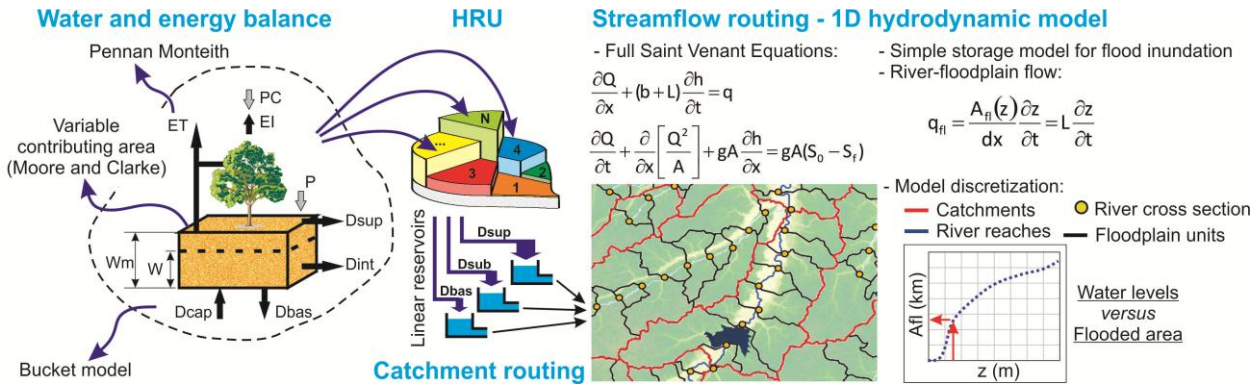

Figure 1. Schematic representation of MGB-IPH hydrological model coupled with a 1D hydrodynamic model.

A.2. Model discretization and hydrological response units

The early version of the MGB-IPH model was based on a square cell discretization of the river basin [*Collischonn et al.*, 2007], while the version described in the present paper uses a division of the basin in small catchments using the ArcHydro methods [*Maidment*, 2002]. Each catchment is subdivided into Hydrological Response Units (HRUs) which are areas with similar hydrological behavior and defined by a combination of soil and land cover maps [*Beven*, 2001; *Kouwen et al.*, 1993]. See scheme shown in Fig. 2.

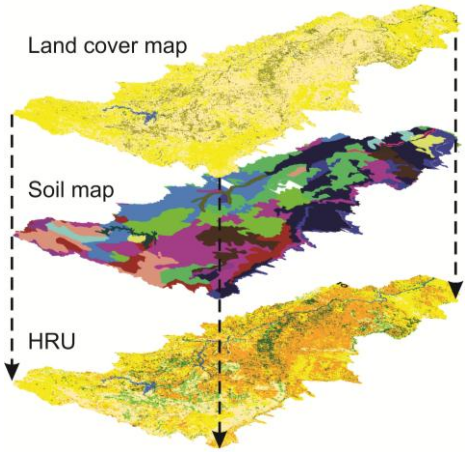

Figure 2. Schematic of a land cover map combined to a soil map to result to provide a Hydrological Response Units (HRU) map.

A.3. Water and energy balance

Vertical water and energy budgets are computed independently for each HRU in each catchment. Soil water balance is computed considering only one soil layer, according to the equation (see Fig. 1):

$$\frac{dW}{dt} = P - ET - D\,\mathrm{sup} - D\,\mathrm{int} - Dbas \tag{1}$$

where W [mm] is the water storage in the soil layer, P [mm.Δt^{-1}] is the rainfall that reaches the soil, ET [mm.Δt^{-1}] is the evapotranspirations from the soil, Dsup [mm.Δt^{-1}] is the surface runoff, Dint [mm.Δt^{-1}] is the subsurface flow and Dbas [mm.Δt^{-1}] is the percolation to groundwater reservoir.

Precipitation (PC) is assumed to be stored on the surface of the vegetation until maximum interception storage capacity is reached, which is determined for each HRU based on the vegetation leaf area index. Energy budget and evapotranspiration from soil, vegetation and canopy to the atmosphere is estimated by the Penman-Monteith equation [*Monteith*, 1965; *Shuttleworth*, 1993; *Allen et al.*, 1998], using an approach similar to that of *Wigmosta et al.* [1994]:

$$ET = \left(\frac{\Delta \cdot A + \rho_A \cdot c_p \dfrac{D}{r_a}}{\Delta + \gamma \left(1 + \dfrac{r_s}{r_a} \right)} \right) \frac{1}{\lambda \cdot \rho_w} \tag{2}$$

where λ [MJ kg^{-1}] is the latent heat of vaporization, Δ [kPa ^{o}C^{-1}] is the gradient of the saturated vapour pressure function, A [MJ m^{-2}s^{-1}] is the available energy, ρ_A [kg m^{-3}] is the density of air, ρ_W [kg m^{-3}] is specific mass of water, c_p [MJ kg^{-1} ^{o}C^{-1}] is the specific heat of moist air, D [kPa] is the vapour pressure deficit, γ [kPa ^{o}C^{-1}] is the psychrometric constant, r_s [s m^{-1}] is the surface resistance of the land cover and r_a [s m^{-1}] is the aerodynamic resistance. Meteorological conditions (air temperature, solar radiation, wind speed, precipitation, relative humidity and atmospheric pressure) are prescribed for each catchment.

Soil infiltration and runoff (*D*sup) are computed based on the variable contributing area concept of the ARNO model [*Todini*, 1996], which is also used in the PDM [*Moore and Clarke*, 1981], VIC2L and LARSIM models. Subsurface flow (*D*int) is computed using an equation similar to the Brooks and Corey unsaturated hydraulic conductivity equation [*Rawls et al.*, 1993]. Percolation from soil layer to groundwater (*D*bas) is calculated according to a simple linear relation between soil water storage and maximum soil water storage. Then, the flow generated within each catchment is routed to the stream network using three linear reservoirs (base flow, subsurface flow and surface flow) as illustrated in Fig. 1.

A.4. River-flood modelling

Originally, the MGB-IPH model performs river flow routing within using the Muskingum Cunge method. Then, a large-scale hydrodynamic model of MGB-IPH was developed by *Paiva et al.* [2011] and it differs from the previous model by its capability of simulating flood inundation and backwater effects. The scheme used is based on the IPH-IV model, first developed by Tucci [1978]. The model solves the full *Saint Venant* equations [*Cunge et al.*, 1980]:

$$\frac{\partial Q}{\partial x} + b\frac{\partial h}{\partial t} = q_{cat} - q_{fl} \tag{3}$$

$$\frac{\partial Q}{\partial t} + \frac{\partial}{\partial x}\left[\frac{Q^2}{A}\right] + gA\frac{\partial h}{\partial x} = gA(S_0 - S_f) \tag{4}$$

where the first and second equations are the 1 D channel mass and momentum conservation laws, Q [m^3.s^{-1}] is river discharge, t [s] is time, x [m] is river longitudinal space coordinate, b [m] is river cross section width at free surface elevation, q_{cat} [m^2.s^{-1}] is local catchment lateral inflow (the sum of the surface, subsurface and base flow from the catchment), q_{fl} [m^2.s^{-1}] is

the river-floodplain flow exchange, h [m] is water depth, g [m.s^{-2}] is acceleration due to gravity, A [m^2] is the cross sectional flow area perpendicular to the flow direction and S_0 [m.m^{-1}] and S_f [m.m^{-1}] are the bed slope and friction slope in the x-direction. Friction slope is estimated using Manning's equation. Flow at river confluences is modeled using a simple mass continuity equation and the energy equation discarding energy losses and the kinetic term [*Cunge et al.*, 1980].

The river reaches are discretized into several river cross sections (Fig. 1) where the hydraulic variables are computed. The model also divides the catchments into floodplain units (Fig. 1), which are areas between two river cross sections where the river-floodplain flow exchange and floodplain water storage is computed.

Flood inundation is simulated using a simple storage model [*Cunge et al.*, 1980], which assumes that (i) the flow velocity parallel to the river direction is null on floodplains, (ii) the floodplain units act only as storage areas and (iii) the floodplain water level equals the water level at the main channel. Considering the model basic assumptions and the mass conservation law, the river-floodplain flow exchange q_{fl} equals:

$$q_{fl} = \frac{Afl(z)}{dx}\frac{\partial h}{\partial t} = L(z)\frac{\partial h}{\partial t} \tag{5}$$

where Afl [m^2] is the flooded area and L [m] is the floodplain equivalent width, measured for each floodplain unit.

The partial differential equations of the model are solved using a linear and implicit finite difference numerical method, similar to the Preissman scheme [*Cunge et al.*, 1980]. Since the model simulates a river network with lots of confluences, the set of discretized equations forms a non symmetric sparse linear system. Then, for better computational efficiency, the matrix solver uses a modified Gauss elimination procedure based on a skyline storage method, avoiding the storage of null elements of the linear system of equations. This method was developed by *Tucci* [1978] and improved by *Paiva et al.* [2011] and is similar to methods used by HEC-RAS model [*USACE*, 2002].

GIS-based algorithms are used to extract river and floodplain geometry parameters mainly from Digital Elevation Models (DEM) [*Paiva et al.*, 2011]. Parameters from a rectangular shape river cross section are estimated using geomorphologic equations and river bottom level is estimated from the DEM using corrections presented in *Paiva et al.* [2011]. The algorithm delineates discrete "floodplain units" for each sub-reach and extracts a z vs Afl

curve from the DEM for each of them. Corrections are applied on the DEM to avoid errors due to vegetation and water level effects. Flood inundation results in terms of 2 D water levels are computed based on 1 D water level outputs and the DEM.

References

Allen, R.G., Pereira, L.S., Raes, D., Smith, M. 1998. Crop evapotranspiration: Guidelines for computing crop water requirements. Irr. & Drain. Paper 56. UN-FAO, Rome, Italy, 174.

Beven, K. 2001. How far can we go in distributed hydrological modelling? Hydrology and Earth System Sciences, 5, 1, 1-12.

Collischonn, B., Collischonn, W., Tucci, C. 2008. Daily hydrological modeling in the Amazon basin using TRMM rainfall estimates. Journal of Hydrology, 207.

Collischonn, W., Allasia, D.G., Silva, B.C., Tucci, C.E.M. 2007. The MGB-IPH model for large-scale rainfall-runoff modeling. Hydrological Sciences Journal, 52, 878-895.

Collischonn, W., Haas, R., Andreolli, I., Tucci, C.E.M. 2005. Forecasting river Uruguay flow using rainfall forecasts from a regional weather-prediction model. J. Hydrol., 305, 87-98.

Cunge, J.A., Holly, F.M., Verney, A. 1980. Practical Aspects of Computational River Hydraulics. Pitman Advanced Publishing Program.

Getirana, A.C.V., Bonnet, M.-P., Rotunno Filho, O.C., Collischonn, W., Guyot, J.-L., Seyler, F., Mansur, W.J. 2010. Hydrological modelling and water balance of the Negro River basin: evaluation based on in situ and spatial altimetry data. Hydrological Processes, 24, 22, 3219-3236.

Kouwen, N. et al. 1993. Grouping Response Units for Distributed Hydrologic Modelling. Journal of Water Resources Management and Planning, ASCE, 119, 3, 289-305.

Liang, X., Lettenmaier, D.P., Wood, E.F., Burges, S.J. 1994. A simple hydrologically based model of land surface water and energy fluxes for general circulation models. Journal of Geophysical Research, 99, D7, 14415-14428.

Ludwig, K., Bremicker, M. 2006. The Water Balance Model LARSIM – Design, Content and Applications. Freiburger Schiriften zür Hydrologie, Band 22, Institut fur Hydrologie der Universität Freiburg.

Maidment, D., 2002. Arc Hydro – GIS for Water Resources. ESRI Press, Redlands, CA.

Monteith, J.L., 1965. Evaporation and environment. In: Proc. 19th Symp. Soc. Exp. Biol. Swansea (1964).

Moore, R.J., Clarke, R.T. 1981. A distribution function approach to rainfall-runoff modeling. Water Resour. Res. 17 (5), 1367–1382.

Nijssem, B., Lettenmaier, D.P., Liang, X., Wetzel, S.W., Wood, E.F. 1997. Streamflow simulation for continental-scale river basins. Water Resour. Res., 33, 4, 711-724.

Paiva, R.C.D., Collischonn, W., Tucci, C.E.M. 2011. Large scale hydrologic and hydrodynamic modeling using limited data and a GIS based approach. Journal of Hydrology, 406, 170–181.

Paiva, R.C.D., Collischonn, W., Buarque, D.C. 2012. Validation of a full hydrodynamic model for large scale hydrologic modelling in the Amazon. Hydrol. Process., DOI: 10.1002/hyp.8425.

Rawls, W.J., Ahuja, L.R., Brakensiek, D.L., Shirmohammadi, A. 1993. Infiltration and soil water movement. In: Maidment, D. R. Handbook of hydrology. McGraw-Hill, New York.

Shuttleworth, W.J. 1993. Evaporation. In: Maidment, D.R. Handbook of Hydrology. McGraw-Hill, New York.

Todini, E. 1996. The ARNO rainfall-runoff model. Journal of Hydrology, 175, 339-382.

Tucci, C.E.M. 1978. Hydraulic and Water Quality Model for a River Network. PhD dissertation, Colorado State University, Fort Collins, USA.

USACE. 2002. HEC-RAS River Analysis System: Hydraulic Reference Manual, Version 3.1. U.S. Army Corps of Engineers, Hydrologic Engineering Center. www.hec.usace.mil.

Wigmosta, M. S., Vail, L. W., Lettenmaier, D. P. 1994. A distributed hydrology-vegetation model for complex terrain. Water Resources Research, 30, 6, 1665-1679.

ANEXO B

Résumé étendu

B.1. Introduction et objectives

Le bassin Amazonien est reconnu comme un des systèmes hydrologiques les plus importants du monde, drainant environ 6 millions de km^2, et contribuant approximativement à 15% des apports en eaux douces à l'océan global [*Molinier et al.*, 1996].

Cette région abrite une des plus grandes forêts tropicales du monde et un écosystème complexe, et ses processus hydrologiques peuvent influencer le climat tant à l'échelle locale que globale [*IPCC*, 2007], le cycle du carbone et en particulier les émissions de méthane et de dioxyde de carbone [*Richey et al.*, 2002, *Melack et al.*, 2004] et plus généralement de nombreux processus biogéochimiques.

De nombreuses caractéristiques hydrologiques particulières rencontrées en Amazonie motivent l'étude de ce système. Cette région présente des précipitations intenses avec une variabilité spatiale forte, au delà d'un régime hydro-climatique contrasté entre différentes régions [*Espinoza et al*., 2009a] et des fleuves extrêmement puissants. Les effets de remous contrôlent les écoulements de quelques uns des principaux fleuves Amazoniens [*Trigg et al.*, 2009; *Meade et al.*, 1991; *Kosuth et al.*, 2009]. De plus, la région Amazonienne présente de vastes plaines d'inondation [*Papa et al.*, 2010; *Hess et al.*, 2008; *Melack e Hess*, 2010] dans lesquelles les écoulements sont complexes [*Bonnet et al.*, 2008; *Alsdorf et al.*, 2007a; *Alsdorf et al.*, 2010] et qui jouent un rôle importante sur le cycle global du carbone [e.g. *Richey et al.*, 2002], sur la dynamique du transport sédimentaire [e.g. *Bourgoin et al.*, 2007] et sur les caractéristiques géochimiques et écologiques des fleuves Amazoniens [*Junk*, 1997, *Richey et al.*, 2002, *Melack et al.*, 2004, *Moreira et al.*, 2004, *Seyler and Boaventura*, 2003].

Cependant, la région Amazonienne s'est dégradée dans les dernières années sous l'impact de différentes activités anthropiques, telles que le déboisement [*Leite et al*, 2012], dont les conséquences sur le régime hydrologique ne sont pas encore totalement comprises. A ceci, s'ajoute l'extension future du système hydro-électrique brésilien pour la région Amazonienne [*BRASIL*, 2007a,b], avec la planification ou la construction actuelle de nombreuses nouvelles centrales hydro-électriques, mais dont les impacts environnementaux possibles sont également méconnus.

En outre, on observe récemment une augmentation de la magnitude des crues et étiages dans les principaux fleuves Amazoniens [e.g. *Espinoza et al.*, 2009b], et l'occurrence d'évènements hydrologiques extrêmes tels que les crues de 2009 et 2012, les étiages de 1996, 2005, 2010 [*Chen et al*., 2010; *Tomasella et al.*, 2010 *Marengo et al*., 2008; *Espinoza et al.*,

2011; *Marengo et al.*, 2011]. Ces crues et sécheresse ont des impacts importants sur la population amazonienne qui dépend fortement des ressources hydriques et qui est particulièrement vulnérable aux crues, la majorité des communes étant concentrée le long des fleuves Amazoniens.

Les modèles hydrologiques à base physique sont un des principaux outils pour (i) aider à la compréhension des processus hydrologiques et leur relation avec d'autres processus géophysiques, et pour (ii) servir de base aux systèmes de prévision hydrologique visant à réduire la vulnérabilité de la population locale aux évènements extrêmes. La modélisation hydrologique est un thème de recherche en continuel développement. Plus spécifiquement, dans le bassin Amazonien et pour la simulation des eaux superficielles, les modèles diffèrent en fonction de leur complexité, depuis les modèles régionaux/globaux qui représentent de forme (i) simplifiée l'écoulement fluvial et des plaines d'inondation [e.g. *Collischonn et al.*, 2008; *Getirana et al.*, 2010; *Beighley et al.*, 2009; *Decharme et al.*, 2011; *Coe et al.*, 2008] ou (ii) plus complète pour les écoulements dans les fleuves [*Paiva et al.*, 2011; *Paiva et al.*, 2012; *Yamazaki et al.*, 2011] e (iii) les modèles détaillés de la plaine d'inondation [*Wilson et al.*, 2007; *Bonnet et al.*, 2008] mais pour des surfaces plus restreintes. Les limitations de ces différents abordages de simulation résultent non seulement des simplifications de la représentation des processus physiques mais également, à la déficience des données d'entrée de ces modèles.

Pourtant, malgré leurs limitations, les modèles hydrologiques à base physique ont récemment commencé à être utilisés dans les systèmes régionaux voire globaux de surveillance et de prévision hydrologique en temps réel [e.g. *Thielen et al.*, 2009; *Wood et al.*, 2002; *Tucci et al.*, 2003; *Collischonn et al.*, 2005; *Alfieri et al.*, 2012]. Cependant, les systèmes de prévision hydrologique basés sur des modèles physiques n'ont pas encore été testés dans la région amazonienne et les études de prévision existantes dans ce bassin sont toutes basées sur des modèles statistiques [e.g. *Uvo e Grahan*, 1998; *Uvo et al.*, 2000; *Schongart e Junk*, 2007; *Cappalaere et al.*, 1995].

Parallèlement aux outils de modélisation hydrologiques, un grand nombre de techniques de télédétection ont été développées dans les dernières années pour l'observation des variables hydrologiques, qui permettent la surveillance de grandes régions difficiles d'accès, comme l'Amazonie, avec une couverture spatio-temporelle bien supérieure aux observations *in situ*. Ces nouveaux produits incluent en particulier, les niveaux d'eau estimés par radar altimétriques [*Frappart et al.*, 2006; *Alsdorf et al.*, 2007; *Santos da Silva et al.*, 2010], la variation du stockage de l'eau terrestre de la mission de gravimétrie GRACE

[*Tapley et al.*, 2004], les estimations de l'humidité du sols de la mission SMOS [*Kerr et al.*, 2001], l'extension des zones inondées [*Hess et al.*, 2003; *Papa et al.*, 2010], les flux d'énergie et d'évapotranspiration [*Vinukollu et al.*, 2011], les données topographiques de modèles numériques de terrain de la mission TRMM [*Farr et al.*, 2007], et les surface inondées et niveaux d'eau de la future mission SWOT [*Durand et al.*, 2010]. Ce type de produits a déjà été utilisé pour la compréhension des processus hydrologique dans le bassin Amazonien [e.g. *Chen et al.*, 2010; *Chen et al.*, 2009; *Alsdorf et al.* 2007; *Alsdorf et al.* 2010; *Frappart et al.*, 2011]. Mais, en outre, ces données peuvent également être utilisées pour la validation et l'investigation des erreurs des modèles hydrologiques [*Getirana et al.*, 2010] ou encore être intégrée à ces modèles.

En ce sens, les techniques d'assimilation de données [*Liu e Gupta*, 2007; *Reichle*, 2008; *Liu et al.*, 2012] sont une alternative pour combiner la grande quantité d'observations hydrologiques basées sur l'observation spatiale avec les modèles hydrologiques avec comme objectifs d'obtenir une estimation optimale des états et flux hydrologiques. Ces techniques peuvent être utilisées dans des études rétrospectives dans lesquelles sont combinées des données historiques avec les résultats de modèles de simulation (e.g. ré-analyse de modèles météorologiques, *Kalnay*, 1996) ou également pour l'actualisation de modèles de prévision en temps réel afin de corriger les erreurs et estimer les états hydrologiques à l'initialisation d'une prévision [e.g. *Collischonn et al.*, 2005]. Diverses applications [e.g. *Andreadis e Lettenmaier*, *Neal et al.*, 2007; *Ricci et al.*, 2011; *Biancamaria et al.*, 2011; *Andreadis et al.*, 2007; *Durand et al.*, 2008c; *Clark et al.*, 2008; *McMillan et al.*, 2012; *Lee et al.*, 2012; *Thirel et al.*, 2010 ; *Kumar et al.*, 2008] de ce type en hydrologie ont été réalisées, notamment l'assimilation de différents types d'observations avec différents types de modèles selon différents types de méthodes, mais dont la plupart utilisent la technique de « Filtre de Kalman d'Ensemble » [*Evensen*, 2003], ou de ses variantes, tel que révisé dans *Liu and Gupta* [2007], *Reichle* [2008] e *Liu et al.* [2012]. Cependant, l'utilisation de l'assimilation de données dans des modules de simulation de l'écoulement dans le réseau de drainage et plaines d'inondation dans les modèles de grande échelle reste encore rare.

Dans la courte introduction présentée ci-dessus, on a souligné l'importance de la compréhension et de la prévision de l'hydrologie du bassin Amazonien et d'autres grands bassins hydrographiques, mais en alertant sur le manque actuel de connaissance sur le fonctionnement de ces systèmes. Ont été également présentés, les types de techniques les plus récentes qui pourraient être utilisés à ces fins– notamment la modélisation hydrologique,

l'observation spatiale, l'assimilation de données et la prévision hydrologique – mais qui sont également des thèmes de recherche actuels.

En ce sens, les questions scientifiques posées ici sont les suivantes:

Comment fonctionne l'hydrologie des grands bassins hydrographiques, en particulier du bassin Amazonien?

Est-il possible de prévoir son fonctionnement, d'anticiper les crues et étiages et de fournir des informations quantitatives pour la gestion des ressources hydriques?

Quels sont les facteurs qui dominent la prévisibilité hydrologique?

Comment les techniques les plus récentes de modélisation hydrologique et hydrodynamique de grande échelle et l'observation par satellite peuvent aider à ces fins?

Ce sont ces questions qui ont motivé le développement de cette thèse qui a eu pour objectif de comprendre et prévoir le fonctionnement hydrologique des grands bassins hydrographiques, plus spécifiquement le bassin Amazonien, avec comme support la modélisation hydrologique et la surveillance des variables hydrologiques par satellite. Plus spécifiquement, cette recherche a visé à :

- Développer des techniques de modélisation hydrologique de grande échelle, d'assimilation de données *in situ* et issues de l'observation spatiale et de prévision des débits dans le bassin Amazonien.
- D'évaluer les performances, les points forts et les limitations de ces techniques de modélisation hydrologique de grande échelle, d'assimilation de données *in situ* et spatiale et de prévision des débits dans le bassin Amazonien.
- De comprendre, avec le support de la modélisation hydrologique et de l'observation spatiale, comment fonctionne le bassin Amazonien en terme de processus hydrologiques dominants et d'identifier quels sont les facteurs qui influencent sa prévisibilité hydrologique.

Ces thèmes et différentes questions scientifiques spécifiques ont été abordées au travers d'une série d'études, présentés sous forme d'articles qui sont résumés ci-dessous.

B.2. Résultats et conclusions

B.2.1.Large-scale hydrologic and hydrodynamic modelling of the Amazon River basin

La recherche développée dans cette thèse débute par une étude de modélisation hydrologique et hydrodynamique du bassin Amazonien en utilisant des techniques qui

relèvent de l'état de l'art de la modélisation physique/conceptuelle des grands bassins hydrographiques et de l'observation spatiale des variables hydrologiques.

Dans ce chapitre sont évaluées les limitations et principales sources d'erreur de la modélisation hydrologique et hydrodynamique pour la représentation des principaux processus hydrologiques dans le bassin Amazonien. En outre, le fonctionnement du bassin Amazonien est étudié au travers des résultats de simulations, en incluant en particulier l'analyse du bilan hydrologique, de la contribution des eaux superficielles, du sol et souterraines à la variabilité du stock d'eau et du rôle de l'hydraulique des fleuves et des plaines d'inondation sur la propagation des ondes de crues le long des fleuves Amazoniens.

Le modèle hydrologique à base physique MGB-IPH « *Modelo de Grandes Bacias* » développé par *Collischonn et al.,* [2007] a été utilisé avec un module de modélisation hydrodynamique de grande échelle récemment développé par *Paiva et al.* [2011], basé sur les équations de *Saint Venant* et sur un modèle de type stockage dans les plaines d'inondation. Des algorithmes de géo-traitement ont été utilisés pour extraire les informations du modèle numérique de terrain (MNT) STRM [*Farr et al.,* 2007] pour le modèle hydrodynamique et le modèle hydrologique a été forcé avec des pluies estimées par le satellite TRMM 3B42 [*Huffman et al.,* 2007]

Une validation détaillée du modèle est présentée en utilisant des observations hydrologiques conventionnelles (débits et cotes aux stations fluviométriques) et dérivées des récentes techniques de l'observation spatiale, incluant les niveaux d'eau estimés par altimétrie spatiale par radar embarqué sur le satellite ENVISAT [*Santos da Silva et al.,* 2010], l'extension des surfaces inondées estimées par les données de plusieurs satellites [*Papa et al.,* 2010] et les variations du stock total d'eau dérivé de la mission de gravimétrie GRACE [*Frappart et al.,* 2010; 2011b].

Conformément aux résultats, le modèle MGB-IPH avec un module hydrodynamique est capable de représenter les principaux processus hydrologiques du bassin Amazonien, représentant de façon satisfaisante les hydrogrammes à différentes échelles spatiales, mais principalement dans les grands fleuves. Les résultats de simulations sont également en accord avec les observations de niveaux d'eau, l'extension des surfaces inondées et les variations du stockage d'eau terrestre.

Cependant, le modèle a présenté une sensibilité principalement aux données de précipitation et aux paramètres liés à la géométrie des fleuves et des plaines d'inondation. Une grande partie des erreurs a lieu dans des régions montagneuses et/ou peu instrumentées, et où, probablement il existe des erreurs importantes dans les données de précipitation utilisées

(produit TRMM 3B42 estimé par satellite). L'incertitude sur les paramètres liés aux fleuves et plaines d'inondation a conduit à des erreurs importantes sur les niveaux d'eau et l'extension des plaines d'inondation, indiquant la nécessité de développer de meilleures méthodologies pour l'estimation de ces paramètres. Sont suggérées quelques alternatives comme des méthodes de correction du MNT SRTM pour retirer les erreurs liées à la végétation, l'estimation de la largeur des fleuves par satellite ou l'utilisation des données de la future mission SWOT.

Le bilan hydrologique global du bassin Amazonien obtenu à partir des résultats de simulation est cohérent avec les estimations précédentes. Les taux moyens de précipitation, d'évapotranspiration et de débit estimé à Óbidos (relativement proche de l'embouchure) sont : P = 5.65 mm.jour^{-1}, ET = 2.72 mm.jour^{-1} and Q = 3.09 mm.jour^{-1}. L'Amazonie présente une variabilité saisonnière marquée dans le stockage d'eau terrestre, avec des amplitudes de variations de 325 mm, pouvant atteindre des valeurs plus grandes de 750 mm en Amazonie centrale. Une telle variabilité est dominée par la dynamique des eaux superficielles (56%), principalement en Amazonie centrale qui présente de vastes plaines d'inondation. L'eau des sols contribue également pour partie (36%) à la variabilité du stock d'eau dans le bassin, tandis que les eaux souterraines ne présentent pas une grande contribution (8%) dans ce comportement.

Le rôle des plaines d'inondation et des effets de remous dans la propagation des ondes de crues le long des fleuves Amazoniens a également été étudié. Il existe une forte interaction entre les niveaux d'eau, les zones inondées et les débits lors du passage des ondes de crue. Les plaines d'inondation agissent en stockant les volumes d'eau dérivés du cours principal du fleuve, atténuant et retardant l'onde de crue, retardant celle-ci de plusieurs mois dans les grands fleuves Amazoniens. Les effets de remous ont également un rôle important, bien que moindre, et ne pas les prendre en compte conduit à des hydrogrammes simulés en avance par rapport aux observations. Ces résultats indiquent l'importance de l'utilisation des approximations presque complètes des équations de *Saint Venant* et de la représentation des plaines d'inondation pour la modélisation du bassin Amazonien ou autres bassins semblables avec les modèles de grande échelle. Bien que les plaines d'inondation jouent un rôle important sur les écoulements dans le bassin Amazonien, leur variation saisonnière n'influe pas apparemment sur le taux d'évapotranspiration et le bilan hydrologique de ce dernier.

Pour conclure, bien qu'il existe quelques limitations dans les résultats de simulation présentés, le modèle MGB-IPH s'est montré très performant pour la représentation des hydrogrammes et par conséquence est approprié pour servir de base aux études de prévision

des débits dans le bassin Amazonien. En outre, le modèle développé dans cette thèse pourra fournir les bases techniques pour la compréhension d'autres aspects hydrologiques non explorés ici ou pour l'évaluation de l'impact hydrologique des récentes activités anthropiques en Amazonie, telles que la déforestation [*Leite et al*., 2012], les changements climatiques [*IPCC*, 2007], et la construction de nouveaux grands barrages hydro-électriques dans les fleuves Amazoniens [*BRASIL*, 2007a,b].

B.2.2. Reduced precipitation over large water bodies in the Brazilian Amazon shown from TRMM data

Dans le chapitre 3, une étude de la variabilité spatiale de la précipitation en Amazonie brésilienne est présentée en utilisant les données d'observation spatiale de la mission TRMM (« *Tropical Rainfall Measurement Mission* ») [*Huffman et al.*, 2007]. La motivation pour cette étude est survenue à l'issue d'une analyse préliminaire des données de précipitation du produit TRMM 3B42 au cours de l'étape de préparation des données pour la modélisation hydrologique et hydrodynamique du bassin Amazonien (Chapitre 2), lorsqu'il a été vérifié étonnamment, que la précipitation était moindre sur les grands plans d'eau Amazoniens. A partir de ce constat, les questions suivantes se sont posées : La réduction de précipitation estimée par TRMM 3B42 sur les grands plans d'eau Amazoniens serait-elle significative ? Serait-ce une réduction artificielle, provoquées par des questions techniques des estimations du TRMM 3B42 ? Ou est-ce réel et une caractéristique des précipitations en Amazonie expliqué par un phénomène physique ?

En résumé, les résultats montrent une réduction claire de la précipitation annuelle moyenne et du nombre de jours pluvieux du TRMM 3B42 sur les grands plans d'eau Amazoniens, tels que les bassins des fleuves Solimões, Amazone, Tapajós, Negro et sur le réservoir de Balbina, confirmée par des tests statistiques. Ce comportement est variable au cours de la journée, étant plus marqué l'après-midi lorsque une grande partie de la précipitation a une origine convective et s'inverse la nuit et le matin. Ces caractéristiques ne sont pas en accord avec des problèmes techniques dans l'estimation des pluies par satellite relatés dans des études précédentes [*Tian and Peters-Lidard*, 2007]. En revanche, les tendances identifiées ici sont en accord avec un phénomène physique appelé brise fluviale provoqué par des différences entre le bilan énergétique de la forêt et de l'eau, qui pourrait provoquer une plus grande formation de nuages et de l'augmentation de la précipitation sur la forêt pendant la journée et le contraire la nuit, et qui a été décrit dans d'autres travaux dans la

région [*Cutrim et al.,* 2000*; Fitzjarrald et al.,* 2008*; Negri et al.,* 2000; *Garstang and Fitzjarrald,* 1999]. Comme la plupart des postes pluviométriques dans le bassin Amazonien sont localisés le long des fleuves, les estimations de précipitation basés sur les pluviomètres pourraient être systématiquement sous-estimées avec d'importantes implications sur les études dans la région. Cependant, l'étude présentée ici n'est pas totalement concluante et ce phénomène pourrait être confirmé par l'analyse de données de radars météorologiques installés *in situ*.

B.2.3. On the sources of hydrological prediction uncertainty in the Amazon

Les caractéristiques de prévisibilité hydrologique dans le bassin Amazonien ont été initialement étudiées dans le chapitre 4 afin de guider le développement d'un prototype de système de prévision hydrologique. Les erreurs dans les résultats des systèmes de prévision hydrologique basés sur des modèles hydrologiques à base physique dérivent normalement de : (i) les incertitudes sur la structure et les paramètres du modèle hydrologique, (ii) les incertitudes sur les forçages météorologiques futurs (iii) les incertitudes des conditions hydrologiques au moment de la prévision [*Liu e Gupta*, 2007].

Ainsi, la connaissance de l'importance relative de chacun de ces termes peut indiquer les actions prioritaires dans le développement du système de prévision hydrologique, pouvant être d'améliorer la structure du modèle, les forçages météorologiques ou les estimations des conditions initiales au travers de système d'assimilation de données.

Dans le chapitre 4, est présentée une étude de prévisibilité hydrologique pour le bassin Amazonien. Le modèle MGB-IPH basé sur l'implémentation présentée dans le chapitre 2 est utilisé. L'importance relative des conditions hydrologiques initiales du modèle et du forçage météorologique, plus spécifiquement des précipitations, est évaluée en tant que sources d'incertitude pour la prévision des débits en Amazonie.

Dans le contexte de la recherche développée ici, cette étape a eu un rôle fondamental – celui d'indiquer le chemin à suivre pour développer un système de prévisions hydrologiques dans le bassin Amazonien basé sur des modèles à base physique.

Pour cette étude nous avons utilisé une approche développée par *Wood and Lettenmaier* [2008] qui compare l'incertitude de prévisions gérées à partir d'un ensemble de conditions initiales et de prévisions gérées à partir d'une même condition initiale mais avec différents forçages météorologiques. A partir des deux ensembles de prévisions, il est possible d'évaluer à partir de quel moment l'incertitude de la prévision gérée par les erreurs de la

précipitation devient plus importante que celle induite par l'incertitude sur les conditions initiales. Nous avons également rechercher comment ces résultats varient spatialement et en fonction de la saison, quelles sont les variables d'état les plus importantes et comment les résultats peuvent être liés aux caractéristiques du bassin Amazonien.

Les résultats de cette étude initiale montrent que l'incertitude sur les conditions hydrologiques initiales domine la prévisibilité hydrologique dans les grands fleuves Amazoniens, même pour des horizons de prévisions élevés (1 à 3 mois), étant plus importante que l'incertitude sur la précipitation future. L'importance des variables d'état liées aux eaux superficielles comme le débit, les hauteurs d'eau et le volume dans les plaines d'inondation est mise en évidence, en particulier dans les fleuves avec une faible pente et de grande plaines d'inondation associé, ceci est probablement du à un temps important de transit des ondes de crues dans ce type de milieu. L'état des eaux souterraines apparaît important dans les périodes d'étiages dans le Sud-Ouest du bassin caractérisé par une saisonnalité plus marquée et pour être formé sur le bouclier Brésilien. Les incertitudes sur la précipitation sont importantes pour les fleuves plus petits et au début de la saison humide lors de la montée des hydrogrammes dans quelques régions spécifiques.

Les résultats suggèrent la potentialité d'un système basé sur un modèle hydrologique forcé par des données météorologiques historiques et utilisant les conditions initiales optimales pour la prévision des débits en temps réel dans le bassin Amazonien. En outre, nous avons montré l'importance de développer des techniques d'assimilation de données dans les modèles hydrologiques pour l'estimation des états hydrologiques qui seront utilisés au début de chaque prévision. Ces conclusions ont motivé le développement et l'évaluation de techniques d'assimilation de données et de prévision de débit et de niveaux d'eau qui sont présentées dans le chapitre 5.

B.2.4. Assimilating in situ and radar altimetry data into a large-scale hydrologic-hydrodynamic model for streamflow forecast in the Amazon River basin

Dans ce chapitre 5, il est présenté les résultats des travaux concernant l'intégration de modèles de simulation avec les observations, tant conventionnelles des stations fluviométriques que issues de l'observation spatiale afin d'améliorer les estimations de ces modèles. Pour la première fois, un schéma d'assimilation a été développé pour un modèle hydrologique et hydrodynamique de grande échelle pour assimiler des informations *in situ* et de l'altimétrie radar par satellite [*Santos da Silva et al.*, 2010]. Le schéma est basé sur la

technique de filtre de Kalman d'ensemble [*Evensen*, 2003] et a été implémenté et évalué pour le modèle MGB-IPH dans sa configuration présentée dans le chapitre 2 pour le bassin Amazonien.

Les performances de ce systèmes sont satisfaisantes pour l'assimilation de données de débits et de niveaux d'eau *in situ* et d'altimétrie radar dans le modèle hydrologique et hydrodynamique de grande échelle. L'assimilation de débits *in situ* a démontré que ce schéma améliore les estimations du modèle pour les postes fluviométriques utilisés pour l'assimilation, mais, contrairement aux tentatives d'études antérieures portant sur des régions plus petites [e.g. in *Clark et al.*, 2008; et dans d'autres travaux résumés *Lee et al.*, 2012], également transfère les informations à des localisations non surveillées, améliorant les résultats bien que dans une moindre mesure.

L'assimilation de données de l'altimétrie radar par le satellite ENVISAT améliore les estimations des niveaux d'eau et de débit dans une moindre mesure, principalement dans les fleuves où les observations ont été assimilées. Un aspect intéressant, est qu'en dépit que les données des radars altimétriques utilisées aient une faible résolution temporelle (35 jours), leur assimilation améliore les résultats du modèle au niveau journalier, probablement grâce à la haute résolution spatiale et la faible variabilité temporelle de l'inondation Amazonienne.

Dans quelques cas, le schéma dégrade les résultats pour des localisations non surveillées, ce qui pourrait être du à (i) la grande dimension de l'espace des variables d'état des modèles hydrologiques distribués à comparer avec l'information contenue dans les données assimilées ; (ii) une caractérisation imparfaites des erreurs du modèle hydrologique ; (iii) des fausses corrélations introduites par des problèmes numériques de la méthode. Ainsi, il reste encore un potentiel pour améliorer ce type de schéma d'assimilation de données au travers de l'utilisation de plus de données observées, une connaissance plus approfondie des erreurs du modèle hydrologique et le développement de méthodes de localisation pour limiter spatialement l'influence des observations.

En résumé, les résultats d'évaluation du schéma d'assimilation de données de débits et d'altimétrie par radar dans les modèles hydrologiques de grande échelle sont encourageants. Ces techniques peuvent être utilisées pour le développement de ré-analyse hydrologiques qui pourraient être utilisées dans des études rétrospectives, comme par exemple des évènements hydrologiques extrêmes qui ont eu lieu récemment en Amazonie. Le même schéma d'assimilation de données pourrait également facilement être appliqué dans d'autres modèles régionaux ou globaux similaires [e.g. *Yamazaki et al.*, 2011; *Decharme et al.*, 2011; *Alfieri et al.*, 2012; *Getirana et al.*, 2012]. Il existe également la possibilité d'améliorer les résultats

présentés dans cette thèse grâce à l'assimilation de données de nouvelles missions qui seront lancées dans le futur, telle que la constellation SENTINEL-3 de l'ESA (« *European Spatial Agency* ») ou de la future mission SWOT [*Durand et al.*, 2008a].

Enfin, pour la première fois a été développé un prototype de système de prévision de débits pour le bassin Amazonien présenté dans le chapitre 5, basé sur le modèle hydrologique et hydrodynamique de l'Amazonie, initialisé avec les conditions initiales optimales estimées par le schéma d'assimilation de données et en utilisant les précipitations estimées par satellite disponibles en temps réel. La technique adoptée «*Ensemble Streamflow Prediction* » [*Day*, 1985], dans laquelle considérant que la pluie future n'est pas connue, il est utilisé les données de précipitations des années passées pour forcer le modèle.

Les résultats de ce système se sont avérés prometteurs et le modèle a été capable de fournir des prévisions avec une bonne précision et exactitude dans le bassin Amazonien. Pour de faibles horizons de prévision (5 à 15 jours), les prévisions concordent avec les données observées dans de nombreuses stations fluviométriques quand pour des horizons plus importants (> 30 jours) les prévisions continuent à être informatives particulièrement dans les grands fleuves. Les résultats en général sont meilleurs pour les postes fluviométriques utilisés pour l'assimilation des données, comme attendu. Les prévisions ont une bonne exactitude le long du fleuve principal Solimões/Amazone même pour des horizons de prévision élevés (90 jours), en étant capable de prévoir, par exemple, la grande sécheresse de 2005 avec une grande antécédence.

Les résultats présentés ici montrent le potentiel de la modélisation hydrologique de grande échelle appuyée par l'information fournie par l'observation spatiale (par exemple, la précipitation, les niveaux d'eau dans les fleuves) pour la prévision des débits avec une importante antécédence dans les grands bassins hydrographiques du monde, comme le bassin Amazonien.